Eugenio Bianchi

Loop Quantum Gravity

TESI DI PERFEZIONAMENTO

SCUOLA NORMALE SUPERIORE

PISA - 2010

Contents

Preface

The topic of this thesis is the problem of quantum gravity, that is the investigation of the physics of gravity in regimes where quantum effects are expected to be important. The focus is on some of the current approaches to this problem, in particular on canonical Loop Quantum Gravity [1, 2, 3], on the path integral quantization of Regge gravity known as Spinfoam models [4, 5, 6], on Matrix Models for 4d Gravity (Group Field Theory) [7, 8, 9], and on topological field theories with defect networks [10, 11]. The recent remarkable convergence of these four approaches [12, 13] is leading to new developments in the field and is making these approaches a promising common direction to explore. In the following I refer to this direction simply as Loop Quantum Gravity (LQG).

The thesis is based on a number of papers [P1-P17] that cover organically various aspects of Loop Quantum Gravity. In particular, they cover the following topics:

- quantum geometry at the Planck scale [P3, P15, P16];
- formulation of the theory using topological field theory methods [P10, P14];
- coherent states and the semiclassical behavior of Loop Quantum Gravity [P4, P5, P6, P7, P11, P13, P15];
- gravitons from Loop Quantum Gravity [P1, P2, P8, P9];
- applications to early cosmology and black hole physics [P12, P17].

My main motivation for this series of papers is that I see the field evolving in a promising direction and I am interested in its formal developement, in assessing its physical viability as a description of gravity at the Planck scale, and in the possibility of extracting physical predictions from it. There is also a contingent motivation: in the effort to develop a simple presentation of the theory, I have been lead to reinvestigate various basic aspects of Loop Quantum Gravity. The simple introduction presented in chapter 1 of this thesis is the result of this attempt.

Parts of this thesis have been written while I was at Scuola Normale Superiore and at the Centre de Physique Théorique de Luminy. I thank both institutions for the lively scientific environement they have provided.

Over the last few years I have had the opportunity to collaborate with a number of colleagues. I would like to thank them for all the time spent together in enjoyable discussions: Carlo Rovelli, Leonardo Modesto, Simone Speziale, Alejandro Satz, Emanuele Alesci, Claudio Perini, Elena Magliaro, Francesca Vidotto, Daniele Regoli, Pietro Donà, Hal Haggard. A special thanks goes to my supervisors, Pietro Menotti and Carlo Rovelli, for all that they have taught me and for all that they keep teaching me everyday.

This thesis is dedicated to my brother Mike and to my parents for all their support and love.

Eugenio Bianchi,
Pisa and Marseille,
November 2010

Publications

[P1] E. Bianchi, L. Modesto, C. Rovelli, and S. Speziale, "Graviton propagator in loop quantum gravity," *Class.Quant.Grav.* **23** (2006) 6989–7028, `gr-qc/0604044`.

[P2] E. Bianchi and L. Modesto, "The Perturbative Regge-calculus regime of loop quantum gravity," *Nucl.Phys.* **B796** (2008) 581–621, `0709.2051`.

[P3] E. Bianchi, "The Length operator in Loop Quantum Gravity," *Nucl.Phys.* **B807** (2009) 591–624, `0806.4710`.

[P4] E. Bianchi and A. Satz, "Semiclassical regime of Regge calculus and spin foams," *Nucl.Phys.* **B808** (2009) 546–568, `0808.1107`.

[P5] E. Alesci, E. Bianchi, E. Magliaro, and C. Perini, "Intertwiner dynamics in the flipped vertex," *Class.Quant.Grav.* **26** (2009) 185003, `0808.1971`.

[P6] E. Alesci, E. Bianchi, E. Magliaro, and C. Perini, "Asymptotics of LQG fusion coefficients," *Class.Quant.Grav.* **27** (2010) 095016, `0809.3718`.

[P7] E. Alesci, E. Bianchi, E. Magliaro, and C. Perini, "Asymptotics of LQG fusion coefficients," *Class.Quant.Grav.* **27** (2010) 095016, `0809.3718`.

[P8] E. Alesci, E. Bianchi, and C. Rovelli, "LQG propagator: III. The New vertex," *Class.Quant.Grav.* **26** (2009) 215001, `0812.5018`.

[P9] E. Bianchi, E. Magliaro, and C. Perini, "LQG propagator from the new spin foams," *Nucl.Phys.* **B822** (2009) 245–269, 0905.4082.

[P10] E. Bianchi, "Loop Quantum Gravity à la Aharonov-Bohm," submitted to *Phys.Rev. D*, 0907.4388.

[P11] E. Bianchi, E. Magliaro, and C. Perini, "Coherent spin-networks," *Phys.Rev.* **D82** (2010) 024012, 0912.4054.

[P12] E. Bianchi, C. Rovelli, and F. Vidotto, "Towards Spinfoam Cosmology," *Phys.Rev.* **D82** (2010) 084035, 1003.3483.

[P13] E. Bianchi, E. Magliaro, and C. Perini, "Spinfoams in the holomorphic representation," submitted to *Phys.Rev. D*, 1004.4550.

[P14] E. Bianchi, D. Regoli, and C. Rovelli, "Face amplitude of spinfoam quantum gravity," *Class.Quant.Grav.* **27** (2010) 185009, 1005.0764.

[P15] E. Bianchi, P. Dona', and S. Speziale, "Polyhedra in loop quantum gravity," submitted to *Phys.Rev. D*, 1009.3402.

[P16] E. Bianchi and H. Haggard, "Volume spectrum from Bohr-Sommerfeld quantization," to appear (2010).

[P17] E. Bianchi, "Black Hole entropy, Loop Gravity, and Polymer Physics," *GR19 - CQG Special Issue* (2010).

Chapter 1

Introduction

Loop Quantum Gravity is a candidate theory for the quantum degrees of freedom of the gravitational field. The theory describes the general-relativistic dynamics of quantum geometry. It provides an implementation of the ideas due to Wheeler, DeWitt, Misner, Hawking and many others about a non-perturbative approach to quantum gravity. In the last few years, Loop Quantum Gravity has evolved into a rich mathematical setting: there is now a simple covariant description of its dynamics, defined in group theoretical terms; moreover, the semiclassical limit of the theory has now been explored and contact with classical General Relativity is now available. Besides the further formal development of the theory, the main focus today is twofold: (i) the development of approximation schemes to address fundamental physics questions and (ii) the study of the agreement of the theory with known physics in the appropriate regimes. Physics questions such as the fate of ultraviolet divergences and of cosmological singularities, or the microscopic origin of black hole entropy, can now be posed within this framework.

In this introduction, I discuss what is the problem addressed by Loop Quantum Gravity, what are the main physical ideas behind this theory, and what is its current status[1].

1.1 The problem addressed

There is a scale – *the Planck scale* – where both Quantum Mechanical effects and General Relativistic effects are expected to be important. At this scale we expect *new physics*, and we don't have yet a theory to describe it. The search for this theory is the problem of Quantum Gravity. The scale of quantum gravitational effects is easy to extimate[2]:

[1]This introduction is based on a series of lectures I have given at the XIX Sigrav school held in October 2010 at Scuola Normale Superiore, Pisa.

[2]In the following, the speed of light c is set to unity, $\hbar$ is the reduced Planck constant and G is the Newton's gravitational constant.

the typical length scale of quantum effects for a system of mass M is its Compton wavelength $\lambda_C = \hbar/M$; the scale of strong gravity effects for the same system is the 'Black-Hole horizon radius' $r_{\mathrm{BH}} = 2GM$. These two typical lengths are of the same order of magnitude at the Planck scale,

$$M_P = \sqrt{\hbar/G} \approx 10^{19}\ \mathrm{GeV}\ , \qquad L_P = \sqrt{\hbar G} \approx 10^{-35}\ \mathrm{m}\ . \tag{1.1}$$

Genuine Quantum Gravity effects are expected to be important in high-energy scattering[3], in the final stages of Black-Hole evaporation (where the effects of the curvature singularity are expected to be important), and in primordial cosmology, close to the Big Bang singularity. In fact, Quantum Gravity effects are expected to *cure* such singularities.

There are several approaches to the problem of Quantum Gravity that are currently being explored: String Theory [14, 15, 16, 17], Loop Quantum Gravity [1, 2, 3], Asymptotically Safe Gravity [18, 19], Causal Dynamical Triangulations [20, 21], Horava-Lifshitz Gravity [22], Non-commutative geometry [23], and others. It is fair to say that the problem is still open: all the approaches are still incomplete, there is no robust prediction yet and no experimental support so far. The topic of this thesis is the loop approach.

Before discussing the loop approach, I believe it is important to state what we do know about quantum gravity. This allows to sharpen the problem to be addressed and to improve the rough extimated of the Planck scale discussed above, formulating it in a well-developed framework: the framework of quantum field theory [24, 25].

An effective description of quantum gravity is available at low-energies: it is provided by a perturbative quantum theory of *gravitons* and matter fields on flat spacetime seen as an Effective Field Theory[4] [27, 28]. This is a phenomenological description: once fixed the energy E of the process of interest and the requested accuracy, it is enough to measure a finite number of coupling constants to predict scattering cross sections and decay rates. The result is given in the form of an expansion in the dimensionless ratio E/M_P, and this sets the accuracy of the prediction.

This perturbative framework breaks down at a scale M_P that it predicts[5] once a finite number of measurements have been made, and this provides a better estimate of the Planck scale. At such scale new physics is expected: the search for an *ultraviolet completion* of this bottom-up approach is the objective of quantum gravity research.

[3] For processes with center-of-mass energy of the order of magnitude of the impact parameter over Newton's constant. See section 6 for further details.

[4] We refer the reader to the lectures by Polchinski [26] for a nice introduction and discussion.

[5] Notice that, from the effective field theory perspective, a non-renormalizable theory (as is the case for perturbative quantum gravity [29, 30]) is not worst than a renormalizable theory – the difference is only in their sensitivity to the physics at microscopic scales. It is thanks to this sensitivity that the perturbative theory is able to predict the scale of its own break down.

In the search for an ultraviolet completion of perturbative quantum gravity we need some guide: which ultraviolet completion? At least in principle, there can be many inequivalent ones. Do we have any hint from the physics we know?

Fortunately, the answer is affirmative: the clue comes from the principles that lie at the basis of our classical theory of gravity, namely Einstein's General Relativity. Key features of General Relativity are (i) general covariance and (ii) the idea that gravity can be understood as the geometry of spacetime. In Loop Quantum Gravity such two features are taken as guiding principles for building a quantum theory of gravity. The theory is a diffeomorphism-invariant theory of quantum geometry with the metric acting as an operator on a space of quantum states. At present, the theory as been developed both in a canonical and in a covariant framework and a number of consistency checks and rigorous mathematical results is available. A crucial feature of this *top down* approach is that it predicts a specific form of ultraviolet completion for the perturbative theory: a remarkable result of Loop Quantum Gravity is the *prediction* of a quantum discreteness of space at the Planck scale [31].

1.2 Principles of Loop Quantum Gravity

The structure of General Relativity is the following:

- It is a field theory defined on a 4-manifold $\mathcal{M}$. The differentiable manifold $\mathcal{M}$ is not equipped with a given fixed metric. The absence of this non-dynamical metric is called *background independence.*

- The degrees of freedom are a Lorentzian metric field $g_{\mu\nu}(x)$ that is dynamical, and matter fields. Gravity is described by the metric field: in General Relativity *gravity is geometry.*

- The theory has a huge local group of symmetry: the action functional is invariant under diffeomorphisms of the manifold, *Diff*$(\mathcal{M})$. This is the mathematical implementation of Einstein's *general covariance.*

- The dynamics is prescribed by a specific action $S = S_{\text{gravity}}[g_{\mu\nu}] + S_{\text{matter}}[\varphi, g_{\mu\nu}]$ for gravity and matter fields $\varphi(x)$ and satisfies the principles above. The gravity part of the action is taken to be the Einstein-Hilbert action $S_{\text{gravity}}[g_{\mu\nu}] = \int \sqrt{-g}R\,dx$.

In Loop Quantum Gravity, the first three points above are taken as guiding principles. On the other hand the forth, the specific classical action, is not regarded as fundamental. The structure of Loop Quantum Gravity is the following:

- It is a framework for *diffeomorphism-invariant* Quantum Field Theory.

- The metric is a field operator, thus we have a theory of *Quantum Geometry.*

- It is a top-down approach: a specific dynamics is postulated at the quantum level in a way that is consistent with the structure and symmetries of the theory. It is given by a sum over quantum geometries.

It is also useful to know what the theory is not. There is no fixed background metric. This is to be opposed to ordinary Quantum Field Theory on fixed or on curved spacetime (and also to perturbative String Theory for instance). Moreover, Loop Quantum Gravity is a non-perturbative approach: it does not consist in the perturbative quantization of fluctuations of a classical metric.

The idea and the need for a non-perturbative quantization of General Relativity is not new. In fact Loop Quantum Gravity can be understood as the evolution and the mathematically well-defined version of the "old" non-perturbative approaches to Quantum Gravity investigated by Wheeler, DeWitt, Misner, Hawking and many others since the fifties. In next section we recall the basic structure of these approaches. Compared to these older attempts, what makes Loop Quantum Gravity mathematically robust is a further technical assumption that characterizes the theory and that we discuss in section 1.2.3: the *loop assumption*.

1.2.1 Old non-perturbative approaches

The conceptual framework of the old non-perturbative approaches to quantum gravity is the same as in Loop Quantum Gravity. In fact, Loop Quantum Gravity has its roots in these approaches. It is useful to describe their structure as it provides an introduction to the ideas of Loop Quantum Gravity, and at the same time highlights the progress done in the loop approach in the last two decades.

Non-perturbative approaches admit a canonical and a covariant version. The canonical version can be understood as the quantization of the Hamiltonian formulation of General Relativity[6] (see appendix A). The phase space of General Relativity consists of a Riemannian metric $q_{ab}(x)$ on a $3d$ manifold Σ and its conjugate momentum $\pi^{ab}(x)$. The manifold Σ represents space and can be understood as a constant-time surface in spacetime. The quantum theory consists of the following ingredients:

- *Space of states.* The quantum theory is formulated in the Schrödinger picture: the reason for this choice is that it allows to disentangle the kinematics from the dynamics.A state is a functional of the spatial metric, $\Psi[q_{ab}]$.

The invariance of the classical theory under diffeomorphisms ϕ of the manifold Σ is implemented in the quantum theory requiring that states are invariant under diffeomorphisms,

$$\Psi[\phi^* q_{ab}] = \Psi[q_{ab}] \ . \tag{1.2}$$

[6] The canonical formulation of General Relativity is mainly due to Dirac, Bergmann, Arnowitt, Deser and Misner.

A diffeomorphism invariant scalar product is introduced in order to promote the linear space of states into a Hilbert space. The scalar product is defined in terms of an integral over metrics $q_{ab}(x)$, modulo diffeomorphisms,

$$\langle\Psi_1|\Psi_2\rangle = \int D[q_{ab}]\,\overline{\Psi_1[q_{ab}]}\,\Psi_2[q_{ab}]\ . \tag{1.3}$$

• *Geometric operators.* Operators measuring the geometry of space can be introduced. For instance the operator that measures the volume of a region R is

$$\hat{V}(R) = \int_R d^3x\sqrt{\det q}\ . \tag{1.4}$$

• *Dynamics.* The dynamics is coded into the Wheeler-DeWitt equation,

$$\hat{H}\ \Psi[q_{ab}] = 0\ , \tag{1.5}$$

where the operator $\hat{H}$ can be understood as the quantization of the Hamiltonian constraint of General Relativity. The dynamics admits a covariant, *spacetime*, formulation. The transition kernel can be defined as the Misner-Hawking path integral over spacetime metrics $g_{\mu\nu}(x)$:

$$G[q'_{ab}, q''_{ab}] = \int_{q'_{ab}, q''_{ab}} \mathcal{D}[g_{\mu\nu}]\ e^{\frac{i}{\hbar}S_{\text{gravity}}[g_{\mu\nu}]} \tag{1.6}$$

Here $g_{\mu\nu}(x)$ are Lorentzian metrics defined on a region $\mathcal{M}$ of spacetime with the topology $\Sigma\times[0,1]$, where Σ is a 3-manifold regarded as space and $[0,1]$ is a temporal interval. We have called $q'_{ab}(x)$, $q''_{ab}(x)$ the 3-metric induced on the initial and the final component of the boundary of the region $\mathcal{M}$.

The transition kernel satisfies Wheeler-DeWitt equation

$$\hat{H}\ W[q_{ab}, q''_{ab}] = 0\ . \tag{1.7}$$

In fact, the transition kernel provides a full definition of the dynamics that is equivalent to the Wheeler-DeWitt equation[7].

The transition amplitude from a state Ψ_1 to a state Ψ_2 involves the kernel (1.6) and is given by the following expression

$$\langle\Psi_2|\hat{G}|\Psi_1\rangle \equiv \int D[q']\int D[q'']\,\overline{\Psi_2[q''_{ab}]}\,G[q'_{ab}, q''_{ab}]\,\Psi_1[q'_{ab}]\ . \tag{1.8}$$

Conditional probabilities are computed out of transition amplitudes[8] [35].

[7]It is useful to discuss the classical analogue of the Wheeler-DeWitt equation as it illustrates the relation between the canonical and the covarian version of the theory. ..

[8]The formalism admits a generalization to connected boundaries [1, 32]. This generalization allows to formulate questions about regions of spacetime (as scattering amplitudes [33]) as opposed to strictly "quantum cosmology" questions that involve the "wavefunction of the universe" [34].

The structure described above provides a *conceptual framework* for Quantum Gravity. It has proven useful in formulating questions. Unfortunately, in this form, it faces important technical difficulties: the expressions above are only formal and no calculation is possible. For instance, we have not declared what is the linear space of states $\Psi[q_{ab}]$. Saying that we consider only the ones that are normalizable with respect to the scalar product (1.3) does not solve the problem as the functional measure over 3-metrics modulo diffeomorphisms still needs to be defined. Moreover, about geometric operators, how do we compute their eigenvalues and eigenstates? Moving to the dynamics: the canonical version (1.5) is difficult to define because of the nonlinear nature of the classical Hamiltonian constraint. There are divergency issues and quantization ambiguities. Besides this, the main problem is the difficulty in finding at all solutions of the Wheeler-DeWitt equation. The covariant path-integral version (1.6) suffers from analogous problems: again there is the ambiguity in the choice of the classical action and the difficulty in defining the functional measure over Lorentzian 4-metric modulo diffeomorphisms. Besides these issues, the main problem is that of *computing*[9] the path-integral in (1.6) and the transition amplitudes defined in (1.8).

To summarize, there is an appealing framework with the conceptual structure that is considered appropriate in a quantum general-relativistic setting. However this construction has remained formal until the end of the Eighties.

Loop Quantum Gravity has the conceptual structure described above. What makes it a mathematically robust framework is a further assumption – the loop assumption. It is this assumption that allows to overcome the difficulties discussed above. Now we turn to it.

1.2.2 Gravity in terms of SU(2) gauge variables

There is a development in the classical description of General Relativity that has been crucial in the formulation of Loop Quantum Gravity: it is Ashtekar's 1988 realization that *gravity can be described in term of* $SU(2)$ *gauge variables* [36, 37].

A classical action for gravity that allows to couple fermions is given by

$$S[e,\omega] = \frac{1}{32\pi G}\Big(\int \epsilon_{IJKL}\, e^I \wedge e^J \wedge F^{KL}(\omega) \;+\frac{2}{\gamma}\int d\big(e_I \wedge T^I\big)\Big) \tag{1.9}$$

where $e^I = e^I_\mu(x) dx^\mu$ is the frame field and $\omega^{IJ} = \omega^{IJ}_\mu(x) dx^\mu$ is a Lorentz connection, F^{IJ}

[9] Notice that the path-integral (1.6) can be computed perturbatively integrating over metrics given by a classical solution of Einstein equations plus a small perturbation. A similar approach is available for the Wheeler-DeWitt equation. This leads to a well-defined framework that is essentially equivalent to standard perturbative quantum gravity: the theory is predictive at low energies, but ultraviolet divergencies are back, together with the need of an ultraviolet completion. This is why this direction is not taken here and the efforts are concentrated on a non-perturbative formulation.

its curvature and T^I is the torsion of the frame field[10]. The spacetime metric is given by $g_{\mu\nu}(x) = \eta_{IJ} e^I_\mu e^J_\nu$. The action above consists of two terms, the first being the standard Einstein-Cartan action. The second term is the Nieh-Yan invariant and does not modify the classical equations of motion[11]: it is a topological term that can be compared to the θ-term present in Yang-Mills gauge theory [40, 25]. The constant γ in front of it is called the Barbero-Immirzi parameter and will be important in the quantum theory.

The action (1.9) admits a phase-space formulation in terms of Ashtekar canonical variables:

- the position "q" is a $SU(2)$ connection $A^i_a(x)$ on the spatial hypersurface Σ;
- the conjugate momentum "p" is a non-abelian electric field $E^a_i(x)$ that plays the role of the spatial metric[12],

with standard canonical Poisson brackets

$$\{A^i_a(x), E^a_i(x')\} = 8\pi\gamma G\ \delta_a{}^b \delta^i{}_j \delta(x, x')\ . \tag{1.10}$$

The kinematics is the same as for a $SU(2)$ Yang-Mills gauge theory[13], but clearly the dynamics is different: we are still describing General Relativity. This description is available only if the Barbero-Immirzi parameter is finite and non-vanishing.

The Schroedinger non-perturbative framework for Gravity described in the previous section can be formulated in terms of $SU(2)$ gauge variables. There is a gain in this reformulation: the *raison d'être* of gauge variables is Wilson loops and is discussed in next section.

1.2.3 States in terms of Wilson loops

The Wilson loop of the Ashtekar connection is a functional of A^i_a defined as the trace of the holonomy of the connection along a closed curve $\curlyvee$ (a loop) embedded in the

[10]Here, in $I, J, ..$ are *internal* Lorentz indices, i.e. they label generators of the Lorentz group $SO(1,3)$ (or of its covering $SL(2,\mathbb{C})$). Indices are raised and lowered with the Lorentz metric η_{IJ}. The curvature of the Lorentz connection is given by $F^{IJ}(\omega) = d\omega^{IJ} + \omega^{IK} \wedge \omega_K{}^L$, the torsion is given by $T^I(e,\omega) = de^I + \omega^I{}_J \wedge e^J$. The frame field and the Lorentz connection are understood as independent variables as in the Palatini formalism.

[11]The Nieh-Yan invariant is P-odd and T-odd. The total derivative of $e_I \wedge T^I$ is

$$d\big(e_I \wedge T^I\big) = T_I \wedge T^I \ - \ e_I \wedge e_J \wedge F^{IJ}(\omega)$$

. The 4-form $e_I \wedge e_J \wedge F^{IJ}(\omega)$ is known as the Holst term [38] and vanishes if the torsion is zero (recall that $e_J \wedge F^{IJ}(\omega) = dT^I + \omega^I{}_J \wedge T^J$). See [39] for further details on torsional invariants.

[12]The relation between the Ashtekar variables and the e, ω variables is the following: the electric field is the density-one inverse-triad, $E^a_i = \frac{1}{2}\epsilon^{abc}\epsilon_{ijk} e^j_b e^k_c$; the connection is related to $(e\omega)$ by $A^i_a = \frac{1}{2}\epsilon^i{}_{kl}\omega^{kl}_a + \gamma\omega^{0i}_a$.

[13]Here $SU(2)$ is the covering of the local rotation group $SO(3)$.

3-manifold Σ:

$$\mathcal{W}_\Upsilon[A] = \mathrm{Tr}\, P \exp\left(i \int_\Upsilon A_a^i(x) \frac{\sigma_i}{2} dx^a\right) . \tag{1.11}$$

The idea proposed by Rovelli and Smolin in 1989 [41] is to build the linear space of states for Gravity from linear combinations of products of Wilson loops

$$\Psi_{\Upsilon_1..\Upsilon_L}[A] = \mathcal{W}_{\Upsilon_1}[A]\mathcal{W}_{\Upsilon_2}[A] \cdots \mathcal{W}_{\Upsilon_L}[A] . \tag{1.12}$$

Different loops can knot, can intersect and can even superpose along a portion of their paths.

On the space of linear superpositions of products of Wilson loops $\Psi_{\Upsilon_1..\Upsilon_L}[A]$, a diffeomorphism invariant scalar product can be introduced: the functional measure $\int D[A]$ is defined in terms of the Haar measure on $SU(2)$ via the Ashtekar-Lewandowski construction. The Hilbert space of states of Loop Quantum Gravity is defined as the Cauchy completion (in norm) of the linear space of products of Wilson loops.

This is the technical assumption that converts the old non-perturbative approach into a robust mathematical framework.

1.2.4 Why loops?

As the loop assumption is so central in the structure of Loop Quantum Gravity, it is important to discuss what is the motivation for this choice and how it helps addressing the technical difficulties discussed in section 1.2.1.

A classical field theory is a system with an infinite number of degrees of freedom. The standard strategy to obtain a quantum theory is to first capture a finite number of them, quantize them, a then define the full theory via a Cauchy completion to all the degrees of freedom. A standar example is the way Fock space is build out of n-particle states (see [42], ch.2). The *loop assumption* consists in using Wilson loops to capture a finite number of degrees of freedom of Gravity.

The state $\Psi_{\Upsilon_1..\Upsilon_L}[A]$ defined in (1.12) captures only a finite number of degrees of freedom of $A(x)$. Each Wilson loop knows only about the flux of the curvature of the Ashtekar connection through the loop. These are the microscopic degrees of freedom of the quantum gravitational field.

Notice that a Wilson loop state transforms covariantly under diffeomorphisms: let $\phi : \Sigma \to \Sigma$ be a diffeomorphism; then the transformation of the connection under a diffeomorphism, $\phi_* A$, pulls back to the loops that label the state,

$$\Psi_{\Upsilon_1..\Upsilon_L}[\phi_* A] = \Psi_{\phi^{-1}\circ(\Upsilon_1..\Upsilon_L)}[A] . \tag{1.13}$$

It is this property that allows to define a diffeomorphism invariant scalar product. Together with the fact that the flux of the electric field E ("the metric") can be promoted to a self-adjoint operator, this puts the kinematics of this approach into a robust mathematical form.

The feature of the loop assumption that has attracted much attention since its proposal [41] is the fact that it drastically simplifies the dynamics: a Wilson loop without self-intersections is an exact solutions of Wheeler-DeWitt equation,

$$\hat{H}\,\mathcal{W}_{\Upsilon}[A] = 0\ . \tag{1.14}$$

When loops intersect, the Hamiltonian constraint operator $\hat{H}$ acts non-trivially on the state $\Psi_{\Upsilon_1..\Upsilon_L}[A]$ only at the intersection of loops. This feature allows to restrict the possible forms of the dynamics and to develop approximation schemes for the solution of the Wheeler-DeWitt equation.

These are the motivations and the mathematical advantages provided by the loop assumption. The question then is: is this assumption *correct*? Clearly, this is not a mathematics issue: the answer depends on the physical predictions of the theory built on it.

In the following section we give a simple presentation of the structure of LQG. Some possible physical implications are discussed in chapter 6.

1.3 Loop Quantum Gravity: a simple presentation

This section is divided in three parts: the Hilbert space of states 1.3.1, the Penrose metric operator and quantum geometry 1.3.2, dynamics and the semiclassical limit.

1.3.1 The Hilbert space of states

We introduce the notion of graph Γ and show that a Hilbert space $\mathcal{H}(\Gamma)$ can be associated to it. The Hilbert space of LQG is defined in terms of this graph Hilbert space.

A graph Γ is a finite set of L elements $\{l_1,..,l_L\}$ denoted 'links' and N elements $\{n_1,..,n_N\}$ denoted 'nodes', together with a boundary relation that associates an ordered couple of nodes $\{s_l,t_l\}$ ('source' and 'target') to each link.

To links l of the graph Γ we can associate $SU(2)$ group elements h_l and consider functions $\psi(h_l)$ that are invariant under $SU(2)$ transformations g_n associated to the nodes of the graph,

$$\psi(g_{t_l} h_l g_{s_l}^{-1}) = \psi(h_l)\ . \tag{1.15}$$

This linear space of functions (the wavefunctions of LQG) can be promoted to an Hilbert space introducing the following scalar product:

$$(\psi_1,\psi_2) = \int_{SU(2)^L} dh_1 \cdots dh_L\ \overline{\psi_1(h_1,..,h_l)}\,\psi_2(h_1,..,h_l)\ , \tag{1.16}$$

where dh is the invariant measure on SU(2) (Haar measure). Taken into account that the wavefunctions $\psi(h_l)$ have the invariance (1.15), the product of $SU(2)$-invariant measures reduces to the Haar measure on the homogeneous space $SU(2)^L/SU(2)^N$ [43]. Correspondingly, the graph Hilbert space $\mathcal{H}(\Gamma)$ is the linear space of square integrable functions on $SU(2)^L/SU(2)^N$,

$$\mathcal{H}(\Gamma) = L^2(SU(2)^L/SU(2)^N, d\mu_{Haar}) \, . \tag{1.17}$$

In order to define the Hilbert space of full LQG, we need to introduce two other notions, the notion of *proper* graph Hilbert space $\mathcal{H}_0(\Gamma)$ and the notion of symmetrizer S.

Notice that, if a graph Γ' is a subset of a graph Γ, then the Hilbert space $\mathcal{H}(\Gamma')$ is a subspace of the Hilbert space $\mathcal{H}(\Gamma)$. The proper graph Hilbert space $\mathcal{H}_0(\Gamma)$ is defined in the following way:

$$\mathcal{H}_0(\Gamma) = \{\text{subspace of } \mathcal{H}(\Gamma) \text{ such that } \forall\, \Gamma' \subset \Gamma,\ \mathcal{H}_0(\Gamma) \perp \mathcal{H}(\Gamma')\} \, . \tag{1.18}$$

From the definition follows that, if Γ' is a subset of the graph Γ, then the proper graph Hilbert space $\mathcal{H}_0(\Gamma)$ is orthogonal to $\mathcal{H}_0(\Gamma')$.

Moreover, notice that a graph can have a non-trivial group of automorphisms, Aut(Γ). We call S the projector on the trivial representation of Aut(Γ). It plays the role of symmetrizer.

The LQG Hilbert space $\mathcal{H}_{LQG}$ is defined as the direct sum over graphs of symmetrized proper-graph Hilbert spaces,

$$\mathcal{H}_{LQG} = \bigoplus_{\Gamma} S\mathcal{H}_0(\Gamma) \, . \tag{1.19}$$

Its definition can be compared to the one of Fock space in terms on N-particle Hilbert spaces $\mathcal{H}_0(N)$,

$$\mathcal{H}_{Fock} = \bigoplus_{N} S\mathcal{H}_0(N) \, , \tag{1.20}$$

where S now is the (anti-)symmetrizer for indistinguishable particles, bosons (fermions).

Notice that $\mathcal{H}_{LQG}$ is a separable Hilbert space for the same reason Fock space is separable (see [42], ch.2): the graph Hilbert space is separable, the sum over graphs is countable, and the full Hilbert space $\mathcal{H}_{LQG}$ is obtained à la Fock via the Cauchy completion of truncated Hilbert spaces up to a maximum graph $\Gamma_{\max}$.

1.3.2 Penrose metric operator and quantum geometry

Let us focus on states belonging to the graph Hilbert space $\mathcal{H}(\Gamma)$. The quantum geometry interpratation of the states $\psi(h_l)$ discussed above comes from looking at the conjugate momentum to the configuration variable h_l. The conjugate momentum goes under the name of *flux* operator E^i_l and is defined as[14]

$$E^i_l = \gamma L_P^2 \hat{J}^i_l \ , \tag{1.21}$$

where $\hat{J}^i_l$ is the left derivative with respect to the group element h_l,

$$\hat{J}^i_l \, \psi(h_l) = -i \, \frac{\partial}{\partial \alpha_i} \psi(h_l \, e^{i\alpha_i \tau^i}) \Big|_{\alpha_i = 0} \ . \tag{1.22}$$

There is a flux operator associated to the source of each link of the graph[15].

There are two main properties of the flux operator that are worth discussing. Let us consider a node of the graph Γ that is the end-point of F links l. We will call it an F-valent node. The first property is that the set of flux operators E^i_l (l=1,. . ,F) satisfy the following *closure* condition

$$\sum_l E^i_l \ = 0 \tag{1.23}$$

as an operator equation in $\mathcal{H}(\Gamma)$. This is a consequence of the 'gauge' symmetry (1.15), the operator (1.23) is infact the generator of this symmetry. The second important property of the flux operator is that it transforms as a vector[16] under $SU(2)$ transformations (rotations) at the node. It can be used as elementary operator in order to build composite scalar operators that act on the Hilbert space $\mathcal{H}(\Gamma)$.

The simplest scalar operator that can be built out of the flux operator is the scalar product $\vec{E}_l \cdot \vec{E}_{l'}$ for two links that share the same source $n = s_l = s_{l'}$. This operator was infact introduced long ago by Penrose in the context of his spin-geometry theorem [44] and goes under the name of *Penrose metric operator*. As we will discuss below, the Penrose metric operator measures the 3-*metric* at each node of the graph Γ. Per each node of the graph, there are as many operators $\vec{E}_l \cdot \vec{E}_{l'}$ as couples of links that end at the node. Notice that such operators do not commute:

$$[\vec{E}_l \cdot \vec{E}_{l'} \ , \ \vec{E}_l \cdot \vec{E}_{l''}] = i\gamma \, L_P^2 \, \vec{E}_l \cdot (\vec{E}_{l'} \times \vec{E}_{l''}) \qquad \text{if } s_l = s_{l'} = s_{l''} \ . \tag{1.24}$$

As a result the metric in LQG is non-commutative, and Heisenberg uncertainty relations for quantum geometry follow.

Out of the set of operators $\vec{E}_l \cdot \vec{E}_{l'}$, we can extract a maximally set of commuting operators. Simultaneous eigenstates of this set of operators provide an orthonormal basis

[14]The flux operator has dimensions of length squared. Here γ and L_P are to be understood as fundamental constants of the theory.

[15]Notice that the flux operator associated to the target of a link is not an independent operator. It can be obtained reversing the orientation of the link and sending the group element h_l into h_l^{-1}. This corresponds to minus the right derivative. In the following we will focus on a node of the graph Γ and assume that the links at the node are all oriented so that the node is the source of the links.

[16]In the following we will use the vector notation $\vec{E}_l$ for the flux operator.

of the Hilbert space $\mathcal{H}(\Gamma)$ and are called *spin-network states*. Let us first introduce the notion of spin-network. A spin-network s is a triple $s = (\Gamma, j_l, i_n)$ consisting of a graph Γ and a labeling of its links and nodes as follows:

- a $SU(2)$ spin j_l is associated to each link of the graph,
- a $SU(2)$ intertwiner i_n to each node of the graph.

A spin-network state $\psi_s(h_l)$ is a state in $\mathcal{H}(\Gamma)$ that is labeled by a spin-network and defined as

$$\psi_s(h_l) = \Big(\bigotimes_{n\subset\Gamma} i_n \Big) \cdot \Big(\bigotimes_{l\subset\Gamma} \sqrt{2j_l+1}\, D^{(j_l)}(h_l) \Big) \,, \tag{1.25}$$

where $D^{(j_l)}(h_l)$ is the j_l-representation matrix of the $SU(2)$ group element h_l associated to the link l, and i_n is an element of an orthonormal basis in the vector space of intertwiners[17] associated to a node n. The notation $\cdot$ in (1.25) stands for a contraction of dual spaces[18] as prescribed by the connectivity of the graph Γ. The fact that spin-network states provide an orthonormal basis of the Hilbert space $\mathcal{H}(\Gamma)$ can also be proved straightforwardly using Peter-Weyl theorem [43].

In Loop Quantum Gravity, the original motivation for understanding the operator $\vec{E}_l \cdot \vec{E}_{l'}$ as a metric is that the electric field discussed in section 1.2.2 codes the metric of

[17] We briefly recall the notion of intertwiner. Intertwiners between F representations of $SU(2)$ form a finite dimensional vector space. They can be understood as follows [45]. Consider F particles of spin $j_1, .., j_F$. Simulateous eigenstates of the operators $\vec{J}_l^2$ and J_l^z, with $l = 1, .., F$,

$$|m_1, .., m_F\rangle = |j_1, m_1\rangle \otimes \cdots \otimes |j_F, m_F\rangle, \tag{1.26}$$

provide an orthonormal basis of the Hilbert space $V^{(j_1..j_F)} = V^{(j_1)} \otimes \cdots \otimes V^{(j_F)}$ of the system. Now we focus on *singlet* states, i.e. on the subspace $V_0^{(j_1..j_F)}$ of $V^{(j_1..j_F)}$ of states that are invariant under rotations. Singlet states $|i\rangle$ are annihilated by the total angular momentum operator,

$$(\vec{J}_1 + \cdots + \vec{J}_F)\,|i\rangle = 0 \tag{1.27}$$

The space $V_0^{(j_1..j_F)}$ is in general non-trivial and its dimension d depends on the value of the F spins. An orthonormal basis of this space can be easily found using standard techniques for the coupling of angular momenta [Landau]. An element $|i\rangle$ of a orthonormal basis of $V_0^{(j_1..j_F)}$ can be expandend on the basis $|m_1, .., m_F\rangle$ of $V^{(j_1..j_F)}$. We call $i^{m_1\cdots m_F}$ its coefficients,

$$|i\rangle = \sum_{m_1,..,m_F} i^{m_1\cdots m_F} |m_1, .., m_F\rangle \,. \tag{1.28}$$

In (1.25), the invariant tensors $i_n^{m_1\cdots m_F}$ label nodes of the graph Γ. They intertwine the representations $j_1, .., j_F$ labeling the links that enter the node n.

[18] To be more explicit we recall that, if $V^{(j)}$ is the vector space where the representation j of $SU(2)$ acts, then the tensor product of representations $D^{(j_l)}(h_l)$ lives in $\otimes_l (V^{(j_l)*} \otimes V^{(j_l)})$ while the tensor product of intertwiners lives precisely in the dual of this space.

space, its flux through a surface can be promoted to an operator, and it coincides with the flux operator discussed above. Here we discuss a different argument that motivates the interpretation of $\vec{E}_l \cdot \vec{E}_{l'}$ as a metric operator. The argument is due to Penrose.

Let us consider a node n of the graph Γ. Associated to the node there is an intertwiner Hilbert space, as discussed above. The operator $\vec{E}_l \cdot \vec{E}_{l'}$ with $n = s_l = s_{l'}$ is defined on this Hilbert space. In particular we can consider the expectation value of the Penrose metric operator on an intertwiner state $|i\rangle$. Considering the $F \times F$ couples of links at the node of the graph, this defines a matrix $T_{ll'}$,

$$T_{ll'} \equiv \langle \frac{\vec{E}_l \cdot \vec{E}_{l'}}{\sqrt{\vec{E}_l^2}\,\sqrt{\vec{E}_{l'}^2}} \rangle \ , \tag{1.29}$$

where the rationalized version of the operator has been considered for convenience. Now let us consider a semiclassical state, that is a state such that the dispersion[19] of $\vec{E}_l \cdot \vec{E}_{l'}$ is small,

$$\frac{\Delta(\vec{E}_l \cdot \vec{E}_{l'})}{\|\vec{E}_l \cdot \vec{E}_{l'}\|} \ll 1 \ , \tag{1.30}$$

What Penrose shows is that, on semiclassical states, the matrix $T_{ll'}$ is very constrained and codes a 3-dimensional Riemannian geometry: the components of $T_{ll'}$ measure the angle between directions in Euclidean space, or equivalently

$$T_{ll'} \approx \vec{n}_l \cdot \vec{n}_{l'} \tag{1.31}$$

where the $\vec{n}_l$ are a set of unit-vectors in Euclidean space and the $\approx$ stands for the fact that the identity is attained in the semiclassical limit (1.30). This result goes under the name of *spin-geometry theorem* [44].

Out of the metric operator we can built geometric quantities and use them to provide a physical interpretation of the spin-network states. In the following, we discuss the area and the volume operator.

There is an area operator A_l associated to each link of the graph Γ. It is given by the square root of the diagonal component l of the metric operator. Its spectrum is discrete and it is immediate to derive it as $\vec{J}_l^2$ is the Casimir of $SU(2)$,

$$A_l = \sqrt{\vec{E}_l \cdot \vec{E}_l} = \gamma L_P^2 \ \sqrt{j_l(j_l+1)} \ . \tag{1.32}$$

Notice that the spectrum has a *Planck scale gap*: the minimum non-vanishing eigenvalue is attained for $j_l = 1/2$ and given by $a_0 = \frac{\sqrt{3}}{2}\gamma L_P^2$.

[19]The dispersion ΔO is defined in the standard way as $\Delta O = \sqrt{\langle O^2\rangle - \langle O\rangle^2}$, where $\langle O\rangle = \langle i|O|i\rangle$ is the expectation value of the operator O on some state $|i\rangle$.

Figure 1.1: A portion of the spectrum of the volume. Points in each column in the plot correspond to the eigenvalues of the volume of a node with 4 links of equal spin j_0. The non-zero eigenvalues are twice degenerate. The vanishing eigenvalues are non-degenerate.

Let us now focus on the volume defined by the metric $\vec{E}_l \cdot \vec{E}_{l'}$. There is a volume operator associated to each node of the graph[20]. The volume of two- and three-valent nodes identically vanishes. The first non-trivial case is for a node that is four-valent. In this case its expression is given by

$$V_n = \frac{\sqrt{2}}{3} \sqrt{\left| \vec{E}_l \cdot (\vec{E}_{l'} \times \vec{E}_{l''}) \right|} \,. \tag{1.33}$$

This operator has a discrete spectrum. A series of eigenvalues is shown in figure 1.1. It has a Planck scale volume gap $v_0 = \frac{1}{\sqrt{2}\,3^{3/4}} \gamma^{3/2} L_P^3$.

From the notion of volumes and areas of states in the graph Hilbert space $\mathcal{H}(\Gamma)$, the following physical picture of spin-network states arises (see figure 1.2):

- nodes of the spin-network represent quantum grains of space with a definite volume; intertwiners are the quantum numbers of the volume;

[20]Notice that a link of the graph can be split into two introducing a 2-valent node. Thus, one can ask what is the volume of a this extra node, or equivalently what is the volume of a link. It turns out that the volume operator for 2-valent nodes identically vanishes. Therefore the volume is truely supported by nodes.

Figure 1.2: The physical picture associated to a spin-network state. Each node of the spin-network graph corresponds to a grain of space with a quantum behavior.

- links of the spin-network represent interfaces between grains of space having definite area; the spins are the quantum numbers of the area;
- the graph of the spin-network codes the connectivity of the grains of space.

To summarize, in Loop Quantum Gravity, space is described by a quantum geometry: the theory predicts a granular structure of space at the Planck scale, with geometric quantities having Planck scale gaps coming from the fact that their spectra come in discrete series, and non-trivial dispersions that satisfy Heisenberg uncertainity relations. The classical geometry proper of General Relativity is recovered looking at the expectation value of the metric on coherent states as described in detail in chapters 2 and 3.

1.3.3 Dynamics and spinfoams

In the previous section we described the quantum geometry of space. The topic of this section is its dynamics, that is quantum spacetime.

Let us start introducing the notion of *spinfoam* (see figure 1.3). A two-complex $\mathcal{C}$ is a finite set consisting of elements f called 'faces', elements e ('edges'), and elements v ('vertices'), together with a boundary relation ∂ that associates a cyclically ordered set of edges to each face, and an ordered couple of vertices (the source and the target) to each edge. Now let us consider the group $SU(2)$ and associate (i) an irreducible representation j_f (a *spin*) to each face of the two-complex $\mathcal{C}$, and (ii) a $SU(2)$ intertwiner i_e to each edge of the two complex. The triple $\sigma = (\mathcal{C}, j_f, i_e)$ is called a spinfoam. Notice that, in general, spinfoams can have boundaries: the boundary of the two-complex is a graph Γ with links that cut a boundary face and nodes that cut boundary edges. Moreover, the labeling of the two-complex induces a labeling of the boundary graph. As a result, the boundary of a spinfoam is a spin-network $s = (\Gamma, j_l, i_n)$. In the following we will restrict

Figure 1.3: A portion of a spinfoam 2-complex. Its boundary is a spin-network graph.

attention to spinfoams with fixed boundary data consisting in an initial spin-network s and a final spin-network s'.

A spinfoam σ with boundary $\partial\sigma = s \cup s'$ represents a quantum spacetime, the quantum version of a 4-metric $g_{\mu\nu}$ that reduces to a given 3-metric q_{ab} and q'_{ab} on the initial and final boundary of the 4-manifold, as discussed in section 1.2.1. Now, analogously to what happens in classical General Relativity where it is not enough to have a metric to describe the dynamics of gravity – we need also an action – here at the quantum level the dynamics is described not just by a spinfoam configuration, but by a weight $W(\sigma)$ associated to each spinfoam. The transition amplitude from an initial spin-network s to a final spin-network s' is determined by a sum over weighted spin-foams and is given by

$$G(s, s') = \sum_{\sigma\,:\,\partial\sigma = s\cup s'} W(\sigma)\ . \tag{1.34}$$

The weight $W(\sigma)$ is given by the following group theoretical expression:

$$W(\sigma) = \prod_f (2j_f + 1)\ \prod_v \Big\{ \bigotimes_{e\in v} I_\gamma(i_e) \Big\}\ . \tag{1.35}$$

The weight is local on the spin-foam two-complex: it is given by a product of amplitudes associated to faces f and vertices v of the two-complex. The face amplitude $2j_f + 1$ is determined by the requirement that the transition amplitude satisfy a composition property. The vertex amplitude is a Lorentz scalar built from Lorentz-covariant intertwining tensors $I_\gamma(i_e)$ associated to edges of the two-complex that end at the vertex. Their contraction is symmetric under exchange of the edges. The Lorentz intertwiner $I_\gamma(i_e)$ associated to edges of the spinfoam provides an embedding in spacetime of the grain of space described by the $SU(2)$ intertwiner i_e associated to nodes of the spin-network. It is defined in the following way.

Let us consider a unitary irreducible representation $V^{(p,j)}$ of the Lorentz group $SL(2,\mathbb{C})$ (the principal series) [46]. Here p is a real number and j an half-integer. In particular let us introduce a constant γ and write the real parameter as $p = \gamma j$. Later, it will turn out that this constant γ coincides with the Immirzi parameter. The representation space $V^{(\gamma j, j)}$ decomposes in an infinite series of $SU(2)$ representations $V^{(j')}$

$$V^{(\gamma j, j)} = \; V^{(j)} \oplus V^{(j+1)} \oplus V^{(j+2)} \oplus \cdots \; . \tag{1.36}$$

Let us call Y_γ the map that identifies the $SU(2)$ representation $V^{(j)}$ with the lowest-weight block $V^{(j)} \subset V^{(\gamma j, j)}$,

$$Y_\gamma : V^{(j)} \to V^{(j)} \subset V^{(\gamma j, j)} \; . \tag{1.37}$$

The $SL(2,\mathbb{C})$ intertwiner $I_\gamma(i_e)$ is obtained embedding the $SU(2)$ intertwiner using the map Y_γ, and then projecting it to the Lorentz invariant space of intertwiners via the projector $P_{SL(2,\mathbb{C})}$,

$$I_\gamma(i_e) = P_{SL(2,\mathbb{C})} \, Y_\gamma \, i_e \; . \tag{1.38}$$

This completes the definition of the spinfoam dynamics. It can be compared to the definition of the Wigner $\{6j\}$ symbol that enters the description of quantum 3d gravity provided by Ponzano and Regge [47].

To summarize. Quite surprisingly, the spinfoam dynamics is largely determined by a few general principles: (i) spacetime locality, (ii) composition property, (iii) crossing symmetry, (iv) local Lorentz invariance. The question then is how this group-theoretical object can know about the action of classical General Relativity and what is the evidence that General Relativity is recovered in the classical limit.

The remarkable result found in [48, 49] is that, in the semiclassical limit $\hbar \to 0$, the weight $W(\sigma)$ reproduces the exponential of the Einstein-Hilbert action, evaluated on a piecewise-flat metric g_σ associated to the spinfoam σ,

$$W(\sigma) \;\approx\; e^{\frac{i}{\hbar} S_{\mathrm{gravity}}[g_\sigma]} \; . \tag{1.39}$$

Thus, the contact with classical General Relativity (and with the old path integral formulation described in section 1.2.1) is recovered in the semiclassical limit[21]. This provides a 4d Lorentzian generalization of the Ponzano and Regge result for 3d gravity[22] [47]. For a more detailed discussion of the semiclassical limit, we refer the reader to chapter 3.

[21] Notice that, in the semiclassical limit, the dependence of the theory on the Immirzi parameter γ drops out.

[22] The asymptotics of the Wigner $\{6j\}$ symbol reproduces the exponential of the 3d gravity action [47].

1.4 Plan of the thesis

The rest of the thesis is organized as follows. We first describe the notion of quantum polyhedra and coherent states (chapter 2), then we discuss how coherent states allow to formulate the problem of the semiclassical limit of spinfoams and derive formula (1.39) (chapter 3). The notions discussed in chapters 2 and 3 are used in chapters 4 and 5 to analyze the graviton regime and the cosmological regime of Loop Quantum Gravity. In chapter 4, we compute two-point correlation functions for the Penrose metric operator. The calculation is done for a coherent state peaked on flat space and is compared to the graviton propagator computed in perturbative quantum gravity. In chapter 5, we study the spinfoam dynamics of a coherent state peaked on a homogeneous and isotropic geometry, study its evolution, and show that the gravity part of Friedmann equation arises in the semiclassical limit. Finally, in chapter 6 we describe some future research directions.

Chapter 2

Quantum polyhedra and coherent states

Loop quantum gravity is a continuous theory, whose Hilbert space is the direct sum of spaces associated to graphs Γ embedded in a three-dimensional hypersurface, $\mathcal{H} = \oplus_\Gamma \mathcal{H}_\Gamma$. It is often convenient to consider a single graph Γ, and the associated Hilbert space $\mathcal{H}_\Gamma$. The truncation captures only a finite number of degrees of freedom of the theory. An important question for us is whether these degrees of freedom can be "packaged" as to provide some *approximate* description of smooth 3d geometries [50, 51]. We specifically think that it would be useful to have a picture of the classical degrees of freedom captured by $\mathcal{H}_\Gamma$ in terms of discrete geometries. Such knowledge is for instance relevant for the interpretation of semiclassical states restricted on $\mathcal{H}_\Gamma$.

As it turns out, useful insights can be gained looking at the structure of $\mathcal{H}_\Gamma$. It decomposes in terms of SU(2)-invariant spaces $\mathcal{H}_F$ associated to each node of valence F. For a 4-valent node, it has been known for quite some time that an intertwiner represents the state of a "quantum tetrahedron" [52, 53], namely the quantization of the space of shapes of a flat tetrahedron in $\mathbb{R}^3$ with fixed areas. For a generic valence F, a natural expectation would be a relation to polyhedra with F faces, as mentioned in [54] and [50]. In this chapter we clarify the details of this correspondence[1].

There are two keys to our result. The first one is the fact that $\mathcal{H}_F$ is the quantization of a certain classical phase space $\mathcal{S}_F$, introduced by Kapovich and Millson in [56]. The second is the fact that there is a unique bounded convex polyhedron with F faces of given areas associated to each point of $\mathcal{S}_F$. This is guaranteed by an old theorem by Minkowski [57]. The correspondence is up to a measure-zero subset of "degenerate" configurations, present also in the 4-valent case. Accordingly, we have the following relations:

$$\text{polyhedra with } F \text{ faces} \longleftrightarrow \text{classical phase space } \mathcal{S}_F \longleftrightarrow \text{intertwiner space } \mathcal{H}_F.$$

[1] This chapter is based on work done together with Simone Speziale and Pietro Donà. The results have been published in [55].

An immediate consequence of these results is a complete characterization of coherent states at a fixed graph: they uniquely define a collection of polyhedra associated to each node of the graph. This provides a simple and compelling picture of the degrees of freedom of $\mathcal{H}_\Gamma$ in terms of discrete geometries, which is associated with a parametrization of the classical holonomy-flux variables in terms of the twisted geometries introduced in [50].

The chapter is ideally divided into two parts, concerning respectively the classical geometry of polyhedra, and the notion of quantum polyhedron together with its relevance to loop gravity. The motivation for the first part comes from the fact that polyhedra have a rich classical geometry. One of the reasons why the notion of quantum tetrahedron has been so fruitful in the developement of loop gravity and spinfoams is the fact that everybody understands the geometry of a classical tetrahedron. To make the extension to higher valence as fruitful, we need first of all to clarify a number of aspects of the geometry of polyhedra.

Minkowski's theorem guarantees that a polyhedron can be reconstructed out of the areas and normals to its faces, just as it happens for the tetrahedron. The new feature here is that there are many possible polyhedra with the same number of faces which differ in their combinatorial structure, i.e. in the adjacency relations of the faces. In the first part of the chapter (sections 2.1 and 2.2) we focus entirely on the classical geometry of polyhedra, and collect and in some cases adapt various results known in the mathematical literature. We discuss the combinatorial classes of polyhedra, and how the phase space of shapes at given areas can be divided into regions of different classes. We show explicitly how a given configuration of areas and normals can be used to reconstruct the polyhedron geometry, including its edge lengths, volume and combinatorial class. Furthermore, we discuss certain *shape matching conditions* which effectively restrict a collection of polyhedra to (a generalization of) Regge geometries.

In the second part of the chapter (sections 2.3 to 2.5) we discuss the quantum theory. We first review the construction of the quantization map between the phase space $\mathcal{S}_F$ and Hilbert space of intertwiners $\mathcal{H}_F$. This leads to the interpretation of an intertwiner state as the state of a quantum polyhedron, and of coherent intertwiners [58, 59] as states describing semiclassical polyhedra. The relevance of polyhedra extend to the whole graph Hilbert space $\mathcal{H}_\Gamma$, via the twisted geometries variables. The result provides an interpretation of coherent spin-network states in $\mathcal{H}_\Gamma$ as a collection of semiclassical polyhedra.

Furthermore, we introduce a new operator which measures the volume of a quantum polyhedron. Its definition is based on the knowledge of the classical system behind the intertwiner space $\mathcal{H}_F$, and has the right semiclassical limit on nodes of any valence. We discuss its relation with the standard volume operator of loop quantum gravity. Finally, we make some brief remarks on the polyhedral picture, Regge calculus and covariant spin foam models.

2.1 The phase space of polyhedra

2.1.1 Convex polyhedra and Minkowski theorem

A convex polyhedron is the convex hull of a finite set of points in 3d Euclidean space. It can be represented as the intersection of finitely many half-spaces as

$$\mathcal{P} = \left\{ x \in \mathbb{R}^3 \,|\, n_i \cdot x \leq h_i, \quad i = 1, \ldots, m \right\}, \tag{2.1}$$

where n_i are arbitrary vectors, and h_i are real numbers. The abstract description (2.1) is non-unique and redundant: the minimal set of half-spaces needed to describe a polyhedron corresponds to taking their number m equal to the number of faces F of the polyhedron. In this chapter we are interested in the description of a convex polyhedron with F faces in terms of variables that have an immediate geometric interpretation: the areas of the faces of the polyhedron and the unit normals to the planes that support such faces.

Let us consider a set of unit vectors $n_i \in \mathbb{R}^3$ and a set of positive real numbers A_i such that they satisfy the *closure* condition

$$C \equiv \sum_{i=1}^{F} A_i \, n_i = 0. \tag{2.2}$$

A convex polyhedron with F faces having areas A_i and normals n_i can be obtained in the following way. For each vector n_i consider the plane orthogonal it. Then translate this plane to a distance h_i from the origin of $\mathbb{R}^3$. The intersection of the half-spaces bounded by the planes defines the polyhedron, $n_i \cdot x \leq h_i$. We can then adjust the heights so that $h_i = h_i(A)$ so that the faces have areas A_i.

Remarkably, a convex polyhedron with such areas and normals always exists. Moreover, it is unique, up to rotations and translations. This result is established by the following theorem due to H. Minkowski [57, 60]:

Theorem (Minkowski, 1897)

(a) *If $n_1, \ldots, n_F$ are non-coplanar unit vectors and $A_1, \ldots, A_F$ are positive numbers such that the closure condition* (2.2) *holds, than there exists a convex polyhedron whose faces have outwards normals n_i and areas A_i.*

(b) *If each face of a convex polyhedron is equal in area to the corresponding face with parallel external normal of a second convex polyhedron and conversely, then the two polyhedra are congruent by translation.*

This unicity will play an important role in the following. Throughout the rest of the paper, we use simply polyhedra to refer to bounded convex polyhedra.

2.1.2 Kapovich-Millson phase space as the space of shapes of polyhedra

Let us consider F vectors in $\mathbb{R}^3$ that have given norms $A_1, \ldots, A_F$ and such that they sum up to zero. The space of such vectors modulo rotations has the structure of a symplectic manifold [56] and is known as the *Kapovich-Millson phase space*[2] $\mathcal{S}_F$,

$$\mathcal{S}_F = \left\{ n_i \in (S^2)^F \mid \textstyle\sum_{i=1}^F A_i n_i = 0 \right\} / \mathrm{SO}(3) \, . \tag{2.3}$$

The Poisson structure on this $2(F-3)$-dimensional space is the one that descends via symplectic reduction from the natural SO(3)-invariant Poisson structure on each of the F spheres S^2.

Action-angle variables for (2.3) are $(F-3)$ pairs (μ_i, θ_i) with canonical Poisson brackets, $\{\mu_i, \theta_j\} = \delta_{ij}$. Here μ_i is the length of the vector $\vec{\mu}_i = A_1 n_1 + \ldots + A_{i+1} n_{i+1}$ (see Fig.2.1), and its conjugate variable θ_i is the angle between the plane identified be the vectors $\vec{\mu}_{i-1}$, $\vec{\mu}_i$ and the plane identified by the vectors $\vec{\mu}_i$, $\vec{\mu}_{i+1}$. At fixed areas, the range of each μ_i is finite.

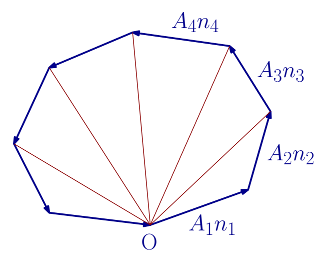

Figure 2.1: A polygon with side vectors $A_i n_i$ and the $(F-3)$ independent diagonals. The space of possible polygons in $\mathbb{R}^3$ up to rotations is a $(2F-6)$-dimensional phase space, with action-angle variables the pairs (μ_i, θ_i) of the diagonal lengths and dihedral angles. For non-coplanar normals, the same data defines also a unique polyhedron thanks to Minkowski's theorem.

Thanks to Minkowski's theorem, a point in $\mathcal{S}_F$ with non-coplanar normals identifies a unique polyhedron. Accordingly, we refer to (2.3) as the *space of shapes of polyhedra at fixed areas*. Notice that (2.3) contains also configurations with coplanar normals: they can be thought of as "degenerate" polyhedra, obtained as limiting cases. The fact that the polyhedra with faces of given areas form a phase space will be important in section (2.3.1) where we discuss the Hilbert space of the quantum polyhedron.

[2]In [56] it is also called the space of shapes of (bended) polygons. To be precise, it is a symplectic manifold up to a finite number of points, corresponding to configurations with one or more consecutive vectors collinear.

2.1.3 Classes of polyhedra with F faces

The phase space $\mathcal{S}_F$ has a rich structure: as we vary the normals of a polyhedron keeping its areas fixed, not only the geometry, but in general also the combinatorial structure of the polyhedron changes; that is, the number of edges and the adjacency of faces. We refer to the combinatorial structure as the *class* of the polyhedron. In other words, there are two components to the shape of a polyhedron: its class, and its geometry (up to rotations) once the combinatorial structure is fixed. The different classes of polyhedra correspond to the different tessellations of a sphere having F faces. Which class is realized, depends on the specific value of the normals. This is a point we would like to stress: one is not free to choose a class, and then assign the data. It is on the contrary *the choice of data that selects the class.* This is an immediate consequence of Minkowski's theorem. Accordingly, the phase space $\mathcal{S}_F$ can be divided into regions corresponding to the different classes of polytopes with F faces.

To visualize the class of a polyhedron it is convenient to use Schlegel diagrams [61, 60]. The Schlegel diagram of a polyhedron is a planar graph obtained choosing a face f, and projecting all the other faces on f as viewed from above. See Fig.2.2 for examples.

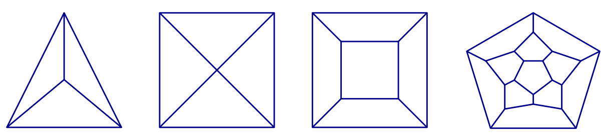

Figure 2.2: Some examples of Schlegel diagrams. From left to right, a tetrahedron, a pyramid, a cube and a dodecahedron.

To understand the division of $\mathcal{S}_F$ into regions of different class, let us first give some examples, and postpone general comments to the end of the Section. In the most familiar $F = 4$ case, there is no partitioning of $\mathcal{S}_4$: there is a unique tessellation of the sphere, the tetrahedron, and it is well known that there is always a unique tetrahedron associated with four closed normals. The first non-trivial case is $F = 5$, where there are two possible classes: a triangular prism, and a pyramid (see Fig. 2.3). Consider then the phase space

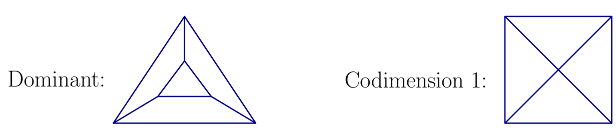

Figure 2.3: Polyhedra with 5 faces: the two possible classes are the triangular prism (left panel) and the pyramid (right panel). The two classes differ in the polygonal faces and in the number of vertices.

$\mathcal{S}_5$. Minkowski's theorem guarantees that the same set (A_i, n_i) cannot be associated to both classes, thus each point in $\mathcal{S}_5$ corresponds to a unique class. One might at first think that $\mathcal{S}_5$ can be more or less equally divided among the two classes, but this is not the case. In fact, notice that the pyramid is just a special case of the prism, obtained by collapsing to a point one of the edges connecting two triangular faces. The existence of a pyramid then requires a non-trivial condition, i.e. the presence of a 4-valent vertex. A moment of reflection shows that this condition can be imposed via an algebraic equation on the variables. Hence the shapes corresponding to pyramids span a codimension one surface in $\mathcal{S}_5$. Generic configurations of areas and normals describe triangular prisms, and the pyramids are measure zero special cases. We call *dominant* the class of maximal dimensionality, e.g. the triangular prism here.

Let us move to $F = 6$, a case of particular interest since regular graphs in $\mathbb{R}^3$ are six-valent. There are *seven* different classes of polyhedra, see Fig.2.4. The most familiar one is the cuboid (top left of Fig.2.4), with its six quadrilateral faces. Remarkably, there is a further dominant class: it is a "pentagonal wedge", i.e. a polyhedron with two triangles, two quadrilaterals and two pentagons as faces (to visualize it, immagine a triangular prism planed down on a corner, so that a vertex is replaced by a triangle). The remaining five classes are subdominant, because non-trivial conditions are required

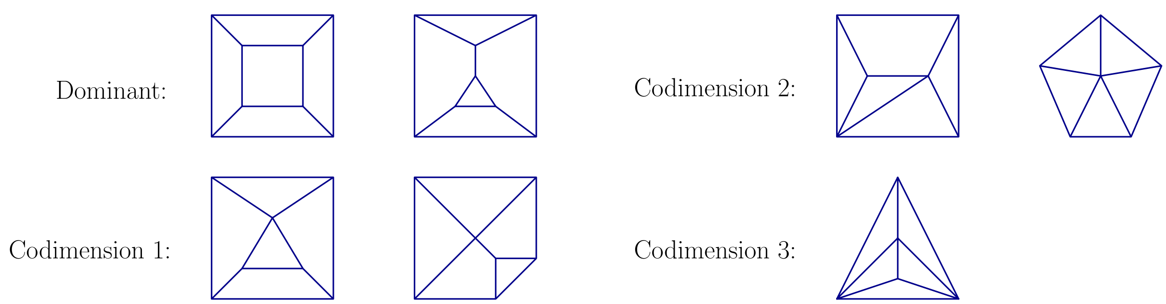

Figure 2.4: The seven classes of polyhedra with 6 faces, grouped according to the dimensionality of their configurations.

for their existence. Subdominant classes have fewer vertices and thus can be seen as special cases with certain edges of zero length.[3]

From the above analysis, we expect that the phase space $\mathcal{S}_6$ can then be divided into regions corresponding to the two dominant classes, separed by the subdominant ones. This is qualitatively illustrated in Figure 2.5. To confirm this picture, we performed

[3]Among these, notice the class of codimension 3. It has six triangular faces and three four-valent vertices. This class is interesting in that it can be seen as two tetrahedra glued along a common triangle. Two arbitrary tetrahedra are defined by 12 independent numbers. In order for them to glue consistently and generate this polyhedron, the shape of the shared triangle has to match. This shape matching requires three conditions (for instance matching of the edge lengths), thus we obtain a 9-dimensional space of shapes. For fixed external areas, this is precisely the codimension 3 subspace in $\mathcal{S}_6$. Hence this

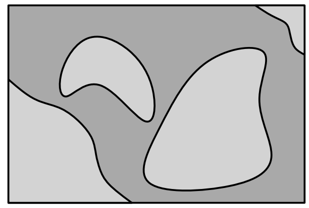

Figure 2.5: Pictorial representation of the phase space: it can be mapped into regions corresponding to the various dominant classes (two in the example). The subdominant classes separe the dominant ones and span measure-zero subspaces.

some numerical investigations. Using the reconstruction algorithm, which we introduce in the next Section, we can assign a class to each point in $\mathcal{S}_6$. In Fig.2.6 we give an explicit example of a 2d and a 3d slice of the 6d space $\mathcal{S}_6$, which shows the subdivision into the two dominant classes.

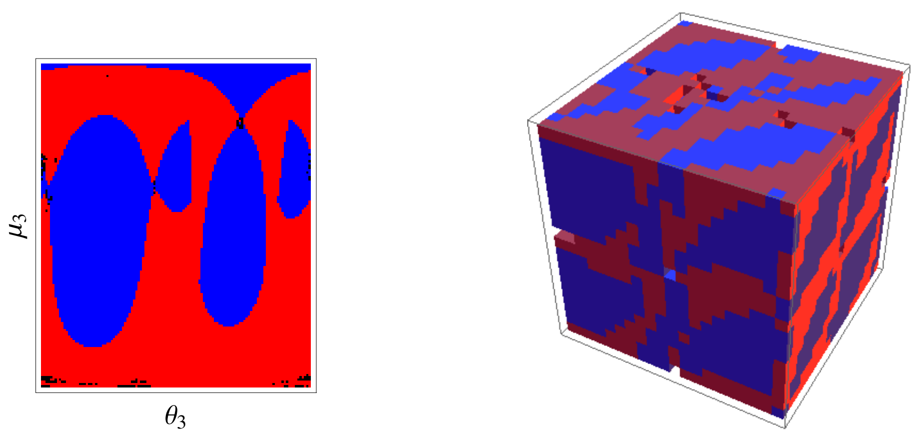

Figure 2.6: Mappings of subspaces of $\mathcal{S}_6$ realized using the reconstruction algorithm of Section 2.2 and Wolfram's Mathematica. We subdivided the phase space into a regular grid, and had Mathematica computing the adjacency matrix of the area-normal configurations lying at the center of the cells. This associates a unique class to each cell of the phase space. The information is colour-coded, cuboids in blue, pentagonal wedges in red. With this mapping of finite resolution we have measure-zero probability of hitting a subdominant class, thus the latter are absent in the figures. The holes are configurations for which our numerical algorithm failed. Concerning the specific values of the example, the areas are taken to be $(9, 10, 11, 12, 13, 13)$. In the left panel, we fixed $\mu_1 = 15$, $\theta_1 = \frac{7}{10}\pi$, $\mu_2 = 13$, $\theta_2 = \frac{13}{10}\pi$, and plotted the remaining pair (μ_3, θ_3). In the right panel, we fixed $\mu_i = (15, 13, 17)$ and plotted the three angles θ_i.

---

class is a special case of two tetrahedra where conditions are imposed for them to glue consistently.

After this brief survey of some specific examples, let us make some general statements.

- The phase space $\mathcal{S}_F$ can be divided into regions corresponding to different classes. The dominant classes, generically more than one, cover it densely, whereas the subdominant ones span measure-zero subspaces. The dominant classes in phase space correspond to polyhedra with all vertices three-valent, that is the dual to the tessellation is a triangulation. This condition maximizes both the number of vertices, $V = 3(F-2)$, and edges, $E = 2(F-2)$. Subdominant classes are special configurations with some edges of zero lengths and thus fewer vertices.

- Since all classes correspond to tessellations of the sphere with F faces, they are connected by Pachner moves [62]. The reader can easily find a sequence of moves connecting all seven classes of Fig.2.4. To start, apply a 2-2 move to the upper edge of the inner square of the cuboid to obtain the pentagonal wedge.

- The lowest-dimensional class corresponds to a maximal number of triangular faces, a condition which minimizes the number of vertices. When *all* the faces are triangular, the polyhedron can be seen as a collection of tetrahedra glued together, and with matching conditions imposed along all shared internal triangles.

Large F and the hexagonal dominance

The number of classes grows very fast with F (see for instance [63] for a tabulation). In the examples above with small F, we have been able to characterize the class looking just at how many faces have a certain valence. However as we increase F we find classes with the same valence distribution, but which differ in the way the faces are connected. To distinguish the classes one needs to identify the complete combinatorial structure of the polyhedron. This information is captured by the *adjacency matrix*, which codes the connectivity of the faces of the polyhedron. Below in Section 2.2.3 we will show how this matrix can be explicitly built as a function of areas and normals, and give some explicit examples.

An interesting question concerns the average valence of a face, defined as $\langle p\rangle = 2E/F$. A simple estimate can be given using the fact that the boundary of any polyhedron is a tessellation of the two-sphere, therefore by the Euler formula $F - E + V = 2$. For the dominant classes, which are dual to triangulations, the additional relation $2E = 3V$ holds, hence $E = 3(F-2)$ and we get $\langle p\rangle = 6(1-2/F)$. For large F, we expect the polyhedron to be dominated by *hexagonal faces*. This expectation is immediately confirmed by a simple numerical experiment. The specimen in Figure 2.7, for instance, has $F = 100$ and $\langle p\rangle \sim 5.88$. Notice also from the image that there are no triangular faces, consistently with the fact that they tend to minimize the number of vertices and are thus highly non-generic configurations.

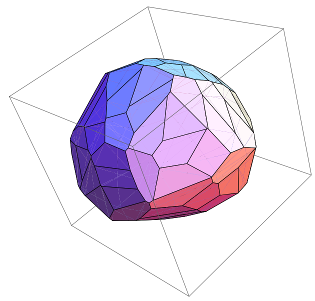

Figure 2.7: A polyhedron with $F = 100$ drawn with Wolfram's Mathematica, using the reconstruction algorithm. The example has all areas equals and normals uniformly distributed on a sphere. Notice that most faces have valence 6, and that triangles are nowhere to be seen.

2.2 Polyhedra from areas and normals: reconstruction procedure

So far we have discussed how a point in $\mathcal{S}_F$ specifies a unique polyhedron, and the existence of different combinatorial structures. We now describe how the polyhedron can be explicitly reconstructed from areas and normals. The reconstruction will allow us to evaluate completely its geometry, including the lengths of the edges and the volume, and to identify its class through the adjacency matrix, thus being able to associate a class with each point of $\mathcal{S}_F$.

The main difficulty in developing a reconstruction algorithm is that, given the areas and the normals, it is not known a priori which faces of the polyhedron are adjacent. The adjacency relations of the faces (and the combinatorial class of the polyhedron) are to be derived together with its geometry. This can be done in two steps. The first step uses an algorithm due to Lasserre [64] that permits to algebraically compute the lengths $\ell_{ij}(h, n)$ of all the edges of the polyhedron as defined by h_i and n_i, as in (2.1). The second step consists of solving a certain quadratic system to obtain the values of the heights h_i for given areas.

2.2.1 Lasserre's reconstruction algorithm

We now review Lasserre's procedure, and adapt it to the three-dimensional case of interest here. The basic idea of the reconstruction algorithm is to compute the length of an edge as the length of an interval in coordinates adapted to the edge. Consider the i-th face. From the defining inequalities (2.1), we know that points $x \in \mathbb{R}^3$ on this face satisfy

$$n_i \cdot x = h_i \tag{2.4a}$$
$$n_j \cdot x \leq h_j, \quad i \neq j. \tag{2.4b}$$

We consider the generic case in which $n_i \cdot n_j \neq \pm 1 \ \forall i, j$ (these special configurations can be obtained as limiting cases). We introduce coordinates y_i adapted to the face, that is

$$n_i \cdot y_i = 0, \qquad y_i = x - (x \cdot n_i) n_i. \tag{2.5}$$

Using (2.4a) we get $x = h_i n_i + y_i$, which inserted in (2.4b) gives

$$y_i \cdot n_j \leq r_{ij}, \quad i \neq j \ , \tag{2.6}$$

where we have defined

$$r_{ij} \equiv h_j - (n_i \cdot n_j) h_i \ . \tag{2.7}$$

Hence, the i-th face can be characterized either in terms of the x or the y_i coordinates,

$$\begin{cases} x \cdot n_i = h_i \\ n_j \cdot x \leq h_j, \quad i \neq j \end{cases} \longrightarrow \quad \begin{cases} y_i \cdot n_i = 0 \\ y_i \cdot n_j \leq r_{ij}(h, n), \quad i \neq j \end{cases} \tag{2.8}$$

Notice that $r_{ij}/\sqrt{1 - (n_i \cdot n_j)^2}$ is the distance of the edge ij from the projection of the origin on the i-th face.

The next step is to iterate this process and describe an edge in terms of its adapted coordinates. We start from the i-th face again, and assume that it is connected to the face j, so that the two faces share an edge. Points on the edge ij between the i-th and the j-th face satisfy

$$y_i \cdot n_i = 0 \tag{2.9}$$
$$y_i \cdot n_j = r_{ij} \tag{2.10}$$
$$y_i \cdot n_k \leq r_{ik}, \qquad k \neq i, j. \tag{2.11}$$

As before, we introduce coordinates z_{ij}, adapted to the edge,

$$n_i \cdot z_{ij} = n_j \cdot z_{ij} = 0, \qquad z_{ij} = y_i - [n_j - (n_i \cdot n_j) n_i] \frac{y_i \cdot n_j}{1 - (n_i \cdot n_j)^2}. \tag{2.12}$$

Using (2.10) we get that for a point in the edge

$$y_i = [n_j - (n_i \cdot n_j) n_i] \frac{h_j - h_i (n_i \cdot n_j)}{1 - (n_i \cdot n_j)^2} + z_{ij}. \tag{2.13}$$

Plugging this in (2.11) gives

$$z_{ij} \cdot n_k \leq b_{ij,k}, \tag{2.14}$$

where we have defined

$$b_{ij,k} \equiv h_k - (n_i \cdot n_k)h_i - \frac{(n_j \cdot n_k) - (n_i \cdot n_j)(n_i \cdot n_k)}{1 - (n_i \cdot n_j)^2} \left[h_j - h_i(n_i \cdot n_j)\right] . \tag{2.15}$$

Summarizing as before, going to adapted coordinates the edge is defined by

$$\begin{cases} y_i \cdot n_i = 0 \\ y_i \cdot n_j = r_{ij}(h,n) \\ y_i \cdot n_k \leq r_{ik}(h,n), \quad k \neq i,j. \end{cases} \longrightarrow \begin{cases} z_{ij} \cdot n_i = 0 \\ z_{ij} \cdot n_j = 0 \\ z_{ij} \cdot n_k \leq b_{ij,k}(h,n), \quad i \neq j \neq k \end{cases} \tag{2.16}$$

At this point we are ready to evaluate the length of each edge. To that end, we parametrize the z_{ij} coordinate vector in terms of its norm, say λ, and its direction which is given by the wedge product of the two normals,

$$z_{ij} = \lambda \frac{n_i \wedge n_j}{\sqrt{1 - (n_i \cdot n_j)^2}}. \tag{2.17}$$

If we define

$$a_{ij,k} \equiv \frac{n_i \wedge n_j \cdot n_k}{\sqrt{1 - (n_i \cdot n_j)^2}}, \tag{2.18}$$

we can rewrite the inequalities in (2.16) as

$$\lambda a_{ij,k} \leq b_{ij,k}. \tag{2.19}$$

Finally, the length of the edge is the length of the interval determined by the tightest set of inequalities, i.e.

$$\min_{k|a_{ij,k}>0} \left\{ \frac{b_{ij,k}}{a_{ij,k}} \right\} - \max_{k|a_{ij,k}<0} \left\{ \frac{b_{ij,k}}{a_{ij,k}} \right\}. \tag{2.20}$$

Here the minimum is taken over all the k's such that $a_{ij,k}$ is positive, and the maximum over all the k's such that $a_{ij,k}$ is negative. This quantity is symmetric [64] and satisfies a key property: it can be defined for *any pair of faces* ij, not only if their intersection defines an edge in the boundary of the polyhedron, and it is *negative* every time the edge does not belong to the polyhedron [64]. Thanks to this property, we can consistently define the edge lengths for any pair of faces ij as

$$\ell_{ij}(h,n) = \max_k \left\{ 0, \min_{k|a_{ij,k}>0} \left\{ \frac{b_{ij,k}}{a_{ij,k}} \right\} - \max_{k|a_{ij,k}<0} \left\{ \frac{b_{ij,k}}{a_{ij,k}} \right\} \right\}. \tag{2.21}$$

The result is a matrix whose entries are the edge lengths (as a functions of the normals and the heights) if the intersection is part of the boundary of the polyhedron, and zero if the intersection is outside the polyhedron.

This formula completes Lasserre's algorithm, and permits one to reconstruct the polyhedron from the set (h_i, n_i). To achieve a description in terms of areas and normals, we need one more step, that is an expression for the heights in terms of the areas. This can be done using (2.21) to compute the areas of the faces. We consider the projection of the origin on the face, and use it to divide the face into triangles. Recall the Lasserre's procedure has provided us with the distance between an edge and the projected origin, see (2.8). We thus can write

$$A_i = \frac{1}{2} \sum_{\substack{j=1 \\ j \neq i}}^{F} \frac{r_{ij}}{\sqrt{1-(n_i \cdot n_j)^2}} \, \ell_{ij}. \tag{2.22}$$

Notice that both $r_{ij}(h,n)$ from (2.7) and $\ell_{ij}(h,n)$ from (2.21) are linear in the heights. Hence, the area is a quadratic function,

$$A_i(h,n) = \sum_{j,k=1}^{F} M_i^{jk}(n_1,\ldots,n_F) h_j h_k, \tag{2.23}$$

where M_i is a matrix depending only on the normals. This homogeneous quadratic system can be solved for $h_i(A,n)$. The existence of a solution with $h_i > 0 \; \forall i$ is guaranteed by Minkowski's theorem. However, the solution is not unique: in fact, we have the freedom of moving the origin around inside the polyhedron, thus changing the value of the heights without changing the shape of the polyhedron. A method which we found convenient to use is to determine a solution minimizing the function

$$f(h_i) \equiv \sum_i \left(A_i(h,n) - A_i\right)^2 \tag{2.24}$$

at areas and normals fixed, with $A_i(h,n)$ given by (2.23). This is the method used in the numerical investigations of Figs. 2.6 and 2.7.[4]

Finally, from the inverse we derive the lengths as functions of areas and normals, which with a slight abuse of notation we still denote in the same way,

$$\ell_{ij}(A,n) = \ell_{ij}(h(A,n),n). \tag{2.25}$$

These expressions are well-defined and can be computed explicitly.

2.2.2 Volume of a polyhedron in terms of areas and normals

Let us call $\mathcal{P}(A_i,n_i)$ the convex subset of $\mathbb{R}^3$ corresponding to the polyhedron. Its volume is simply the integral on this region of the Euclidean volume density:

$$V(A_i,n_i) = \int_{\mathcal{P}(A_i,n_i)} d^3x. \tag{2.26}$$

[4] Concerning Fig. 2.6, we can also give now more details on the holes: these are configurations for which the numerical algorithm to solve (2.23) failed. This limitation can be easily improved with a better inversion algorithm, or by choosing a configuration slighly off the center of the cell.

An interesting question is how to compute efficiently the volume integral (2.26). The simplest way is to use the algorithm described in the previous section: we chop the region $\mathcal{P}(A_i, n_i)$ into pyramids with a common vertex in its interior and bases given by the faces of the polyhedron. In this way the volume is just the sum of the volumes of the pyramids, i.e.

$$V(A_i, n_i) = \frac{1}{3} \sum_{i=1}^{F} h_i \, A_i \ . \tag{2.27}$$

Here $h_i = h_i(A, n)$ are the heights of the pyramids expressed in terms of the areas and normals via Lasserre's algorithm.

The volume can be used to define a volume function on the phase space $\mathcal{S}_F$. To that end, notice that (2.27) is not defined for configurations with coplanar normals, which on the other hand do enter $\mathcal{S}_F$. However, it can be straightforwardly extended to a function on the whole $\mathcal{S}_F$ by defining it to be zero for coplanar configurations. Furthermore, the resulting phase space function is continuous.[5] Since the volume is manifestly invariant under rotations, it can also be written as a function of the reduced phase space variables only, that is, $V(A_i, \mu_k, \theta_k)$. To do so explicitly, one uses the relation $n_i = n_i(\mu_k, \theta_k)$, which is straightforward to derive once a reference frame is chosen.

The volume of the polyhedron as a function of areas and normals has a number of interesting properties:

C1. *Non-negative phase-space function.* The volume is by construction non-negative, and at given areas, it vanishes only when the normals n_i lie in a plane. This in particular implies that the volume vanishes for $F = 2$ and 3.

C2. *Boundedness.* For fixed areas A_i, the volume is a bounded function of the normals. We call $V_{\max}(A_i)$ the volume of the polyhedron with maximum volume,[6]

$$V_{\max}(A_i) \equiv \sup_{n_i} \{V(A_i, n_i)\} \ . \tag{2.28}$$

In particular, $V_{\max}(A_i)$ is smaller that the volume of the sphere that has the same surface area as the polyhedron. Therefore we have the bound

$$0 \leq V(A_i, n_i) < \frac{\left(\sum_i A_i\right)^{\frac{3}{2}}}{3\sqrt{4\pi}} \ . \tag{2.29}$$

[5] In order to to see this, one shows that the limit of coplanar normals exists and the volume tends to zero in this limit. From property (C3) – see below, a general F-valent coplanar configuration can be obtained from a $F+1$ configuration in the limit of zero base's area.

[6] Notice that there can be more than one polyhedron that attains maximum volume. For instance, in the case $F = 4$, there are two parity-related tetrahedra with maximal volume.

C3. *Face-consistency.* If we set to zero one of the areas such that the result is still a non-degenerate polyhedron, the function (2.27) automatically measures the volume of the reduced polyhedron with $F-1$ faces.

In conclusion, a point in $\mathcal{S}_F$ determines uniquely the whole geometry of a polyhedron and in particular its edge-lengths ℓ_{ij} (2.21) and its volume (2.27).[7] Now we show how these data can be used to identify the class of the polyhedron.

2.2.3 Adjacency matrix and the class of the polyhedron

The adjacency matrix A of the polyhedron is defined as

$$A_{ij} = \begin{cases} 1 & \text{if the faces } i \text{ and } j \text{ are adjacent} \\ 0 & \text{otherwise} \end{cases} \qquad i,j = 1,\ldots,F \tag{2.30}$$

Notice that A_{ij} coincides with the matrix ℓ_{ij} in (2.21) with all the non-zero entries normalized to 1: the recontruction algorithm gives us the adjacency matrix for free.

The symmetric matrix A_{ij} contains information on the connectivity of the faces as well as on the valence of each face, thus the class of the polyhedron can be identified uniquely from it. The valence p_i of the face i can be extracted taking the sum of the columns for each row,

$$p_i = \sum_{j=1}^{F} A_{ij}. \tag{2.31}$$

For example, for the two classes with $F=5$ of Fig.2.3 we have

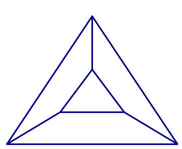

$$\longrightarrow \quad A = \begin{pmatrix} 0 & 0 & 1 & 1 & 1 \\ 0 & 0 & 1 & 1 & 1 \\ 1 & 1 & 0 & 1 & 1 \\ 1 & 1 & 1 & 0 & 1 \\ 1 & 1 & 1 & 1 & 0 \end{pmatrix} \quad \longrightarrow \quad p = (3,3,4,4,4)$$

[7] It is worth adding that the problem of computing the volume of a given polyhedron is a complex and well studied topic in computational mathematics [65, 66], hence better procedures than the one used here could in principle be found. However, the usual starting point for common algorithms is the knowledge of the coordinates of vertices, or the system of inequalities (2.1). Therefore the methods need to be adapted to obtain formulas in terms of areas and normals. The main difficulty is clearly that the adjacency relations of the faces are to be derived together with the geometry. We found Lasserre's algorithm to be the most compatible with these necessities, thanks to the fact that the lengths are reconstructed algebraically. Numerical algorithms for the volume and shape reconstruction from areas and normals are developed in the study of extended Gaussian images in informatics [67], however there are no analytical results.

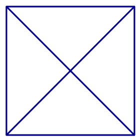

$$\longrightarrow \quad A = \begin{pmatrix} 0 & 1 & 1 & 1 & 1 \\ 1 & 0 & 1 & 0 & 1 \\ 1 & 1 & 0 & 1 & 0 \\ 1 & 0 & 1 & 0 & 1 \\ 1 & 1 & 0 & 1 & 0 \end{pmatrix} \quad \longrightarrow \quad p = (4, 3, 3, 3, 3)$$

From graph theory [68], we known that (2.30) has a number of interesting properties that can be related to the geometrical parameters of the polyhedron. For instance, the number of walks from the face i to the face j of length r is given by the matrix elements of the r-th power $(A^r)_{ij}$. From this property we deduce that the number E of edges of the polyhedron is

$$E = \frac{1}{2}\,\mathrm{Tr}A^2 = \frac{1}{2}\sum_i p_i. \tag{2.32}$$

This expression generalizes the value $E = 3(F-2)$ valid for the dominant classes.

Higher traces are related to the number of loops of a given lengh. For instance, the number of closed loops of length 3 is given by $(1/6)\,\mathrm{Tr}A^3$.

Through the adjacency matrix, obtained via the reconstruction procedure, areas and normals identify a unique class, and thus permits the division of $\mathcal{S}_F$.

2.2.4 Shape-matching conditions

Knowing the complete geometry of the polyhedra allows us also to address the following situation. Suppose that we are given two polyhedra in terms of their areas and normals, and that we want to glue them by a common face. Even if we choose the area of the common face to be the same, there is no guarantee that the shape of the face will match: The two sets of data will in general induce different shapes of the face. That is, the face has the same area but it can be two different polygons altogether. In order to glue the polyhedra nicely, one needs shape matching conditions guaranteeing that the shared face has the same geometry in both polyhedra.

If both polyhedra are tetrahedra, the problem has been solved in [69]. One uses the fact that the shape of the common triangle matches if two lengths, or two internal angles, are the same. The internal angles α can be expressed in terms of the 3d dihedral angles of the tetrahedron as follows,

$$\cos\alpha^i_{jk} = \frac{\cos\phi_{ij} + \cos\phi_{ik}\cos\phi_{jk}}{\sin\phi_{ik}\sin\phi_{jk}}. \tag{2.33}$$

Here the faces i, j and k all share a vertex, and α^i_{jk} is the angle between the edge ij and the edge ik inside the triangle i. See left panel of Figure 2.8. Consider now the adjacent tetrahedron. Its geometry induces for the same angle the value

$$\cos\alpha^i_{j'k'} = \frac{\cos\phi'_{ij'} + \cos\phi'_{ik'}\cos\phi'_{j'k'}}{\sin\phi'_{ik'}\sin\phi'_{jk'}}. \tag{2.34}$$

Hence, for the shape to match it is sufficient to require

$$\mathcal{C}_{kl,ij}(\phi) \equiv \cos\alpha^i_{jk} - \cos\alpha^i_{j'k'} = 0 \tag{2.35}$$

for two of the three angles of the triangle. These *shape matching conditions* are conditions on the normals of the two tetrahedra.

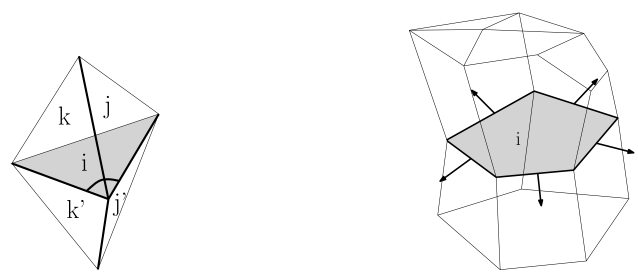

Figure 2.8: The geometric meaning of equation (2.35): the 2d angle $\alpha_{ij,kl}$ belonging to the shaded triangle can be expressed in terms of 3d angles associated the thick edges of the tetrahedron k, or equivalenty of the tetrahedron l.

The simplicity of the conditions (2.35) is a consequence of the fact that two triangles with the same area are congruent if two angles match. For the general case, the face to glue is now a polygon and the number of conditions greater. One needs to make sure that the valence p of the polygon is the same. Then, the number of independent parameters of a polygon on the plane is $2p-3$, hence giving the edge lengths is not enough, and $p-2$ additional conditions are needed. A convenient procedure is the following. Identify the faces of the two polyhedra that, having the same area, we want to match. From the reconstruction algorithm, we know the edge lengths ℓ_{ij} of the face viewed from one polyhedron. Then, for all j such that $\ell_{ij} \neq 0$, we consider the face normals n_j projected on the plane of the i-th face,

$$\tilde{n}_j = \frac{n_j - (n_i \cdot n_j)n_i}{|n_j - (n_i \cdot n_j)n_i|} = \frac{n_j - \cos\phi_{ij} n_i}{\sin\phi_{ij}}. \tag{2.36}$$

The set $(\ell_j, \tilde{n}_j)$ defines a unique polygon in the plane identified by n_i, thanks to a two-dimensional version of Minkowski's theorem. Then, we do the same with the second polyhedron, obtaining a second set $(\ell'_j, \tilde{n}'_j)$ living in the plane identified by n'_i. Finally, the shape matching conditions consist of imposing the equivalence of these two flat polygons up to rotations in three-dimensional space. Notice that the shape matching are now conditions on both the normals and the areas of the two polyhedra.

2.3 Relation to loop quantum gravity

Thus far we have been discussing classical properties of polyhedra. In the rest of the paper, we discuss the relevance of polyhedra for loop quantum gravity. The relation comes from the following two key results:

(i) Intertwiners are the building blocks of spin-network states, an orthonormal basis of the Hilbert space of loop quantum gravity [70, 71]

(ii) Intertwiners are the quantization of the phase space of Kapovich and Millson [72, 59, 73] (see also [74, 75]), i.e. of the space of shapes of polyhedra with fixed areas discussed in the previous sections.

Therefore an intertwiner can be understood as the state of a *quantum polyhedron*, and spin-network states as a collection of quantum polyhedra associated with each vertex.

In this section we review how (ii) and the notion of quantum polyhedron are established, observe that coherent intertwiners are peaked on the geometry of a classical polyhedron and discuss the relevance of this fact for the relation between semiclassical states of loop quantum gravity and twisted geometries.

2.3.1 The quantum polyhedron

Let us consider the space of vectors in 3d Euclidean space with norm j. This is a phase space, the Poisson structure being the rotationally invariant one proper of the 2-sphere S^2_j of radius j. As is well known, its quantization[8] is the representation space $V^{(j)}$ of SU(2). We are interested in the phase space $\mathcal{S}_F$, that is the space of F vectors that sum to zero, up to rotations. The Poisson structure on $\mathcal{S}_F$ is obtained via the symplectic reduction of the Poisson structure on the product of F spheres of given radius. Thanks to Guillemin-Sternberg's theorem that quantization commutes with reduction [76], we can quantize first the unconstrained phase space $\times_i S^2_{j_i}$, and then reducing it at the quantum level extracting the subspace of $\otimes_i V^{(j_i)}$ that is invariant under rotations. This gives precisely the intertwiner space $\mathcal{H}_F = \mathrm{Inv}\big[\otimes_{i=1}^F V^{(j_i)}\big]$. The situation is summarized by the commutativity of the following diagram,

$$\begin{array}{ccccc} & \times_i S^2_{j_i} & \longrightarrow & \otimes_i V^{j_i} & \\ \text{Symplectic reduction} & \downarrow & & \downarrow & \text{Quantum reduction} \\ & \mathcal{S}_F & \longrightarrow & \mathcal{H}_F & \end{array}$$

The correspondence between classical quantities and their quantization is the following: up to a dimensionful constant, the generators $\vec{J}_i$ of SU(2) acting on each representation space $V^{(j_i)}$ are understood as the quantization of the vectors $A_i n_i$. In LQG

[8] Notice that, as usual, the quantum theory requirers the quantization of some classical quantities. In this case the norm of the vector has to be a half-integer j, the *spin*.

the dimensionful constant is chosen to be the Immirzi parameter γ times Planck's area $8\pi L_P^2$,

$$A_i n_i \qquad \longrightarrow \qquad \hat{E}_i = 8\pi\gamma L_P^2 \, \vec{J}_i. \tag{2.37}$$

The closure condition (2.2) on the normals of the polyhedron is promoted to an operator equation,

$$\sum_{i=1}^{F} \vec{J}_i = 0. \tag{2.38}$$

This condition defines the space of intertwiners, and corresponds to the Gauss constraint of classical General Relativity in Ashtekar-Barbero variables.

One can then proceed to associate operators to geometric observables through the quantization map (2.37). The area of a face of the quantum polyhedron is

$$\hat{A}_i = \sqrt{\hat{E}_i \cdot \hat{E}_i} = 8\pi\gamma L_P^2 \sqrt{j_i(j_i+1)} \tag{2.39}$$

and produces an equispaced quantization of the area $A_i \sim j_i$ for large spins, i.e. up to quantum corrections.[9] The scalar product between the generators of $SU(2)$ associated to two faces of the polyhedron measure the angle θ_{ij} between them [77],

$$\hat{\theta}_{ij} = \arccos \frac{\vec{J}_i \cdot \vec{J}_j}{\sqrt{j_i(j_i+1)\, j_j(j_j+1)}}. \tag{2.40}$$

Notice that the angle operators do not commute among themselves, therefore it is not possible to find a state for a quantum polyhedron that has a definite value of all the angles between its faces. Moreover, the adjacency relations of the faces is not prescribed a priori, thus $\hat{\theta}_{ij}$ might not even be a true dihedral angle of the polygon. Therefore an eigenstate of a maximal commuting set of angles is far from the state of a classical polyhedron: it is an infinite superposition of polyhedra of different shapes, including different combinatorial classes. Semiclassical states for a quantum polyhedron are discussed in the next section.

2.3.2 Coherent intertwiners and semiclassical polyhedra

Coherent intertwiners for $\mathcal{H}_F$ were introduced in [58] and furtherly developed in [59, 73] (for previous related work, see [78]). These Livine-Speziale (LS) coherent intertwiners are defined as the SU(2)-invariant projection of a tensor product of states $|j_i, n_i\rangle \in V^{(j_i)}$,

$$\| j_i, n_i \rangle \equiv \int \mathrm{d}g \; D^{(j_1)}(g) |j_1, n_1\rangle \cdots D^{(j_F)}(g) |j_F, n_F\rangle. \tag{2.41}$$

[9] Notice that an ordering can be chosen so that the area is exactly $\hat{A}_i = 8\pi\gamma L_P^2 j_i$.

The states $|j, n\rangle$ are SU(2) coherent states peaked on the direction n of the spin [79, 80],

$$\langle j, n|\vec{J}|j, n\rangle = jn. \tag{2.42}$$

In (2.41), the unit-vectors n_i can be assumed to close, $\sum_i j_i n_i = 0$. The reduced states are still an overcomplete basis of $\mathcal{H}_F$, as a consequence of the Guillemin-Sternberg theorem [59, 81].

Coherent intertwiners are semiclassical states for a quantum polyhedron: the areas are sharp, and the expectation value of the non-commuting angle operators $\hat{\theta}_{ij}$ reproduces the classical angles between faces of the polyhedron in the large spin limit,

$$\frac{\langle j_i, n_i \| \cos\hat{\theta}_{ij} \| j_i, n_i\rangle}{\langle j_i, n_i \| j_i, n_i\rangle} \approx n_i \cdot n_j. \tag{2.43}$$

Moreover, the dispersions are small compared to the expectation values.

A useful fact is that coherent intertwiners can be labeled directly by a point in the phase space $\mathcal{S}_F$ of Kapovich and Millson, and therefore by a unique polyhedron. This provides a resolution of the identity in intertwiner space as an integral on $\mathcal{S}_F$. To realize this reduction, it is convenient to parametrize $\mathcal{S}_F$ via $F-3$ complex numbers Z_k, instead of (μ_k, θ_k) [59]. Let us choose an orientation in $\mathbb{R}^3$ and consider the stereographic projection z_i of the unit-vectors n_i into the complex plane.[10] The $F-3$ complex variables Z_k are the cross-ratios

$$Z_k = \frac{(z_{k+3} - z_1)(z_2 - z_3)}{(z_{k+3} - z_3)(z_2 - z_1)}, \quad k = 1, \dots, F-3. \tag{2.44}$$

Given an orientation in $\mathbb{R}^3$, a set of normals n_i that satisfy the closure condition (2.2) can be obtained as a function of the cross-ratios,

$$n_i = n_i(Z_k) \ . \tag{2.45}$$

Coherent intertwiners can then be obtained via geometric quantization [59]: they are labeled by the variables Z_k, that is $|j_i, Z_k\rangle$, and are equal to the states $\| j_i, n_i\rangle | = | j_i, n_i(Z_k)\rangle$ up to a normalization and phase.[11] The resolution of the identity is given by an integral over the variables Z_k,

$$\mathbb{1}_{\mathcal{H}_F} = \int_{\mathbb{C}^{F-3}} \mathrm{d}\mu(Z_k)\ |j_i, Z_k\rangle\langle j_i, Z_k| \ , \tag{2.46}$$

[10] The relation between the unit-vector $n = (n_x, n_y, n_z)$ and the stereographic projection is

$$z = -\frac{n_x - i n_y}{1 - n_z} = -\tan\frac{\theta}{2}\, e^{-i\phi},$$

where θ and ϕ are the zenith and azimuth angles of S^2, and we have chosen to project from the south pole.

[11] The states $|j_i, Z_k\rangle$ also define an holomorphic representation of the quantum algebra of functions $\psi(Z_k) \equiv \langle j_i, \bar{Z}_k|\psi\rangle$, see [73]. We will not use this representation in this paper.

where the integration measure $\mathrm{d}\mu(Z_k) = K_{j_i}(Z_k, \bar{Z}_k)\prod_k \mathrm{d}^2 Z_k$ depends parametrically on the spins j_i and is given explicitly in [59]. The relevance of this formula for the following discussion is that it provides a resolution of the identity in intertwiner space as a sum over semiclassical states, each one representing a classical polyhedron: the intertwiner space can be fully described in terms of polyhedra.[12]

2.3.3 Coherent states on a fixed graph and twisted geometries

The states $|j_i, Z_k\rangle$ provide coherent states for the space of intertwiners only, and should not be confused with coherent spin-network states for loop quantum gravity. Nevertheless, classical polyhedra and coherent intertwiners are relevant to the full theory, as we now discuss.

To relate polyhedra to loop quantum gravity, consider a truncation of the theory to a single graph Γ, with L links and N nodes. The associated gauge-invariant Hilbert space $\mathcal{H}_\Gamma = L_2[\mathrm{SU}(2)^L/\mathrm{SU}(2)^N]$ decomposes in terms of intertwiner spaces $\mathcal{H}_{F(n)} \equiv \mathrm{Inv}[\otimes_{l\in n} V^{(j_l)}]$ as

$$\mathcal{H}_\Gamma = \oplus_{j_l}\left(\otimes_n \mathcal{H}_{F(n)}\right). \tag{2.48}$$

This Hilbert space is the quantization of a classical space[13] $S_\Gamma = T^*\mathrm{SU}(2)^L//\mathrm{SU}(2)^N$, which corresponds to (gauge-invariant) holonomies and fluxes associated with links and dual faces of the graph. The key result is that this space admits a decomposition analogous to (2.48). In fact, it can be parametrized as [50]

$$S_\Gamma = \bigtimes_l T^*S^1 \bigtimes_n \mathcal{S}_{F(n)}, \tag{2.49}$$

where T^*S^1 is the cotangent bundle to a circle, F the valence of the node n, and $\mathcal{S}_F$ is the phase space of Kapovich and Millson.

The parametrization is achieved through an isomorphism between holonomy-fluxes and a set of variables dubbed "twisted geometries". These are the assignment of an area A_l and an angle ξ_l to each link, and of F normals n_i, satisfying the closure condition (2.2),

[12] Recently [54, 82, 83] attention has been given to a second space for which polyhedra are relevant. This is a sum of intertwiner spaces such that the total spin is fixed,

$$\mathcal{H}_J = \bigoplus_{\substack{j_1..j_F \\ \sum_i j_i = J}} \mathrm{Inv}\big[\otimes_{i=1}^F V^{(j_i)}\big]. \tag{2.47}$$

The interest in this space is that it is a representation of the unitary group U(F). Vectors in this space represent quantum polyhedra with fixed number of faces and fixed total area, but fuzzy individual areas as well as shapes as before. Coherent states for (2.47) can be built using U(F) coherent states [82]. These are also peaked on classical polyhedra like the LS states (2.41), thus the results in this paper are relevant for them as well.

[13] Again, this is a symplectic manifold up to singular points [84].

to each node. See [50, 51] for details and discussions. In this parametrization, a point of S_Γ describes a collection of polyhedra associated to each node. The two polyhedra belonging to nodes connected by a link l share a face. The area of this face is uniquely assigned to both polyhedra A_l (notice that this fact alone does not imply that the shape of the face matches – more on this below). The extra angles ξ_l carry information on the extrisic geometry between the polyhedra.

The isomorphism (2.49) and the unique correspondence between closed normals and polyhedra means that *each classical holonomy-flux configuration on a fixed graph can be visualized as a collection of polyhedra, together with a notion of parallel transport between them.* Just as the intertwiners are the building blocks of the quantum geometry of spin networks, polyhedra are the building blocks of the classical phase space (2.49) in the twisted geometries parametrization.

What is the relevance of this geometric construction to the quantum theory? Coherent states for loop quantum gravity have been introduced and extensively studied by Thiemann and collaborators [85, 86, 87, 88, 89, 84]. Although the states for the full theory have components on each graph, one needs to cut off the number of graphs to make them normalizable. In practice, it is often convenient to truncate the theory to a single graph. This truncation provides a useful computational tool, to be compared to a perturbative expansion, and has found many applications, from the study of propagators [90] to cosmology [91]. In many of these applications, control of the semiclassical limit requires a notion of semiclassical states in the truncated space $\mathcal{H}_\Gamma$. The truncation can only capture a finite number of degrees of freedom, thus coherent states in $\mathcal{H}_\Gamma$ are not peaked on a smooth classical geometry. Twisted geometries offer a way to see them as peaked on a discrete geometry, to be viewed as an approximation of a smooth geometry on a cellular decomposition dual to the graph Γ. The above results provide a compelling picture of these twisted geometries in terms of polyhedra, and thus of coherent states as a collection of semiclassical polyhedra.

There is one subtlety with this geometric picture that should be kept in mind, which justifies the name "twisted" geometries: they define a metric which is locally flat, but *discontinuous*. To understand this point, consider the link shared by two nodes. Its dual face has area proportional to A_l. However, the shape of the face is determined *independently* by the data around each node (i.e. the normals and the other areas), thus generic configurations will give two different shapes. In other words, the reconstruction of two polyhedra from holonomies and fluxes does not guarantee that the shapes of shared faces match. Hence, the metric of twisted geometries is discontinuous across the face [50, 51].[14] See left panel of Figure 2.8.

One can also consider a special set of configurations for which the shapes match, see right panel of Figure 2.8. This is a subset of the phase space S_Γ where the shape

[14] Aspects of this discontinuity have been discussed also in [92, 93]

matching conditions, discussed earlier in Section 2.2.4, hold. This subset corresponds to piecewise flat *and continuous* metrics. For the special case in which all the polyhedra are tetrahedra, this is the set-up of Regge calculus, and those holonomies and fluxes indeed describe a 3d Regge geometry: twisted geometries with matching conditions amount to edge lengths and extrinsic curvature dihedral angles [50, 51]. This relation between twisted geometry and Regge calculus implies that holonomies and fluxes carry *more* information than the space of Regge calculus. This is not in contradiction with the fact that the Regge variables and the LQG variables on a fixed graph both provide a truncation of general relativity: simply, they define two distinct truncations of the full theory. See [51] for a discussion of these aspects.

For an arbitrary graph, the shape-matching subset describes a generalization of 3d Regge geometry to arbitrary cellular decompositions. In this case however the variables are not equivalent any longer to edge lengths, since as already discussed these do not specify uniquely the geometry of polyhedra. Rather, such cellular Regge geometry must use areas and normals as fundamental variables.

Finally, let us make some comments on the coherent states themselves. The discussion so far is largely independent of the details of the coherent states on $\mathcal{H}_\Gamma$. All that is required is that they are properly peaked on a point in phase space. The states most commonly used are the heat-kernel ones of Thiemann and collaborators. Notice that these are not written in terms of the LS coherent intertwiners (2.41). Nevertheless, it was shown in [94] that they do reproduce coherent intertwiners in the large area limit. Alternative coherent states based directly on coherent intertwiners appear in [95]. These results show that coherent intertwiners can be used as building blocks of coherent spin networks.

2.4 On the volume operator

At the classical level, the volume of a polyhedron is a well-defined quantity. In this section we investigate the quantization of this quantity and its relation with the volume operators used in loop quantum gravity.

2.4.1 The volume of a quantum polyhedron

Let us consider the phase space $\mathcal{S}_F$ of polyhedra with F faces of given area. The volume of the polyhedron is a well-defined function on this phase spase, as discussed in Section 2.2.2. Coherent intertwiners provide a natural tool to promote this quantity to an operator in $\mathcal{H}_F$.

In the following we use the parametrization of the phase space $\mathcal{S}_F$ in terms of the cross ratios Z_k. In particular, the F normals n_i are understood as functions of the cross-ratios, $n_i(Z_k)$. Accordingly we call $V(j_i, Z_k)$ the volume of a polyhedron with faces of area[15] $A_i(j_i) = 8\pi\gamma L_P^2 j_i$ and normals $n_i(Z_k)$,

$$V(j_i, Z_k) \equiv V(A(j_i), n(Z_k)) \ . \tag{2.50}$$

Let us consider now the Hilbert space of intertwiners $\mathcal{H}_F$ associated to the phase space $\mathcal{S}_F$. The volume of a quantum polyhedron can be defined in terms of coherent intertwiners $|j_i, Z_k\rangle$ and of the classical volume as follows:

$$\hat{V} = \int d\mu(Z_k)\ V(j_i, Z_k)\ |j_i, Z_k\rangle\langle j_i, Z_k| \ . \tag{2.51}$$

This integral representation of the operator in terms of its classical version[16] is of the kind considered originally by Glauber [98] and Sudarshan [99]. It has a number of interesting properties that we now discuss:

Q1. The operator $\hat{V}$ is positive semi-definite, i.e.

$$\langle\psi|\hat{V}|\psi\rangle = \int d\mu(Z_k)\ V(j_i, Z_k)\ |\langle j_i, Z_k|\psi\rangle|^2 \quad \geq 0 \ , \tag{2.52}$$

for every $|\psi\rangle$ in $\mathcal{H}$. This is a straightforward consequence of the fact that the classical volume is a positive function, $V(j_i, Z_k) \geq 0$. Furthermore, $\hat{V}$ vanishes for $F = 2$ and 3.

Q2. $\hat{V}$ is a bounded operator in $\mathcal{H}_F$. Its norm $||\hat{V}|| = \sup_\psi \langle\psi|\hat{V}|\psi\rangle/\langle\psi|\psi\rangle$ is bounded from above by the maximum value of the classical volume of a polyhedron with fixed areas,

$$\frac{\langle\psi|\hat{V}|\psi\rangle}{\langle\psi|\psi\rangle} = \int d\mu(Z_k)\ V(j_i, Z_k)\ |\langle j_i, Z_k|\psi\rangle|^2 \quad \leq \quad \sup_{Z_k} \{V(j_i, Z_k)\} \ \equiv V_{max}(j_i) \ . \tag{2.53}$$

Q3. *0-spin consistency.* Let us consider the operator $\hat{V}$ defined on the Hilbert space $\mathcal{H}_{F+1}$ associated to spins $j_1, \ldots, j_F, j_{F+1}$, and the one defined on the Hilbert space

[15] We assume here an ordering of operators such that the area is linear in the spin. Other possibilities can be considered as well.

[16] In the literature [79], the classical function $V(j_i, Z_k)$ is called the P-symbol of the operator $\hat{V}$. On the other hand, the expectation value of the operator $\hat{V}$ on a set of coherent states, i.e.

$$Q(j_i, Z_k) \equiv \langle j_i, Z_k|\hat{V}|j_i, Z_k\rangle \ ,$$

is called the Q-symbol. When the P-symbol and the Q-symbol of an operator exist, then the operator is fully determined by either of them. The properties of these symbols and of the operator they define have been studied by Berezin in [96, 97]

$\mathcal{H}_F$ associated to spins $j_1, \ldots, j_F$. When the spin j_{F+1} vanishes, the two operators coincide. This is a consequence of the fact that the classical volume of a polyhedron with $F+1$ faces coincides with the volume of a polyhedron with F faces and the same normals when one of the areas is sent to zero.

These three properties are the quantum version of C1, C2, C3 discussed in Section 2.2.2. Moreover, using the fact that for large spins two coherent intertwiners become orthogonal,

$$|\langle j_i, Z_k | j_i, Z'_k\rangle|^2 \to \delta(Z_k, Z'_k), \tag{2.54}$$

we have that the expectation value $\langle \hat{V}\rangle$ of the volume operator on a coherent state $|j_i, Z_k\rangle$ reproduces the volume of the classical polyhedron with shape (j_i, Z_k),

$$\langle \hat{V}\rangle \equiv \frac{\langle j_i, Z_k|\hat{V}|j_i, Z_k\rangle}{\langle j_i, Z_k|j_i, Z_k\rangle} \approx V(A_i(j_i), n_i(Z_k)). \tag{2.55}$$

This fact allows to estimate the largest eigenvalue of the volume: in the large spin limit, the largest eigenvalue is given by $V_{max}(A_i)$, the volume of the largest polyhedron in $\mathcal{S}_F$.

The spectrum of the operator $\hat{V}$ can be computed numerically. Let us focus on the case $F=4$ for concreteness. The matrix elements of $\hat{V}$ in the conventional recoupling basis are given by

$$V_{kk'} = \langle j_i, k|\hat{V}|j_i, k'\rangle = \int \mathrm{d}\mu(Z)\, V(j_i, Z)\, \langle j_i, k|j_i, Z\rangle\langle j_i, Z|j_i, k'\rangle. \tag{2.56}$$

The matrix $V_{kk'}$ can be diagonalized numerically to obtain its eigenvalues.[17] We focused for simplicity on the simplest case where all the four spins j_i are equal to j_0. The results using Wolfram's Mathematica are shown in Fig. 2.9 and confirm that the maximum eigenvalue is below the volume of the regular tetrahedron. Notice also that the spectrum has a gap. One of the interesting questions to investigate in the future is whether this gap survives at higher valence, or it is dumped as for the standard volume operator [100].

It is interesting to notice that the volume operator introduced above commutes with the parity operator. This is the operator that sends the normals to their opposite,

$$\hat{\mathcal{P}}|j, n\rangle = |j, -n\rangle. \tag{2.57}$$

In terms of the stereographic projection, the maps $n \mapsto -n$ amounts to $z \mapsto -1/\bar{z}$, thus its action on coherent intertwiners labeled by the single cross-ratios Z is simply

$$\hat{\mathcal{P}}|j_i, Z\rangle = |j_i, \bar{Z}\rangle. \tag{2.58}$$

[17] The overlaps, $\langle j, k|j_i, Z\rangle = \frac{(-1)^{2k}}{2j+k+1}\frac{(2j!)^2}{(2j+k)!(2j-k)!}L_k(1-2Z)$, where L_k is the k-th Legendre polynomial, and the measure, can be found in [59].

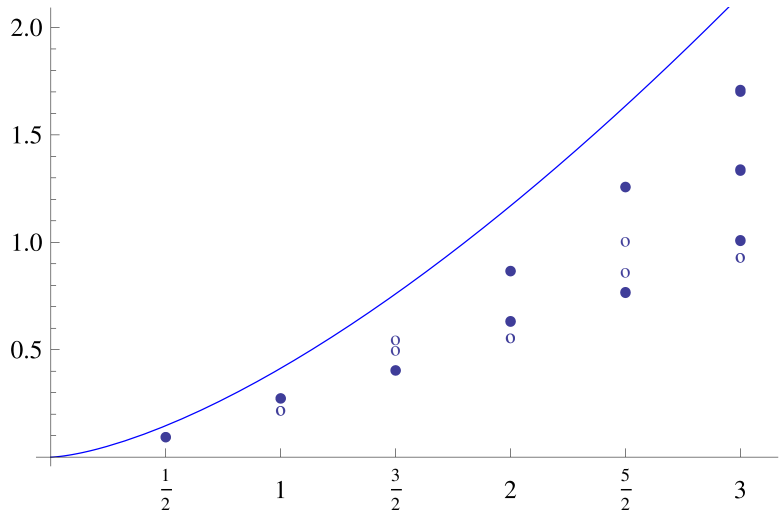

Figure 2.9: Some eigenvalues of $\hat{V}$. For comparison, the curve is the classical volume of an equilateral tetrahedron as a function of the area $A = j$ (units $8\pi\gamma L_P^2 = 1$). The empty circles are single eigenvalues, the full circles have double degeneracy. The spectrum is gapped and bounded from the above by the classical maximal volume, which provides a large spin asymptote.

Notice that $V(j_i, Z_k) = V(j_i, \bar{Z}_k)$ thanks to the invariance of the classical volume under parity. Moreover the measure $\mathrm{d}\mu(Z_k)$ is invariant under the transformation $Z_k \to \bar{Z}_k$. As a result, the operator (2.51) commutes with parity,

$$\hat{\mathcal{P}}\hat{V}\hat{\mathcal{P}}^\dagger = \int \mathrm{d}\mu(Z)\, V(j_i, Z)|j_i, \bar{Z}\rangle\langle j_i, \bar{Z}| = \int \mathrm{d}\mu(\bar{Z})\, V(j_i, \bar{Z})|j_i, Z\rangle\langle j_i, Z| = \hat{V}. \quad (2.59)$$

This explains the degeneracies seen in the spectrum.

Clearly, there are other possibilities for the volume of a quantum polyhedron. All of them share the same classical limit, but can have a different spectrum for small eigenvalues. An interesting variant is $\hat{\tilde{V}} = \sqrt{|\hat{U}|}$, where $\hat{U}$ is the oriented-volume square operator, defined as

$$\hat{U} = \int d\mu(Z_k)\; s(Z_k) V^2(j_i, Z_k)\; |j_i, Z_k\rangle\langle j_i, Z_k|. \quad (2.60)$$

Here $s(Z_k)$ is the parity of the polyhedron, i.e. $s(Z_k) = \pm 1$ and $s(\bar{Z}_k) = -s(Z_k)$.

The operator $\hat{U}$ anticommutes with the parity, and so does $\hat{\tilde{V}}$. Therefore, under the assumption that the spectrum is non-degenerate, we have that the eigenvalues appear in pairs $\pm u$. In particular, a zero eigenvalue is present when the Hilbert space $\mathcal{H}_F$ is odd-dimensional. This operator is similar in spirit to the the volume of a quantum tetrahedron introduced by Barbieri [52], $\hat{V}_B = (8\pi\gamma)^{\frac{3}{2}} L_P^3 \frac{\sqrt{2}}{3}\sqrt{|J_1 \cdot (J_2 \times J_3)|}$. In Fig. 2.10 we show some eigenvalues of $\hat{\hat{V}}$ and a comparison with $\hat{V}_B$.

For more on semiclassical aspects of the spectrum of the volume, see [101].

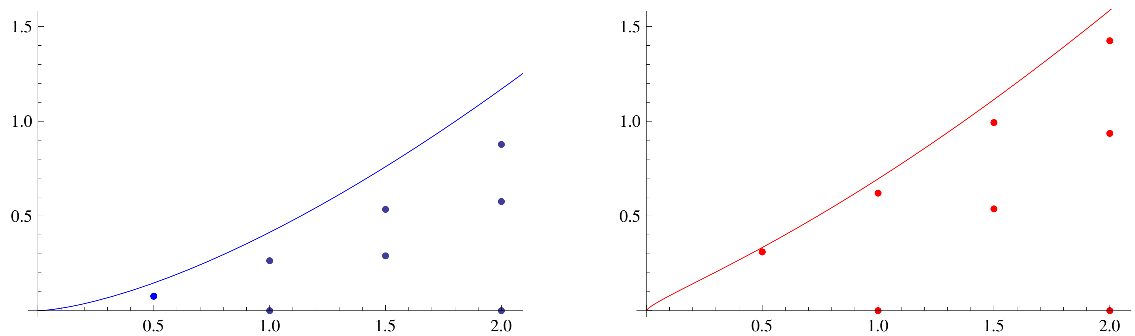

Figure 2.10: Left panel. Some eigenvalues of $\hat{\hat{V}}$. For comparison, the curve is the classical volume of an equilateral tetrahedron as a function of the area $A = j$ (units $8\pi\gamma L_P^2 = 1$). All but the zero eigenvalue have double degeneracies. Right panel. Same region of the spectrum for Barbieri's operator $\hat{V}_B$. Notice that here the asymptotic curve is the equilateral volume with areas $A = \sqrt{j(j+1)}$.

2.4.2 LQG volume operator and the quantum polyhedron

In LQG, the operator associated to the volume of a region in space is a well studied quantity [31, 102, 103, 104]. It is defined on the graph Hilbert space $\mathcal{H}_\Gamma$ as a sum over contributions $\hat{V}_n$ from each node n of the graph within the region R,

$$\hat{V}_\Gamma(R) = \sum_{n \subset R} \hat{V}_n. \tag{2.61}$$

In order to admit a lifting from $\mathcal{H}_\Gamma$ to the full Hilbert space of LQG, the operator $\hat{V}_\Gamma(R)$ has to satisfy a number of consistency conditions that go under the name of "cylindrical consistency" [3]. In particular, these conditions are satisfied by the operator $\hat{V}_n$ if (i) it commutes with the area of dual surfaces, so that $\hat{V}_n$ reduces to an operator on the intertwiner space $\mathcal{H}_{F(n)}$, and (ii) it satisfies a *0-spin consistency condition* so that the operators defined on different intertwiner spaces coincide when these spaces are identified.

In the previous section we have introduced an operator $\hat{V}_n$, given by (2.51) for the given node, that satisfies these conditions. Condition (i) holds because by construction the operator acts within $\mathcal{H}_{F(n)}$, and condition (ii) follows from property Q3 in Section 2.4. This operator is based on the knowledge of the classical system behind the intertwiner space $\mathcal{H}_{F(n)}$. The single node operator $\hat{V}_n$ measures the volume of a quantum polyhedron dual to the node, and the operator $\hat{V}_\Gamma(R)$ built as in (2.61) the volume of a region in a twisted geometry. It has a good semiclassical limit by construction.

The standard strategy in LQG is on the other hand rather different. The starting point is the classical expression for the volume of a region,

$$V(R) = \int_R \mathrm{d}^3x \sqrt{\frac{1}{3!}\left|\epsilon^{ijk}\epsilon_{abc}E_i^a E_j^b E_k^c\right|}\ , \tag{2.62}$$

$E_i^a(x)$ being the Ashtekar-Barbero triad. The key step is to rewrite this quantity in terms of fluxes, which are the fundamental operators of the theory. This step introduces a regularization procedure which is adapted to a graph Γ embedded in space. Then, the regularized quantity is promoted to an operator in the Hilbert space $\mathcal{H}_\Gamma$ and the limit of vanishing regulator exists and it is well-defined. Two volume operators have been constructed in this way, one by Rovelli-Smolin [31], and one by Ashtekar-Lewandowski [102]. Both these operators have the form (2.61), and differ in the regularization procedure and in details on the exact form of $\hat{V}_n$. For the Ashtekar-Lewandowski volume operator, the node contribution is defined on the intertwiner space $\mathcal{H}_F$ as

$$\hat{V}_n^{AL} = (8\pi\gamma)^{3/2} L_P^3 \sqrt{\frac{1}{8}\Big|\sum_{1\leq i<j<k\leq F} \epsilon(e_i,e_j,e_k)\ \vec{J}_i\cdot(\vec{J}_j\wedge\vec{J}_k)\Big|}, \tag{2.63}$$

where $\epsilon(e_i,e_j,e_k)=\pm1,0$ is the orientation of the tangents e_i to the links at the node. The overall coefficient is fixed by a consistency requirement known as 'triad test' [105]. There is a large amount of analytical and numerical results on the spectrum of this operator (e.g. [106, 100]), particularly because it enters Thiemann's construction of the Hamiltonian constraint [107] and thus it is relevant to understand the quantum dynamics of the theory. Moreover its semiclassical behaviour has been investigated in detail with the conclusion that only *cubulations*, that is regular graphs with 6-valent nodes, have a good semiclassical limit [108]. In the light of the quantum polyhedron introduced in this chapter, this result can be understood as follows.

On semiclassical states,[18] $\langle\vec{J}_i\rangle = \vec{A}_i \equiv A_i n_i$ (see discussion in Section 2.3 and cf. (2.37) and (2.42)), and the expectation value of (2.63) is – at zero order in $\hbar$ [108]

$$\langle\hat{V}_n^{AL}\rangle = \sqrt{\frac{1}{8}\Big|\sum_{1\leq i<j<k\leq F} \epsilon(e_i,e_j,e_k)\ \vec{A}_i\cdot(\vec{A}_j\wedge\vec{A}_k)\Big|}. \tag{2.64}$$

[18] The semiclassical states used in the analysis of [108] are the heat-kernel coherent states developed by Thiemann and collaborators [85, 86, 87, 88]. However, the details on the coherent states do not matter for our argument, all that is required is that they are peaked on a given point in the classical phase space S_Γ.

As discussed earlier, the variables $\vec{A}_i$ of the semiclassical state define a polyhedron around the node n. The key observation is that (2.64) is *not* the volume of that polyhedron. The volume of a convex polyhedron with F faces is in general a rather complicated function of the areas and normals (see the discussion in Section 2.2.2). There is however a case where this expression simplifies greatly, and in this case it coincides with (2.64): it happens for *parallelepipeds*. Parallelepipeds are a subset of the phase space $\mathcal{S}_F$ for $F = 6$ with areas that are equal in pairs. They live within the combinatorial class of cuboids: they are cuboids with three couples of parallel faces.[19] The volume of a parallelepiped is

$$V = \sqrt{|\vec{A}_1 \cdot (\vec{A}_2 \wedge \vec{A}_3)|}, \tag{2.65}$$

where (123) are any three faces sharing a vertex. It is straightforward to see that this coincides with (2.64) for the semiclassical state of a cubic analytic node[20] with areas equals in pairs and normals parallel pairwise.

This fact explains why the expectation value of the operator (2.63) on a semiclassical states reproduces the volume of a parallelepiped for $F = 6$, but not the volume of other polyhedra.[21]

2.5 On dynamics and spin foams

Spin foam models for the dynamics of loop quantum gravity are usually built starting from a discretization of the spacetime manifold in terms of a simplicial triangulation Δ. A certain control over the dynamics comes from a connection with Regge calculus in the large spin limit. Specifically, in this limit the transition amplitudes are related to exponentials of the Regge action [59, 81, 48, 49]. This result is generally regarded as a promising step towards understanding the low-energy physics of the theory, since discrete general relativity on Δ is reproduced. On the other hand, complete transition amplitudes for LQG require the use of more general 2-complexes than those those dual to simplicial manifolds.[22]

Just as Regge calculus is useful to study the semiclassical behaviour on simplicial manifolds, a generalization thereof to arbitrary cellular decompositions could be relevant to the full theory, and allow us to test whether models such as the one proposed in [109]

[19] Notice that parallelepipeds are a set of measure zero among the cuboids. Moreover, cuboids are not the only dominant class in phase space $\mathcal{S}_F$ with $F = 6$.

[20] That is, the link are the analytic continuations of each other across the nodes.

[21] It goes without saying that an expression like (2.63) works also for a tetrahedron, as we saw with $\hat{V}_B$ earlier. But that requires a different numerical coefficient in (2.63) – an extra $\sqrt{2}/3$.

[22] Although a direct construction of the path integral for arbitrary graph has not been attempted so far, in [109] a model valid for arbitrary graph was proposed, based on a natural extension of some algebraic properties of the EPR model [110, 5].

can be related to (discrete) general relativity. In this final Section, we would like to make two remarks on this idea.

The first remark concerns Regge calculus on arbitrary cellular decompositions. The point is that edge lengths are not good variables to capture the (discrete) metric of the manifold. This is simply because a generic 4d polyhedron at fixed edge lengths is not rigid. Therefore a piecewise-linear metric can not be described by the edge lengths of the polyhedra alone. The solution to this problem can be found looking again at Minkowski's theorem, which holds in any dimension. The theorem implies that a generic polyhedron in $\mathbb{R}^n$, sometimes called an n-polytope, is uniquely characterized by $nF - n(n+1)/2$ numbers: the volumes of the F "faces" (which are now $(n-1)$-polytopes) and the normals satisfying the n-dimensional closure condition. On the other hand, n-simplexes are polytopes with a minimal number of faces, $F = n + 1$. In this case, assigning their $n(n+1)/2$ edge lengths suffices, thus edge lengths fix a unique flat metric on each n-simplex and can be used as fundamental variables in the full triangulation.

Let us fix $n = 4$. To identify the geometry of each 4-polytope, we need volumes V_m and 4d unit normals N_m of each polyhedron m in its boundary, satisfying the closure condition. For these to extend to a piecewise-linear, continuous metric on the whole cellular decomposition, we additionally need shape matching conditions, of the sort described in Section 2.2.4 for three dimensions. A tentative Regge-like action can then be written as

$$S[V_m, N_m] = \sum_f A_f(V_m, N_m)\epsilon_f(V_m, N_m) + \text{constraints}, \tag{2.66}$$

where f are the 2d faces of the cellular decomposition, and ϵ the deficit angles, defined as usual as 2π minus the sum of dihedral angles of each 4-polytope sharing the face. The constraints are the closure and shape matching conditions. In principle, we can interpret (2.66) as an "effective" Regge action in which the internal edge lengths of an initial simplicial triangulation have been evaluated on the flat solution.

The second remark concerns the link between spin foam amplitudes and Regge calculus. A lesson from the recent asymptotics studies of the EPR model is that the amplitude is dominated by exponentials of the Regge action when the boundary data satisfy certain conditions, which guarantee the existence of a unique 4-simplex in the bulk. This suggest that the dominant contributions to models on arbitrary graphs could come from requesting the existence of a unique 4-polytope, and that the amplitude could be related to a form of the Regge action specialized to the 4-polytope, such as the one described above. So the question is whether, as for the 4-simplex, the conditions for the existence of the 4-polytope can be mapped into conditions on the boundary data, such as 3d closure and non-degeneracy conditions, and shape matching. This is a key question that we leave open for future work. We believe that the answer, and these considerations in general, will be relevant to tackle the problem of the semiclassical limit of spin foams on arbitrary graphs, such as the one proposed in [109].

2.6 Summary

In this chapter we discussed a number of properties of classical polyhedra which are of interest to loop quantum gravity. A polyhedron can be uniquely identified by the areas and the normals to its faces (Minkowski's theorem, Section 2.1). The identification includes the knowledge of its geometry (edge lengths, volume), and its combinatorial class (the adjacency of the faces). This information can be explicitly derived from the areas and normals through the reconstruction procedure presented in section 2.2. We observed that the space of polyhedra of given areas is a phase space, previously introduced by Kapovich and Millson, and used our reconstruction algorithm to divide this space into regions corresponding to different classes.

We then discussed the relevance of polyhedra to the quantum theory. We first recalled (section 2.3) that the quantization of Kapovich and Millson phase space gives the SU(2)-invariant space of intertwiners, and thus observed that the LS coherent intertwiners can be interpreted as semiclassical polyhedra. The polyhedral picture can be extended to a whole graph using the twisted-geometry parametrization of the holonomy-flux variables. The knowledge of the classical space behind intertwiners was then used to introduce a new operator, which measures the volume of a quantum polyhedron (section 2.4), and by construction has the correct semiclassical limit. We performed some numerical analysis of its spectrum for the simplest 4-valent case. We discussed its relation to the volume operators commonly used in loop quantum gravity. Finally (section 2.5), we used the four-dimensional version of Minkowski's theorem to make some remarks on Regge calculus on non-simplicial discretizations and its possible relevance to spin foam models on graphs of arbitrary valence.

Our hope is that the notion of a quantum polyhedron can find useful applications in future developments of loop quantum gravity, and that the results in this chapter pose a first stone in that direction.

Chapter 3

Spinfoams: semiclassical behavior

Spinfoams [4, 111] provide a covariant formulation of the dynamics of Loop Quantum Gravity (LQG) [1, 2, 3] (see [12] for an up-to-date status report). The dynamics is described in terms of transition amplitudes between states belonging to the kinematical Hilbert space of LQG. In particular, when the spin-network basis is used, the transition amplitude is a function of spins and intertwiners associated to the links and the nodes of the spin-network graph. In the recent literature [58, 5, 6, 109], spinfoams are generally defined in terms of these variables: a space-time configuration in the spinfoam sum is understood as a 2-complex with faces labeled by $SU(2)$-spins and edges labeled by $SU(2)$-intertwiners.

Different representations of the Hilbert space of LQG can be lifted to the covariant level in spinfoams. In this chapter we consider two representations for spinfoams. The first is a *holonomy representation*. This representation allows to write spinfoams into a form closer to a Feynman path-integral: as an integral over the Ashtekar connection smeared along links that slice faces of the spinfoam 2-complex. The second is the *holomorphic representation*: it is based on the Segal-Bargmann transform for theories of connections introduced by Ashtekar, Lewandowski, Marolf, Mourão and Thiemann [112].

Clearly, spinfoams in different representations have the same physical content. What the new representations provide is new insights and new calculational tools. In particular, the holomorphic representation offers a new way of understanding the semiclassical behavior of spinfoams. The holomorphic representation is associated to coherent spin-network states [85, 113, 114, 115],[94]. These states are peaked on a classical intrinsic *and* extrinsic discrete geometry of space. This fact has a remarkable consequence that we discuss below.

Recently, the large scale asymptotics of the $4d$ spinfoam vertex has been derived [81, 49]. The analysis has been done using the representation in terms of spins and normals introduced by Livine and Speziale [58]. For a geometric set of boundary data, the asymptotics of the Lorentzian vertex features a sum over two classical solutions. This leads to a cosine of Regge action, similarly to what happens in 3d for the Ponzano-Regge model. We argue that the presence of the second undesired classical solution in the semiclassical expansion is an artifact of the representation used: the representation in terms of spins and normals diagonalizes the area operator; as a result, it has a maximal spread on its conjugate momentum and cannot completely identify a point in phase space. On the other hand, the holomorphic representation discussed in this chapter is based on coherent spin-networks. These states are peaked both on the area and on its conjugate variable, an extrinsic angle. This is enough to select one of the two classical solutions in the semiclassical expansion.

This chapter is organized as follows[1]. In section 3.1 we discuss the holonomy representation of spinfoams and its relation with the two representations mostly used in the literature: the 'spin and intertwiner' representation and the 'spin and normals' representation. Then, in section 3.2, we introduce the holomorphic representation as the Segal-Bargmann transform of the holonomy representation. Moreover we discuss the interpretation of the complex variables used in terms of discrete classical geometries. In sections 3.3 and 3.4, we derive the expression of the Euclidean and the Lorentzian spinfoam vertex both in the holonomy and in the holomorphic representation. In section 3.5, we discuss an application of the derived formulae: we show how the peakedness on the extrinsic geometry allows to select a single classical solution in the analysis of the large scale asymptotics of the Lorentzian spinfoam vertex.

3.1 Spin Foams in various representations

In LQG, the Hilbert space associated to an embedded graph Γ is $\mathcal{H}_\Gamma = L^2(SU(2)^L/SU(2)^N)$ where L is the number of links of the graph and N the number of nodes. In the 'holonomy representation', a state is a gauge invariant function of $SU(2)$ group elements h_l ($l = 1,..,L$) that is invariant under $SU(2)$ gauge transformations at nodes,

$$\Psi(h_l) = \Psi(g_{n_l}\, h_l\, g_{n'_l}^{-1}). \tag{3.1}$$

Here n_l and n'_l are respectively the node that is source/target of the link l.

Spinfoams provide the transition amplitude from an 'in' state to an 'out' state: they are maps that correspond to the formal expression

$$W[g^{(3)}_{\text{in}}, g^{(3)}_{\text{out}}] = \int_{g^{(3)}_{\text{in}}}^{g^{(3)}_{\text{out}}} Dg^{(4)}\ \exp iS[g^{(4)}]. \tag{3.2}$$

for the transition amplitude of 3-geometries in terms of a sum over 4-geometries [117, 118]. The formalism admits a generalization to 'boundary amplitudes' [1, 32]. Let $\mathcal{H}_\Gamma$

[1] This chapter is based on work done together with Elena Magliaro and Claudio Perini. The results have been published in [94, 116].

be the Hilbert space associated to a graph on the boundary of a 4-dimensional ball. The boundary amplitude of a state $\Psi \in \mathcal{H}_\Gamma$ is given by

$$\langle W|\Psi\rangle = \int \prod_l dh_l \, W(h_l) \, \Psi(h_l), \tag{3.3}$$

where $W(h_l)$ is the spinfoam model in the holonomy representation. The quantity $W(h_l)$ is *local* in space-time, i.e. it is given by a product of elementary vertex-amplitudes $W_v(h_{vl})$ integrated over bulk variables h_{vl}:

$$W(h_l) = \sum_\sigma \int dh_{vl}^{\text{bulk}} \prod_{v\subset\sigma} W_v(h_{vl}) \prod_{f\subset\sigma} \delta(\prod_{v\in\partial f} h_{vl}). \tag{3.4}$$

Here, the sum is over 2-complexes σ with boundary given by the graph Γ. A "face amplitude" is present: it is given by a delta function of a product of the holonomies h_{vl} bounding a face f of the 2-complex. It is needed in order to guarantee the composition law of the spinfoam amplitude [119]. Notice that we are associating a boundary graph to each vertex of the 2-complex, therefore the holonomies h_{vl} have a vertex label v and a link label l. The construction is the following: we consider a 4-ball that contains a single vertex of the 2-complex σ; the boundary graph associated to the vertex is defined as the intersection of the portion of the 2-complex contained in the 4-ball and the boundary of the 4-ball. In particular, the boundary graph has as many links as faces of the 2-complex intersecting at the vertex. The bulk variables h_{vl}^{bulk} are $SU(2)$ holonomies associated to these links.

As an example, the vertex amplitude of the Ponzano-Regge model for 3d gravity is given by

$$W_v^{PR}(h_l) = \int \prod_{n=1}^{4} dg_n \, \prod_{l=1}^{6} \delta(g_{n_l} \, h_l \, g_{n'_l}^{-1}). \tag{3.5}$$

In the case of the Ponzano-Regge model, the boundary graph is a complete graph with 4 nodes. Similarly, the vertex proposed by Engle-Pereira-Rovelli-Livine and Freidel-Krasnov (EPRL-FK) [5, 6] was originally defined on a complete graph with 5 nodes. More recently, Kaminski-Kisielowski-Lewandowski have proposed a version of the EPRL-FK vertex that provides a generalization to arbitrary boundary graphs [109].

Above we have defined spinfoams directly in the holonomy representation. In the literature, spinfoam vertices are generally presented using a different representation: the 'spin and intertwiner' representation, $W_v(j_l, i_n)$. This representation is related to the holonomy representation by the Peter-Weyl transform (see table 3.1). This is the representation associated to an orthonormal basis of the boundary Hilbert space $\mathcal{H}_\Gamma$. Let $\Psi_{j_l,i_n}(h_l)$ be a spin-network state,

$$\Psi_{j_l,i_n}(h_l) = \Big(\bigotimes_n i_n\Big) \cdot \Big(\bigotimes_l D^{(j_l)}(h_l)\Big). \tag{3.6}$$

Here $D^{(j)}$ are $SU(2)$ representation matrices and i_n intertwining tensors. The spinfoam vertex in the 'spin and intertwiner' representation is given by the amplitude of an element of the spin-network basis

$$W_v(j_l, i_n) = \langle W_v | \Psi_{j_l, i_n} \rangle. \tag{3.7}$$

For instance, in this representation, the Ponzano-Regge vertex is simply given by a Racah $6j$-symbol [47],

$$W_v^{PR}(j_l) = \{6j\}. \tag{3.8}$$

In the definition and in the analysis of the asymptotics of the new spinfoam vertices, a third representation has turned out to be useful [120, 48, 81, 49, 121]. It is a representation in terms of a spin and two unit-normals per link of the graph. This representation is associated to spin-networks with nodes labeled by Livine-Speziale coherent intertwiners [58, 59]. A coherent intertwiner in $\mathrm{Inv}(\otimes_{e=1}^{E} H^{(j_e)})$ is labeled by E unit-vectors $\vec{n}_e$ satisfying the closure condition $\sum_e j_e \vec{n}_e = 0$. They are defined in terms of Bloch $SU(2)$-coherent states[2] $|j_e, \vec{n}_e\rangle$ and are given by the following formula

$$\Phi(\vec{n}_e) = \int_{SU(2)} dg \, \bigotimes_{e=1}^{E} D^{(j_e)}(g) |j_e, \vec{n}_e\rangle. \tag{3.9}$$

A spin-network state with coherent intertwiners at nodes is given by

$$\Psi_{j_l, \vec{n}_l, \vec{n}'_l}(h_l) = \Big(\bigotimes_n \Phi_n(\vec{n}_l) \Big) \cdot \Big(\bigotimes_l D^{(j_l)}(h_l) \Big). \tag{3.10}$$

These states form an overcomplete basis of the Hilbert space $\mathcal{H}_\Gamma$ with the measure on normals derived in [59].

A spinfoam vertex can be written in the 'spin and normals' representation,

$$W_v(j_l, \vec{n}_l, \vec{n}'_l) = \langle W_v | \Psi_{j_l, \vec{n}_l, \vec{n}'_l} \rangle. \tag{3.11}$$

The reason why this representation is so useful in the semiclassical analysis of the vertex is that the normals $\vec{n}$ are classical variables, as opposed to the intertwiners in (3.7) that are quantum numbers. This is in fact the original motivation of [58] for introducing coherent intertwiners. On the other hand, the spins j_l are still quantum numbers. In the following we introduce a new representation where the classical counterparts of the spins and of their conjugate momenta appear.

[2]Let $R_{\vec{n}}$ be the matrix that rotates the vector $\vec{e}_3 = (0,0,1)$ into the unit-vector $\vec{n}$, leaving the vector $\vec{e}_3 \times \vec{n}$ invariant; we call $h_{\vec{n}}$ the associated $SU(2)$ element, $h_{\vec{n}} = D^{(1/2)}(R_{\vec{n}})$. A Bloch coherent state in direction $\vec{n}$ is obtained rotating the maximum-eigenvalue eigenstate of the spin in the direction $\vec{e}_3$ to the direction $\vec{n}$, i.e. $|j, \vec{n}\rangle = D^{(j)}(h_{\vec{n}})|j, +j\rangle$. These are the states used in the description of the magnetic moment of a nucleus in an external magnetic field [122].

$$\begin{tikzcd} W(h_l) \arrow[r, "SB"] \arrow[d, "PW"'] & W(H_l) \arrow[d, dotted] \\ W(j_l, i_n) \arrow[r, "LS"] & W(j_l, \vec{n}_l, \vec{n}'_l) \end{tikzcd}$$

Table 3.1: The various representations of spinfoams are related by transforms as shown in the diagram. The Peter-Weyl transform (PW) sends the holonomy representation $W(h_l)$ in the 'spin and intertwiner' representation $W(j_l, i_n)$. The 'spin and normals' representation $W(j_l, \vec{n}_l, \vec{n}'_l)$ is obtained from the 'spin and intertwiner' representation via the Livine-Speziale transform (LS). The topic of this chapter is the holomorphic representation $W(H_l)$. It is obtained from the holonomy representation via the Segal-Bargmann transform (SB). The expression for the 4d vertex amplitudes in the holomorphic representation is eq. (3.29) for the Euclidean case, and eq. (3.40) for the Lorentzian case. In the semiclassical analysis of spinfoams, there is an interesting interplay of the holomorphic and the 'spin and normals' representations. This is discussed in section 3.5.

3.2 The holomorphic representation

In this section we introduce a new representation of spinfoams, a representation based on *coherent spin-networks* [94],[85, 113, 114, 115]. Coherent spin-network states provide an overcomplete basis of the boundary Hilbert space $\mathcal{H}_\Gamma$. They are labeled by an element H_l of $SL(2,\mathbb{C})$ per link of the graph and are defined by

$$\Psi_{H_l}(h_l) = \int \prod_n dg_n \, \prod_l K_{t_l}(g_{n_l}\, h_l\, g^{-1}_{n'_l}\, H_l^{-1}). \tag{3.12}$$

Here, t_l are positive real numbers and K_t is the analytic continuation to $SL(2,\mathbb{C})$ of the heat-kernel on $SU(2)$,

$$K_t(h) = \sum_j (2j+1) e^{-j(j+1)\frac{t}{2}} \, \mathrm{Tr}\, D^{(j)}(h). \tag{3.13}$$

As shown in [112], coherent spin-networks provide a Segal-Bargmann transform for Loop Quantum Gravity. Given a state $\Psi_f(h_l)$, its scalar product with a coherent spin-network $\Psi_{H_l}(h_l)$ defines a function $\Phi_f(H_l)$ that is holomorphic in H_l,

$$\Phi_f(H_l) = \langle \Psi_f | \Psi_{H_l} \rangle = \int \prod_l dh_l \, \overline{\Psi_f(h_l)} \, \Psi_{H_l}(h_l), \tag{3.14}$$

and belongs to the Hilbert space

$$\mathcal{H}L^2(SL(2,\mathbb{C})^L, d\nu_t(H)^L) \tag{3.15}$$

of holomorphic functions normalizable with respect to a measure $d\nu_t(H)^L$ (see [112] and the appendix of [94] for details). This result is based on the seminal work of Hall [123]. Moreover the $SL(2,\mathbb{C})$ labels H_l provide a parametrization of the phase space of the theory as captured by a graph. The peakedness properties of these states and their geometrical interpretation in terms of classical holonomies and fluxes is well-studied within Loop Quantum Gravity [85, 113, 114, 115]. However their use in spinfoams has remained largely unexplored until recently [94]. In the following we show how coherent spin-networks and the associated holomorphic representation can be fruitfully used in the spinfoam setting.

A spinfoam vertex can be expressed in the holomorphic representation using formula (3.3),

$$W_v(H_l) = \langle W_v | \Psi_{H_l} \rangle. \tag{3.16}$$

As an example, the Ponzano-Regge vertex amplitude (3.5) in the holomorphic representation is given by the following formula:

$$W_v^{PR}(H_l) = \int \prod_n dg_n \, \prod_l K_{t_l}(\,(g_{n_l}\, H_l\, g^{-1}_{n'_l})^{-1}). \tag{3.17}$$

The advantage of using the holomorphic representation is that the $SL(2,\mathbb{C})$ labels admit a clear interpretation in terms of classical discrete geometries. Here we discuss two equivalent descriptions of the discrete geometry associated to the $SL(2,\mathbb{C})$ variables: the first (a) is the one proper of canonical LQG and is due to Sahlmann-Thiemann-Winkler [85, 113, 114], the second (b) is the one mostly used in the covariant spinfoam setting, it is in terms of Freidel-Speziale variables for twisted geometries [50] and has been introduced by the authors in [94].

(a) Let Σ be the boundary 3-manifold and choose a classical configuration of the Ashtekar connection A and its conjugate momentum, the electric field E. Moreover, let Δ_Σ be a cellular decomposition of Σ and Γ a graph dual to this decomposition. The flux of the electric field through a face f_l of Δ_Σ determines a $su(2)$ algebra element $E_l = \int_{f_l} E$. The holonomy of the connection along a link l of the graph Γ determines a $SU(2)$ group element $h_l = P \exp \int_l A$. The set of couples (h_l, E_l), one per link of the graph, determines a point in a truncation of the phase space of General Relativity as captured by the graph Γ. The couple (h_l, E_l) can be written as an element of the complexification of $SU(2)$ using the polar decomposition of $SL(2,\mathbb{C})$:

$$H_l = \; h_l \; \exp(\frac{E_l}{8\pi G\hbar\gamma} t_l). \tag{3.18}$$

Coherent spin-networks with labels as in (3.18) are peaked on the classical configuration (h_l, E_l).

(b) Let Δ_Σ be a cellular decomposition of the boundary 3-manifold Σ (the cells of the decomposition can be simplicial or even polyhedral). Equip separately each cell with a Euclidean 3-geometry. As a result, the shape of each cell is fixed and the area and the normals to its faces can be computed. Now we consider two cells that share a face, and require that the area of the face is the same when seen from either of the two cells. Therefore, for each face f_l of Δ_Σ, we have as variables its area $\mathscr{A}_l$ and two normals $\vec{n}_l$ and $\vec{n}'_l$. In general the geometry these data determine is twisted in the sense of [50]. A special case is the one where shared faces have congruent shapes. In this case, a piecewise-flat geometry is obtained. In the case of a simplicial decomposition, this is a Regge geometry[3] [127].

Besides areas and 3-normals, there is another quantity of interest. Let us consider two cells sharing a face f_l and think them as embedded in 4-dimensional Minkowski space. We call N_l^I and $N_l'^I$ the 4-normals to the two cells. Their scalar product determines an angle Θ_l with the meaning of extrinsic curvature, $\cosh\Theta_l = -\eta_{IJ} N_l^I N_l'^J$, where η_{IJ} is the Minkowski metric. We call ξ_l the extrinsic angle times the Immirzi parameter γ,

$$\xi_l = \gamma \Theta_l. \tag{3.19}$$

Summarizing, for each link of the graph Γ dual to Δ_Σ, we have the following set of variables:

- an area $a_l = \frac{\mathscr{A}_l}{8\pi G\hbar\gamma}$,
- an *extrinsic* angle ξ_l,
- two unit-normals $\vec{n}_l$ and $\vec{n}'_l$.

Out of these variables we can build a $SL(2,\mathbb{C})$ element H_l given by the following expression

$$H_l = h_{\vec{n}_l}\, e^{-iz_l \frac{\sigma_3}{2}}\, h^{-1}_{-\vec{n}'_l}, \tag{3.20}$$

where the complex number z_l is given in terms of ξ_l and a_l by

$$z_l = \xi_l + i a_l t_l, \tag{3.21}$$

and $h_{\vec{n}}$ is the $SU(2)$ element associated to a vector $\vec{n}$ as explained in the footnote[2]. The reason for this parametrization is that coherent spin-networks (3.12) with $SL(2,\mathbb{C})$ labels specified as in (3.20), for large area a_l reduce to superpositions over spins of Livine-Speziale spin-networks (3.10) [94]. Moreover, the superposition over spins is a Gaussian centered in $j_l \approx a_l$ times a phase term $\exp(-i\xi_l j_l)$. This is the superposition originally proposed by Rovelli in the analysis of the graviton propagator [128]. The interpretation

[3] On the encoding of simplicial geometry in a lattice gauge theory formulation of quantum gravity, see [124, 125, 93]. For a discussion of the matching of lengths in LQG see sec.5 of [92]. For a non-commutative flux representation of LQG and its simplicial interpretation see [126].

of the $SL(2,\mathbb{C})$ labels in terms of twisted geometries will be important in section 3.5 where we discuss the semiclassical behavior of spinfoams.

The relation between the description in terms of fluxes and holonomies (a) and the description in terms of areas, angles and normals (b) can be easily derived. Writing (3.20) as

$$H_l = \big(h_{\vec{n}_l}\, e^{-i\gamma\Theta_l \frac{\sigma_3}{2}}\, h^{-1}_{-\vec{n}'_l}\big)\ \exp\big(i\frac{\mathscr{A}_l}{8\pi G\hbar\gamma}\vec{n}'_l\cdot\frac{i\vec{\sigma}}{2}\,t_l\big);, \tag{3.22}$$

we recognize the variables used in (3.18),

$$h_l = P\exp\int_l A = h_{\vec{n}_l}\, e^{-i\gamma\Theta_l\frac{\sigma_3}{2}}\, h^{-1}_{-\vec{n}'_l}, \tag{3.23}$$

$$E_l = \int_{f_l} E = \mathscr{A}_l\, \vec{n}'_l\cdot\frac{i\vec{\sigma}}{2}. \tag{3.24}$$

3.3 4d Euclidean vertex amplitude in the holomorphic representation

The 4d spinfoam vertex amplitude [5, 6] is generally defined in terms of its components on a spin-network basis. In the Euclidean case, for Immirzi parameter $0<\gamma<1$, it is given by

$$W_v(j_l,i_n) = \sum_{i_n^+,i_n^-}\{15J\}(j_l^+,i_n^+;j_l^-,i_n^-)\ \prod_n f^{i_n}_{i_n^+,i_n^-} \tag{3.25}$$

with $j_l^\pm = \frac{1\pm\gamma}{2}j_l$, $\{15J\}$ the $15j$-symbol for $SU(2)\times SU(2)$ and the fusion coefficients $f^{i_n}_{i_n^+,i_n^-}$ defined in [5] (see also [129]). This representation has been used in numerical investigations [130]. Contracting it with the spin-network basis (3.6) leads to a rather simple integral formula for the vertex in the holonomy representation.

Let Y be a map from the representation $H^{(j)}$ of $SU(2)$ to the representation $H^{(j^+,j^-)}$ of the Euclidean group $Spin(4)\simeq SU(2)\times SU(2)$. The map Y is such that it commutes with the diagonal action of $SU(2)$ on $SU(2)\times SU(2)$. In the canonical basis, the map Y is given by Clebsh-Gordan coefficients

$$Y_m^{m^+,m^-} = \langle j^+,m^+;j^-,m^-|j,m\rangle. \tag{3.26}$$

Notice that $j^+ + j^- = j$, therefore the map Y corresponds to a projection to the highest weight representation in the tensor product $H^{(j^+)}\otimes H^{(j^-)}$. Using this map, the vertex amplitude in the holonomy representation can be written as

$$W_v(h_l) = \int_{Spin(4)^5}\prod_n dG_n\ \prod_l P(h_l, G_{n_l}G^{-1}_{n'_l}). \tag{3.27}$$

The integrals on $Spin(4)$ impose the Euclidean invariance of the vertex, and the integrand is given by a product of 'face' terms P given by

$$P(h,G) = \sum_j (2j+1)\mathrm{Tr}\Big(D^{(j)}(h)\, Y^\dagger D^{(j^+,j^-)}(G^{-1})Y\Big). \tag{3.28}$$

Expression (3.27) can be easily put in the holomorphic representation using the Segal-Bargamann transform [112]:

$$W(H_l) = \int_{Spin(4)^5} \prod_n dG_n \, \prod_l P_{t_l}(H_l, G_{n_l} G_{n'_l}^{-1}) \tag{3.29}$$

where

$$\begin{aligned} P_t(H,G) = &\sum_j (2j+1)\, e^{-j(j+1)\frac{t}{2}} \, \times \\ &\times\ \mathrm{Tr}\Big(D^{(j)}(H)\, Y^\dagger D^{(j^+,j^-)}(G^{-1})Y\Big). \end{aligned} \tag{3.30}$$

3.4 4d Lorentzian vertex amplitude in the holomorphic representation

In this section we discuss the definition of the 4d Lorentzian vertex [131, 5] and derive its holonomy and its holomorphic representation.

Let $\Psi(h_l)$ be a gauge invariant state on a graph bounding the spinfoam vertex

$$\Psi(h_l) = \sum_{j_l} \Psi^{(j_l)} \cdot \big(\bigotimes_l D^{(j_l)}(h_l)\big). \tag{3.31}$$

The 4d Lorentzian vertex amplitude for this state is obtained in two steps:

(i) we map the $SU(2)$-boundary state $\Psi(h_l)$ into a $SL(2,\mathbb{C})$-boundary state $(f \circ \Psi)(G_l)$ using a (γ dependent) map f defined below;

(ii) we impose Lorentz invariance at nodes.

This provides a compact definition of the vertex amplitude as[4]

$$\langle W_v|\Psi\rangle = \int_{SL(2,\mathbb{C})^N} \prod_n dG_n \ (f\circ\Psi)(G_{n_l} G_{n'_l}^{-1}). \tag{3.32}$$

[4]Notice that one of the integrals over $SL(2,\mathbb{C})$ has to be gauge-fixed in order to avoid having a divergent expression [132].

The EPRL-FK vertex corresponds to a specific choice of f defined as follows. Let us consider the unitary irreducible representation $(\rho = \gamma 2j, n = 2j)$ of $SL(2,\mathbb{C})$ [46]. It decomposes into irreducible representations of a subgroup $SU(2)$ as

$$H^{(\rho=\gamma 2j,n=2j)}_{SL(2,\mathbb{C})} = H^{(j)}_{SU(2)} \oplus H^{(j+1)}_{SU(2)} \oplus \cdots \tag{3.33}$$

Let Y be the embedding of $H^{(j)}_{SU(2)}$ into the lowest weight representation of $H^{(\gamma 2j,2j)}_{SL(2,\mathbb{C})}$. Calling $|(\gamma 2j, 2j); j', m'\rangle$ its canonical basis, the map Y is given by

$$Y = \sum_{m=-j}^{+j} |(\gamma 2j, 2j); j, m\rangle\langle j, m|. \tag{3.34}$$

Now we define the map

$$f : L^2(SU(2)^L/SU(2)^N) \to L^2(SL(2,\mathbb{C})) \tag{3.35}$$

in terms of Y as follows. Given the state (3.31), we have

$$(f \circ \Psi)(G_l) = \sum_{j_l} \Psi^{(j_l)} \cdot \big(\bigotimes_l Y^\dagger D^{(\gamma 2j_l,2j_l)}(G_l)Y\big). \tag{3.36}$$

Using the definition (3.32),(3.36) of the Lorentzian vertex, it is easy to derive its holonomy representation. Let $\Psi_{h'_l}(h_l)$ be the $SU(2)$ gauge invariant delta function on the boundary graph

$$\Psi_{h'_l}(h_l) = \int_{SU(2)^N} \prod_n dg_n \prod_l \delta(g_{n_l}\, h_l g^{-1}_{n'_l}\, h'^{-1}_l). \tag{3.37}$$

Its vertex amplitude provides the holonomy representation of the Lorentzian vertex. It is given by the following integral expression

$$W_v(h_l) = \langle W_v|\Psi_{h_l}\rangle = \int \prod_n dG_n\ \prod_l P(h_l, G_{n_l}G^{-1}_{n'_l}), \tag{3.38}$$

where the integral is over $SL(2,\mathbb{C})^N$ and the 'face' term is

$$P(h, G) = \sum_j (2j+1)\mathrm{Tr}\Big(D^{(j)}(h)\ Y^\dagger D^{(\gamma 2j,2j)}(G^{-1})Y\Big) \tag{3.39}$$

similarly to what happens in the Euclidean case. Its Segal-Bargmann transform corresponds to the vertex amplitude of a coherent spin-network. It is given by

$$W_v(H_l) = \langle W_v|\Psi_{H_l}\rangle = \int \prod_n dG_n\ \prod_l P_{t_l}(H_l, G_{n_l}G^{-1}_{n'_l}), \tag{3.40}$$

where the 'face' term now is

$$P_t(h,G) = \sum_j (2j+1) e^{-j(j+1)\frac{t}{2}} \times \\ \times \operatorname{Tr}\Big(D^{(j)}(H)\, Y^\dagger D^{(\gamma 2j,2j)}(G^{-1}) Y\Big). \tag{3.41}$$

We report also the 'spin and normals' representation of the Lorentzian vertex

$$W_v(j_l,\vec{n}_l,\vec{n}'_l) \equiv \langle W_v|\Psi_{j_l,\vec{n}_l,\vec{n}'_l}\rangle = \\ = \int \prod_n dG_n \prod_l \langle j_l, -\vec{n}_l|Y^\dagger D^{(\gamma 2j,2j)}(G_{n_l}G^{-1}_{n'_l})Y|j_l,\vec{n}'_l\rangle. \tag{3.42}$$

This expression is the one used in the analysis of the asymptotics of the vertex [49]. In next section we uncover an interesting interplay of the representations (3.40) and (3.42) of the spinfoam vertex in the analysis of its semiclassical behavior.

3.5 Semiclassical analysis: role of the extrinsic curvature

The holomorphic representation is associated to a set of states that have semiclassical properties. This fact makes the holomorphic representation the appropriate tool for studying the semiclassical behavior of spinfoams. We illustrate this point using a simple quantum mechanical system, and then discuss it in the case of the 4d Lorentzian vertex amplitude.

Let us consider a particle on a line. The evolution operator in the position representation is given by

$$W(x_1,x_2) = \langle x_2|e^{-\frac{i}{\hbar}HT}|x_1\rangle = \int_{x_1}^{x_2} D[x(t)]\; e^{\frac{i}{\hbar}S[x(t)]}, \tag{3.43}$$

where H is the Hamiltonian operator for the particle, T the evolution time, and $S[x(t)]$ the classical action. In the formal semiclassical limit $\hbar \to 0$, the path integral in (3.43) is dominated by classical solutions $x_{(k)}(t)$ starting at x_1 and ending at x_2. There can be more than a single classical solution and the stationary phase approximation of the path integral is given by a sum over all classical contributions [133]

$$W(x_1,x_2) \overset{\hbar\to 0}{\approx} \sum_k A_{(k)}(x_1,x_2)\; e^{\frac{i}{\hbar}S_{(k)}(x_1,x_2)}. \tag{3.44}$$

Here $S_{(k)}(x_1,x_2) = S[x_{(k)}(t)]$ is the Hamilton function, that is the action evaluated on one of the classical solutions. $A_{(k)}(x_1,x_2)$ is a slowly varying function of x_1 and x_2.

Notice that, if we expand the Hamilton function around the points $x_1 = q_1$ and $x_2 = q_2$, the linear terms in the expansion are proportional to the initial and final momenta. In fact the derivatives of the Hamilton function are

$$\begin{aligned} p_2^{(k)}(x_1,x_2) &= \frac{\partial}{\partial x_2} S_{(k)}(x_1,x_2), \\ p_1^{(k)}(x_1,x_2) &= -\frac{\partial}{\partial x_1} S_{(k)}(x_1,x_2) \end{aligned} \tag{3.45}$$

where $p_1^{(k)}(x_1,x_2)$ and $p_2^{(k)}(x_1,x_2)$ are the initial and final momenta of the classical solution $x_{(k)}(t)$. This fact has two important consequences:

(i) Let us consider a Gaussian wave packet peaked at the initial position q_1 and initial momentum p_1, and study its evolution with the dynamics (3.43). In the $\hbar \to 0$ limit, only one of the terms in the sum over classical solutions in (3.44) contributes to its evolution. Specifically, the term that contributes is the exponential of the Hamilton function for the classical solution $x_{(0)}(t)$ that has q_1, p_1 as initial conditions.

(ii) The transition amplitude to a Gaussian wave packet that is peaked at a final position q_2 and final momentum p_2 is suppressed unless these are the final position and momentum of the classical solution $x_{(0)}(t)$ that has q_1, p_1 as initial conditions.

These two facts make the holomorphic representation especially well-suited for the analysis of the semiclassical behavior of the dynamics.

The holomorphic representation for a particle on a line is associated with coherent states given by the analytic continuation in x_0 of the heat-kernel on a line

$$K_t(x,x_0) = \frac{1}{\sqrt{2\pi t}} e^{-\frac{(x-x_0)^2}{2t}}. \tag{3.46}$$

When x_0 is continued to the complex number $z_0 = q_0 + \frac{i}{\hbar} p_0 t$, the state $K_t(x,z)$ is peaked both on the position q_0 of the particle *and* on its momentum p_0. In fact the state has a phase term $\exp \frac{i}{\hbar} x p_0$ coding the peakedness on the momentum,

$$K_t(x,z_0) = \frac{1}{\sqrt{2\pi t}} e^{-\frac{(x-q_0)^2}{2t}}\; e^{+\frac{i}{\hbar}(x-q_0)p_0}\; e^{+\frac{t}{2\hbar^2}p_0^2}. \tag{3.47}$$

The holomorphic representation of the evolution operator is

$$W(z_1,z_2) = \int dx_1 \int dx_2\, \overline{K_t(x_2,z_2)}\, W(x_1,x_2)\, K_t(x_1,z_1). \tag{3.48}$$

We call the couple $(z_1,z_2) = (q_1,p_1;q_2,p_2)$ *classical* if it corresponds to the boundary conditions of a classical solution $x_{(0)}(t)$ of the dynamics. In the $\hbar \to 0$ limit, the transition amplitude $W(z_1, z_2)$ is maximized when the couple (z_1, z_2) corresponds to a classical solution. Otherwise, if (z_1, z_2) is not classical, a rapidly oscillating term $\exp \frac{i}{\hbar}(p_{(k)} - p_1)x_1$ appears in the integral (3.48) with the effect that the transition amplitude $W(z_1, z_2)$ is suppressed.

To summarize: the feature of the holomorphic representation is that at most one classical trajectory contributes to the semiclassical expansion of the transition amplitude. A similar phenomenon happens in spinfoams.

Let us consider the Lorentzian spinfoam vertex (3.40) and focus on the case of a graph Γ dual to the boundary of a 4-simplex as originally done in [131, 5]. The amplitude $W_v(H_l)$ depends on ten elements of $SL(2,\mathbb{C})$, one per link of the graph. We can parametrize them in terms of twisted geometries using the variables $(a_l, \xi_l, \vec{n}_l, \vec{n}'_l)$, as explained in section 3.2. The semiclassical limit $\hbar \to 0$ corresponds to the large area asymptotics, $a_l \gg 1$. In the following, we discuss the large area asymptotics of $W_v(H_l)$.

Notice that the large a_l asymptotics of $D^{(j)}(e^{a_l \frac{\sigma_3}{2}})$ is proportional to the projector to the highest magnetic number $|j, +j\rangle\langle j, +j|$. As shown in [94], a consequence of this fact is that the large area asymptotics of H_l in the definition of coherent spin-networks reproduces a Gaussian with a phase on spins, times Bloch coherent states:

$$\begin{aligned} e^{-j_l(j_l+1)\frac{t}{2}} D^{(j_l)}(H_l) \overset{a_l \gg 1}{\approx} & \exp(-i\xi_l j_l) \times \\ & \times \exp\big(-(j_l - a_l)^2 \frac{t}{2} + a_l^2 \frac{t}{2}\big)\ |j_l, \vec{n}_l\rangle\langle j_l, -\vec{n}'_l|. \end{aligned} \tag{3.49}$$

When gauge invariance at nodes is imposed, Bloch coherent states intertwine and reproduce Livine-Speziale states. As a result, the large area asymptotics of the spinfoam vertex in the holomorphic representation is given by the vertex in the 'spin and normals' representation (3.42), summed over spins with a Gaussian weight times a phase in spins:

$$\begin{aligned} W(H_l) \overset{a_l \gg 1}{\approx} \sum_{j_l} W(j_l, \vec{n}_l, \vec{n}'_l)\ & \exp(-i \sum_l \xi_l j_l) \times \\ & \times \exp(-\sum_l (j_l - a_l)^2 \frac{t_l}{2} + \sum_l a_l^2 \frac{t}{2}). \end{aligned} \tag{3.50}$$

Now we consider the sum over spins. The Gaussian in the second line of (3.50) is peaked on a large value of the spins, $j_l \approx a_l \gg 1$. As a result, if we want to estimate the sum over spins, it is enough to know the large spin behavior of the quantity $W(j_l, \vec{n}_l, \vec{n}'_l)$. This quantity has been studied in detail by Barrett-Dowdall-Fairbairn-Hellmann-Pereira [49]. We briefly recall their results. They compute the large spin asyptotics of the 4d Lorentzian vertex in the spins-normals representation (3.42). The result found is the following:

(i) when the spins and the normals identify the geometry of the boundary of a 4-simplex in 4d Minkowski space, the asymptotics gets two contributions:

$$W(j_l,\vec{n}_l,\vec{n}'_l) \overset{j_l\gg 1}{\approx} \sum_{p=\pm 1} A_{(p)}\ \exp(p\, i \sum_l \gamma j_l\ \Theta_l). \tag{3.51}$$

Each contribution features a rapidly oscillating phase term given by the Regge action for discrete gravity [127],

$$S_{\rm R}(j_l,\vec{n}_l,\vec{n}'_l) = \sum_l \gamma j_l\ \Theta_l(j_l,\vec{n}_l,\vec{n}'_l). \tag{3.52}$$

This is the action for a single 4-simplex with faces of area $A_l = 8\pi G\hbar\,\gamma j_l$, extrinsic angle Θ_l, and a given choice of parity.

(ii) On the other hand, if the boundary data $(j_l,\vec{n}_l,\vec{n}'_l)$ do not identify the edge lengths of a 4-simplex but give only a twisted geometry, then the vertex amplitude is exponentially suppressed.

The two semiclassical contributions $p=\pm 1$ in (3.51) correspond to parity-reversed classical solutions. We argue here that the appearence of a sum over classical solutions in the asymptotics of $W(j_l,\vec{n}_l,\vec{n}'_l)$ is exactly analogous to what happens in the simpler case discussed at the beginning of this section (3.44): it is due to the fact that the 'spin and normals' representation does not identify a point in phase space. Let us see now what happens in the holomorphic representation (3.50) when we use the result (3.51).

Our boundary data now are not just areas and normals $(a_l,\vec{n}_l,\vec{n}'_l)$, there are also the angles ξ_l that are conjugate to the areas. Let us assume that the areas and the normals are compatible with the edge-lengths of a 4-simplex[5]. Plugging (3.51) into (3.50) we have

$$\begin{aligned} W(H_l) \overset{a_l\gg 1}{\approx} \sum_{p=\pm 1}\sum_{j_l} A_{(p)}\ \exp\big(p\, i S_R(j_l) - i\sum_l \xi_l j_l\big)\times \\ \times \exp(-\sum_l (j_l-a_l)^2\frac{t_l}{2} + \sum_l a_l^2\frac{t}{2}). \end{aligned} \tag{3.53}$$

In the sum over spins there is now a rapidly oscillating phase term

$$\exp i(p\,\gamma\Theta_l^{(0)} - \xi_l) j_l. \tag{3.54}$$

Analogously to expression (3.45), the quantity $\Theta_l^{(0)}$ is the momentum computed out of Regge action for given boundary data:

$$\Theta_l^{(0)} = \frac{\partial S_R}{\partial(\gamma j_l)}(a_l) = \Theta_l(a_l). \tag{3.55}$$

[5]If it is not the case the amplitude is suppressed because $W(j_l,\vec{n}_l,\vec{n}'_l)$ is.

Therefore the sum over spins is suppressed unless the variable ξ_l in the boundary data is chosen to coincide with $+\gamma\Theta_l^{(0)}$ or $-\gamma\Theta_l^{(0)}$. In either case, only one of the two classical solutions contributes to the semiclassical behavior of the vertex.

3.6 Summary and perspectives

In this chapter we have introduced a holomorphic representation for spinfoams. The 4d spinfoam vertex for gravity has a rather elegant expression in this representation: it is given by formula (3.29,3.30) in the Euclidean case and by (3.40,3.41) in the Lorentzian case. This new representation is obtained introducing first a holonomy representation and then computing its Segal-Bargmann transform. A spinfoam amplitude in the holomorphic representation is a function $W(H_l)$ of $SL(2,\mathbb{C})$ elements H_l, one per link of the boundary graph Γ. The set of variables H_l describe a truncation of the phase space of General Relativity as captured by the graph Γ. They admit a parametrization in terms of the variables generally used for describing the classical boundary geometry of a spinfoam configuration: (i) 3-normals to faces of a cellular decomposition of space, (ii) the area of faces, (iii) an angle associated to faces that measures the extrinsic curvature at the interface of two cells. These data describe the intrinsic and extrinsic geometry of the boundary and can be coded into $SL(2,\mathbb{C})$ elements H_l via equation (3.20). Therefore, we have a description of spinfoams in terms of variables with a clear geometrical meaning.

The holomorphic representation of spinfoams can be fruitfully used for analyzing their semiclassical behavior. In section 3.5, we focused on a spinfoam vertex in the holomorphic representation and showed that a single exponential of the Regge action contributes to the large scale asymptotics. What selects one of the two exponentials appearing in the "spin and normals" representation is the peakedness of the boundary state on a prescribed extrinsic curvature. It is important to understand if this feature extends beyond the single vertex level. A way to attack the problem is to derive an action in holomorphic variables following the method introduced in [48] and then checking if a mechanism of cancellation of phases as proposed in [134] is at work.

Finally, we suggest a way to use the holomorphic representation to make a bridge with the Hamiltonian framework. Roughly, let us consider a holomorphic transition amplitude (propagation kernel) $W(H_i, H_f)$ between an initial state labeled by complex variables H_i and a final state labeled by H_f. Suppose there is a differential operator $\hat{C}$ acting on either the initial or the final variables which annihilates the amplitude:

$$\hat{C}\, W(H_i, H_f) = 0. \tag{3.56}$$

The previous equation can then be interpreted as the Wheeler-DeWitt equation for pure gravity satisfied by the propagation kernel in the holomorphic representation. A recent result [91] in the context of spinfoam cosmology shows that the holomorphic amplitude for a transition between two homogeneous metrics is, in a suitable approximation, in the kernel of a differential operator which is (the quantization of) the Friedmann-Robertson-Walker Hamiltonian in the absence of matter. We find this result encouraging and it urges us to further explore this line of research.

Chapter 4

Gravitons from LQG

In this chapter[1] we compute metric correlations in Loop Quantum Gravity (LQG) [1, 3, 2] and we compare them with the scaling and the tensorial structure of the graviton propagator in perturbative Quantum Gravity [136, 137, 28]. The strategy is the one introduced in [128] and developed in [138, 139, 140, 141, 142, 143, 135, 144]. In particular, we use the boundary amplitude formalism [1, 32, 145, 146]. The dynamics is implemented in terms of (the group field theory expansion of) the new spin foam models introduced by Engle, Pereira, Rovelli and Livine (EPRL_γ model) [5] and by Freidel and Krasnov (FK_γ model) [6]. We restrict attention to Euclidean signature and Immirzi parameter smaller than one: $0 < \gamma < 1$. In this case the two models coincide.

Previous attempts to derive the graviton propagator from LQG adopted the Barrett-Crane spin foam vertex [147] as model for the dynamics [128, 138, 139, 140, 141, 142, 143, 135, 144] (see also [148, 149, 150] for investigations in the three-dimensional case). The analysis of [142, 143] shows that the Barrett-Crane model fails to give the correct scaling behavior for off-diagonal components of the graviton propagator. The problem can be traced back to a missing coherent cancellation of phases between the intertwiner wave function of the semiclassical boundary state and the intertwiner dependence of the model. The attempt to correct this problem was part of the motivation for the lively search of *new* spin foam models with non-trivial intertwiner dependence [110, 151, 5, 6, 58]. The intertwiner dynamics of the new models was investigated numerically in [130, 152, 153, 154]. The analysis of the large spin asymptotics of the vertex amplitude of the new models was performed in [120, 48, 59] and in [81]. In [135], the obstacle that prevented the Barrett-Crane model from yielding the correct behaviour of the propagator was shown to be absent for the new models: the new spin foams feature the correct dependence on intertwiners to allow a coherent cancellation of phases with the boundary semiclassical state. In this chapter we restart from scratch the calculation and derive

[1] This chapter is based on work done together with Elena Magliaro, Claudio Perini, Emanuele Alesci e Carlo Rovelli. The results of this work have been published in [90, 135]

the graviton propagator from the new spin foam models.

In this introduction we briefly describe the quantity we want to compute. We consider a manifold $\mathcal{R}$ with the topology of a 4-ball. Its boundary is a 3-manifold Σ with the topology of a 3-sphere S^3. We associate to Σ a boundary Hilbert space of states: the LQG Hilbert space $\mathcal{H}_\Sigma$ spanned by (abstract) spin networks. We call $|\Psi\rangle$ a generic state in $\mathcal{H}_\Sigma$. A spin foam model for the region $\mathcal{R}$ provides a map from the boundary Hilbert space to $\mathbb{C}$. We call this map $\langle W|$. It provides a sum over the bulk geometries with a weight that defines our model for quantum gravity. The dynamical expectation value of an operator $\mathcal{O}$ on the state $|\Psi\rangle$ is defined via the following expression[2]

$$\langle \mathcal{O} \rangle = \frac{\langle W|\mathcal{O}|\Psi\rangle}{\langle W|\Psi\rangle} \,. \tag{4.2}$$

The operator $\mathcal{O}$ can be a geometric operator as the area, the volume or the length [31, 155, 102, 156, 77, 157, 92]. The geometric operator we are interested in here is the (density-two inverse-) metric operator $q^{ab}(x) = \delta^{ij} E^a_i(x) E^b_j(x)$. We focus on the *connected* two-point correlation function $G^{abcd}(x,y)$ on a semiclassical boundary state $|\Psi_0\rangle$. It is defined as

$$G^{abcd}(x,y) = \langle q^{ab}(x)\, q^{cd}(y)\rangle - \langle q^{ab}(x)\rangle \, \langle q^{cd}(y)\rangle \,. \tag{4.3}$$

The boundary state $|\Psi_0\rangle$ is semiclassical in the following sense: it is peaked on a given configuration of the intrinsic and the extrinsic geometry of the boundary manifold Σ. In terms of Ashtekar-Barbero variables these boundary data correspond to a couple (E_0, A_0). The boundary data are chosen so that there is a solution of Einstein equations in the bulk which induces them on the boundary. A spin foam model has good semiclassical properties if the dominant contribution to the amplitude $\langle W|\Psi_0\rangle$ comes from the bulk configurations close to the classical 4-geometries compatible with the boundary data (E_0, A_0). By *classical* we mean that they satisfy Einstein equations.

The classical bulk configuration we focus on is flat space. The boundary configuration that we consider is the following: we decompose the boundary manifold S^3 in five tetrahedral regions with the same connectivity as the boundary of a 4-simplex; then we choose the intrinsic and the extrinsic geometry to be the ones proper of the boundary of a Euclidean 4-simplex. By construction, these boundary data are compatible with flat space being a classical solution in the bulk.

[2]This expression corresponds to the standard definition in (perturbative) quantum field theory where the *vacuum* expectation value of a product of local observables is defined as

$$\langle O(x_1)\cdots O(x_n)\rangle_0 = \frac{\displaystyle\int D[\varphi] O(x_1)\cdots O(x_n) e^{iS[\varphi]}}{\displaystyle\int D[\varphi] e^{iS[\varphi]}} \equiv \frac{\displaystyle\int D[\phi] W[\phi] O(x_1)\cdots O(x_n) \Psi_0[\phi]}{\displaystyle\int D[\phi] W[\phi] \Psi_0[\phi]} \,. \tag{4.1}$$

The vacuum state $\Psi_0[\phi]$ codes the boundary conditions at infinity.

For our choice of boundary configuration, the dominant contribution to the amplitude $\langle W|\Psi_0\rangle$ is required to come from bulk configurations close to flat space. The connected two-point correlation function $G^{abcd}(x,y)$ probes the fluctuations of the geometry around the classical configuration given by flat space. As a result it can be compared to the graviton propagator computed in perturbative quantum gravity.

The plan of the chapter is the following: in section 4.1 we introduce the metric operator and construct a semiclassical boundary state; in section 4.2 we recall the form of the new spin foam models; in section 4.3 we define the LQG propagator and provide an integral formula for it at the lowest order in a vertex expansion; in section 4.4 we compute its large spin asymptotics; in section 4.5 we discuss expectation values of metric operators; in section 4.6 we present our main result: the scaling and the tensorial structure of the LQG propagator at the leading order of our expansion; in section 4.7 we attempt a comparison with the graviton propagator of perturbative quantum gravity.

4.1 Semiclassical boundary state and the metric operator

Semiclassical boundary states are a key ingredient in the definition of boundary amplitudes. Here we describe in detail the construction of a boundary state peaked on the intrinsic and the extrinsic geometry of the boundary of a Euclidean 4-simplex. The construction is new: it uses the coherent intertwiners of Livine and Speziale [58] (see also [59]) together with a superposition over spins as done in [128, 138]. It can be considered as an improvement of the boundary state used in [142, 143, 135] where Rovelli-Speziale gaussian states [78] for intertwiners were used.

We consider a simplicial decomposition Δ_5 of S^3. The decomposition Δ_5 is homeomorphic to the boundary of a 4-simplex: it consists of five cells t_a which meet at ten faces f_{ab} ($a,b=1,..,5$ and $a<b$). Then we consider the sector of the Hilbert space $\mathcal{H}_\Sigma$ spanned by spin network states with graph Γ_5 dual to the decomposition Δ_5. Γ_5 is a complete graph with five nodes. We call v_a its nodes and l_{ab} ($a<b$) its ten links. Spin network states supported on this graph are labelled by ten spins j_{ab} ($a<b$) and five intertwiners i_a. We denote them by $|\Gamma_5, j_{ab}, i_a\rangle$ and call $\mathcal{H}_{\Gamma_5}$ the Hilbert space they span. On $\mathcal{H}_{\Gamma_5}$ we can introduce a *metric operator* smearing the electric field on surfaces dual to links, i.e. considering scalar products of fluxes. We focus on the node n and consider a surface f_{na} which cuts the link from the node n to the node a. The flux operator through the surface f_{na}, parallel transported in the node n, is denoted[3] $(E_n^a)_i$. It has the following three non-trivial properties:

(i) the flux operators $(E_n^a)_i$ and $(E_a^n)_i$ are related by a $SU(2)$ parallel transport g_{an} from the node a to the node n together with a change of sign which takes into account the

[3]Throughout the chapter $i,j,k\ldots=1,2,3$ are indices for vectors in $\mathbb{R}^3$.

different orientation of the face f_{an},

$$(E^a_n)_i = -(R_{an})_i{}^j \, (E^n_a)_j \; , \tag{4.4}$$

where R_{an} is the rotation which corresponds to the group element g_{an} associated to the link l_{an}, i.e. $R_{an} = D^{(1)}(g_{ab})$;
(ii) the commutator of two flux operators for the same face f_{na} is[4]

$$[\,(E^a_n)_i\, , \,(E^a_n)_j\,] = i\gamma\epsilon_{ij}{}^k \, (E^a_n)_k \; ; \tag{4.5}$$

(iii) a spin network state is annihilated by the sum of the flux operators over the faces bounding a node

$$\sum_{c\neq n}(E^c_n)_i|\Gamma_5, j_{ab}, i_a\rangle = 0 \; . \tag{4.6}$$

This last property follows from the $SU(2)$ gauge invariance of the spin network node.

Using the flux operator we can introduce the density-two inverse-metric operator at the node n, projected in the directions normal to the faces f_{na} and f_{nb}. It is defined as $E^a_n \cdot E^b_n = \delta^{ij}(E^a_n)_i(E^b_n)_j$. Its diagonal components $E^a_n{\cdot}E^a_n$ measure the area square of the face f_{na},

$$E^a_n{\cdot}E^a_n\,|\Gamma_5, j_{ab}, i_a\rangle = \Big(\gamma\sqrt{j_{na}(j_{na}+1)}\Big)^2\,|\Gamma_5, j_{ab}, i_a\rangle \; . \tag{4.7}$$

Spin network states are eigenstates of the diagonal components of the metric operator. On the other hand, the off-diagonal components $E^a_n{\cdot}E^b_n$ with $a \neq b$ measure the dihedral angle between the faces f_{na} and f_{nb} (weighted with their areas). It reproduces the angle operator [77]. Using the recoupling basis for intertwiner space, we have that in general the off-diagonal components of the metric operator have non-trivial matrix elements

$$E^a_n{\cdot}E^b_n\,|\Gamma_5, j_{ab}, i_a\rangle = \sum_{i'_c}\big(E^a_n{\cdot}E^b_n\big)_{i_c}{}^{i'_c}\,|\Gamma_5, j_{ab}, i'_a\rangle \; . \tag{4.8}$$

We refer to [142, 143] for a detailed discussion. In particular, from property (ii), we have that some off-diagonal components of the metric operator at a node do not commute [156]

$$[\,E^a_n{\cdot}E^b_n\, , \,E^a_n{\cdot}E^c_n\,] \neq 0 \; . \tag{4.9}$$

From this non-commutativity an Heisenberg inequality for dispersions of metric operators follows. Here we are interested in states which are peaked on a given value of *all* the off-diagonal components of the metric operator and which have dispersion of the order of Heisenberg's bound. Such states can be introduced using the technique of coherent

[4]Throughout the chapter we put $c = \hbar = G_{\mathrm{Newton}} = 1$.

intertwiners [58, 59]. A coherent intertwiner between the representations $j_1, .., j_4$ is defined as[5]

$$\Phi^{m_1\cdots m_4}(\vec{n}_1, .., \vec{n}_4) = \frac{1}{\sqrt{\Omega(\vec{n}_1, .., \vec{n}_4)}} \int_{SU(2)} dh \prod_{a=1}^{4} \langle j_a, m_a | D^{(j_a)}(h) | j_a, \vec{n}_a \rangle \tag{4.10}$$

and is labelled by four unit vectors $\vec{n}_1, .., \vec{n}_4$ satisfying the closure condition

$$j_1 \vec{n}_1 + \cdots + j_4 \vec{n}_4 = 0 \; . \tag{4.11}$$

The function $\Omega(\vec{n}_1, .., \vec{n}_4)$ provides normalization to one of the intertwiner. The function $\Phi^{m_1\cdots m_4}$ is invariant under rotations of the four vectors $\vec{n}_1, .., \vec{n}_4$. In the following we always assume that this invariance has been fixed with a given choice of orientation[6].

Nodes of the spin network can be labelled with coherent intertwiners. In fact such states provide an overcomplete basis of $\mathcal{H}_{\Gamma_5}$. Calling $v_i^{m_1\cdots m_4}$ the standard recoupling basis for intertwiners, we can define the coefficients

$$\Phi_i(\vec{n}_1, .., \vec{n}_4) = v_i^{m_1\cdots m_4} \Phi_{m_1\cdots m_4}(\vec{n}_1, .., \vec{n}_4) \; . \tag{4.12}$$

We define a *coherent spin network* $|\Gamma_5, j_{ab}, \Phi_a\rangle$ as the state labelled by ten spins j_{ab} and 4×5 normals $\vec{n}_{ab}$ and given by the superposition

$$|\Gamma_5, j_{ab}, \Phi_a(\vec{n})\rangle = \sum_{i_1\cdots i_5} \Big(\prod_{a=1}^{5} \Phi_{i_a}(\vec{n}_{ab}) \Big) |\Gamma_5, j_{ab}, i_a\rangle \; . \tag{4.13}$$

The expectation value of the metric operator on a coherent spin network is simply

$$\langle \Gamma_5, j_{ab}, \Phi_a | E_c^a \cdot E_c^b | \Gamma_5, j_{ab}, \Phi_a \rangle \simeq \gamma^2 j_{ca} j_{cb} \, \vec{n}_{ca} \cdot \vec{n}_{cb} \tag{4.14}$$

in the large spin limit. As a result we can choose the normals $\vec{n}_{ab}$ so that the coherent spin network state is peaked on a given intrinsic geometry of Σ.

Normals in different tetrahedra cannot be chosen independently if we want to peak on a Regge geometry [127]. The relation between normals is provided by the requirement

[5]The state $|j, \vec{n}\rangle$ is a spin coherent state. It is labelled by a unit vector $\vec{n}$ or equivalently by a point on the unit sphere. Given a $SU(2)$ transformation g which acts on the vector $+\vec{e}_z$ sending it to the vector $\vec{n} = Re_z$, a spin coherent state is given by $|j, \vec{n}\rangle = D^{(j)}(g)|j, +j\rangle$. As a result, it is defined up to a phase $e^{i\alpha j}$ corresponding to a transformation $\exp(i\alpha \vec{n} \cdot \vec{J})|j, \vec{n}\rangle = e^{i\alpha j}|j, \vec{n}\rangle$. A phase ambiguity in the definition of the coherent intertwiner (4.10) follows. Such ambiguity becomes observable when a superposition over j is considered.

[6]For instance we can fix this redundancy assuming that the sum $j_1\vec{n}_1 + j_2\vec{n}_2$ is in the positive z direction while the vector $\vec{n}_1 \times \vec{n}_2$ in the positive y direction. Once chosen this orientation, the four unit-vectors $\vec{n}_1, .., \vec{n}_4$ (which satisfying the closure condition) depend only on two parameters. These two parameters can be chosen to be the dihedral angle $\cos\theta_{12} = \vec{n}_1 \cdot \vec{n}_2$ and the twisting angle $\tan\phi_{(12)(34)} = \frac{(\vec{n}_1\times\vec{n}_2)\cdot(\vec{n}_3\times\vec{n}_4)}{|\vec{n}_1\times\vec{n}_2| \, |\vec{n}_3\times\vec{n}_4|}$.

that they are computed from the lengths of the edges of the triangulation Δ_5. In fact, a state with generic normals (satisfying the closure condition (4.11)) is peaked on a discontinuous geometry. This fact can be seen in the following way: let us consider an edge of the triangulation Δ_5; this edge is shared by three tetrahedra; for each tetrahedron we can compute the expectation value of the length operator for an edge in its boundary [92]; however in general the expectation value of the length of an edge seen from different tetrahedra will not be the same; this fact shows that the geometry is *discontinuous*. The requirement that the semiclassical state is peaked on a Regge geometry amounts to a number of relations between the labels $\vec{n}_{ab}$. In the case of the boundary of a Euclidean 4-simplex (excluding the 'rectangular' cases discussed in [158]), the normals turn out to be completely fixed once we give the areas of the ten triangles or equivalently the ten spins j_{ab},

$$\vec{n}_{ab} = \vec{n}_{ab}(j_{cd}) \ . \tag{4.15}$$

This assignment of normals guarantees that the geometry we are peaking on is Regge-like. In particular, in this chapter we are interested in the case of a 4-simplex which is approximately regular. In this case the spins labelling the links are of the form $j_{ab} = j_0 + \delta j_{ab}$ with $\frac{\delta j_{ab}}{j_0} \ll 1$ and a perturbative expression for the normals solving the continuity condition is available:

$$\vec{n}_{ab}(j_0 + \delta j) = \vec{n}_{ab}(j_0) + \sum_{cd} v^{(ab)(cd)} \delta j_{cd} \ . \tag{4.16}$$

The coefficients $v^{(ab)(cd)}$ can be computed in terms of the derivative of the normals $\vec{n}_{ab}$ (for a given choice of orientation, see footnote 6) with respect to the ten edge lengths, using the Jacobian of the transformation from the ten areas to the ten edge lengths of the 4-simplex.

In the following we are interested in superpositions over spins of coherent spin networks. As coherent intertwiners are defined only up to a spin-dependent arbitrary phase, a choice is in order. We make the canonical choice of phases described in [81]. We briefly recall it here. Consider a non-degenerate Euclidean 4-simplex; two tetrahedra t_a and t_b are glued at the triangle $f_{ab} \equiv f_{ba}$. Now, two congruent triangles f_{ab} and f_{ba} in $\mathbb{R}^3$ can be made to coincide via a unique rotation $R_{ab} \in SO(3)$ which, together with a translation, takes one outward-pointing normal to minus the other one,

$$R_{ab} \vec{n}_{ab} = -\vec{n}_{ba} \ . \tag{4.17}$$

The canonical choice of phase for the spin coherent states $|j_{ab}, \vec{n}_{ab}\rangle$ and $|j_{ab}, \vec{n}_{ba}\rangle$ entering the coherent intertwiners Φ_a and Φ_b is given by lifting the rotation R_{ab} to a $SU(2)$ transformation g_{ab} and requiring that

$$|j_{ab}, \vec{n}_{ba}\rangle = D^{(j_{ab})}(g_{ab}) \, J |j_{ab}, \vec{n}_{ab}\rangle \tag{4.18}$$

where $J : \mathcal{H}_j \to \mathcal{H}_j$ is the standard antilinear map for $SU(2)$ representations defined by

$$\langle\epsilon|\big(|\alpha\rangle \otimes J|\beta\rangle\big) = \langle\beta|\alpha\rangle \quad \text{with} \quad |\alpha\rangle, |\beta\rangle \in \mathcal{H}_j \tag{4.19}$$

and $\langle\epsilon|$ is the unique intertwiner in $\mathcal{H}_j \otimes \mathcal{H}_j$. In the following we will always work with coherent spin networks $|\Gamma_5, j_{ab}, \Phi_a(\vec{n}(j))\rangle$ satisfying the continuity condition, and with the canonical choice for the arbitrary phases of coherent states. From now on we use the shorter notation $|j, \Phi(\vec{n})\rangle$.

Coherent spin networks are eigenstates of the diagonal components of the metric operator, namely the area operator for the triangles of Δ_5. The extrinsic curvature to the manifold Σ measures the amount of change of the 4-normal to Σ, parallel transporting it along Σ. In a piecewise-flat context, the extrinsic curvature has support on triangles, that is it is zero everywhere except that on triangles. For a triangle f_{ab}, the extrinsic curvature K_{ab} is given by the angle between the 4-normals N_a^μ and N_b^μ to two tetrahedra t_a and t_b sharing the face f_{ab}. As the extrinsic curvature is the momentum conjugate to the intrinsic geometry, we have that a semiclassical state cannot be an eigenstate of the area as it would not be peaked on a given extrinsic curvature. In order to define a state peaked both on intrinsic and extrinsic geometry, we consider a superposition of coherent spin networks,

$$|\Psi_0\rangle = \sum_{j_{ab}} \psi_{j_0,\phi_0}(j) |j, \Phi(\vec{n})\rangle \ , \tag{4.20}$$

with coefficients $\psi_{j_0,\phi_0}(j)$ given by a gaussian times a phase,

$$\psi_{j_0,\phi_0}(j) = \frac{1}{N} \exp\Big(-\sum_{ab,cd} \alpha^{(ab)(cd)} \, \frac{j_{ab} - j_{0ab}}{\sqrt{j_{0ab}}} \, \frac{j_{cd} - j_{0cd}}{\sqrt{j_{0cd}}} \Big) \ \exp\Big(-i \sum_{ab} \phi_0^{ab} \, (j_{ab} - j_{0ab}) \Big) \ . \tag{4.21}$$

As we are interested in a boundary configuration peaked on the geometry of a regular 4-simplex, we choose all the background spins to be equal, $j_{0ab} \equiv j_0$. Later we will consider an asymptotic expansion for large j_0. The phases ϕ_0^{ab} are also chosen to be equal. The extrinsic curvature at the face f_{ab} in a regular 4-simplex is $K_{ab} = \arccos N_a \cdot N_b = \arccos(-\frac{1}{4})$. In Ashtekar-Barbero variables (E_0, A_0) we have

$$\phi_0 \equiv \phi_0^{ab} = \gamma K_{ab} = \gamma \arccos(-1/4) \ . \tag{4.22}$$

The 10×10 matrix $\alpha^{(ab)(cd)}$ is assumed to be complex with positive definite real part. Moreover we require that it has the symmetries of a regular 4-simplex. We introduce the matrices $P_k^{(ab)(cd)}$ with $k = 0, 1, 2$ defined as

$$P_0^{(ab)(cd)} = 1 \quad \text{if} \quad (ab) = (cd) \quad \text{and zero otherwise,} \tag{4.23}$$
$$P_1^{(ab)(cd)} = 1 \quad \text{if} \quad \{a = c, b \neq d\} \ \text{or a permutation of it} \quad \text{and zero otherwise,} \tag{4.24}$$
$$P_2^{(ab)(cd)} = 1 \quad \text{if} \quad (ab) \neq (cd) \quad \text{and zero otherwise.} \tag{4.25}$$

Their meaning is simple: a couple (ab) identifies a link of the graph Γ_5; two links can be either coincident, or touching at a node, or disjoint. The matrices $P_k^{(ab)(cd)}$ correspond to these three different cases. Using the basis $P_k^{(ab)(cd)}$ we can write the matrix $\alpha^{(ab)(cd)}$ as

$$\alpha^{(ab)(cd)} = \sum_{k=0}^{2} \alpha_k \, P_k^{(ab)(cd)} \,. \tag{4.26}$$

As a result our ansatz for a semiclassical boundary state $|\Psi_0\rangle$ is labelled by a (large) half-integer j_0 and has only three complex free parameters, the numbers α_k.

4.2 The new spin foam dynamics

The dynamics is implemented in terms of a spin foam functional $\langle W|$. Here we are interested in its components on the Hilbert space spanned by spin networks with graph Γ_5. The sum over two-complexes can be implemented in terms of a formal perturbative expansion in the parameter λ of a Group Field Theory [9]:

$$\langle W|\Gamma_5, j_{ab}, i_a\rangle = \sum_\sigma \lambda^{N_\sigma} W(\sigma) \tag{4.27}$$

The sum is over spinfoams (colored 2-complexes) whose boundary is the spin network (Γ_5, j_{ab}, i_a), $W(\sigma)$ is the spinfoam amplitude

$$W(\sigma) = \prod_{f\subset\sigma} W_f \prod_{v\subset\sigma} W_v \tag{4.28}$$

where W_v and W_f are the vertex and face amplitude respectively. The quantity N_σ in (4.27) is the number of vertices in the spin foam σ, therefore the formal expansion in λ is in fact a *vertex expansion*.

The spin foam models we consider here are the EPRL$_\gamma$ [5] and FK$_\gamma$ [6] models. We restrict attention to $0 < \gamma < 1$; in this case the two models coincide. The vertex amplitude is given by

$$W_v(j_{ab}, i_a) = \sum_{i_a^+ \, i_a^-} \{15j\}\big(j_{ab}^+, i_a^+\big) \ \{15j\}\big(j_{ab}^-, i_a^-\big) \ \prod_a f^{i_a}_{i_a^+ i_a^-}(j_{ab}) \tag{4.29}$$

where the unbalanced spins j^+, j^- are

$$j_{ab}^\pm = \gamma^\pm j_{ab}, \qquad \gamma^\pm = \frac{1\pm\gamma}{2} \,. \tag{4.30}$$

This relation puts restrictions[7] on the value of γ and of j_{ab}. The fusion coefficients $f^{i_a}_{i_a^+ i_a^+}(j_{ab})$ are defined in [5] (see also [129]) and built out of the intertwiner $v_i^{m_1 \cdots m_4}$ in $\mathcal{H}_{j_1} \otimes \cdots \otimes \mathcal{H}_{j_4}$ and the intertwiners $v_{i_\pm}^{m_1^\pm \cdots m_4^\pm}$ in $\mathcal{H}_{j_1^\pm} \otimes \cdots \otimes \mathcal{H}_{j_4^\pm}$. Defining a map $Y : \mathcal{H}_j \to \mathcal{H}_{j^+} \otimes \mathcal{H}_{j^-}$ with matrix elements $Y^m_{m^+ m^-} = \langle j^+, m^+; j^-, m^- | \, Y | j, m \rangle$ given by Clebsh-Gordan coefficients, we have that the fusion coefficients $f^{i_a}_{i_a^+ i_a^+}$ are given by

$$f^{i_a}_{i_a^+ i_a^+} = Y_{m_1 m_1^+ m_1^-} \cdots Y_{m_4 m_4^+ m_4^-} \;\; v_i^{m_1 \cdots m_4} \;\; v_{i_+}^{m_1^+ \cdots m_4^+} \;\; v_{i_-}^{m_1^- \cdots m_4^-} \; . \tag{4.31}$$

Indices are raised and lowered with the Wigner metric.

Throughout this chapter we will restrict attention to the lowest order in the vertex expansion. To this order, the boundary amplitude of a spin network state with graph Γ_5 is given by

$$\langle W | \Gamma_5, j_{ab}, i_a \rangle = \mu(j_{ab}) W_v(j_{ab}, i_a) \; , \tag{4.32}$$

i.e. it involves a single spin foam vertex.

The function μ is defined as $\mu(j) = \prod_{ab} W_{f_{ab}}(j)$. A natural choice for the face amplitude is $W_f(j^+, j^-) = (2j^+ + 1)(2j^- + 1) = (1 - \gamma^2) j^2 + 2j + 1$. Other choices can be considered. We assume that $\mu(\lambda j_{ab})$ scales as λ^p for some p for large λ. We will show in the following that, at the leading order in large j_0, the LQG propagator (4.3) is in fact independent from the choice of face amplitude, namely from the function $\mu(j)$.

4.3 LQG propagator: integral formula

In this section we define the LQG propagator and then provide an integral formula for it. The dynamical expectation value of an operator $\mathcal{O}$ on the state $|\Psi_0\rangle$ is defined via the following expression

$$\langle \mathcal{O} \rangle = \frac{\langle W | \mathcal{O} | \Psi_0 \rangle}{\langle W | \Psi_0 \rangle} \; . \tag{4.33}$$

The geometric operator we are interested in is the metric operator $E^a_n \cdot E^b_n$ discussed in section 4.1. We focus on the *connected* two-point correlation function G^{abcd}_{nm} on a semiclassical boundary state $|\Psi_0\rangle$. It is defined as

$$G^{abcd}_{nm} = \langle E^a_n \cdot E^b_n \; E^c_m \cdot E^d_m \rangle - \langle E^a_n \cdot E^b_n \rangle \, \langle E^c_m \cdot E^d_m \rangle \; . \tag{4.34}$$

We are interested in computing this quantity using the boundary state $|\Psi_0\rangle$ introduced in section 4.1 and the spin foam dynamics (4.29). This is what we call the *LQG propagator.*

[7] Formula (4.29) is well-defined only for $j^\pm$ half-integer. As a result, for a fixed value of γ, there are restrictions on the boundary spin j. For instance, if we choose $\gamma = 1/n$ with n integer, then we have that j has to be integer and $j \geq n$, i.e. $j \in \{n, n+1, n+2, \cdots\}$.

As the boundary state is a superposition of coherent spin networks, the LQG propagator involves terms of the form $\langle W|\mathcal{O}|j,\Phi(\vec{n})\rangle$. Its explicit formula is

$$G^{abcd}_{nm} = \frac{\sum_j \psi(j)\langle W|E^a_n\cdot E^b_n\, E^c_m\cdot E^d_m|j,\Phi(\vec{n})\rangle}{\sum_j \psi(j)\langle W|j,\Phi(\vec{n})\rangle} - \frac{\sum_j \psi(j)\langle W|E^a_n\cdot E^b_n|j,\Phi(\vec{n})\rangle}{\sum_j \psi(j)\langle W|j,\Phi(\vec{n})\rangle}\frac{\sum_j \psi(j)\langle W|E^c_m\cdot E^d_m|j,\Phi(\vec{n})\rangle}{\sum_j \psi(j)\langle W|j,\Phi(\vec{n})\rangle} \quad (4.35)$$

In the following two subsections we recall the integral formula for the amplitude of a coherent spin network $\langle W|j,\Phi(\vec{n})\rangle$ [120, 59],[81] and derive analogous integral expressions for the amplitude with metric operator insertions $\langle W|E^a_n\cdot E^b_n|j,\Phi(\vec{n})\rangle$ and $\langle W|E^a_n\cdot E^b_n\, E^c_m\cdot E^d_m|j,\Phi(\vec{n})\rangle$.

4.3.1 Integral formula for the amplitude of a coherent spin network

The boundary amplitude of a coherent spin network $|j,\Phi(\vec{n})\rangle$ admits an integral representation [120, 59],[81]. Here we go through its derivation as we will use a similar technique in next section.

The boundary amplitude $\langle W|j,\Phi(\vec{n})\rangle$ can be written as an integral over five copies of $SU(2)\times SU(2)$ (with respect to the Haar measure):

$$\langle W|j_{ab},\Phi_a(\vec{n})\rangle = \sum_{i_a}\Big(\prod_a \Phi_{i_a}(\vec{n})\Big)\langle W|j_{ab},i_a\rangle = \mu(j)\int\prod_{a=1}^{5}\mathrm{d}g^+_a\mathrm{d}g^-_a\,\prod_{ab}P^{ab}(g^+,g^-)\ . \quad (4.36)$$

The function $P^{ab}(g^+,g^-)$ is given by

$$P^{ab}(g^+,g^-) = \langle j_{ab},-\vec{n}_{ba}|\,Y^\dagger D^{(j^+_{ab})}\big((g^+_a)^{-1}g^+_b\big)\otimes D^{(j^-_{ab})}\big((g^-_a)^{-1}g^-_b\big)Y|j_{ab},\vec{n}_{ab}\rangle\ . \quad (4.37)$$

where the map Y is defined in section 4.2. Using the factorization property of spin coherent states,

$$Y|j,\vec{n}\rangle = |j^+,\vec{n}\rangle\otimes|j^-,\vec{n}\rangle\ , \quad (4.38)$$

we have that the function $P^{ab}(g^+,g^-)$ factorizes as

$$P^{ab}(g^+,g^-) = P^{ab+}(g^+)\,P^{ab-}(g^-) \quad (4.39)$$

with

$$P^{ab\pm} = \langle j_{ab},-\vec{n}_{ba}|D^{(j^\pm_{ab})}\big((g^\pm_a)^{-1}g^\pm_b\big)|j_{ab},\vec{n}_{ab}\rangle = \Big(\langle\frac{1}{2},-\vec{n}_{ba}|(g^\pm_a)^{-1}g^\pm_b|\frac{1}{2},\vec{n}_{ab}\rangle\Big)^{2j^\pm_{ab}}\ . \quad (4.40)$$

In the last equality we have used (again) the factorization property of spin coherent states to exponentiate the spin $j^\pm_{ab}$. In the following we will drop the $1/2$ in $|\frac{1}{2},\vec{n}_{ab}\rangle$ and write always $|\vec{n}_{ab}\rangle$ for the coherent state in the fundamental representation.

The final expression we get is

$$\langle W|j,\Phi(\vec{n})\rangle = \mu(j)\int\prod_{a=1}^{5}\mathrm{d}g_a^+\mathrm{d}g_a^-\;e^S \tag{4.41}$$

where the "action" S is given by the sum $S = S^+ + S^-$, with

$$S^\pm = \sum_{ab} 2j_{ab}^\pm \log\langle -\vec{n}_{ab}|(g_a^\pm)^{-1}g_b^\pm|\vec{n}_{ba}\rangle\;. \tag{4.42}$$

4.3.2 LQG operators as group integral insertions

In this section we use a similar technique to derive integral expressions for the expectation value of metric operators. In particular we show that

$$\langle W|E_n^a\cdot E_n^b|j_{ab},\Phi_a(\vec{n})\rangle = \mu(j)\int\prod_{a=1}^{5}\mathrm{d}g_a^+\mathrm{d}g_a^-\;\; q_n^{ab}(g^+,g^-)\;e^S \tag{4.43}$$

and that

$$\langle W|E_n^a\cdot E_n^b\;E_m^c\cdot E_m^d|j_{ab},\Phi_a(\vec{n})\rangle = \mu(j)\int\prod_{a=1}^{5}\mathrm{d}g_a^+\mathrm{d}g_a^-\;\; q_n^{ab}(g^+,g^-)\;q_m^{cd}(g^+,g^-)\;e^S \tag{4.44}$$

where we assume[8] $n\neq m$ and $a,b,c,d\neq n,m$. The expression for the insertions $q_n^{ab}(g^+,g^-)$ in the integral is derived below.

We start focusing on $\langle E_n^a{\cdot}E_n^b\rangle$ in the case $a\neq b$. The metric field $(E_a^b)_i$ acts on a state $|j_{ab},m_{ab}\rangle$ as γ times the generator J_i of $SU(2)$. As a result we can introduce a quantity Q_i^{ab} defined as

$$Q_i^{ab}(g^+,g^-) = \langle j_{ab},-\vec{n}_{ba}|\,Y^\dagger D^{(j_{ab}^+)}\big((g_a^+)^{-1}g_b^+\big)\otimes D^{(j_{ab}^-)}\big((g_a^-)^{-1}g_b^-\big)Y(E_a^b)_i|j_{ab},\vec{n}_{ab}\rangle\;, \tag{4.45}$$

so that

$$\langle W|E^{na}\cdot E^{nb}|j,\Phi(\vec{n})\rangle = \int\prod_{a=1}^{5}\mathrm{d}g_a^+\mathrm{d}g_a^-\;\delta^{ij}Q_i^{na}Q_j^{nb}{\prod_{cd}}'P^{cd}(g^+,g^-)\;. \tag{4.46}$$

The product $\prod'$ is over couples (cd) different from $(na),(nb)$. Thanks to the invariance properties of the map Y, we have that

$$Y\,J_i^{ab}|j_{ab},m_{ab}\rangle = (J_i^{ab+}+J_i^{ab-})Y|j_{ab},m_{ab}\rangle\;. \tag{4.47}$$

[8]Similar formulae can be found also in the remaining cases but are not needed for the calculation of the LQG propagator.

Thus Q_i^{ab} can be written as

$$Q_i^{ab} = Q_i^{ab+}\, P^{ab-} + P^{ab+}\, Q_i^{ab-} \tag{4.48}$$

with

$$Q_i^{ab\pm} = \gamma\, \langle j_{ab}^{\pm}, -\vec{n}_{ba}| D^{(j_{ab}^{\pm})}\big((g_a^{\pm})^{-1} g_b^{\pm}\big)\, J_i^{ab\pm} | j_{ab}^{\pm}, \vec{n}_{ab}\rangle \;. \tag{4.49}$$

Now we show that $Q_i^{ab\pm}$ is given by a function $A_i^{ab\pm}$ linear in the spin $j_{ab}^{\pm}$, times the quantity $P^{ab\pm}$ defined in (4.40),

$$Q_i^{ab\pm} = A_i^{ab\pm}\; P^{ab\pm} \;. \tag{4.50}$$

The function $A_i^{ab\pm}$ is determined as follows. The generator $J_i^{ab\pm}$ of $SU(2)$ in representation $j_{ab}^{\pm}$ can be obtained as the derivative

$$i\, \frac{\partial}{\partial \alpha^i} D^{(j_{ab}^{\pm})}\big(h(\alpha)\big)\Big|_{\alpha^i=0} = J_i^{ab\pm} \tag{4.51}$$

where the group element $h(\alpha)$ is defined via the canonical parametrization $h(\alpha) = \exp(-i\alpha^i \frac{\sigma_i}{2})$. Therefore, we can write $Q_i^{ab\pm}$ as

$$\begin{aligned} Q_i^{ab\pm} &= i\,\gamma\, \frac{\partial}{\partial \alpha^i}\Big(\langle j_{ab}^{\pm}, -\vec{n}_{ba}| D^{(j_{ab}^{\pm})}\big((g_a^{\pm})^{-1} g_b^{\pm}\big)\, D^{(j_{ab}^{\pm})}\big(h(\alpha)\big) | j_{ab}^{\pm}, \vec{n}_{ab}\rangle \Big)\Big|_{\alpha^i=0} \\ &= i\,\gamma\, \frac{\partial}{\partial \alpha^i}\Big(\gamma\, \langle -\vec{n}_{ba}| (g_a^{\pm})^{-1} g_b^{\pm} h(\alpha) |\vec{n}_{ab}\rangle \Big)^{2j_{ab}^{\pm}}\Big|_{\alpha^i=0} \\ &= \gamma\, j_{ab}^{\pm}\, \langle -\vec{n}_{ba}| (g_a^{\pm})^{-1} g_b^{\pm} \sigma^i |\vec{n}_{ab}\rangle \big(\langle -\vec{n}_{ba}| (g_a^{\pm})^{-1} g_b^{\pm} |\vec{n}_{ab}\rangle \big)^{2j_{ab}^{\pm}-1} \;. \end{aligned} \tag{4.52}$$

Comparing expression (4.52) with (4.50) and (4.40), we find that $A_i^{na\pm}$ is given by

$$A_i^{na\pm} = \gamma j_{na}^{\pm} \frac{\langle -\vec{n}_{an}| (g_a^{\pm})^{-1} g_n^{\pm} \sigma^i |\vec{n}_{na}\rangle}{\langle -\vec{n}_{an}| (g_a^{\pm})^{-1} g_n^{\pm} |\vec{n}_{na}\rangle} \;. \tag{4.53}$$

A vectorial expression for $A_i^{na\pm}$ can be given, introducing the rotation $R_a^{\pm} = D^{(1)}(g_a^{\pm})$,

$$A_i^{na\pm} = \gamma j_{na}^{\pm}\, (R_n^{\pm})^{-1} \frac{R_n^{\pm} n_{na} - R_a^{\pm} n_{an} - i(R_n^{\pm} n_{na} \times R_a^{\pm} n_{an})}{1 - (R_a^{\pm} n_{an}) \cdot (R_n^{\pm} n_{na})} \;. \tag{4.54}$$

Thanks to (4.48) and (4.50), we have that the expression for Q_i^{ab} simplifies to

$$Q_i^{ab} = A_i^{ab}\; P^{ab} \tag{4.55}$$

with

$$A_i^{ab} = A_i^{ab+} + A_i^{ab-} \;. \tag{4.56}$$

As a result, equation (4.46) reduces to

$$\langle W|E^a_n\cdot E^b_n|j,\Phi(\vec{n})\rangle = \int \prod_{a=1}^{5} \mathrm{d}g^+_a \mathrm{d}g^-_a \; \delta^{ij} A^{na}_i A^{nb}_j \prod_{cd} P^{cd}(g^+,g^-) \;, \tag{4.57}$$

which is of the form (4.41) with the insertion $A^{na}\cdot A^{nb}$. Therefore, comparing with equation (4.43), we have that

$$q^{ab}_n(g^+,g^-) = A^{na}\cdot A^{nb} \tag{4.58}$$

for $a\neq b$. The case with $a=b$ can be computed using a similar technique but the result is rather simple and expected, thus we just state it

$$q^{aa}_n(g^+,g^-) = \gamma^2 j_{na}(j_{na}+1)\;. \tag{4.59}$$

As far as $\langle E^a_n\cdot E^b_n\, E^c_m\cdot E^d_m\rangle$ a similar result can be found. In particular, for $n\neq m$ and $a,b,c,d\neq n,m$ the result is stated at the beginning of this section, equation (4.44), with the same expression for the insertion $q^{ab}_n(g^+,g^-)$ as in equation (4.58) and equation (4.59).

Substituting (4.43)-(4.44) in (4.35) we obtain a new expression for the propagator in terms of group integrals:

$$G^{abcd}_{nm} = \frac{\sum_j \mu(j)\psi(j)\int \mathrm{d}g^{\pm}\; q^{ab}_n\, q^{cd}_m\, e^S}{\sum_j \mu(j)\psi(j)\int \mathrm{d}g^{\pm}\, e^S} - \frac{\sum_j \mu(j)\psi(j)\int \mathrm{d}g^{\pm}\; q^{ab}_n\, e^S}{\sum_j \mu(j)\psi(j)\int \mathrm{d}g^{\pm}\, e^S}\frac{\sum_j \mu(j)\psi(j)\int \mathrm{d}g^{\pm}\; q^{cd}_m\; e^S}{\sum_j \mu(j)\psi(j)\int \mathrm{d}g^{\pm}\, e^S}\;. \tag{4.60}$$

This expression with metric operators written as insertions in an integral is the starting point for the large j_0 asymptotic analysis of next section.

4.4 LQG propagator: stationary phase approximation

The correlation function (4.60) depends on the scale j_0 fixed by the boundary state. We are interested in computing its asymptotic expansion for large j_0. The technique we use is an (extended) stationary phase approximation of a multiple integral over both spins and group elements. In 4.4.1 we put expression (4.60) in a form to which this approximation can be applied. Then in 4.4.2 we recall a standard result in asymptotic analysis regarding connected two-point functions and in 4.4.3-4.4.4 we apply it to our problem.

4.4.1 The total action and the extended integral

We introduce the "total action" defined as $S_{\mathrm{tot}} = \log\psi + S$ or more explicitly as

$$S_{\mathrm{tot}}(j_{ab}, g_a^+, g_a^-) = -\frac{1}{2}\sum_{ab,cd}\alpha^{(ab)(cd)}\,\frac{j_{ab}-j_{0ab}}{\sqrt{j_{0ab}}}\,\frac{j_{cd}-j_{0cd}}{\sqrt{j_{0cd}}} - i\sum_{ab}\phi_0^{ab}\,(j_{ab}-j_{0ab}) + S^+(j_{ab}, g_a^+) + S^-(j_{ab}, g_a^-)\;. \tag{4.61}$$

Notice that the action $S^+ + S^-$ is a homogeneous function of the spins j_{ab} therefore, rescaling the spins j_{0ab} and j_{ab} by an interger λ so that $j_{0ab} \to \lambda j_{0ab}$ and $j_{ab} \to \lambda j_{ab}$, we have that the total action goes to $S_{\mathrm{tot}} \to \lambda S_{\mathrm{tot}}$. We recall also that $q_n^{ab} \to \lambda^2 q_n^{ab}$. In the large λ limit, the sums over spins in expression (4.60) can be approximated with integrals over continuous spin variables[9]:

$$\sum_j \mu \int \mathrm{d}^5 g^{\pm}\; q_n^{ab}\, e^{\lambda S_{\mathrm{tot}}} = \int \mathrm{d}^{10} j\, \mathrm{d}^5 g^{\pm}\; \mu\, q_n^{ab}\, e^{\lambda S_{\mathrm{tot}}} + O(\lambda^{-N}) \qquad \forall N>0\;. \tag{4.62}$$

Moreover, notice that the action, the measure and the insertions in (4.60) are invariant under a $SO(4)$ symmetry that makes an integration $\mathrm{d}g^+\mathrm{d}g^-$ redundant. We can factor out one $SO(4)$ volume, e.g. putting $g_1^+ = g_1^- = 1$, so that we end up with an integral over $\mathrm{d}^4 g^{\pm} = \prod_{a=2}^5 \mathrm{d}g_a^+ \mathrm{d}g_a^-$.

As a result we can re-write expression (4.60) in the following integral form

$$G_{nm}^{abcd} = \lambda^4\Big(\frac{\int \mathrm{d}^{10} j\, \mathrm{d}^4 g^{\pm} \mu\; q_n^{ab}\, q_m^{cd}\, e^{\lambda S_{\mathrm{tot}}}}{\int \mathrm{d}^{10} j\, \mathrm{d}^4 g^{\pm} \mu\, e^{\lambda S_{\mathrm{tot}}}} - \frac{\int \mathrm{d}^{10} j\, \mathrm{d}^4 g^{\pm} \mu\; q_n^{ab}\, e^{\lambda S_{\mathrm{tot}}}}{\int \mathrm{d}^{10} j\, \mathrm{d}^4 g^{\pm} \mu\, e^{\lambda S_{\mathrm{tot}}}}\frac{\int \mathrm{d}^{10} j\, \mathrm{d}^4 g^{\pm} \mu\, q_m^{cd}\; e^{\lambda S_{\mathrm{tot}}}}{\int \mathrm{d}^{10} j\, \mathrm{d}^4 g^{\pm} \mu\, e^{\lambda S_{\mathrm{tot}}}}\Big)\;. \tag{4.63}$$

To this expression we can apply the standard result stated in the following section.

4.4.2 Asymptotic formula for connected two-point functions

Consider the integral

$$F(\lambda) = \int \mathrm{d}x\, f(x)\, e^{\lambda S(x)} \tag{4.64}$$

over a region of $\mathbb{R}^d$, with $S(x)$ and $f(x)$ smooth complex-valued functions such that the real part of S is negative or vanishing, $\mathrm{Re}S \leq 0$. Assume also that the stationary points x_0 of S are isolated so that the Hessian at a stationary point $H = S''(x_0)$ is non-singular, $\det H \neq 0$. Under these hypothesis an asymptotic expansion of the integral F for large λ is available: it is an extension of the standard stationary phase approximation that

[9] The remainder, i.e. the difference between the sum and the integral, can be estimated via Euler-Maclaurin summation formula. This approximation does not affect any finite order in the computation of the LQG propagator.

takes into account the fact that the action S is complex [159]. A key role is played by *critical points*, i.e. stationary points x_0 for which the real part of the action vanishes, $\mathrm{Re}S(x_0) = 0$. Here we assume that there is a unique critical point. Then the asymptotic expansion of $F(\lambda)$ for large λ is given by

$$F(\lambda) = \left(\frac{2\pi}{\lambda}\right)^{\frac{d}{2}} \frac{e^{i\,\mathrm{Ind}\,H} e^{\lambda S(x_0)}}{\sqrt{|\det H|}} \left(f(x_0) + \frac{1}{\lambda}\Big(\frac{1}{2} f''_{ij}(x_0)(H^{-1})^{ij} + D\Big) + \mathcal{O}(\tfrac{1}{\lambda^2})\right) \tag{4.65}$$

with $f''_{ij} = \partial^2 f / \partial x^i \partial x^j$ and $\mathrm{Ind}\,H$ is the index[10] of the Hessian. The term D does not contain second derivatives of f, it contains only[11] $f(x_0)$ and $f'_i(x_0)$. Now we consider three smooth complex-valued functions g, h and μ. A connected 2-point function relative to the insertions g and h and w.r.t. the measure μ is defined as

$$G = \frac{\int \mathrm{d}x\, \mu(x)\, g(x) h(x)\, e^{\lambda S(x)}}{\int \mathrm{d}x\, \mu(x)\, e^{\lambda S(x)}} - \frac{\int \mathrm{d}x\, \mu(x)\, g(x)\, e^{\lambda S(x)}}{\int \mathrm{d}x\, \mu(x)\, e^{\lambda S(x)}} \frac{\int \mathrm{d}x\, \mu(x)\, h(x)\, e^{\lambda S(x)}}{\int \mathrm{d}x\, \mu(x)\, e^{\lambda S(x)}} \,. \tag{4.67}$$

Using (4.65) it is straightforward to show that the (leading order) asymptotic formula for the connected 2-point function is simply

$$G = \frac{1}{\lambda}\, (H^{-1})^{ij}\, g'_i(x_0)\, h'_j(x_0)\; + \mathcal{O}(\tfrac{1}{\lambda^2}) \,. \tag{4.68}$$

Notice that both the measure function μ and the disconnected term D do not appear in the leading term of the connected 2-point function; nevertheless they are present in the higher orders (loop contributions). The reason we are considering the quantity G, built from integrals of the type (4.64), is that the LQG propagator has exactly this form. Specifically, in sections 4.4.3 we determine the critical points of the total action, in 4.4.4 we compute the Hessian of the total action and the derivative of the insertions evaluated at the critical points, and in 4.6 we state our result.

[10] The index is defined in terms of the eigenvalues of h_k of the Hessian as $\mathrm{Ind}\,H = \frac{1}{2}\sum_k \arg(h_k)$ with $-\frac{\pi}{2} \leq \arg(h_k) \leq +\frac{\pi}{2}$.

[11] More explicitly, the term D is given by

$$D = f'_i(x_0) R'''_{jkl}(x_0)(H^{-1})^{ij}(H^{-1})^{kl} + \frac{5}{2} f(x_0) R'''_{ijk}(x_0) R'''_{mnl}(x_0)(H^{-1})^{im}(H^{-1})^{jn}(H^{-1})^{kl} \tag{4.66}$$

with $R(x) = S(x) - S(x_0) - \frac{1}{2}H_{ij}(x_0)(x-x_0)^i(x-x_0)^j$.

4.4.3 Critical points of the total action

The real part of the total action is given by

$$\mathrm{Re}S_{\mathrm{tot}} = -\sum_{ab,cd}(\mathrm{Re}\,\alpha)^{(ab)(cd)}\,\frac{j_{ab}-j_{0ab}}{\sqrt{j_{0ab}}}\,\frac{j_{cd}-j_{0cd}}{\sqrt{j_{0cd}}}+ \tag{4.69}$$

$$+\sum_{ab} j^-_{ab}\log\frac{1-(R^-_a n_{ab})\cdot(R^-_b n_{ba})}{2}+\sum_{ab} j^+_{ab}\log\frac{1-(R^+_a n_{ab})\cdot(R^+_b n_{ba})}{2}\ . \tag{4.70}$$

Therefore, having assumed that the matrix α in the boundary state has positive definite real part, we have that the real part of the total action is negative or vanishing, $\mathrm{Re}S_{\mathrm{tot}} \leq 0$. In particular the total action vanishes for the configuration of spins j_{ab} and group elements $g^\pm_a$ satisfying

$$j_{ab} = j_{0ab}\ , \tag{4.71}$$

$$g^\pm_a \ \text{ such that }\ R^\pm_a n_{ab}(j) = -R^\pm_b n_{ba}(j)\ . \tag{4.72}$$

Now we study the stationary points of the total action and show that there is a unique stationary point for which $\mathrm{Re}S_{\mathrm{tot}}$ vanishes.

The analysis of stationary points of the action $S^+ + S^-$ with respect to variations of the group variables $g^\pm_a$ has been performed in full detail by Barrett et al. in [81]. Here we briefly summarize their result as they apply unchanged to the total action. We invite the reader to look at the original reference for a detailed derivation and a geometrical interpretation of the result.

The requirement that the variation of the total action with respect to the group variables $g^\pm_a$ vanishes, $\delta_g S_{\mathrm{tot}} = 0$, leads to the two sets of equations (respectively for the real and the imaginary part of the variation):

$$\sum_{b\neq a} j^\pm_{ab}\frac{R^\pm_a n_{ab} - R^\pm_b n_{ba}}{1-(R^\pm_a n_{ab})\cdot(R^\pm_b n_{ba})} = 0 \quad , \quad \sum_{b\neq a} j^\pm_{ab}\frac{(R^\pm_a n_{ab})\times(R^\pm_b n_{ba})}{1-(R^\pm_a n_{ab})\cdot(R^\pm_b n_{ba})} = 0\ . \tag{4.73}$$

When evaluated at the maximum point (4.72), these two sets of equations are trivially satisfied. Infact the normals $\vec{n}_{ab}$ in the boundary state are chosen to satisfy the closure condition (4.11) at each node. Therefore the critical points in the group variables are given by all the solutions of equation (4.72).

For normals $\vec{n}_{ab}$ which define non-degenerate tetrahedra and satisfy the continuity condition (4.15), the equation $R_a n_{ab} = -R_b n_{ba}$ admits two distinct sets of solutions, up to global rotations. These two sets are related by parity. The two sets can be lifted to $SU(2)$. We call them $\bar{g}^+_a$ and $\bar{g}^-_a$. Out of them, four classes of solutions for the couple (g^+_a, g^-_a) can be found. They are given by

$$(\bar{g}^+_a,\bar{g}^-_a),\ (\bar{g}^-_a,\bar{g}^+_a),\ (\bar{g}^+_a,\bar{g}^+_a),\ (\bar{g}^-_a,\bar{g}^-_a)\ . \tag{4.74}$$

The geometrical interpretation is the following. The couples $(j_{ab}\vec{n}_{ab}, j_{ab}\vec{n}_{ab})$ are interpreted as the selfdual and anti-selfdual parts (with respect to some "time" direction, e.g. $(0,0,0,1)$) of area bivectors associated to triangles in 4-dimensions; since these bivectors are diagonal, they live in the 3-dimensional subspace of $\mathbb{R}^4$ orthogonal to the chosen "time" direction. Because of the closure condition (4.11), for a fixed n the four bivectors $(j_{na}\vec{n}_{na}, j_{na}\vec{n}_{na})$ define an embedding of a tetrahedron in $\mathbb{R}^4$. The two group elements g_a^+ and g_a^- of the action (4.42) define an SO(4) element which rotates the "initial" tetrahedron. The system (4.72) is a gluing condition between tetrahedra. The first two classes of solutions in (4.74) glue five tetrahedra into two Euclidean non-degenerate 4-simplices related by a reflection, while the second two classes correspond to degenerate configurations with the 4-simplex living in the three-dimensional plane orthogonal to the chosen "time" direction.

The evaluation of the action $S(j_{ab}, g_a^+, g_a^-) = S^+(j_{ab}, g_a^+) + S^-(j_{ab}, g_a^-)$ on the four classes of critical points gives

$$S(j_{ab}, \bar{g}_a^+, \bar{g}_a^-) = +\, S_{\text{Regge}}(j_{ab}) \,, \tag{4.75}$$

$$S(j_{ab}, \bar{g}_a^-, \bar{g}_a^+) = -\, S_{\text{Regge}}(j_{ab}) \,, \tag{4.76}$$

$$S(j_{ab}, \bar{g}_a^+, \bar{g}_a^+) = +\, \gamma^{-1} S_{\text{Regge}}(j_{ab}) \,, \tag{4.77}$$

$$S(j_{ab}, \bar{g}_a^-, \bar{g}_a^-) = -\, \gamma^{-1} S_{\text{Regge}}(j_{ab}) \,, \tag{4.78}$$

where $S_{\text{Regge}}(j_{ab})$ is Regge action for a single 4-simplex with triangle areas $A_{ab} = \gamma j_{ab}$ and dihedral angles $\phi_{ab}(j)$ written in terms of the areas

$$S_{\text{Regge}}(j_{ab}) = \sum_{ab} \gamma j_{ab} \phi_{ab}(j) \,. \tag{4.79}$$

Now we focus on stationarity of the total action with respect to variations of the spin labels j_{ab}. We fix the group elements (g_a^+, g_a^-) to belong to one of the four classes (4.74). For the first class we find

$$0 = \left.\frac{\partial S_{\text{tot}}}{\partial j_{ab}}\right|_{(\bar{g}_a^+, \bar{g}_a^-)} = -\sum_{cd} \frac{\alpha^{(ab)(cd)}(j_{cd} - j_{0cd})}{\sqrt{j_{0ab}}\sqrt{j_{0cd}}} - i\phi_0^{ab} + i\frac{\partial S_{\text{Regge}}}{\partial j_{ab}} \,. \tag{4.80}$$

The quantity $\partial S_{\text{Regge}}/\partial j_{ab}$ is γ times the extrinsic curvature at the triangle f_{ab} of the boundary of a 4-simplex with triangle areas $A_{ab} = \gamma j_{ab}$. As the phase ϕ_0^{ab} in the boundary state is choosen to be exactly γ times the extrinsic curvature, we have that equation (4.80) vanishes for $j_{ab} = j_{0ab}$. Notice that, besides being a stationary point, this is also a critical point of the total action as stated in (4.71).

On the other hand, if equation (4.80) is evaluated on group elements belonging to the classes $(\bar{g}_a^-, \bar{g}_a^+)$, $(\bar{g}_a^-, \bar{g}_a^-)$, $(\bar{g}_a^+, \bar{g}_a^+)$, we have that there is no cancellation of phases and therefore no stationary point with respect to variations of spins. This is the feature of the phase of the boundary state: it selects a classical contribution to the asymptotics of a spin foam model, a fact first noticed by Rovelli for the Barrett-Crane model in [128].

4.4.4 Hessian of the total action and derivatives of the insertions

Here we compute the Hessian matrix of the total action $S_{\rm tot}$ at the critical point $j_{ab} = j_{0ab}$, $(g_a^+, g_a^-) = (\bar{g}_a^+, \bar{g}_a^-)$. We introduce a local chart of coordinates $(\vec{p}_a^{\,+}, \vec{p}_a^{\,-})$ in a neighborhood of the point $(\bar{g}_a^+, \bar{g}_a^-)$ on $SU(2) \times SU(2)$. The parametrization is defined as follows: we introduce

$$g_a^{\pm}(p_a^{\pm}) = h(p_a^{\pm})\, \bar{g}_a^{\pm} \tag{4.81}$$

with $h(p_a^{\pm}) = \sqrt{1 - |\vec{p}_a^{\,\pm}|^2} + i\vec{p}_a^{\,\pm} \cdot \vec{\sigma}$. The vector $\vec{p}_a^{\,\pm}$ is assumed to be in a neighborhood of the origin, which corresponds to the critical point $\bar{g}_a^{\pm}$. We introduce also the notation $n_a^{\pm}$

$$n_a^{\pm} = \bar{R}_a^{\pm} n_a \tag{4.82}$$

where $\bar{R}_a^{\pm}$ is the rotation associated to the $SU(2)$ group element $\bar{g}_a^{\pm}$. The bivectors $(j_{ab} n_{ab}^+, j_{ab} n_{ab}^-)$ have the geometrical interpretation of area bivectors associated to the triangles of a 4-simplex with faces of area proportional to j_{ab}.

The Hessian matrix is obtained computing second derivatives of the total action with respect to j_{ab}, p_a^+ and p_a^-, and evaluating it at the point $j_{ab} = j_{0ab}$ and $p_a^{\pm} = 0$. With this definitions we have that the (gauge-fixed) Hessian matrix is a $(10{+}12{+}12) \times (10{+}12{+}12)$ matrix (as it does not contain derivatives w.r.t. $g_1^{\pm}$) and has the following structure:

$$S''_{\rm tot} = \begin{pmatrix} \frac{\partial^2 S_{\rm tot}}{\partial j \partial j} & 0_{10\times 12} & 0_{10\times 12} \\ 0_{12\times 10} & \frac{\partial^2 S_{\rm tot}}{\partial p^+ \partial p^+} & 0_{12\times 12} \\ 0_{12\times 10} & 0_{12\times 12} & \frac{\partial^2 S_{\rm tot}}{\partial p^- \partial p^-} \end{pmatrix} \tag{4.83}$$

as

$$\left.\frac{\partial^2 S_{\rm tot}}{\partial p_a^{i\pm} \partial p_b^{j\mp}}\right|_{\vec{p}=0} = 0 \ , \quad \left.\frac{\partial^2 S_{\rm tot}}{\partial j_{ab} \partial p_c^{j\mp}}\right|_{\vec{p}=0} = 0 \ . \tag{4.84}$$

For the non-vanishing entries we find

$$Q_{(ab)(cd)} = \left.\frac{\partial^2 S_{\rm tot}}{\partial j_{ab} \partial j_{cd}}\right|_{\vec{p}=0} = -\frac{\alpha^{(ab)(cd)}}{\sqrt{j_{0ab}}\sqrt{j_{0cd}}} + (S''_{\rm Regge})_{(ab)(cd)} \ , \tag{4.85}$$

$$H^{\pm}_{(ai)(bj)} = \left.\frac{\partial^2 S_{\rm tot}}{\partial p_a^{i\pm} \partial p_b^{j\pm}}\right|_{\vec{p}=0} = 2i\gamma^{\pm} j_{0ab} (\delta^{ij} - n_{ab}^{i\pm} n_{ab}^{j\pm} + i\epsilon^{ijk} n_{ab}^{k\pm}) \ , \tag{4.86}$$

$$H^{\pm}_{(ai)(aj)} = \left.\frac{\partial^2 S_{\rm tot}}{\partial p_a^{i\pm} \partial p_a^{j\pm}}\right|_{\vec{p}=0} = -2i\gamma^{\pm} \sum_{b\neq a} j_{0ab} (\delta^{ij} - n_{ab}^{i\pm} n_{ab}^{j\pm}) \ , \tag{4.87}$$

where we have defined the $10{\times}10$ matrix of second derivatives of the Regge action

$$(S''_{\rm Regge})_{(ab)(cd)} = \left.\frac{\partial^2 S_{\rm Regge}}{\partial j_{ab} \partial j_{cd}}\right|_{j_{0ab}} \ . \tag{4.88}$$

We report also the first derivatives of the insertion $q_n^{ab}(g^+, g^-)$ evaluated at the critical point:

$$\left.\frac{\partial q_n^{ab}}{\partial \vec{p}_a^{\pm}}\right|_{\vec{p}=0} = i\gamma^2\gamma^{\pm} j_{0na} j_{0nb} (\vec{n}_{nb}^{\pm} - \vec{n}_{na}\cdot\vec{n}_{nb}\,\vec{n}_{na}^{\pm} + i\,\vec{n}_{na}^{\pm}\times\vec{n}_{nb}^{\pm})\;, \tag{4.89}$$

$$\left.\frac{\partial q_n^{ab}}{\partial \vec{p}_n^{\pm}}\right|_{\vec{p}=0} = -i\gamma^2\gamma^{\pm} j_{0na} j_{0nb} (\vec{n}_{na}^{\pm} + \vec{n}_{nb}^{\pm})(1 - \vec{n}_{na}\cdot\vec{n}_{nb})\;, \tag{4.90}$$

$$\left.\frac{\partial q_n^{ab}}{\partial j_{cd}}\right|_{\vec{p}=0} = \gamma^2 \left.\frac{\partial (j_{na}\vec{n}_{na}\cdot j_{nb}\vec{n}_{nb})}{\partial j_{cd}}\right|_{j_{0ab}} . \tag{4.91}$$

We recall that in all these expressions the normals $\vec{n}_{ab}$ are functions of j_{ab} as explained in section 4.1. These expressions will be used in section 4.6 to compute the leading order of the LQG propagator.

4.5 Expectation value of metric operators

Before focusing on the LQG propagator, i.e. on the two-point function, here we briefly discuss the one-point function $\langle E_n^a \cdot E_n^b\rangle$. Its meaning is the dynamical expectation value of the metric operator. The fact that it is non-vanishing provides the background for the propagator. Using the technique developed in the previous sections we can compute it at the leading order in the large spin expansion. We use the integral formula for the metric operator (4.43)-(4.44) and the stationary phase analysis of section 4.4 and find that the expectation value of the metric operator is simply given by the evaluation of the insertion $q_n^{ab}(g^+, g^-)$ at the critical point

$$\langle E_n^a \cdot E_n^b\rangle = q_n^{ab}(g^+, g^-)\big|_{j_{0ab},\bar{g}^+,\bar{g}^-} + \mathcal{O}(j_0). \tag{4.92}$$

For the diagonal components $a = b$ we have that the insertion is simply given by $q_n^{aa} = (\gamma j_{na})^2$ so that its evaluation at the critical point gives the area square of the triangle f_{na}. For the off-diagonal components we have that $q_n^{ab} = A_n^a \cdot A_n^b$ where A_n^{ai} is given in equation (4.54). Its evaluation at the critical point can be easily found using equation (4.72) in expression (4.54). We find

$$\vec{A}^{na}\Big|_{j_{0ab},\bar{g}^+,\bar{g}^-} = \vec{A}^{na+}\Big|_{j_{0ab},\bar{g}^+} + \vec{A}^{na-}\Big|_{j_{0ab},\bar{g}^-} = \gamma j_{0na}^+\vec{n}_{na}(j_0) + \gamma j_{0na}^-\vec{n}_{na}(j_0) = \gamma j_{0na}\vec{n}_{na}(j_0) \tag{4.93}$$

so that $\vec{A}^{na}$ at the critical point evaluates to the classical value $\vec{E}_{n\mathrm{cl}}^a = \gamma j_{0na}\vec{n}_{na}(j_0)$, the normal to the face a of the tetrahedron n (normalized to the area of the face). It is the classical counterpart of the operator $(E_n^a)^i$. Therefore we have that at the leading order the expectation value of the off-diagonal components is given by the dihedral angle between two faces of a tetrahedron

$$\begin{aligned}\langle E_n^a \cdot E_n^b \rangle &= \vec{E}^a_{n\mathrm{cl}} \cdot \vec{E}^b_{n\mathrm{cl}} + \mathcal{O}(j_0) \\ &= \gamma^2 j_{0na} j_{0nb}\, \vec{n}_{na}(j_0) \cdot \vec{n}_{nb}(j_0) + \mathcal{O}(j_0)\;. \end{aligned} \tag{4.94}$$

They have the expected geometrical meaning. We observe that the same quantities computed with the Barrett-Crane spinfoam dynamics do not show the right behavior when the off-diagonal components of the metric operator are considered.

Using the same technique we can evaluate the leading order of the two-point function. We have that

$$\langle E_n^a \cdot E_n^b\, E_m^c \cdot E_m^d \rangle = E^a_{n\mathrm{cl}} \cdot E^b_{n\mathrm{cl}}\, E^c_{m\mathrm{cl}} \cdot E^d_{m\mathrm{cl}} + \mathcal{O}(j_0^3)\;. \tag{4.95}$$

The quantity we are specifically interested in in this chapter is the *connected* two-point function. It is of order $\mathcal{O}(j_0^3)$, therefore it requires the next-to-leading orders in equations (4.94) and (4.95). Such orders depend on the measure $\mu(j)$. However in the computation of the connected part, these contributions cancel. The technique we use in next section for the calculation of the connected two-point function is the one introduced in section (4.4.2) and captures directly the leading order.

4.6 LQG propagator: the leading order

We have defined the LQG propagator as the connected two-point function $G^{abcd}_{nm} = \langle E_n^a \cdot E_n^b\, E_m^c \cdot E_m^d \rangle - \langle E_n^a \cdot E_n^b \rangle \langle E_m^c \cdot E_m^d \rangle$. Using the integral formula (4.43)-(4.44) and the result (4.68) for the asymptotics of connected two-point functions, we can compute the LQG propagator in terms of (the inverse of) the Hessian of the total action and of the derivative of the metric operator insertions at the critical point. These two ingredients are computed in section 4.4.4. Using them, we find that the LQG propagator is given by

$$\begin{aligned} G^{abcd}_{nm}(\alpha) = \sum_{p,q,r,s} & Q^{-1}_{(pq)(rs)} \frac{\partial q_n^{ab}}{\partial j_{pq}} \frac{\partial q_m^{cd}}{\partial j_{rs}} + \\ & + \sum_{r,s=2}^{5} \sum_{i,k=1}^{3} \left((H^+)^{-1}_{(ri)(sk)} \frac{\partial q_n^{ab}}{\partial p_r^{i+}} \frac{\partial q_m^{cd}}{\partial p_s^{k+}} + (H^-)^{-1}_{(ri)(sk)} \frac{\partial q_n^{ab}}{\partial p_r^{i-}} \frac{\partial q_m^{cd}}{\partial p_s^{k-}} \right) \\ & + \mathcal{O}(j_0^2) \end{aligned} \tag{4.96}$$

where all the terms appearing in this expression are defined in section 4.4.4. From this expression we can extract the dependence on the boundary spin j_0 and on the Immirzi parameter γ. We notice that the combinations

$$R_{nm}^{abcd} = \frac{1}{\gamma^3 j_0^3} \sum_{p<q,r<s} Q^{-1}_{(pq)(rs)} \frac{\partial q_n^{ab}}{\partial j_{pq}} \frac{\partial q_m^{cd}}{\partial j_{rs}} \,, \tag{4.97}$$

$$X_{nm}^{abcd} = \frac{1}{2\gamma^4 j_0^3} \sum_{r,s=2}^{5} \sum_{i,k=1}^{3} \Big(\frac{1}{\gamma^+} (H^+)^{-1}_{(ri)(sk)} \frac{\partial q_n^{ab}}{\partial p_r^{i+}} \frac{\partial q_m^{cd}}{\partial p_s^{k+}} + \frac{1}{\gamma^-} (H^-)^{-1}_{(ri)(sk)} \frac{\partial q_n^{ab}}{\partial p_r^{i-}} \frac{\partial q_m^{cd}}{\partial p_s^{k-}} \Big) \,, \tag{4.98}$$

$$Y_{nm}^{abcd} = \frac{1}{2\gamma^4 j_0^3} \sum_{r,s=2}^{5} \sum_{i,k=1}^{3} \Big(\frac{1}{\gamma^+} (H^+)^{-1}_{(ri)(sk)} \frac{\partial q_n^{ab}}{\partial p_r^{i+}} \frac{\partial q_m^{cd}}{\partial p_s^{k+}} - \frac{1}{\gamma^-} (H^-)^{-1}_{(ri)(sk)} \frac{\partial q_n^{ab}}{\partial p_r^{i-}} \frac{\partial q_m^{cd}}{\partial p_s^{k-}} \Big) \,, \tag{4.99}$$

are in fact independent from j_0 and from γ. In terms of these quantities we have that the LQG propagator has the following structure

$$G_{nm}^{abcd}(\alpha) = (\gamma j_0)^3 \big(R_{nm}^{abcd}(\alpha) + \gamma X_{nm}^{abcd} + \gamma^2 Y_{nm}^{abcd} \big) \, + \mathcal{O}(j_0^2) \tag{4.100}$$

where the dependence on γ and on j_0 has been made explicit now. The matrices R_{nm}^{abcd}, X_{nm}^{abcd} and Y_{nm}^{abcd} can be evaluated algebraically. Only the matrix R_{nm}^{abcd} depends on the three parameters $\alpha_0, \alpha_1, \alpha_2$ appearing on the boundary state. We find that

$$R_{nm}^{abcd} = \left(\begin{array}{ccc} \begin{pmatrix} c_1 & c_3 & c_3 \\ c_3 & c_2 & c_4 \\ c_3 & c_4 & c_2 \end{pmatrix} & \begin{pmatrix} c_3 & c_5 & c_6 \\ c_5 & c_3 & c_6 \\ c_6 & c_6 & c_4 \end{pmatrix} & \begin{pmatrix} c_3 & c_6 & c_5 \\ c_6 & c_4 & c_6 \\ c_5 & c_6 & c_3 \end{pmatrix} \\ \begin{pmatrix} c_3 & c_5 & c_6 \\ c_5 & c_3 & c_6 \\ c_6 & c_6 & c_4 \end{pmatrix} & \begin{pmatrix} c_2 & c_3 & c_4 \\ c_3 & c_1 & c_3 \\ c_4 & c_3 & c_2 \end{pmatrix} & \begin{pmatrix} c_4 & c_6 & c_6 \\ c_6 & c_3 & c_5 \\ c_6 & c_5 & c_3 \end{pmatrix} \\ \begin{pmatrix} c_3 & c_6 & c_5 \\ c_6 & c_4 & c_6 \\ c_5 & c_6 & c_3 \end{pmatrix} & \begin{pmatrix} c_4 & c_6 & c_6 \\ c_6 & c_3 & c_5 \\ c_6 & c_5 & c_3 \end{pmatrix} & \begin{pmatrix} c_2 & c_4 & c_3 \\ c_4 & c_2 & c_3 \\ c_3 & c_3 & c_1 \end{pmatrix} \end{array} \right) \tag{4.101}$$

where

$$c_1 = 4\beta_1 \ \ , \ \ c_2 = 4\beta_2 \ \ , \ \ c_3 = -\frac{2}{3}\,(2\beta_0 - 3\beta_1 + 3\beta_2) \ , \tag{4.102}$$

$$c_4 = \frac{1}{3}\,(8\beta_0 - 12\beta_1) \ , \ c_5 = \frac{1}{9}\,(49\beta_0 - 93\beta_1 + 48\beta_2) \ , \ c_6 = -\frac{1}{9}\,(23\beta_0 - 42\beta_1 + 15\beta_2) \ , \tag{4.103}$$

and[12]

$$\beta_0 = \frac{1}{10}\left(-\frac{1}{\alpha_0+6\alpha_1+3\alpha_2}+\frac{32}{-8\alpha_0-8\alpha_1+16\alpha_2+i\sqrt{15}}-\frac{5}{\alpha_0-2\alpha_1+\alpha_2+i\sqrt{15}}\right)\ , \tag{4.106}$$

$$\beta_1 = \frac{1}{30}\left(-\frac{3}{\alpha_0+6\alpha_1+3\alpha_2}+\frac{16}{-8\alpha_0-8\alpha_1+16\alpha_2+i\sqrt{15}}+\frac{5}{\alpha_0-2\alpha_1+\alpha_2+i\sqrt{15}}\right)\ , \tag{4.107}$$

$$\beta_2 = \frac{1}{30}\left(-\frac{3}{\alpha_0+6\alpha_1+3\alpha_2}-\frac{64}{-8\alpha_0-8\alpha_1+16\alpha_2+i\sqrt{15}}-\frac{5}{\alpha_0-2\alpha_1+\alpha_2+i\sqrt{15}}\right)\ . \tag{4.108}$$

The matrices X^{abcd}_{nm} and Y^{abcd}_{nm} turn out to be proportional

$$X^{abcd}_{nm} = \frac{7}{36}Z^{abcd}_{nm} \quad , \quad Y^{abcd}_{nm} = -i\frac{\sqrt{15}}{36}Z^{abcd}_{nm}\ , \tag{4.109}$$

with the matrix Z^{abcd}_{nm} given by

$$Z^{abcd}_{nm} = \begin{pmatrix} \begin{pmatrix} 0 & 0 & 0 \\ 0 & 0 & 0 \\ 0 & 0 & 0 \end{pmatrix} & \begin{pmatrix} 0 & -1 & e^{i\frac{\pi}{3}} \\ -1 & 0 & e^{-i\frac{\pi}{3}} \\ e^{i\frac{\pi}{3}} & e^{-i\frac{\pi}{3}} & 0 \end{pmatrix} & \begin{pmatrix} 0 & e^{-i\frac{\pi}{3}} & -1 \\ e^{-i\frac{\pi}{3}} & 0 & e^{i\frac{\pi}{3}} \\ -1 & e^{i\frac{\pi}{3}} & 0 \end{pmatrix} \\ \begin{pmatrix} 0 & -1 & e^{i\frac{\pi}{3}} \\ -1 & 0 & e^{-i\frac{\pi}{3}} \\ e^{i\frac{\pi}{3}} & e^{-i\frac{\pi}{3}} & 0 \end{pmatrix} & \begin{pmatrix} 0 & 0 & 0 \\ 0 & 0 & 0 \\ 0 & 0 & 0 \end{pmatrix} & \begin{pmatrix} 0 & e^{i\frac{\pi}{3}} & e^{-i\frac{\pi}{3}} \\ e^{i\frac{\pi}{3}} & 0 & -1 \\ e^{-i\frac{\pi}{3}} & -1 & 0 \end{pmatrix} \\ \begin{pmatrix} 0 & e^{-i\frac{\pi}{3}} & -1 \\ e^{-i\frac{\pi}{3}} & 0 & e^{i\frac{\pi}{3}} \\ -1 & e^{i\frac{\pi}{3}} & 0 \end{pmatrix} & \begin{pmatrix} 0 & e^{i\frac{\pi}{3}} & e^{-i\frac{\pi}{3}} \\ e^{i\frac{\pi}{3}} & 0 & -1 \\ e^{-i\frac{\pi}{3}} & -1 & 0 \end{pmatrix} & \begin{pmatrix} 0 & 0 & 0 \\ 0 & 0 & 0 \\ 0 & 0 & 0 \end{pmatrix} \end{pmatrix}\ . \tag{4.110}$$

This is the main result of the chapter, the scaling and the tensorial structure of metric correlations in LQG. In the following we collect some remarks on this result:

[12] We notice that the inverse of the matrix $Q_{(ab)(cd)}$ can be written in terms of the parameters β_k using the formalism (4.26) introduced in section 4.1,

$$(Q^{-1})^{(ab)(cd)} = \sum_{k=0}^{2} j_0 \beta_k P_k^{(ab)(cd)}\ . \tag{4.104}$$

The matrix $Q_{(ab)(cd)}$ is defined in equation (4.85) and is given by

$$Q^{(ab)(cd)} = \frac{1}{j_0}\sum_{k=0}^{2}(ih_k-\alpha_k)P_k^{(ab)(cd)}\ , \tag{4.105}$$

with $h_0 = -\frac{9}{4}\sqrt{\frac{3}{5}}$, $h_1 = \frac{7}{8}\sqrt{\frac{3}{5}}$, $h_2 = -\sqrt{\frac{3}{5}}$.

- The LQG propagator scales as j_0^3, as expected for correlations of objects with dimensions of area square, $E_n^a \cdot E_n^b \sim (\gamma j_0)^2$.

- The off-diagonal components are not suppressed as happened for the Barrett-Crane model [142, 143] and have the same scaling as the diagonal ones.

- The contribution R_{nm}^{abcd} in (4.100) matches exactly with the matrix of correlations of areas and angles computed in perturbative quantum Regge calculus with a boundary state as done in [140].

- On the other hand, the 'γ-terms' in (4.100), $\gamma X_{nm}^{abcd} + \gamma^2 Y_{nm}^{abcd}$, are new and proper of the spin foam model. They come from $SU(2) \times SU(2)$ "group" fluctuations. They don't contribute to area-area correlations, nor to area-angle correlations. On the other hand, their contribution to angle-angle correlations is non-trivial.

- In the limit $\gamma \to 0$ and $j_0 \to \infty$ with $\gamma j_0 = \text{const} = A_0$, only the Regge contribution survives. It is interesting to notice that the same limit was considered in [160] in the context of loop quantum cosmology.

- The 'γ-terms' have an interesting feature that we now describe. Let us focus on the tensorial components $G_4 = G_{12}^{(34)(45)}$ and $G_5 = G_{12}^{(35)(45)}$. They are related by a permutation of the vertices 4 and 5, keeping the other three vertices fixed. The 'Regge-term' is invariant under this permutation, $R_{12}^{(34)(45)} = R_{12}^{(35)(45)}$. On the other hand the 'γ-terms' are not. In particular we have that

$$\gamma X_{12}^{(35)(45)} + \gamma^2 Y_{12}^{(35)(45)} = e^{i\frac{2\pi}{3}} \left(\gamma X_{12}^{(34)(45)} + \gamma^2 Y_{12}^{(34)(45)} \right) . \tag{4.111}$$

  It would be interesting to identify the origin of the phase $\frac{2\pi}{3}$. We notice that the permutation of the vertex 4 with the vertex 5 of the boundary spin network corresponds to a parity transformation of the four-simplex. In this sense the 'γ-terms' are parity violating.

In next section we investigate the relation of the result found with the graviton propagator computed in perturbative quantum field theory.

4.7 Comparison with perturbative quantum gravity

The motivation for studying the LQG propagator comes from the fact that it probes a regime of the theory where predictions can be compared to the ones obtained perturbatively in a quantum field theory of gravitons on flat space [136, 137, 28]. Therefore it is interesting to investigate this relation already at the preliminary level of a single spin foam vertex studied in this chapter. In this section we investigate this relation within the setting discussed in [142, 143, 135].

In perturbative quantum gravity[13], the graviton propagator in the harmonic gauge is given by

$$\langle h_{\mu\nu}(x)h_{\rho\sigma}(y)\rangle = \frac{-1}{2|x-y|^2}(\delta_{\mu\rho}\delta_{\nu\sigma}+\delta_{\mu\sigma}\delta_{\nu\rho}-\delta_{\mu\nu}\delta_{\rho\sigma}). \tag{4.112}$$

Correlations of geometrical quantities can be computed perturbatively in terms of the graviton propagator. For instance the angle at a point x_n between two intersecting surfaces f_{na} and f_{nb} is given by[14]

$$q_n^{ab} = g_{\mu\nu}(x_n)g_{\rho\sigma}(x_n)B^{\mu\rho}_{na}(x_n)B^{\nu\sigma}_{nb}(x_n) \tag{4.113}$$

where $B^{\mu\nu}$ is the bivector associated to the surface[15]. As a result the angle fluctuation can be written in terms of the graviton field

$$\delta q_n^{ab} = h_{\mu\nu}(x_n)\,(T_n^{ab})^{\mu\nu}\ , \tag{4.115}$$

where we have defined the tensor $(T_n^{ab})^{\mu\nu} = 2\delta_{\rho\sigma}B^{\mu\rho}_{na}(x_n)B^{\nu\sigma}_{nb}(x_n)$. The angle correlation $(G^{abcd}_{nm})_{\rm qft}$ is simply given by

$$(G^{abcd}_{nm})_{\rm qft} = \langle h_{\mu\nu}(x_n)h_{\rho\sigma}(x_m)\rangle\ (T_n^{ab})^{\mu\nu}(T_m^{cd})^{\rho\sigma}\ . \tag{4.116}$$

In particular, this quantity can be computed for couples of surfaces identified by triangles of area A_0 living on the boundary of a regular Euclidean 4-simplex. This quantity has been computed in [143] and we report it here for reference,

$$\left(G^{abcd}_{nm}\right)_{\rm qft} = \frac{-A_0^3}{18\sqrt{3}\times 512}\begin{pmatrix} \begin{pmatrix} -16 & 6 & 6\\ 6 & -28 & 16\\ 6 & 16 & -28\end{pmatrix} & \begin{pmatrix} 6 & 4 & -7\\ 4 & 6 & -7\\ -7 & -7 & 16\end{pmatrix} & \begin{pmatrix} 6 & -7 & 4\\ -7 & 16 & -7\\ 4 & -7 & 6\end{pmatrix}\\ \begin{pmatrix} 6 & 4 & -7\\ 4 & 6 & -7\\ -7 & -7 & 16\end{pmatrix} & \begin{pmatrix} -28 & 6 & 16\\ 6 & -16 & 6\\ 16 & 6 & -28\end{pmatrix} & \begin{pmatrix} 16 & -7 & -7\\ -7 & 6 & 4\\ -7 & 4 & 6\end{pmatrix}\\ \begin{pmatrix} 6 & -7 & 4\\ -7 & 16 & -7\\ 4 & -7 & 6\end{pmatrix} & \begin{pmatrix} 16 & -7 & -7\\ -7 & 6 & 4\\ -7 & 4 & 6\end{pmatrix} & \begin{pmatrix} -28 & 16 & 6\\ 16 & -28 & 6\\ 6 & 6 & -16\end{pmatrix}\end{pmatrix}$$

[13]Here we consider the Euclidean case.

[14]We thank E. Alesci for a discussion on this point.

[15]To be more specific, we consider local coordinates (σ^1,σ^2) for a surface t and call $t^\mu(\sigma)$ its embedding in the $4d$ manifold. The bivector $B_t^{\mu\nu}(x)$ is defined as

$$B_t^{\mu\nu}(x) = \frac{\partial t^\mu}{\partial\sigma^\alpha}\frac{\partial t^\nu}{\partial\sigma^\beta}\epsilon^{\alpha\beta}\ . \tag{4.114}$$

The question we want to answer here is if the quantity $(G^{abcd}_{nm})_{\rm qft}$ and the leading order of the LQG propagator given by equation (4.100) can match. As we can identify γj_0 with the area A_0, we have that the two have the same scaling. The non-trivial part of the matching is the tensorial structure. Despite the fact that we have 9×9 tensorial components, only six of them are independent as the others are related by symmetries of the configuration we are considering. On the other hand the semiclassical boundary state $|\Psi_0\rangle$ we used in the LQG calculation has only three free parameters, $\alpha_0, \alpha_1, \alpha_2$. Therefore we can ask if there is a choice of these 3 parameters such that we can satisfy the 6 independent equations given by the matching condition

$$\Big(G^{abcd}_{nm}(\alpha)\Big)_{\rm lqg} = \Big(G^{abcd}_{nm}\Big)_{\rm qft} \,. \tag{4.117}$$

We find that a solution in terms of the parameters α_k can be found only in the limit of vanishing Immirzi parameter, keeping constant the product $\gamma j_0 = A_0$. In this limit we find a unique solution for α_k given by

$$\alpha_0 = \frac{1}{100}(495616\sqrt{3} - 45\sqrt{15}\, i) \,, \tag{4.118}$$

$$\alpha_1 = \frac{1}{200}(-299008\sqrt{3} + 35\sqrt{15}\, i) \,, \tag{4.119}$$

$$\alpha_2 = \frac{1}{25}(31744\sqrt{3} - 5\sqrt{15}\, i) \,. \tag{4.120}$$

Therefore the matching condition (4.117) can be satisfied, at least in the specific limit considered. Having found a non-trivial solution, it is interesting to study the real part of the matrix $\alpha^{(ab)(cd)}$ in order to determine if it is positive definite. Its eigenvalues (with the associated degeneracy) are

$$\lambda_5 = 9216\sqrt{3} \,, \quad \deg = 5 \,, \tag{4.121}$$

$$\lambda_4 = \frac{4608\sqrt{3}}{5} \,, \quad \deg = 4 \,, \tag{4.122}$$

$$\lambda_1 = -\frac{1024\sqrt{3}}{5} \,, \quad \deg = 1 \,. \tag{4.123}$$

We notice that all the eigenvalues are positive except one, λ_1. The corresponding eigenvector represents conformal rescalings of the boundary state, $j_{0ab} \to \lambda j_{0ab}$. It would be interesting to determine its origin and to understand how the result depends on the choice of gauge made for the graviton propagator (4.112).

4.8 Summary

In this chapter we have studied correlation functions of metric operators in loop quantum gravity. The analysis presented involves two distinct ingredients:

- The first is a setting for defining correlation functions. The setting is the boundary amplitude formalism. It involves a boundary semiclassical state $|\Psi_0\rangle$ which identifies the regime of interest, loop quantum gravity operators $E_n^a \cdot E_n^b$ which probe the quantum geometry on the boundary, a spin foam model $\langle W|$ which implements the dynamics. The formalism allows to define semiclassical correlation functions in a background-independent context.

- The second ingredient consists in an approximation scheme applied to the quantity defined above. It involves a vertex expansion and a large spin expansion. It allows to estimate the correlation functions explicitly. The explicit result can then be compared to the graviton propagator of perturbative quantum gravity. In this chapter we focused on the lowest order in the vertex expansion and the leading order in the large spin expansion.

The results found in the chapter can be summarized as follows:

1. In section 4.1 we have introduced a semiclassical state $|\Psi_0\rangle$ peaked on the intrinsic and the extrinsic geometry of the boundary of a regular Euclidean 4-simplex. The technique used to build this state is the following: (i) we use the coherent intertwiners introduced in [58, 59] to define coherent spin networks as in [81]; (ii) we choose the normals labelling intertwiners so that they are compatible with a simplicial 3-geometry (4.15). This addresses the issue of discontinuous lengths identified in [92]; (iii) then we take a gaussian superposition over coherent spin networks in order to peak on extrinsic curvature as in [128, 138]. This state is an improvement of the ansatz used in [142, 143, 135], as it depends only on the three free parameters $\alpha_0, \alpha_1, \alpha_2$.

2. In section 4.3 we have defined expectation values of geometric observables on a semiclassical state. The LQG propagator is defined in equation (4.34) as a connected correlation function for the product of two metric operators

$$G_{nm}^{abcd} = \langle E_n^a \cdot E_n^b \; E_m^c \cdot E_m^d \rangle - \langle E_n^a \cdot E_n^b \rangle \, \langle E_m^c \cdot E_m^d \rangle \; . \tag{4.124}$$

   This is the object that in principle can be compared to the graviton propagator on flat space: the background is coded in the expectation value of the geometric operators and the propagator measures correlations of fluctuations over this background.

3. In section 4.3.2 we have introduced a technique which allows to write LQG metric operators as insertions in a $SO(4)$ group integral. It can be interpreted as the covariant version of the LQG operators. The formalism works for arbitrary fixed triangulation. Having an integral formula for expectation values and correlations of metric operators allows to formulate the large spin expansion as a stationary phase approximation. The problem is studied in detail restricting attention to the lowest order in the vertex expansion, i.e. at the single-vertex level.

4. The analysis of the large spin asymptotics is performed in section 4.4. The technique used is the one introduced by Barrett et al in [81]. There, the large spin asymptotics of the boundary amplitude of a coherent spin network is studied and four distinct critical points are found to contribute to the asymptotics. Two of them are related to different orientations of a 4-simplex. The other two come from selfdual configurations. Here, our boundary state is peaked also on extrinsic curvature. The feature of this boundary state is that it selects only one of the critical points, extracting $\exp iS_{\text{Regge}}$ from the asymptotics of the EPRL spin foam vertex. This is a realization of the mechanism first identified by Rovelli in [128] for the Barrett-Crane model.

6. In 4.5 we compute expectation values of LQG metric operators at leading order and find that they reproduce the intrinsic geometry of the boundary of a regular 4-simplex.

7. Computing correlations of geometric operators requires going beyond the leading order in the large spin expansion. In section 4.4.2 we derive a formula for computing directly the *connected* two-point correlation function to the lowest non-trivial order in the large spin expansion. The formula is used in section 4.4.4.

8. The result of the calculation, the LQG propagator, is presented in section 4.6. We find that the result is the sum of two terms: a "Regge term" and a "γ-term". The Regge term coincides with the correlations of areas and angles computed in Regge calculus with a boundary state [140]. It comes from correlations of fluctuations of the spin variables and depends on the parameters α_k of the boundary state. The "γ-term" comes from fluctuations of the $SO(4)$ group variables. An explicit algebraic calculation of the tensorial components of the LQG propagator is presented.

9. The LQG propagator can be compared to the graviton propagator. This is done in section 4.7. We find that the LQG propagator has the correct scaling behaviour. The three parameters α_k appearing in the semiclassical boundary state can be chosen so that the tensorial structure of the LQG propagator matches with the one of the graviton propagator. The matching is obtained in the limit $\gamma \to 0$ with γj_0 fixed.

Now we would like to put these results in perspective with respect to the problem of extracting the low energy regime of loop quantum gravity and spin foams.

Deriving the LQG propagator at the level of a single spin foam vertex is certainly only a first step. Within the setting of a vertex expansion, an analysis of the LQG propagator for a finite number of spinfoam vertices is needed. Some of the techniques developed in this chapter generalize to this more general case. In particular superpositions of coherent spin networks can be used to build semiclassical states peaked on the intrinsic and the extrinsic curvature of an arbitrary boundary Regge geometry. Moreover, the expression of the LQG metric operator in terms of $SO(4)$ group integrals presented in this chapter works for an arbitrary number of spin foam vertices and allows to derive an integral representation of the LQG propagator in the general case, analogous to the one of [120] but with non-trivial insertions. This representation is the appropriate one for the analysis of the large spin asymptotics along the lines discussed for Regge calculus in [134]. The non-trivial question which needs to be answered then is if the semiclassical boundary state is able to enforce semiclassicality in the bulk. Another feature identified in this chapter which appears to be general is that, besides the expected Regge contribution, correlations of LQG metric operators have a non-Regge contribution which is proper of the spin foam model. It would be interesting to investigate if this contribution propagates when more than a single spin foam vertex is considered.

Chapter 5

Towards Spinfoam cosmology

The dynamics of loop quantum gravity (LQG) can be given in covariant form by using the *spinfoam* formalism. In this chapter[1] we apply this formalism to cosmology. In other words, we introduce a spinfoam formulation of quantum cosmology, or a "spinfoam cosmology". We obtain two results. The first is that physical transition amplitudes can be computed, in an appropriate expansion. We compute explicitly the transition amplitude between homogeneous isotropic coherent states, at first order. The second and main result is that this amplitude is in the kernel of an operator $\hat{C}$, and the classical limit of $\hat{C}$ turns out to be precisely the gravity part of the Hamiltonian constraint of the Friedmann dynamics of homogeneous isotropic cosmology. In other words, we show that LQG yields the Friedmann equation in a suitable limit. Since we work in the absence of matter, thought, the dynamics of the model we consider is still rather trivial.

LQG has seen momentous developments in the last few years. We make use of several of these developments here, combining them together. The first ingredient we utilize is the "new" spinfoam vertex [110, 58, 151, 6, 5]. The second is the Kaminski-Kisielowski-Lewandowski extension of this to vertices of arbitrary-valence [109]. The third ingredient is the coherent state technology [123, 112, 85, 86, 87, 88, 113, 114, 115, 84, 108, 50, 95], and in particular the holomorphic coherent states discussed in detailed in [94]. These states define a holomorphic representation of LQG [112, 116], and we work here in this representation.

Our strategy is the following. We consider the standard Hilbert space of canonical LQG and we assume the dynamics to be given by the new vertex. We consider holomorphic coherent states in this Hilbert space and we work in the holomorphic representation they define.

We truncate LQG down to a graph with a finite number of links. In particular, the calculation is based on the "dipole" graph formed by two nodes connected by four links

[1] This chapter is based on work done together with Carlo Rovelli and Francesca Vidotto. The results of this chapter have been published in [91].

[161]. This choice determines a Hilbert space, which describes a finite number of the degrees of freedom of the gravitational field. These degrees of freedom can be identified as the lowest modes in a multipole expansion of the metric in hyper-spherical harmonics on S_3 [162]. That is, they describe a closed cosmology, with anisotropies and a few low-mode inhomogeneities.

In particular, we consider coherent states that are peaked on homogeneous isotropic geometries. We emphasize the fact that these states are just peaked on homogeneous and isotropic geometries, but they also include fluctuations of the inhomogeneous and anisotropic degrees of freedom. So, the dynamics of the quantum theory we consider *does* include inhomogeneous and anisotropic degrees of freedom. Homogeneous-isotropic coherent states are labelled by two parameters which capture the scale factor a of standard cosmology and its time derivative $\dot{a}$; or, equivalently, the p and c canonical variables used in Loop Quantum Cosmology (LQC). In the holomorphic representation, these two quantities appear in the complex combination $z = \alpha c + i\beta p$, and therefore the states we consider are labelled by the complex number z. The transition amplitude between two such states is then an analytic function $W(z, z')$ of two complex variables.

We write this transition amplitude at first order in a vertex expansion. We view this as the analog of a first order calculation in, say, QED perturbation theory. We compute explicitly $W(z, z')$ in the limit in which the geometry is large compared to the Planck scale.

In other words, we compute the transition amplitude between macroscopical homogeneous isotropic cosmological spaces in LQG, taking three approximations from the complete theory: (i) the truncation of the degrees of freedom to those defined on a finite graph; (ii) the restriction to first order in the vertex expansion; (iii) the large volume limit. The validity of these approximation can only be justified a posteriori, from the correctness of the result.

Our next step is to notice that the transition amplitude computed solves the equations $H\,W(z, z') = 0$ for a certain operator $H = H(z, \hbar\frac{\mathrm{d}}{\mathrm{d}z})$. This fact implies that the amplitude defines a quantum dynamics where the operator constraint $H = 0$ holds. The corresponding classical dynamics will be governed by (the $\hbar \to 0$ limit of) the classical constraint $H(z, \bar{z}) = 0$. When written in terms of p and c, this turns out to be precisely the Hamiltonian constraint that governs (the gravitational part of) the dynamics of a classical Friedmann cosmology, in the limit of large volume. Therefore LQG yields the Friedmann dynamics in this limit.

Several words of caution are necessary. First, we work in the Euclidean theory. Second, the cosmological dynamics that we obtain is the one in the large volume limit and since we do not have any matter present, this has only the solution $a = \mathit{constant}$, which is flat space. With these caveats, our result is that there is an approximation in LQG that leads to classical cosmology.

This result can be compared with those of LQC [163, 164]. In LQC, one first reduces the classical theory to a cosmological system with a finite number of degrees of freedom, and then applies a "loop quantization" to this symmetry reduced model. Thus, one has a complete quantum theory of a truncation of the classical theory. Here, instead, we start from the full quantum theory and take an approximation. Therefore in LQC one studies the exact solution in a truncated system, while here we study approximated solutions in the (hopefully) exact quantum theory. The possibility of introducing a spinfoam-like expansion starting from LQC has been considered in the papers [165, 166, 167]. These papers and the present work can be seen as two converging attempts to construct a spinfoam version of quantum cosmology.

Finally, in our opinion a main reason of interest of the result we present here is that it represents an example of a complete calculation of physical transition amplitude in background independent quantum gravity. It complements the calculation of the two-point function [128, 138, 142, 143, 135], that has been recently completed [90].

In Section 5.1, we briefly recall the definition of the full quantum theory. In Section 5.2, we discuss the approximation that selects a cosmological sector, we compute the resulting transition amplitude. In Section 5.3, we study the classical limit and recover the Friedmann dynamics.

5.1 The theory

5.1.1 Kinematics

The theory is defined on the Hilbert space

$$\mathcal{H} = \bigoplus_{\Gamma} \mathcal{H}_\Gamma \tag{5.1}$$

The sum runs over the abstract graphs Γ. A graph Γ is here a set of L links ℓ and N nodes n, together with two relations s (source) and t (target) assigning a source node $s(\ell)$ and a target node $t(\ell)$ to every link ℓ. The Hilbert space $\mathcal{H}_\Gamma$ is defined to be

$$\mathcal{H}_\Gamma = L_2[SU(2)^L/SU(2)^N] \tag{5.2}$$

where the action of $SU(2)^N$ on the states $\psi(U_l) \in L_2[SU(2)^L]$ is

$$\psi(U_l) \to \psi(V_{s(\ell)} U_l V_{t(\ell)}^{-1}) \ , \qquad V_n \in SU(2)^N \, . \tag{5.3}$$

Two sets of operators are defined on each space $\mathcal{H}_\Gamma$. For each link we have the "holonomy" multiplicative operator $\hat{U}_\ell \, \psi(U_\ell) = U_\ell \, \psi(U_\ell)$ and the "triad" operator $\hat{E}^i_\ell \, \psi(U_\ell) = (8\pi G\hbar\gamma) \, L^i_\ell \, \psi(U_\ell)$ where G is the Newton constant and L^i_ℓ is the left-invariant vector field acting on the variable U_ℓ.

Finally, the state space of the theory is obtained by factoring $\mathcal{H}$ by an equivalence relation, defined as follows. If Γ is a subgraph of Γ' then $\mathcal{H}_\Gamma$ can be naturally identified with a subspace of $\mathcal{H}_{\Gamma'}$. Two states are equivalent if they can be related by this identification, or if they are mapped into each other by the discrete group of the automorphisms of Γ.

These states are to be thought as "boundary states" in the quantum theory. That is, $\mathcal{H}$ must be identified with the space $\mathcal{H}^*_{out} \otimes \mathcal{H}_{in}$ of the initial and final states of non-relativistic quantum mechanics.

Coherent states

An overcomplete basis of coherent states in the Hilbert space $\mathcal{H}_\Gamma$ is provided by the holomorphic states

$$\Psi_{H_\ell}(U_\ell) = \int_{SU(2)^N} \delta g_n \prod_\ell K_t(g^{-1}_{s(\ell)} U_\ell \; g_{t(\ell)} \, H_\ell^{-1}\,). \tag{5.4}$$

Here $H_\ell \in SL(2,\mathbb{C})$, and K_t is (the analytic continuation to $SL(2,\mathbb{C})$ of) the *heat kernel* function on $SU(2)$. This is a function concentrated on the origin of the group, with a spread of order t. Its explicit form is[2]

$$K_t(U) = \sum_j (2j+1) e^{-2t\hbar\, j(j+1)} \; \mathrm{Tr}[D^j(U)] \tag{5.5}$$

where $D^j(U)$ is the Wigner matrix of the spin-j representation of $SU(2)$.

As shown in [94], these states: (i) are the basis of the holomorphic representation [112, 116], (ii) are a special case of Thiemann's complexifier's coherent states [85, 86, 87, 88, 113, 114, 115, 84, 108], (iii) induce Speziale-Livine coherent tetrahedra [58, 59, 73] on the nodes, and (iv) are equal to the the Freidel-Speziale coherent states [50, 95] for large spins.

The states (5.4) are gauge-invariant semiclassical wave packets. The integral in (5.4) projects ("group averages") on the gauge invariant states. If H_ℓ is in the $SU(2)$ subgroup of $SL(2,\mathbb{C})$, the heat kernel peaks each U_ℓ on H_ℓ. The extension of H_ℓ to $SL(2,\mathbb{C})$ has the same effect as taking a gaussian function $\psi(x) = e^{(x-z_o)^2/2} \sim e^{(x-x_o)^2/2} e^{ip_o x}$ for a complex $z_o = x_o + ip_o$; that is, it adds a phase which peaks the states on a value of the variable conjugate to U_ℓ. Thus, the states (5.4) are peaked on the variables U_ℓ as well as on their conjugate momenta.

[2] We choose a parameter t with the dimension of an inverse action, and put $\hbar$ explicitly in the definition of the coherent states, in order to emphasize the fact that the small t limit is the classical limit, and to keep track of the corresponding dependence on $\hbar$. The factor 2 is for later convenience.

The $SL(2,\mathbb{C})$ labels H_ℓ can be given two related interpretations. First, we can decompose each $SL(2,\mathbb{C})$ label in the form

$$H_\ell = e^{i4tE_\ell/8\pi G\gamma}\ U_\ell \tag{5.6}$$

where $U_\ell \in SU(2)$ and $2tE_\ell/(8\pi G\hbar\gamma) \in su(2)$. Then it is not hard to show that U_ℓ and E_ℓ determine the expectation value of the operators $\hat{U}_\ell$ and $\hat{E}_\ell$ on the state ψ_{H_ℓ}

$$\frac{\langle\psi_{H_\ell}\,|\,\hat{U}_\ell\,|\,\psi_{H_\ell}\rangle}{\langle\psi_{H_\ell}\,|\,\psi_{H_\ell}\rangle} = U_\ell\ , \quad \frac{\langle\psi_{H_\ell}\,|\,\hat{E}_\ell\,|\,\psi_{H_\ell}\rangle}{\langle\psi_{H_\ell}\,|\,\psi_{H_\ell}\rangle} = E_\ell\ , \tag{5.7}$$

and that the corresponding spread is small[3]

$$\Delta U_\ell \sim \ \sqrt{t\hbar}, \qquad \Delta E_\ell \sim G\sqrt{\hbar/t}. \tag{5.8}$$

Alternatively, we can decompose each $SL(2,\mathbb{C})$ label in the form

$$H_\ell = n_{s,\ell}\ e^{-i(\xi_\ell + i\eta_\ell)\frac{\sigma_3}{2}}\ n_{t,\ell}^{-1}\ ; \tag{5.9}$$

$\vec{\sigma} = \{\sigma_i\}, i = 1,2,3$ are the Pauli matrices and $n_{s,\ell}, n_{t,\ell} \in SU(2)$. Freidel and Speziale discuss a compelling geometrical interpretation for the $(\vec{n}_s, \vec{n}_t, \xi, \eta)$ labels of each link [50] (here and below, unit-length vectors $\vec{n}$ and $SU(2)$ elements n are related by $\vec{n}\cdot\vec{\sigma} = n\sigma_3 n^{-1}$). For appropriate four-valent states representing a Regge 3-geometry with intrinsic and extrinsic curvature, the vectors $\vec{n}_s, \vec{n}_t$ are the $3d$ normals to the triangles the tetrahedra bounded by the triangle; ξ is the extrinsic curvature at the triangle and η is the area of the triangle divided by $8\pi G\hbar$. For general states, the interpretation extends to a simple generalization of Regge geometries, that Freidel and Speziale have baptized "twisted geometries".

Thus, the holomorphic coherent states provide a convenient basis of wave packets with good geometrical interpretation.

5.1.2 Dynamics

The spinfoam formalism associates an amplitude

$$\langle W\,|\,\psi\rangle = \sum_\sigma \prod_f d_f(\sigma) \prod_v W_v(\sigma) \tag{5.10}$$

to each boundary state $\psi \in \mathcal{H}$. The sum is over the spinfoams σ bounded by ψ. See [5] for a description of this formalism and for the notation. The vertex amplitude is

[3] If we fix a length scale $L \gg \sqrt{\hbar G}$ and choose $2\hbar t = \hbar G/L^2$ we have $\Delta U_\ell \sim \ \sqrt{\hbar G}/L$ and $\Delta E_\ell \sim \sqrt{\hbar G}\,L$.

$W_v(\sigma) = \langle W_v|\psi_v(\sigma)\rangle$, where $\psi_v(\sigma)$ is the spin network obtained by cutting σ with a small 3-sphere surrounding v and the the vertex amplitude that defines the dynamics of LQG is [5, 5, 58, 6, 109]

$$\langle W_v|\psi\rangle = (f\psi)(\mathbb{I}) \ . \tag{5.11}$$

Here $f : \mathcal{H}_\Gamma \to L_2[SO(4)^L/SO(4)^N]$ is defined as follows. Let

$$j^\pm = \frac{1\pm\gamma}{2} j \tag{5.12}$$

and let Y be the map

$$\begin{array}{rccc} Y: & \mathcal{H}^{(j)} & \longrightarrow & \mathcal{H}^{(j^+,j^-)} \\ & |j,m\rangle & & |j^+,m^+;j^-,m^-\rangle \end{array} \tag{5.13}$$

whose matrix elements are given by the Clebsh-Gordan coefficients.

$$Y_m^{m^+m^-} = \langle j^+,m^+;j^-,m^- \,|\, j,m\rangle \ . \tag{5.14}$$

Consider the Peter-Weyl decomposition of $L_2[SU(2)^L]$ and, respectively $L_2[(SO(4)^L]$. Then f is defined by mapping with Y each $\mathcal{H}_j$ terms of the first into the corresponding $\mathcal{H}_{j^+,j^-}$ of the second.

Explicitly, the generalized state W_v in (5.11) is given by

$$W_v(U_\ell) = \int_{SO(4)^N} \delta G_n \ \prod_\ell P_o(U_\ell\,,\, G_{s(\ell)}G^{-1}_{t(\ell)}) \tag{5.15}$$

where

$$P_o(U,G) = \sum_j (2j+1) \ \mathrm{Tr}\Big[D^{(j)}(U)\,Y^\dagger\,D^{(j^+,j^-)}(G)\,Y\Big]. \tag{5.16}$$

Here $D^{(j)}$ is the Wigner matrix of the spin-j representation of $SU(2)$, while $D^{(j^+,j^-)}$ is the Wigner matrix of the spin-(j^+,j^-) representation of $SO(4)$. The first has has dimension $2j+1$ while the second has dimension $(2j^++1)(2j^-+1)$. These matrices with different dimensions are glued by the map Y.

The vertex amplitude takes a simple form on the holomorphic basis defined by the coherent states. By combining the definition (5.15) of the vertex and the definition (5.4) of the coherent states, one obtains the holomorphic form of the vertex amplitude [116]

$$\begin{aligned} W_v(H_\ell) \ &\equiv\ \langle W_v\,|\,\psi_{H_\ell}\rangle = \int_{SU(2)^L} \delta U_\ell \ W(U_\ell)\ \psi_{H_\ell}(U_\ell) \\ &= \int_{SO(4)^N} \delta G_n \ \prod_\ell P_t(H_\ell\,,\, G_{s(\ell)}G^{-1}_{t(\ell)}) \end{aligned} \tag{5.17}$$

where

$$P_t(H,G) = \sum_j (2j+1)e^{-2t\hbar j(j+1)}\mathrm{Tr}\Big[D^{(j)}(H)Y^\dagger D^{(j^+,j^-)}(G)Y\Big]. \tag{5.18}$$

Here $D^{(j)}$ is the analytic continuation of the Wigner matrix from $SU(2)$ to $SL(2,\mathbb{C})$. Below, we use this last expression to compute the quantum evolution in cosmology.

5.2 The cosmological approximation

5.2.1 Graph expansion

There is no physics without approximations. The first approximation we take is to truncate $\mathcal{H}$ to a single fixed graph Γ. Notice that the states with support on smaller graphs (subgraphs of Γ) are all contained in $\mathcal{H}_\Gamma$; therefore the truncation amounts to disregard all states that have support on graphs "larger" that Γ.

We choose Γ to be the graph formed by two disconnected components Γ_i and Γ_f. We think at these as carrying an initial and a final state. In particular we choose $\Gamma_\mathrm{i} = \Gamma_\mathrm{f} = \Delta_2^*$, where the "dipole" graph Δ_2^* is defined by the set of two nodes $\{n_1, n_2\}$, by the set of four links $\{\ell_1, \ell_2, \ell_3, \ell_4\}$, and by the source and target relations $s(\ell) = n_1$ and $t(\ell) = n_2, \forall \ell$. That is

$\Delta_2^* =$ 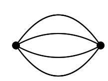 .

The operators defined on the Hilbert space $\mathcal{H}_{\Delta_2^*}$ are (U_ℓ, E_ℓ). These can be interpreted as follows. Consider a space M with the topology of a three sphere, carrying a triad field E and a connection A. Choose an immersion of Δ_2^* into M, and a cellular decomposition Δ_2 of M, dual to Δ_2^*. Δ_2 is the triangulation of the 3-sphere formed by 2 tetrahedra with all their faces identified.[4] We can then identify U_ℓ with the holonomy of A on the link ℓ and E_ℓ with the flux of the triad through the triangle cut by the link ℓ, parallel transported to n_1.

Homogeneous isotropic coherent states

Consider the coherent states on $\mathcal{H}_{\Delta_2^*}$. These are labelled by four $SL(2,\mathbb{C})$ elements $H_\ell = e^{iE_\ell}U_\ell$. We are interested here in homogeneous isotropic coherent states. To find

[4]The metric structure defined by E determines a preferred immersion, up to degeneracies. Pick two points n_1 and n_2 at maximal distance from each other (the "north" and "south" pole in M), and let the equator be the set of points equidistant from the poles. Chose four points on the equator at maximal distance from one another, and connect them to the poles with geodesic links ℓ (this gives the four meridians). The "equator" gets partitioned into four (Voronoï) triangles [168], each cut by one of the links, defined by the minimal distance from the cuts.

them, let us compute (U_ℓ, E_ℓ) for the case of a homogeneous isotropic space. Let A and E to define such a space. Then we can write $A = c \wedge$ and $E = p \wedge$ where $\wedge = g^{-1}dg$ is the fiducial connection defined by the $SU(2)$ Maurer-Cartan connection, upon identification of M with the $SU(2)$ group manifold [169]. Notice that A is here the Ashtekar-Barbero connection, which is determined by both the spin-connection and the extrinsic curvature. The spin connection of a three-sphere is $\Gamma = \wedge$, so that in terms of the scale factor a we have $c = 1 + \gamma\dot{a}$. Choose n_1 to be the identity $\mathbb{I}$ and n_2 to be $-\mathbb{I}$, and choose the links to be given by exponentiating a quadruplet $\vec{n}_\ell$ of vectors in $su(2)$ normal to the faces of a regular tetrahedron centered on the origin. There is an $SO(3)$ freedom in choosing the normals at each node. We choose $n_{1\,\ell} = n_{2\,\ell} := n_\ell$. This gives a realization of the immersion defined in the footnote 4. Then we can compute U_ℓ and E_ℓ [162]

$$U_\ell = n_\ell \, e^{-i\alpha c\frac{\sigma_3}{2}} \, n_\ell^{-1} \ , \ \ E_\ell = -in_\ell \, \frac{2\pi G\gamma}{t}\beta p\frac{\sigma_3}{2} \, n_\ell^{-1}, \tag{5.19}$$

where n_ℓ are $SU(2)$ group elements such that $n_\ell \sigma_3 n_\ell^{-1} = \vec{n}_\ell \cdot \vec{\sigma}$, and α and β are constants that we do not determine here. This implies that in (5.9) we have $n_{s,\ell} = n_{t,\ell} = n_\ell$ and

$$\xi_\ell = \xi = \alpha c, \quad \eta_\ell = \eta = \beta p \ , \tag{5.20}$$

that is

$$H_\ell(\xi, \eta) = n_\ell \; e^{-i(\xi + i\eta)\frac{\sigma_3}{2}} \; n_\ell^{-1} \ . \tag{5.21}$$

The independence of ξ_ℓ and η_ℓ from ℓ can be seen as the effect of isotropy and the equality of of $n_{s,\ell}$ and $n_{t,\ell}$ can be seen as the effect of homogeneity. The two numbers $c = \xi/\alpha$ and $p = \eta/\beta$ label the homogeneous isotropic coherent states.

Remarkably, the same states can be obtained by using the Friedel-Speziale geometrical interpretation [50, 95]. Consider a Regge geometry formed by two equal regular tetrahedra with their faces identified and where the extrinsic curvature is the same at each triangle. This fixes the labels (n_s, n_t, ξ, η) at each triangle ℓ, and determines via (5.9) an $SL(2, \mathbb{C})$ group element which is precisely (5.21).

Finally, the quantity that we want to calculate is

$$W(\xi_{\rm i}, \eta_{\rm i}; \xi_{\rm f}, \eta_{\rm f}) = W(H_l(\xi_{\rm i}, \eta_{\rm i}), H_l(\xi_{\rm f}, \eta_{\rm f})) \tag{5.22}$$

Notice that this is an holomorphic function of $z_{\rm i}$ and $z_{\rm f}$ where

$$z \equiv \xi + i\,\eta \ . \tag{5.23}$$

Thus we can write it as

$$W(z_{\rm i}, z_{\rm f}) = W(\xi_{\rm i}, \eta_{\rm i}; \xi_{\rm f}, \eta_{\rm f}) \ . \tag{5.24}$$

This is the transition amplitude between a homogeneous isotropic universe with scale factor (square) $p_{\rm i}$ and extrinsic curvature $c_{\rm i}$, to a a homogeneous isotropic universe with scale factor (square) $p_{\rm f}$ and extrinsic curvature $c_{\rm f}$.

By writing the in and out states

$$\psi_z(U_\ell) := \psi_{H_\ell(z(c,p))}(U_\ell) := \langle U_\ell \,|\, z\rangle, \tag{5.25}$$

we can interpret $W(z_{\rm i}, z_{\rm f})$ as the physical scalar product between (the projection on the physical state space of) the state $|z\rangle_{\rm i}$ and (the projection on the physical state space of) the state $|z\rangle_{\rm f}$. That is[5]

$$W(z_{\rm i}, z_{\rm f}) = \langle \bar z_{\rm f} \,|\, z_{\rm i}\rangle_{\rm physical} \tag{5.26}$$

We now compute this quantity, to first order in the vertex expansion.

5.2.2 Vertex expansion

At first order in the vertex expansion, the amplitude (5.26) is given by the spinfoam formed by a single vertex bounded by four edges and eight faces.

Δ_2^*

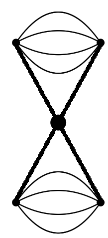

Δ_2^*

in this approximation (5.22) is given by the amplitude of the single vertex v

$$W(z_{\rm i}, z_{\rm f}) = W_v(H_\ell(z_{\rm i}), H_\ell(z_{\rm f})) \tag{5.27}$$

Using (5.17,5.18) this becomes

$$\begin{aligned} W(z_{\rm i}, z_{\rm f}) \;&=\; \int_{SO(4)^4} \delta G_1^{\rm i}\, \delta G_2^{\rm i}\, \delta G_1^{\rm f}\, \delta G_2^{\rm f} \;\; \times \\ &\prod_{\ell^{\rm i}} P_t(H_\ell(z_{\rm i})\,,\, G_1^{\rm i} G_2^{{\rm i}\,-1}) \prod_{\ell^{\rm f}} P_t(H_\ell(z_{\rm f})\,,\, G_1^{\rm f} G_2^{{\rm f}\,-1}) \\ &=\; \int_{SO(4)^2} \delta G^{\rm i}\, \delta G^{\rm f} \;\; \times \\ &\prod_{\ell^{\rm i}} P_t(H_\ell(z_{\rm i})\,,\, G^{\rm i}) \prod_{\ell^{\rm f}} P_t(H_\ell(z_{\rm f})\,,\, G^{\rm f}) \end{aligned}$$

[5]In standard quantum mechanics, the transition amplitude $Z(z_{\rm f}, z_{\rm i}) = \langle z_{\rm f} \,|\, \exp iHt \,|\, z_{\rm i}\rangle$ is anti-linear in the first variable, therefore one may expect (5.26) to be anti-holomorphic in $z_{\rm f}$. However, since here we treat the past and future surfaces as two components of the boundary of the spacetime region between the two, the initial surface is oriented the towards the future and the final surface towards the past. If we change the orientation of the final surface, $z_{\rm f}$ goes to $-\bar z_{\rm f}$.

Notice that this expression factorizes

$$W(z_{\rm i}, z_{\rm f}) = W(z_{\rm i})\; W(z_{\rm f}) \tag{5.28}$$

where

$$W(z) = \int_{SO(4)} \delta G\; \prod_\ell P_t(H_\ell(z), G) \tag{5.29}$$

This factorization happens only at first order. At this order, therefore, the physical projector projects on a single state, and (5.29) can be viewed as a Hartle-Hawking *no-boundary* state [34, 170].

5.2.3 Large volume expansion

Let us now compute (5.29) in the limit in which the universe is large. This limit is given by taking large p in (5.6). Consider the factor $D^{(j)}(H)$ in (5.18). Using (5.6), this reads

$$D^{(j)}(H_\ell) = D^{(j)}(n_\ell)\; D^{(j)}(e^{-iz\frac{\sigma_3}{2}})\; D^{(j)}(n_\ell^{-1})\ . \tag{5.30}$$

For $p \gg 8\pi G\hbar\gamma$, namely $\eta \gg 1$ we have

$$D^{(j)}(e^{-i(\xi+i\eta)\frac{\sigma_3}{2}}) = e^{-i(\xi+i\eta)j}\; P\ . \tag{5.31}$$

where P is the projector on the eigenstate of L_3 with maximum eigenvalue $m = j$. It is easy to see that this terms dominates in the limit [116]. Inserting this result in the previous equation gives

$$D^{(j)}(H_\ell) = e^{-izj}\; D^{(j)}(n_\ell)\; P\; D^{(j)}(n_\ell^{-1}) := e^{-izj}\; P_\ell\ . \tag{5.32}$$

Using this in (5.18) gives

$$P_t(H_\ell, G) {=} \sum_j (2j{+}1) e^{-2t\hbar j(j+1)-izj} \mathrm{Tr}\Big[P_\ell Y^\dagger D^{(j^+, j^-)}(G) Y\Big].$$

We show later that the trace gives a contribution polinomial in j. Therefore we can compute the sum by approximating it with a Gaussian integral. This is peaked on the value $j \sim j_o = -iz/4t\hbar$. Notice that the real part of j_o is given by the imaginary part of z, namely p. For large p, we have $j_o \sim \beta p/4t\hbar$. The gaussian integral gives

$$P_t(H_\ell, G) = \sqrt{\frac{\pi}{t}}\; e^{-\frac{z^2}{8t\hbar}}\; 2j_o \mathrm{Tr}\Big[P_\ell\, Y^\dagger\, D^{(j_o^+, j_o^-)}(G)\, Y\Big]. \tag{5.33}$$

Using this in (5.29) yields

$$W(z) = \left(\sqrt{\frac{\pi}{t}}\; e^{-\frac{z^2}{8t\hbar}}\; 2j_o\right)^4 N_j \tag{5.34}$$

where

$$N_{j_o} = \int_{SO(4)} \delta G \;\; \prod_{\ell} \; \mathrm{Tr}\Big[P_\ell \, Y^\dagger \, D^{(j_o^+, j_o^-)}(G) \, Y\Big]. \tag{5.35}$$

This is norm squared of the Livine-Speziale coherent regular tetrahedron of size j_o. It is given [58] by $N_{j_o} = N_o j_o^{-3}$. Using this and $j_o = -\frac{i}{4t\hbar} z$, we conclude

$$W(z) = N z e^{-\frac{z^2}{2t\hbar}} \tag{5.36}$$

where $N = -2i(\pi/t\hbar)^2 N_o$. Finally, inserting into (5.28) we have

$$W(z_{\rm i}, z_{\rm f}) = N^2 \; z_{\rm i} \, z_{\rm f} \; e^{-\frac{1}{2t\hbar}(z_{\rm i}^2 + z_{\rm f}^2)} \; . \tag{5.37}$$

This is the transition amplitude between two cosmological homogeneous isotropic coherent states.

5.3 Classical limit

We now observe that the transition amplitude (5.37) satisfies the equation

$$\frac{3}{8\pi G (4\alpha\beta\gamma)^2} \left(z^2 - t^2\hbar^2 \frac{\mathrm{d}^2}{\mathrm{d}z^2} - 3t\hbar \right)^2 W(z, z') = 0 \tag{5.38}$$

(the square and the overall factor are for later convenience). Therefore this amplitude describes a quantum system where the operator equation

$$\hat{H} := \frac{3}{8\pi G (4\alpha\beta\gamma)^2} \left(z^2 - t^2\hbar^2 \frac{\mathrm{d}^2}{\mathrm{d}z^2} - 3t\hbar \right)^2 = 0 \tag{5.39}$$

holds. Let us now look for a corresponding classical system. Assume that z is the coordinate of a classical phase space with symplectic structure

$$\omega = \frac{i}{t} \, dz \wedge d\bar{z} \; ; \tag{5.40}$$

that is

$$\{z, \bar{z}\} = it \; . \tag{5.41}$$

The corresponding operators in the quantum theory, that satisfy $[z, \bar{z}] = i\hbar\{z, \bar{z}\}$ are therefore

$$\hat{z} = z \; , \qquad \hat{\bar{z}} = t\hbar \frac{\mathrm{d}}{\mathrm{d}z} \; . \tag{5.42}$$

We can thus rewrite (5.39) as

$$\hat{H} = \frac{3}{8\pi G (4\alpha\beta\gamma)^2} \left(\hat{z}^2 - \hat{\bar{z}}^2 - 2 \right)^2 = 0 \; . \tag{5.43}$$

Let us now take the classical limit of this equation. Replacing operators with classical variables, we have

$$\begin{aligned} H &= \frac{3}{8\pi G(4\alpha\beta\gamma)^2}\left(z^2-\bar{z}^2-2\right)^2 \\ &= \frac{3}{8\pi G(4\alpha\beta\gamma)^2}\left(4i\xi\eta-2\right)^2=0 \end{aligned} \tag{5.44}$$

Using (5.20), this is

$$H=\frac{3}{8\pi G(4\alpha\beta\gamma)^2}\left(4i\,\alpha\beta\,cp-2\hbar\right)^2=0\ . \tag{5.45}$$

In the large p limit we have

$$H=-\frac{3}{8\pi G\gamma^2}\ c^2p^2=0\ . \tag{5.46}$$

Dividing by the volume of space $Vol\sim p^{3/2}>0$, we have

$$H=-\frac{3}{8\pi G\gamma^2}\ \sqrt{p}c^2=0\ . \tag{5.47}$$

In the large volume limit and in the absence of matter the dynamics of the universe approaches the flat ($k=0$) case and the Friedmann hamiltonian constraint becomes

$$H_{cl}=-\frac{3}{8\pi G}\ \dot{a}^2a=0\ ; \tag{5.48}$$

in this regime $c=\gamma\dot{a}$ and $p=a^2$ and this equation is precisely (5.47).

5.4 Summary

We have introduced a spinfoam formulation of quantum cosmology.

We have obtained two results. The first is that it is possible to compute quantum transition amplitudes explicitly in suitable approximations. In detail, we have studied three approximations: (i) cutting the theory to a finite dimensional graph (the dipole), (ii) cutting the spinfoam expansion to just one term with a single vertex and (iii) the large volume limit. The main hypothesis on which this work is based is that the regime of validity in which these approximations are viable includes the semiclassical limit of the dynamics of large wavelengths. "Large" means here of the order to the size of the universe itself. This regime includes of course the standard Friedmann cosmology.

The second result is that the transition amplitude computed appears to give the correct Friedmann dynamics in the classical limit. This results must be taken with caution, for a number of reasons. First, we have used the Euclidean theory, instead than the physical Lorentzian theory. Second, the dynamics we have obtained is in fact trivial due to the absence of matter. The solution of the constraint equation (5.47) is either $p = 0$ or $c = 0$; that is, either the universe has no volume, or it is flat. This is physically correct, since in absence of a matter and in the limit of infinitely large radius one obtain precisely a flat spacetime. But it is only a weak indication that the full Friedmann dynamics is recovered. Whether the result still holds with matter, or a cosmological constant, must still be checked. Also, in the derivation of the classical limit, the symplectic structure (5.40) has been taken as an input. It can be shown that this choice reproduces the symplectic structures of the LQC variables[6] (c, p) or the one of the LQG variables (E_ℓ, U_ℓ). Finally, the system that the approximation defines admits obvious improvements. In particular, transitions must be computed on a larger graph, and at the next order in the vertex amplitude, in order to investigate the validity of the approximation, and it is important to understand what are the first order corrections to the Friedman equation without matter. Can these be computed and if yes, what is the expected physics from these terms?

We have noticed that at first order the transition amplitude factorizes (see eq.(5.26)). To this order, the "projector" on physical states $P = \sum_n \langle n \,|\, n\rangle$ defined by $\langle \psi_\mathrm{f} \,|\, P \,|\, \psi_\mathrm{i}\rangle = \langle W \,|\, \bar{\psi}_\mathrm{f} \otimes \psi_\mathrm{i}\rangle$ projects on a single state, say $|0\rangle$, which can be identified as the Hartle-Hawking "wave function of the universe" defined by the so called "no boundary proposal" [171]. We do not expect this factorization to survive higher orders, where the projector can regain its general form.

From the point of view of cosmology, the system we have described opens in principle the way to the description of inhomogeneous degrees of freedom at the bounce, circumventing the difficulties of the model given in [161]. In particular, the covariant dynamics used here can readily be extended to larger graphs. Coherent states have been largely used in loop quantum cosmology (see for instance [172, 173, 174, 175]) in particular in relation to the problem of finding effective equations or in numerical simulations [176, 177, 178]. Here, however, homogeneous and isotropic states appear naturally as states peaked on homogeneous and isotropic *mean values* of the quantum states, in the context of a formalism which – we stress – is not a reduction of the dynamics to homogeneous and isotropic degrees of freedom. In physical terms, these states represent a universe where inhomogeneous and anisotropic degrees of freedom are taken into account but fluctuate around zero. This provides also an elegant solution of the problem of having to choose between coordinate or momenta in imposing a symmetry reduction in cosmology [179, 180]. Ideally, this formalism could describe inhomogeneous and anisotropic quantum fluctuations of the geometry at the bounce.

[6] This fixes the product $\alpha\beta = 3t/16\pi G\gamma$. Then α can be determined by noticing that for $c = 1$ the connection A is the Cartan connection and its holonomy from the identity to g is g itself. Taking $n_s = \mathbb{I}$ and $n_t = -\mathbb{I}$ gives easily $\alpha = 2\pi$.

The comparison of our results with those of standard loop quantum cosmology requires more work, and opens several issues. In LQC the “natural” quantum dynamics based on c and p requires care, because of the consequent p dependence of the affine parameter, and the possible dependence of the formalism on the “fiducial cell” [181]. Here the same problem does not appear since we do not use such fiducial structure; however the issue deserves to be investigated in more detail. One of the purposes of the present chapter is precisely to open a path for understanding the relation between these peculiar aspects of loop quantum cosmology and the full loop theory of quantum gravity.

Chapter 6

Future research directions

In this chapter I would like to outline three problems I wish to focus on in the next few years.

6.1 Scattering in LQG.

In LQG we don't have yet a theory of scattering. There is nevertheless a promising framework that allows to pose the problem of scattering: it consists in considering finite regions of spacetime (boundary amplitude formalism) [33, 146]. Within this framework, I would like to investigate the notions of asymptotic flatness, ADM energy and scattering states.

Four distinct scattering regimes can be expected in LQG (see the diagram in Fig. 6.1). In the following, E is the center-of-mass energy, b the impact parameter, and G Newton's constant. I believe it is important to investigate separately each one of these regimes.

I. Born scattering regime, $GE \ll b$.
The Born scattering regime corresponds to low energy and large impact parameter. The question to be addressed is if LQG admits an effective field theory description in terms of gravitons in I. The calculation of 2-point correlation functions for the metric operator on semiclassical states [128, 138, 139, 142, 143, 135, 90] provides support for the existence of an effective field theory (see chapter 4). It is important to extend these calculations to n-point functions, and to compute next-to-leading order corrections.

So far all the calculations are done for pure gravity. There is the possibility of coupling fermions considering supersymmetric spinfoams [182]. Moreover, at the effective field theory level, I would like to investigate possible parity-violating effects [183, 184] that come from fermionic loops in the presence of the (Immirzi parameter dependent) Nieh-Yan topological term. The question is if there is any gravitational analogue of the

Figure 6.1: LQG scattering diagram

effect the theta-term has in QCD, a gravitational analogue of the neutron electric dipole moment.

II. Genuine quantum gravity regime, $GE \sim b$.
For high-energy scattering with the Schwarzschild radius GE of the same order of magnitude as the impact parameter, genuine quantum gravity effects are expected. Recently, a possible quantum-geometry effect in high-enegy scattering as been explored [185]. In Loop Quantum Gravity the angle between two directions in space is quantized. In particular, the discreteness of the spectrum of the angle can affect the angular distribution of scattering cross-sections at the Planck scale. The effect is purely kinematical: it depends only on the structure of quantum geometry proper of Loop Quantum Gravity and not on the specific interaction of matter with gravity. In this sense, it can play the role the Stern-Gerlach experiment has played in the development of quantum mechanics. I would like to investigate the corrections to low-energy scattering coming from angle quantization. The goal is to find a phenomenological parametrization of these effects and to put experimental constraints on the scale of Loop Quantum Gravity.

III. Strong gravity regime, $GE \gg b$.
In the strong gravity regime, the production of a large classical black hole is expected and cross-sections can be computed using *classical* General Relativity. The question here

is to assess that LQG reproduces General Relativity in this regime. The recent results about the Regge-gravity limit of spinfoams [48, 49, 116] are a first step in this direction.

IV. Trans-Planckian regime, $b < L_P$.
The main feature of LQG is that it has no trans-Planckian degrees of freedom. This is due to the presence of Planck scale gaps in the spectrum of geometric operators [31, 155, 102, 156, 157, 92]. This feature makes LQG into a candidate ultraviolet completion for a perturbative theory of gravitons. How do Planck-scale gaps affect trans-Planckian scattering cross-sections? Can the effect be coded into a property of the S-matrix [186]?

6.2 Possible LQG effects in early cosmology

Loop Quantum Cosmology [169, 187] is a well-explored framework for quantum effects in early cosmology. It consists in a loop-inspired quantization of symmetry-reduced General Relativity. Recently, a new line of research – spinfoam cosmology [91, 165, 166, 83] – has started to develop (see chapter 5). It consists in the analysis of the spinfoam dynamics of semiclassical spin-networks peaked on a homogenous and isotropic geometry [91, 94]. The effective dynamics of the model reproduces the gravitational part of Friedmann's equation, with quantum corrections. The resulting description is remarkably close to Loop Quantum Cosmology. The advantage of starting from spinfoams is that their dynamics is largely determined by few general principles as spacetime locality and local Lorentz invariance. To develop further this approach, it is important to introduce a non-trivial spinfoam matter content and a cosmological constant (for instance via spinfoams with a quantum lorentz group).

LQG effects like the Planck scale discreteness and Heisenberg uncertainty relations for quantum geometry are expected to modify the acceleration equation for densities close to the Planck scale. It is possible that these effects can be modeled in an effective way and that observational bounds can be put on the parameters of the model, for instance via the dependence on the parameters of the computed primordial tensor power spectrum of gravitational waves [188, 189] and the B-type CMB polarization. This line of research is particularly timely as experiments as PLANCK [190], BICEP [191] and QUIET [192] are partly devoted to the search of the B-mode.

6.3 Microscopic description of Black Hole entropy

In Loop Quantum Gravity, there is a large body of work regarding the derivation of the entropy of a Black Hole from the statistical mechanics of horizon degrees of freedom [193, 194, 195]. A success of this calculation is the reproduction of the area law. There are however a few shortcomings I can see. It is desirable to have a derivation of the coefficient 1/4 in the area law, starting from the quantum theory. Moreover, in the present calculation, the ensemble of microstates is identified by the area of the horizon of the black hole, and not by its mass and angular momentum. As a result, it is not clear how to the determine the variation of the entropy with respect to the mass and to associate to it a temperature.

Recently, I have explored a semiclassical description of the LQG calculation of Black Hole entropy [196]. The description amounts to a statistical counting of shapes of the horizon [197], with a physical cut-off coming from LQG: the microstates are given by the (intrinsic and extrinsic) geometry of a tessellated horizon. I would like to explore the relation of this description with the membrane paradigm [198] and with the notion of quasinormal modes [199, 200].

Appendix A

The Hamiltonian formulation of General Relativity

The dynamical content of General Relativity is fully expressed by Einstein's equations, $G_{\mu\nu} + \Lambda g_{\mu\nu} = T_{\mu\nu}$. Nevertheless, for many purposes it is convenient to have Lagrangian and Hamiltonian formulations and derive the solutions of Einstein's equations as stationary points of an action. At a classical level, having a Lagrangian action makes the symmetries of the theory manifest, while the Hamiltonian formulation yields insights into the nature of the dynamics. Moreover formulating a quantum field theory associated with a classical theory generally requires that the classical theory is expressed in a Lagrangian or Hamiltonian form.

General relativity is usually presented as a theory of metrics. However, it can also be recast as a dynamical theory of connections. Such a reformulation brings general relativity closer to gauge theories in the sense that, in the Hamiltonian framework, they now share the same kinematics. The difference, of course, lies in the dynamics. In particular, while the dynamics of gauge theories requires a background metric structure, that of general relativity does not.

A.1 Action, diffeomorphism invariance and observability

Consider a 4-dimensional manifold $\mathcal{M}$ on which we introduce local coordinates x^μ. Einstein's equations of general relativity can be derived from an action which is the sum of an action for gravity which depends on a lorentian metric field $g_{\mu\nu}(x)$, and an action for matter which depends on both the matter fields $\varphi(x), A_\mu(x), \ldots$ and the metric $g_{\mu\nu}(x)$:

$$
\begin{aligned}
S[g_{\mu\nu}(x),\varphi(x),\ldots] =& \frac{1}{16\pi G}\int_{\mathcal{M}} dx\sqrt{-g(x)}(R(x)-2\Lambda) + \text{boundary terms} + \\
&+\int_{\mathcal{M}} dx\sqrt{-g(x)}(-g^{\mu\nu}(x)\partial_\mu\varphi(x)\partial_\nu\varphi(x) - M^2\varphi(x)\varphi(x)) + \\
&+\ldots\,,
\end{aligned}
\tag{A.1}
$$

where only the term for a free scalar field has been given explictly. The *boundary terms* indicated correspond to an integral on the boundary of the manifold $\mathcal{M}$ of a boundary density depending exclusively on the metric. This term is needed for the action to have an extremum, given the boundary data. In other words, the action (A.1) without the proper boundary terms is not correct from a variational point of view.

Notice that the action depends in a highly nonlinear way on the metric - through the inverse of the metric present in the Ricci scalar and in the matter Lagrangian and through the square root of the determinant of the metric, needed to provide a scalar density. Nevertheless, taking into account boundary terms, it can be shown that it is quadratic in the time derivatives of the metric and this suggests that it admits an appropriate initial value formulation as will be discussed later.

The action (A.1) is invariant under the group of 4-dimensional diffeomorphisms $\mathrm{Diff}(\mathcal{M})$ of the manifold $\mathcal{M}$. Recall that a diffeomorphism F is a C^∞ map between manifolds that is one-to-one, onto and has a C^∞ inverse. In other words, the diffeomorphism group is formed by the set of mappings $F:\mathcal{M}\to\mathcal{M}$ which preserve the structure of $\mathcal{M}$. We consider diffeomorphisms which are given in local coordinates by the smooth maps

$$
F: x^\mu \to F^\mu(x). \tag{A.2}
$$

We have that, for any given configuration $\{\bar{g}_{\mu\nu}(x),\bar{\varphi}(x),\ldots\}$, the action satisfies

$$
S[\tilde{g}_{\mu\nu}(x),\tilde{\varphi}(x),\ldots] = S[\bar{g}_{\mu\nu}(x),\bar{\varphi}(x),\ldots]\,, \tag{A.3}
$$

where

$$
\tilde{g}_{\mu\nu}(x) = \frac{\partial F^\rho(x)}{\partial x^\mu}\frac{\partial F^\sigma(x)}{\partial x^\nu}\bar{g}_{\rho\sigma}(F(x)) \quad , \quad \tilde{\varphi}(x) = \bar{\varphi}(F(x)) \quad , \quad \ldots \tag{A.4}
$$

Now, suppose the configuration $\{\bar{g}_{\mu\nu}(x),\bar{\varphi}(x),\ldots\}$ is an extremum for the action (A.1), i.e. it's a classical solution. Then, due to (A.3), also the configuration $\{\tilde{g}_{\mu\nu}(x),\tilde{\varphi}(x),\ldots\}$ is an extremum for the action. This means that, given a classical solution, we can use the map F to generate a huge set of classical solutions.

Suppose now the configuration $\{\bar{g}_{\mu\nu}(x),\bar{\varphi}(x),\ldots\}$ is a classical solution corresponding to certain initial data prescribed at $x^0 = t_*$ and consider a diffeomorphism F which is the identity for $x^0 \leq t_*$ and generic[1] for x^0 greater than t_*. As a result we obtain a new classical solution satisfying the same initial data. Then, for the theory to be physically meaningfull, i.e to allow physical predictions, the observables of the theory have to be invariant under diffeomorphisms so that they have the same value, given the same initial data.

This argument continues to hold for more general *general relativistic classical field theories* which do not yield standard general relativity, provided they admit a well posed initial value problem[2].

A.2 Dirac analysis of systems with a local symmetry

Let's consider a system described by the following action

$$S[q_i(\lambda)] = \int_{\lambda_0}^{\lambda_1} d\lambda \, L(q_i(\lambda), \dot{q}_i(\lambda)) \; . \tag{A.5}$$

The conjugate momentum to the variable q_i can be defined as

$$p^i = \frac{\partial L}{\partial \dot{q}_i} \; . \tag{A.6}$$

The canonical Hamiltonian for the system is given by the Legendre transform of $L(q_i, \dot{q}_i)$ with respect to $\dot{q}_i$, i.e.

$$H_c(q_i, p^i) = p^i \dot{q}_i - L(q_i, \dot{q}_i) \tag{A.7}$$

with $\dot{q}_i = \dot{q}_i(q, p)$.

If $p_i = p_i(q, \dot{q})$ cannot be inverted with respect to $\dot{q}$, i.e. if $\dot{q}_i = \dot{q}_i(q, p)$ is not unique, then the Lagrangian $L(q, \dot{q})$ is said to be singular. Necessary and sufficient condition for L to be singular is that

$$\det \frac{\partial^2 L}{\partial \dot{q}_i \partial \dot{q}_j} = 0 \; . \tag{A.8}$$

This means that a set of constraints is present, called *primary constraints*

$$\varphi_m(q, p) \approx 0 \qquad m = 1, \dots M \tag{A.9}$$

which follow from the form of the Lagrangian. They are *weakly* zero, "≈ 0", in the sense that the classical solutions live on a surface $\bar{\Gamma} = \{(q, p) \in \Gamma | \, \varphi_m(q, p) = 0\}$ in phase space

[1] Notice that the requirement of analiticity is too strong and is to be considered as technical only. For most purposes, a map F that is C^2, one-to-one, onto and has a C^2 inverse is enough. See [201] for a discussion.

[2] Some "higher derivative" theories of gravity also have been shown to have a well defined well posed initial value formulation (Noakes 1983, [202] pag. 267). However, it should be emphasized that the existence of a well posed initial value formulation is far from an automatic feature.

Γ where the constraints vanish and nevertheless, as they are defined throughout phase space, they can have non trivial Poisson brackets with phase space functions $A(q,p)$.

Thus, the canonical Hamiltonian H_c is not unique as a linear combination of primary constraint can be added to it,

$$H = H_c + u_m \varphi_m \approx H_c \,. \tag{A.10}$$

For the system to be consistent, the derivative with respect to λ of the constraints φ_m has to be weakly zero:

$$0 \approx \dot{\varphi}_n = \{\varphi_n, H\} = \{\varphi_n, H_c\} + u_m \{\varphi_n, \varphi_m\} \,. \tag{A.11}$$

If this does not happen automatically, then the equation (A.11) has to be imposed. There are two possibilities:

- it does not give any new information, but simply requires the u_m to satisfy some conditions;
- (A.11) gives new relations $\phi_k(q,p) \approx 0$ among positions and momenta, independently of the u_n.

If we are in the second case, the constraints $\phi_k(q,p) \approx 0$ have to be added to the primary constraints and are said *secondary*.

Then, the same procedure has to be repeated for secondary constraints, finding possibly further (*tertiary*) constraints, until all the constraints are consistent with the dynamics.

The extended Hamiltonian H_E is given by the canonical Hamiltonian H_c with all the constraints found added with arbitrary multipliers. From this point of view, the distinction among primary constraints, secondary constraints, ... is irrelevant at the Hamiltonian level.

A function $A(q_i, p^i)$ defined on phase space is called *first class* if it has weakly vanishing Poisson brackets with all the constraints. In case this does not happen, the function A is said to be *second class*. Hamiltonian constraints can now be devided in this two classes: in the two examples of constrained systems which follow, namely YM theory and GR, only first class constraints are present, i.e. all the constraints $\mathcal{H}_\alpha$ have vanishing Poisson brackets among each other

$$\{\mathcal{H}_\alpha, \mathcal{H}_\beta\} = {\kappa_{\alpha\beta}}^{\gamma}(q,p)\, \mathcal{H}_\gamma \approx 0 \,.$$

The classical solutions of the dynamics identify curves $(q_{cl}(\lambda), p_{cl}(\lambda))$ in phase space Γ satisfying the constraints,

$$\mathcal{H}_\alpha(q_{cl}, p_{cl}) = 0 \,.$$

Then, if you consider two functions $A(q,p)$ and $B(q,p)$ related by

$$B(q,p) = A(q,p) + u^\alpha \mathcal{H}_\alpha(q,p) \approx A(q,p) \ ,$$

they coincide on classical solutions,

$$B(q_{cl}(\lambda), p_{cl}(\lambda)) = A(q_{cl}(\lambda), p_{cl}(\lambda)) \ .$$

Nevertheless, let's consider a third function $O(q,p)$ on phase space and its Poisson brackets with A and with B,

$$\{O(q,p), A(q,p)\} \, , \tag{A.12}$$

$$\{O(q,p), B(q,p)\} = \{O(q,p), A(q,p)\} + u^\alpha \{O(q,p), \mathcal{H}_\alpha(q,p)\} \, . \tag{A.13}$$

If we require them too to coincide on classical solutions, then we have that O has to have vanishing Poisson brackets with the constraints:

$$\{O, A\}(q_{cl}, p_{cl}) = \{O, B\}(q_{cl}, p_{cl}) \qquad \Rightarrow \qquad \{O, \mathcal{H}_\alpha\} \approx 0 \ .$$

One finds then that the observables have weakly vanishing Poisson brackets with the constraints, i.e. the transformations generated by the constraints on the observables are trivial when the constraints are satisfied. These transformations are called *gauge* transformations.

A.2.1 Yang-Mills gauge theory

We illustrate here the general procedure introduced above on the case of Yang-Mills gauge theory. The action is a functional of the gauge field connection A

$$S[A] = -\frac{1}{2g^2} \int_{\mathcal{M}} \mathrm{Tr}\ F \wedge {}^*F \, , \tag{A.14}$$

and depends on the spacetime metric through the Hodge dual. For definiteness, we choose the gauge group to be $SU(2)$ and the background metric to be Minkowski. We can write the action in local coordinates expressing the $su(2)$-valued one-form A as $A(x) = A^i_\mu(x) \tau_i \, dx^\mu$,

$$S[A^i_\mu(x)] = -\frac{1}{8g^2} \int_{\mathcal{M}} d^4x \ \delta_{ij} \left(\eta^{\mu\rho}\eta^{\nu\sigma} - \eta^{\mu\sigma}\eta^{\nu\rho}\right) F^i_{\mu\nu}(x) F^j_{\rho\sigma}(x) \, . \tag{A.15}$$

The curvature of the connection is defined as

$$F(x) = F^i_{\mu\nu}(x) \, \tau_i \, dx^\mu \wedge dx^\nu \tag{A.16}$$

$$= \left(\partial_\mu A^i_\nu(x) - \partial_\nu A^i_\mu(x) + \epsilon^i{}_{kl} A^k_\mu(x) A^l_\nu(x)\right) \ \tau_i \, dx^\mu \wedge dx^\nu \, , \tag{A.17}$$

where τ_i is a basis of the adjoint representation of $su(2)$ satisfying the orthonormality condition $\mathrm{Tr}\,(\tau_i \tau_j) = \delta_{ij}$. The dual basis is simply given by $\tau^i = \delta^{ij}\tau_j$. The structure constants are defined by the commutation relation $[\tau_i, \tau_j] = i\epsilon^k{}_{ij}\,\tau_k$ and the τ_i can be written in terms of the Pauli matrices, $\tau_i = \sigma_i/2$.

The Hamiltonian analysis starts expressing the action as the time integral of a Lagrangian, $S[A] = \int dt\, L[A]$. This amounts to a choice of a function f and a vector field t^μ on spacetime such that the surfaces Σ_t of constant f, $f(x) = t$, are spacelike Cauchy surfaces with respect to the background metric and such that $t^\mu \partial_\mu f = 1$. The vector field t^μ may be interpreted as describing the "flow of time" in the spacetime and can be used to identify each Σ_t with the initial surface Σ_0. In Minkowski spacetime the choice of f and t^μ can be made via a global inertial coordinate system. In this case, the time flow t^μ is also a globally timelike Killing vector. Writing the spacetime connection in terms of the spatial connection A^i_a and a temporal component A_0, the action assumes the following form

$$S[A^i_a, A^i_0] = \int dt\; \frac{1}{2g^2}\int d\vec{x}\,\delta_{ij}\delta^{ab}(\dot{A}^i_a - \partial_a A^i_0 + \epsilon^i{}_{kl}A^k_a A^l_0)(\dot{A}^j_b - \partial_b A^j_0 + \epsilon^j{}_{kl}A^k_b A^l_0) + \tag{A.18}$$

$$-\frac{1}{4}\delta_{ij}(\delta^{ac}\delta^{bd} - \delta^{ad}\delta^{bc})F^i_{ab}F^j_{cd}\,. \tag{A.19}$$

Notice that, while A^i_a has a kinetic term, i.e. a term quadratic in the time derivatives, the temporal component A^i_0 does not. The next step is to find the conjugate momentum to A^i_a

$$E^a_i(\vec{x}) = \frac{\delta L}{\delta \dot{A}^i_a(\vec{x})} = \frac{1}{g^2}\delta_{ij}\delta^{ab}(\dot{A}^i_b - \partial_b A^i_0 + \epsilon^i{}_{kl}A^k_b A^l_0)\,, \tag{A.20}$$

which is propotional to the electric field, and the conjugate momentum to A^i_0,

$$\Pi^0_i(\vec{x}) = \frac{\delta L}{\delta \dot{A}^i_0(\vec{x})} = 0\,. \tag{A.21}$$

They satisfy the following Poisson brackets:

$$\{A^i_a(\vec{x}), E^b_j(\vec{x}')\} = \delta^i_j \delta^b_a\,\delta(\vec{x} - \vec{x}')\,, \tag{A.22}$$

$$\{A^i_0(\vec{x}), \Pi^0_j(\vec{x}')\} = \delta^i_j\,\delta(\vec{x} - \vec{x}')\,, \tag{A.23}$$

with all the others identically zero, and there is one primary constraint Φ_i,

$$\Phi_i(\vec{x}) = \Pi^0_i(\vec{x}) \approx 0\,. \tag{A.24}$$

The canonical Hamiltonian H_c is found to be

$$H_c[A^i_a, E^a_i, A^i_0, \Pi^0_i] = \frac{1}{2}\int d\vec{x}\,\delta_{ab}\delta^{ij}(g^2 E^a_i E^b_j + g^{-2} B^a_i B^b_j) - \int d\vec{x}\,A^i_0(D_a E^a_i)\,, \tag{A.25}$$

where we have introduced the covariant derivative $D_a v_i = \partial_a v_i + \epsilon^k{}_{ij} A^j_a v_k$ and the magnetic field, i.e. the dual of the field strenght of the spatial connection, $B^a_i = \delta_{ij}\epsilon^{abc}(\partial_b A^j_c - \partial_c A^j_b + \epsilon^j{}_{kl} A^k_b A^l_c)$. The total Hamiltonian is given by $H = H_c + \int d\vec{x}\,\lambda^i(\vec{x})\Phi_i(\vec{x})$, with $\lambda^i(\vec{x})$ arbitrary Lagrangian multiplier. Now we require the primary constraint to be consistent with the dynamics,

$$0 \approx \dot{\Phi}_i(\vec{x}) = \{\Phi_i(\vec{x}), H\} = \{\Pi^0_i(\vec{x}), H_c\} + \int d\vec{x}\,\lambda^j(\vec{x}')\{\Pi^0_i(\vec{x}), \Pi^0_j(\vec{x}')\} = D_a E^a_i(\vec{x})\,. \tag{A.26}$$

This yields the secondary constraint $\mathcal{G}_i$,

$$0 \approx \mathcal{G}_i = D_a E^a_i = \partial_a E^a_i + \epsilon^k{}_{ij} A^j_a E^a_k\,, \tag{A.27}$$

which is recognized as the Gauss law. There is no further constraint because $D_a E^a_i$ commutes with the Hamiltonian due to Bianchi identity for the field strenght. Thus, the extended Hamiltonian is given by

$$H_E[A^i_a, E^a_i, A^i_0, \Pi^0_i, \lambda^i, \Lambda^i] = \frac{1}{2}\int d\vec{x}\,\delta_{ab}\delta^{ij}(g^2 E^a_i E^b_j + g^{-2} B^a_i B^b_j) + \tag{A.28}$$

$$+ \int d\vec{x}\,\lambda^i \Pi^0_i + \int d\vec{x}\,(\Lambda^i - A^i_0)(D_a E^a_i)\,. \tag{A.29}$$

All the constraints are first class. The canonical variable A^i_0 can be absorbed by a redefinition of the arbitray Lagrange multiplier Λ^i. One can eliminate the fields λ^i, Π^0_i by means of their trivial equations of motion, which leads finally to the action

$$S[A^i_a(\vec{x}), E^a_i(\vec{x}), \Lambda^i(\vec{x})] = \int dt \int d\vec{x}\,E^a_i \dot{A}^i_a - \frac{1}{2}\delta_{ab}\delta^{ij}(g^2 E^a_i E^b_j + g^{-2} B^a_i B^b_j) - \Lambda^i(D_a E^a_i)\,. \tag{A.30}$$

This action has still all the gauge invariance of the original action[3] and could have been obtained directly from (A.15) by making the Legendre transform only with respect to A^i_a, considering A^i_0 as a Lagrangian multiplier from the start as it has no kinetic term.

[3] The gauge transformation corresponding to $A_0 \to A_0 + \partial_0\epsilon$ is still present, even if it is not implemented as the canonical transformation generated by a constraint, but as the transformation law of the multiplier Λ which garanties that, not only the Hamiltonian, but also the action is invariant under gauge transformations. A similar argument applies to the ADM formulation of general relativity.

In this case one finds directly that the dynamical variables are the spatial connection and the electric field and that the temporal component A^i_0 is the Lagrange multiplier for the Gauss law.

Introducing the smeared Gauss contraint, $G[\Lambda(\vec{x})] = \int d\vec{x}\, \Lambda^i(\vec{x})\mathcal{G}_i(\vec{x})$, we find that the constraint algebra is given by

$$\big\{G[\Lambda^i_1(\vec{x})], G[\Lambda^i_2(\vec{x})]\big\} = G[\epsilon^k{}_{ij}\Lambda^i_1(\vec{x})\Lambda^j_2(\vec{x})]\,,$$

and it generates the gauge transformations

$$\big\{A^i_a(\vec{x}), G[\Lambda^i(\vec{x})]\big\} = D_a\Lambda^i(\vec{x}) \quad , \quad \big\{E^a_i(\vec{x}), G[\Lambda^i(\vec{x})]\big\} = -\epsilon^k{}_{ij}E^a_k(\vec{x})\Lambda^j(\vec{x})\,,$$

which are the differential versions of the finite gauge transformations $A'_a = UA_aU^{-1} + U\partial_aU^{-1}$, $E'^a = UE^aU^{-1}$. The observable are functions of A^i_a and E^a_i with vanishing Poisson brackets with the Gauss constraint. The counting of dynamical degrees of freedom for a gauge group of dimension n is as follows[4]: the phase space $\Gamma = (A^i_a, E^a_i)$ is $2 \times 3n$-dimensional, there are n constraints on initial conditions which are automatically mantained along the evolution, and the evolution is arbitrary due to n arbitrary Lagrange multipliers; hence we have $6n - n - n = 2 \times$ dof. For $n = 1$, these are the two polarizations of the photon.

In the following sections we will analyse the Hamiltonian formulation of general relativity. Similarly to what as been done above, we choose a time function and describe the dynamics as an evolution in it. Notice, however, that in this case one cannot interpret the evolution in terms of physical measurements using clocks as the spacetime metric is the unkwown field variable to be determined - only after a solution of Einstein equations has been found, the interpretation holds. In absence of a background time, the strategy is the following: (i) we study the temporal foliations of a spacetime $(\mathcal{M}, g_{\mu\nu})$ which has a good causal structure (but which is not required to be "classical" spacetime, i.e. a solution); (ii) we introduce the foliation in the action evaluated on such a metric; (iii) we give a Hamiltonian formulation of the action in terms of the foliation; (iv) we take the new action as a starting point and show that initial data determine a solution which is a spacetime with a good causal structure. As in the Yang-Mills case, despite the long route the final form has its own elegance.

A.3 Causal structure and initial value problem

In general relativity, the causal structure of spacetime is locally of the same qualitative nature as the one of flat spacetime in special relativity. However, significant differences can occur globally because of nontrivial topology, horizons, boundaries and singularities.

[4]As an example, for $SU(N)$ we have $n = \dim SU(N) = N^2 - 1$

Let $(\mathcal{M}, g_{\mu\nu})$ be a $d+1$ dimensional spacetime and Σ be a slice defined as a d dimensional manifold embedded in $\mathcal{M}$ and spacelike with respect to $g_{\mu\nu}$ [203, 202][5].

The future domain of dependence of Σ, $\mathcal{D}^+(\Sigma)$, is the set of points p belonging to $\mathcal{M}$ such that *every* past inextendible causal curve through p intersects Σ. Physically, this means that events in $\mathcal{D}^+(\Sigma)$ are completely determined by conditions given on Σ. The domain of dependence of Σ is defined as $\mathcal{D}(\Sigma) = \mathcal{D}^+(\Sigma) \cup \mathcal{D}^-(\Sigma)$ with $\mathcal{D}^-(\Sigma)$ past domain of Σ.

A slice Σ for which the domain of dependence coincides with all the spacetime manifold

$$\mathcal{D}^+(\Sigma) \cup \mathcal{D}^-(\Sigma) = \mathcal{M} \tag{A.31}$$

is called a *Cauchy surface*. Not every spacetime admits a Cauchy surface; a spacetime which possesses a Cauchy surface is said to be *globally hyperbolic*. Physically, knowing the dynamical varables of the theory on a Cauchy surface is enough to determine all the events in spacetime. Conversely, the absence of a Cauchy surface indicates a breakdown of global predictability.

If $(\mathcal{M}, g_{\mu\nu})$ is globally hyperbolic then a function f exists (cite Geroch)

$$f : \mathcal{M} \to \mathbb{R} \, , \tag{A.32}$$

in local coordinates $f(x^\mu) = t$, such that each surface of constant f is a Cauchy surface for $(\mathcal{M}, g_{\mu\nu})$. Thus $\mathcal{M}$ can be foliated by Cauchy surfaces of constant f,

$$\Sigma_t = \{x^\mu \in \mathcal{M} \,|\, f(x^\mu) = t\} \, , \tag{A.33}$$

and the topology of $\mathcal{M}$ is $\mathcal{M} = \mathbb{R} \times \Sigma$.

If the topology of $\mathcal{M}$ is of this kind, it can be shown that general relativity admits a well-posed initial value formulation ([202], Theorem 10.2.2): given a Riemannian metric on a surface Σ_0 (the spatial metric) and a symmetric tensor field on Σ_0 (the extrinsic curvature), satisfying certain constraint equations, a unique spacetime $(\mathcal{M}, g_{\mu\nu})$ exists, it is called the maximal Cauchy development of the initial conditions and satisfies the following properties:

- $(\mathcal{M}, g_{\mu\nu})$ is a solution of Einstein equations;
- $(\mathcal{M}, g_{\mu\nu})$ is globally hyperbolic with Σ_0 as a Cauchy surface;
- the metric and the extrinsic curvature induced on Σ_0 by $(\mathcal{M}, g_{\mu\nu})$ are those assigned as initial conditions;
- every other spacetime $(\mathcal{M}, \tilde{g}_{\mu\nu})$ satisfying the first three properties can be mapped isometrically into a subset of $(\mathcal{M}, g_{\mu\nu})$.

[5] Here we follow the nomenclature of Wald [202].

Moreover the solution $g_{\mu\nu}$ on $\mathcal{M}$ depends continously and in a stably causal manner on the initial conditions and a diffeomorphism on the initial conditions reconstructs metrics $g_{\mu\nu}$ which are diffeomorphic.

In the following we assume that $\mathcal{M}$ has the product topology, $\mathcal{M} = \mathbb{R} \times \Sigma$, with Σ a compact d-dimensional manifold without boundary. If this restriction is appropriate in quantum gravity is an open question.

A.4 Arnowitt-Deser-Misner metric formulation

Foliation and ADM decomposition

The function $f : \mathcal{M} \to \mathbb{R}$ introduced in the preceding section (A.32) determines a foliation of spacetime: introducing local coordinates $\{x^\mu\}$ on $\mathcal{M}$, the equation

$$f(x^\mu) = t \tag{A.34}$$

identifies surfaces Σ_t in $\mathcal{M}$.

The normal to the slices Σ_t can be defined in terms of the function f

$$n^\mu = \frac{-g^{\mu\nu}\partial_\nu f}{\sqrt{-g^{\rho\sigma}\partial_\rho f \partial_\sigma f}} \; . \tag{A.35}$$

As defined, the normal is normalized to $g_{\mu\nu}n^\mu n^\nu = -1$ (timelike) and is future directed.

Moreover, the function f defines a vector t^μ called *time flow* and defined by the condition

$$t^\mu \partial_\mu f = +1 \; . \tag{A.36}$$

The vector t^μ can be written in terms of a component normal to the surface, Nn^μ, and a component N^μ tangent to it, $N^\mu \partial_\mu f = 0$:

$$t^\mu = N n^\mu + N^\mu \; . \tag{A.37}$$

The equation (A.36) determines N,

$$N = \frac{1}{\sqrt{-g^{\mu\nu}\partial_\mu f \partial_\nu f}} \; , \tag{A.38}$$

but it does not determine N^μ. The scalar N is called *lapse*, the vector N^μ *shift*.

Let's introduce now local coordinates $\{\vec{x}\}$ on Σ and consider a map X from Σ to $\mathcal{M}$

$$\begin{aligned} X : \Sigma &\to \mathcal{M} \\ \vec{x} &\mapsto X^\mu(\vec{x}) \; . \end{aligned}$$

The surface Σ_t is described in $\mathcal{M}$ by the *embedding*

$$x^\mu = X_t^\mu(\vec{x}) \tag{A.39}$$

which satisfies the condition

$$f(X_t^\mu) = t \; . \tag{A.40}$$

Deriving this expression with respect to the parameter t, we find the relation

$$1 = \frac{\partial}{\partial t} f(X_t^\mu) = \frac{\partial X_t^\mu}{\partial t} \partial_\mu f \tag{A.41}$$

which defines the time flow vector t^μ in terms of the embedding

$$t^\mu(x) = \left. \frac{\partial X_t^\mu(\vec{x})}{\partial t} \right|_{x = X_t^\mu(\vec{x})} \; . \tag{A.42}$$

Moreover, deriving equation (A.40) with respect to x^a we find

$$0 = \frac{\partial X_t^\mu}{\partial x^a} \partial_\mu f \tag{A.43}$$

i.e. $\frac{\partial X_t^\mu}{\partial x^a}$ is spacelike, $n_\mu \frac{\partial X_t^\mu}{\partial x^a} = 0$. As a result, the shift functions N^μ can be written as a vector N^a in Σ,

$$N^\mu(X_t^\mu(\vec{x})) = \frac{\partial X_t^\mu}{\partial x^a} N^a(\vec{x}, t) \; , \tag{A.44}$$

called the shift, too. Analogously for the lapse N we have

$$N(X_t(\vec{x})) = N(\vec{x}, t) \; . \tag{A.45}$$

The spacetime metric $g_{\mu\nu}(x)$ induces on Σ_t a spatial metric $h_{ab}(\vec{x}, t)$ given by

$$h_{ab}(\vec{x}, t) = g_{\mu\nu}(X_t^\mu(\vec{x})) \frac{\partial X_t^\mu(\vec{x})}{\partial x^a} \frac{\partial X_t^\nu(\vec{x})}{\partial x^b} \; . \tag{A.46}$$

As $n_\mu \frac{\partial X_t^\mu}{\partial x^a} = 0$, we can introduce a tensor in $\mathcal{M}$

$$h_{\mu\nu} = n_\mu n_\nu + g_{\mu\nu} \tag{A.47}$$

which is spatial, in the sense that $h_{\mu\nu} n^\nu = 0$, and it is related to $h_{ab}(\vec{x}, t)$ by

$$h_{ab} = h_{\mu\nu} \frac{\partial X_t^\mu}{\partial x^a} \frac{\partial X_t^\nu}{\partial x^b} \; . \tag{A.48}$$

Notice that ${h_\mu}^\nu$ acts as a projector from $\mathcal{M}$ to Σ,

$$ {h_\mu}^\nu \partial_\nu f = 0, \tag{A.49} $$

$$ \frac{\partial X_t^\mu}{\partial x^a} {h_\mu}^\nu = \frac{\partial X_t^\nu}{\partial x^a} \,. \tag{A.50} $$

The quantities h_{ab}, N, N^a were introduced by Arnowitt, Deser and Misner [204] and are known as ADM variables. Introducing a foliation of spacetime, the metric $g_{\mu\nu}$ can be written in terms of these variables. This follows from the fact that the embedding $X_t^\mu(\vec{x})$ is a diffeomorphism of $\mathcal{M}$: for each fixed t , $X_t : \Sigma \to \mathcal{M}$ is an embedding, i.e. a global injective immersion. Nevertheless the one-parameter family $X_t^\mu(\vec{x})$ defines a diffeomorphism from $\mathbb{R} \times \Sigma$ to $\mathcal{M}$. Thus, changing from x^μ to $(\vec{x}, t)$ coordinates with $x^\mu = X_t^\mu(\vec{x})$, we find that the metric $g_{\mu\nu}(x)$ has the following form

$$ \begin{aligned} & g_{\mu\nu}(x) dx^\mu \otimes dx^\nu = \\ & = g_{\mu\nu}\big(X_t(\vec{x})\big) \Big[\frac{\partial X_t^\mu}{\partial t} dt + \frac{\partial X_t^\mu}{\partial x^a} dx^a\Big] \otimes \Big[\frac{\partial X_t^\nu}{\partial t} dt + \frac{\partial X_t^\nu}{\partial x^b} dx^b\Big] \\ & = g_{\mu\nu} \Big[N n^\mu dt + \frac{\partial X_t^\mu}{\partial x^a} N^a dt + \frac{\partial X_t^\mu}{\partial x^a} dx^a\Big] \otimes \Big[N n^\nu dt + \frac{\partial X_t^\nu}{\partial x^b} N^b dt + \frac{\partial X_t^\nu}{\partial x^b} dx^b\Big] \\ & = N^2 g_{\mu\nu} n^\mu n^\nu dt \otimes dt + g_{\mu\nu} \frac{\partial X_t^\mu}{\partial x^a} \frac{\partial X_t^\nu}{\partial x^b} (dx^a + N^a dt) \otimes (dx^b + N^b dt) \\ & = -N^2 dt \otimes dt + h_{ab} (dx^a + N^a dt) \otimes (dx^b + N^b dt) \,. \end{aligned} \tag{A.51} $$

From equation (A.51) we can read off the components of the metric $g_{\mu\nu}$ in ADM variables

$$ g_{\mu\nu}(\vec{x}, t) = \left(\begin{array}{c|c} -N^2 + h_{ab} N^a N^b & h_{ab} N^b \\ \hline h_{ab} N^a & h_{ab} \end{array} \right) \tag{A.52} $$

As a reference, we give also its inverse

$$ g^{\mu\nu}(\vec{x}, t) = \left(\begin{array}{c|c} -1/N^2 & N^a/N^2 \\ \hline \frac{N^b}{N^2} & h^{ab} - \frac{N^a N^b}{N^2} \end{array} \right) \tag{A.53} $$

The manifold Σ supplied with the metric h_{ab} is a d-dimensional Riemmanian space (Σ, h_{ab}). On it, a metric compatible covariant derivative $\mathcal{D}_a$ can be defined, $\mathcal{D}_c h_{ab} = 0$. It can be written in terms of a Christoffel connection, $\mathcal{D}_a v^b = \partial_a v^b + \Gamma^b_{ac} v^c$. The Riemann tensor is defined as

$$ {\mathcal{R}_{abc}}^d \, u_d = [\mathcal{D}_a, \mathcal{D}_b] \, u_c \,. \tag{A.54} $$

As Σ is embedded in $\mathcal{M}$, some relations between the structures induced on Σ by $(\mathcal{M}, g_{\mu\nu}, \nabla_\sigma)$ and the structure $(\Sigma, h_{ab}, \mathcal{D}_k)$ are expected to hold. In the following we establish these relations as they will be essential in writing the Hamiltonian action for general relativity.

The spacetime tensor $h_\mu{}^\nu$ plays the role of projector from the tangent space to $\mathcal{M}$ to the tangent space to Σ. By construction $h_{\mu\nu}$ is the metric induced on Σ by $(\mathcal{M}, g_{\mu\nu})$. The covariant derivatives associated to the two metrics are related in the following way

$$\mathcal{D}_\mu u_\nu = h_\mu{}^\rho h_\nu{}^\sigma \nabla_\rho u_\sigma \,, \tag{A.55}$$

with $\mathcal{D}_\mu u_\nu$ defined as

$$\mathcal{D}_a u_b = \mathcal{D}_\mu u_\nu \frac{\partial X_t^\mu}{\partial x^a} \frac{\partial X_t^\nu}{\partial x^b} \,. \tag{A.56}$$

Indeed $\mathcal{D}_\mu$ introduced in equation (A.55) satisfies the defining properties of a derivative operator and furthermore we have

$$\mathcal{D}_\sigma h_{\mu\nu} = h_\mu{}^{\mu'} h_\nu{}^{\nu'} h_\sigma{}^{\sigma'} \nabla_{\sigma'} (g_{\mu'\nu'} + n_{\mu'} n_{\nu'}) = 0 \tag{A.57}$$

since $\nabla_\sigma g_{\mu\nu} = 0$ and $h_{\mu\nu} n^\nu = 0$. Thus, $\mathcal{D}_\mu$ is the *unique* derivative associated with $h_{\mu\nu}$.

The *extrinsic curvature* of Σ in $(\mathcal{M}, g_{\mu\nu})$ is defined as the Lie derivative of the metric $h_{\mu\nu}$ with respect to the normal to Σ,

$$K_{\mu\nu} = \frac{1}{2}\, \mathcal{L}_n^{(\mathcal{M})} h_{\mu\nu} = \frac{1}{2} (n^\sigma \partial_\sigma h_{\mu\nu} + h_{\mu\sigma} \partial_\nu n^\sigma + h_{\nu\sigma} \partial_\mu n^\sigma) \,. \tag{A.58}$$

With the substitution of ordinary derivatives with covariant derivatives and recalling that $g_{\mu\nu} n^\nu n^\mu = -1$, we find

$$K_{\mu\nu} = \frac{1}{2} (h_\mu{}^\sigma \nabla_\sigma n_\nu + h_\nu{}^\sigma \nabla_\sigma n_\mu) \,. \tag{A.59}$$

The terms $h_\mu{}^\sigma \nabla_\sigma n_\nu$ are already symmetric under exchange $(\mu\nu)$ since $n_\mu = \alpha \partial_\mu f$ and ∇_μ is torsionless. Thus we have

$$K_{\mu\nu} = h_\mu{}^\sigma \nabla_\sigma n_\nu \,. \tag{A.60}$$

As a result, we find that the extrinsic curvature measures the change of the normal to Σ parallel trasporting it along Σ.

The tensor $K_{\mu\nu}$ is spatial, $K_{\mu\nu} n^\nu = 0$. Let's consider now the tensor K_{ab} defined on Σ as

$$K_{ab} = K_{\mu\nu} \frac{\partial X_t^\mu}{\partial x^a} \frac{\partial X_t^\nu}{\partial x^b} \,. \tag{A.61}$$

Since $K_{\mu\nu}$ is spatial, K_{ab} contains the same amount of information as $K_{\mu\nu}$. Using the definition (A.58) of $K_{\mu\nu}$ we show that the "extrinsic curvature" K_{ab} can be written in terms of h_{ab}, N, N^a. We start introducing in (A.58) the relation $n^\mu = (t^\mu - N^\mu)/N$,

$$K_{\mu\nu} = \frac{1}{2N}\left[(t^\sigma \partial_\sigma h_{\mu\nu} + h_{\mu\sigma}\partial_\nu t^\sigma + h_{\nu\sigma}\partial_\mu t^\sigma) - (N^\sigma \partial_\sigma h_{\mu\nu} + h_{\mu\sigma}\partial_\nu N^\sigma + h_{\nu\sigma}\partial_\mu N^\sigma)\right].$$

As an example, we analyse the first term in brackets: using the relation (A.42) and (A.48) we find

$$\begin{aligned}
&(t^\sigma \partial_\sigma h_{\mu\nu} + h_{\mu\sigma}\partial_\nu t^\sigma + h_{\nu\sigma}\partial_\mu t^\sigma)\frac{\partial X_t^\mu}{\partial x^a}\frac{\partial X_t^\nu}{\partial x^b} = \\
&= \frac{\partial X_t^\sigma}{\partial t}\partial_\sigma h_{\mu\nu}\frac{\partial X_t^\mu}{\partial x^a}\frac{\partial X_t^\nu}{\partial x^b} + h_{\mu\nu}\frac{\partial}{\partial x^a}\Big(\frac{\partial X_t^\mu}{\partial t}\Big)\frac{\partial X_t^\nu}{\partial x^b} + h_{\mu\nu}\frac{\partial X_t^\mu}{\partial x^a}\frac{\partial}{\partial x^b}\Big(\frac{\partial X_t^\nu}{\partial t}\Big) = \\
&= \frac{\partial}{\partial t}\Big(h_{\mu\nu}(X_t^\mu)\frac{\partial X_t^\mu}{\partial x^a}\frac{\partial X_t^\nu}{\partial x^b}\Big) = \dot{h}_{ab}(\vec{x},t)\ .
\end{aligned}$$

With a similar calculation for the remaining term, we have in the end

$$K_{ab}(\vec{x},t) = \frac{1}{2N}\left[\,\dot{h}_{ab} - (N^c\partial_c h_{ab} + h_{ac}\partial_b N^c + h_{bc}\partial_a N^c)\right]. \tag{A.62}$$

In the term in round brackets we recognize the Lie derivative in Σ of the metric h_{ab} with respect to the vector N^c, $\mathcal{L}_N^{(\Sigma)} h_{ab}$. Hence, the extrinsic curvature can be written in a manifestly Diff(Σ)-invariant form,

$$K_{ab} = \frac{1}{2N}\left[\,\dot{h}_{ab} - \mathcal{D}_a N_b - \mathcal{D}_b N_a\right]. \tag{A.63}$$

It is rather surprising that the *extrinsic* curvature of Σ in $\mathcal{M}$ can be completely described in terms of quantities defined in Σ.

From equation (A.55) one can derive relations between projections of the spacetime curvature and the intrinsic and extrinsic curvature of Σ:

$$h_\mu{}^{\mu'} h_\nu{}^{\nu'} h_\rho{}^{\rho'} h^\sigma{}_{\sigma'} R_{\mu'\nu'\rho'}{}^{\sigma'} = \mathcal{R}_{\mu\nu\rho}{}^\sigma + K_{\rho\mu}K_\nu{}^\sigma + K_{\rho\nu}K_\mu{}^\sigma\,, \tag{A.64}$$

$$h_\mu{}^\rho R_{\rho\sigma} n^\sigma = \mathcal{D}_\rho K^\rho{}_\mu - \mathcal{D}_\mu K^\rho{}_\rho\,, \tag{A.65}$$

$$R_{\mu\nu}n^\mu n^\nu = -\left(K_{\mu\nu}K^{\mu\nu} - \left(K^\mu{}_\mu\right)^2\right) + \nabla_\nu\left(n^\mu\nabla_\mu n^\nu - n^\nu\nabla_\mu n^\mu\right). \tag{A.66}$$

These relations are known as *Gauss-Codazzi relations*. Combining them, we find that the Ricci scalar can be written as

$$\begin{aligned}
R &= h^{\mu\rho}h^\nu{}_\sigma R_{\mu\nu\rho}{}^\sigma - 2R_{\mu\nu}n^\mu n^\nu = \\
&= K_{\mu\nu}K^{\mu\nu} - \left(K^\mu{}_\mu\right)^2 + \mathcal{R} - 2\nabla_\nu\left(n^\mu\nabla_\mu n^\nu - n^\nu\nabla_\mu n^\mu\right)\ .
\end{aligned} \tag{A.67}$$

Action in ADM variables

Consider a manifold $\mathcal{M}$ with topology $\Sigma \times \mathbb{R}$ with $\partial\Sigma = \emptyset$. The action for general relativity on the region $\mathcal{R} = \Sigma \times [0,1]$

$$S_{\mathcal{R}}[g_{\mu\nu}] = \int_{\mathcal{R}} dx\,\sqrt{-g}R - 2\int_{\Sigma_0}^{\Sigma_1} d\vec{x}\,\sqrt{h}K$$

can be written in ADM variables using the results of the previous section[6]

$$S_L[h_{ab}, N, N^k] = \int_{t_0}^{t_1} dt \int_{\Sigma_t} d\vec{x}\; N\sqrt{h}\,\left[\, H^{abcd}K_{ab}K_{cd} + \mathcal{R}\,\right] \;. \tag{A.71}$$

The boundary term in $S_{\mathcal{R}}[g_{\mu\nu}]$ is cancelled by the anologous term appearing in (A.67). Being of the form $S_L = \displaystyle\int dt\, L[h_{ab}, N, N^k]$, the conjugate momentum to the metric h_{ab} can be calculated immediately

$$\pi^{ab}(\vec{x}) = \frac{\delta L}{\delta \dot{h}_{ab}(\vec{x})}\;.$$

A canonical analysis of (A.71) along the same lines followed in the Yang-Mills case yields

$$S_H[h_{ab}, \pi^{ab}, N, N^a] = \int_{t_0}^{t_1} dt \int_{\Sigma_t} d\vec{x}\;\left(\pi^{ab}\dot{h}_{ab} - N\mathcal{H} - N^a\mathcal{H}_a\right)\;. \tag{A.72}$$

Hence the lapse N and the shift N^a appear as Lagrange multipliers for the constraints

$$\mathcal{H} = \frac{1}{\sqrt{h}} {H^{-1}}_{abcd}\pi^{ab}\pi^{cd} - \sqrt{h}\,\mathcal{R} \approx 0 \tag{A.73}$$

$$\mathcal{H}_a = \,-\,2h_{ab}\mathcal{D}_c\pi^{cb} \approx 0\;. \tag{A.74}$$

[6]The tensor H^{abcd} is given by

$$H^{abcd} = \frac{1}{2}(h^{ac}h^{bd} + h^{ad}h^{bc}) - h^{ab}h^{cd}\;. \tag{A.68}$$

Its “inverse” ${H^{-1}}_{abcd}$ is given by

$${H^{-1}}_{abcd} = \frac{1}{2}(h_{ac}h_{bd} + h_{ad}h_{bc}) - \frac{1}{d-1}h_{ab}h_{cd} \tag{A.69}$$

so that

$${H^{-1}}_{abef}H^{efcd} = \frac{1}{2}({\delta_a}^c{\delta_b}^d + {\delta_a}^d{\delta_b}^c)\;. \tag{A.70}$$

As can be read from the term $\int dt \int dx\, \pi^{ab} \dot{h}_{ab}$, we have that h_{ab} and π^{ab} are a canonical couple. Introducing Poisson brackets

$$\{A, B\}_t = \int_{\Sigma_t} d\vec{x} \, \left(\frac{\delta A}{\delta h_{ab}(\vec{x})} \frac{\delta B}{\delta \pi^{ab}(\vec{x})} - \frac{\delta B}{\delta h_{ab}(\vec{x})} \frac{\delta A}{\delta \pi^{ab}(\vec{x})} \right) \tag{A.75}$$

we have the canonical brackets

$$\{h_{ab}(\vec{x}\,'), \pi^{cd}(\vec{x}\,'')\}_t = \frac{1}{2}(\delta_a{}^c \delta_b{}^d + \delta_a{}^d \delta_b{}^c)\, \delta(\vec{x}\,', \vec{x}\,'') \tag{A.76}$$

with $\delta(\vec{x}\,', \vec{x}\,'')$ defined in the following way

$$\int d\vec{x}\,' \, \delta(\vec{x}, \vec{x}\,') f(\vec{x}\,') = f(\vec{x}) \; .$$

Notice that it is a weight one density.

Constraint algebra

The constraints $\mathcal{H}$, $\mathcal{H}_a$ satisfy *Dirac algebra*:

$$\{\mathcal{H}_a(\vec{x}\,'), \mathcal{H}_b(\vec{x}\,'')\} = \mathcal{H}_a(\vec{x}\,'')\partial'_b \delta(\vec{x}\,', \vec{x}\,'') - \mathcal{H}_b(\vec{x}\,')\partial''_a \delta(\vec{x}\,', \vec{x}\,'') \tag{A.77}$$

$$\{\mathcal{H}_a(\vec{x}\,'), \mathcal{H}(\vec{x}\,'')\} = \mathcal{H}(\vec{x}\,')\partial'_a \delta(\vec{x}\,', \vec{x}\,'') \tag{A.78}$$

$$\{\mathcal{H}(\vec{x}\,'), \mathcal{H}(\vec{x}\,'')\} = h^{ab}(\vec{x}\,')\mathcal{H}_a(\vec{x}\,')\partial''_b \delta(\vec{x}\,', \vec{x}\,'') - h^{ab}(\vec{x}\,'')\mathcal{H}_a(\vec{x}\,'')\partial'_b \delta(\vec{x}\,', \vec{x}\,'') \; . \tag{A.79}$$

Notice that $\{\mathcal{H}(\vec{x}\,'), \mathcal{H}(\vec{x}\,'')\}$ is zero for $\vec{x}\,' = \vec{x}\,''$, but "different from zero" for $\vec{x}\,' \neq \vec{x}\,''$. This is due to the fact that $\mathcal{H}(\vec{x})$ is not algebraic in h_{ab}. Indeed the term which contributes to the brackets is $\{\pi^{ab}, \mathcal{R}\}$ and $\delta\mathcal{R}$ is quasilocal in δh_{ab}.

The constraints generate gauge transformations on phase space variables. Let's introduce the quantities

$$V[\xi^a] \, = \int_\Sigma d\vec{x} \; \xi^a(\vec{x}) \, \mathcal{H}_a(\vec{x}) \qquad , \qquad H[\zeta] \, = \int_\Sigma d\vec{x} \; \zeta(\vec{x})\mathcal{H}(\vec{x}) \; . \tag{A.80}$$

They have both the role of *smearing* of the constraints on test functions and of generators with parameters ξ^a, ζ. Notice that the integrals are invariant under diffeomorphisms as the constraints are densities of weight one.

The vector constraint $V[\xi^a]$ generates diffeomorphisms

$$\{h_{ab}, V[\xi^c]\} = \xi^c \partial_c h_{ab} + h_{ca}\partial_b \xi^c + h_{cb}\partial_a \xi^c = \; \mathcal{L}^{(\Sigma)}_\xi h_{ab}$$
$$\{\pi^{ab}, V[\xi^c]\} = \xi^c \partial_c \pi^{ab} - \pi^{ac}\partial_c \xi^b - \pi^{bc}\partial_c \xi^a + \pi^{ab}\partial_c \xi^c = \; \mathcal{L}^{(\Sigma)}_\xi \pi^{ab}$$

where the volume expansion term $\pi^{ab}\partial_c\xi^c$ is due to the fact that π^{ab} is a density of weight one.

As can be read from (A.77), the constraints $\mathcal{H}_a$ form a Lie sub-algebra of Dirac algebra. This has the simple geometric meaning that the composition of spatial diffeomorphisms is still a diffeomorphism

We give also the transformations generated by $H[\zeta]$

$$\{h_{ab}, H[\zeta]\} = 2\zeta H^{-1}{}_{abcd}\frac{\pi^{cd}}{\sqrt{h}} \tag{A.81}$$

$$\begin{aligned}\{\pi^{ab}, H[\zeta]\} =& -\frac{2\zeta}{\sqrt{h}}\big(h_{cd}\pi^{ac}\pi^{bd} - \frac{1}{d-1}h_{cd}\pi^{cd}\pi^{ab}\big) \\ &+ \sqrt{h}H^{abcd}\mathcal{D}_c\mathcal{D}_d\zeta - \zeta\sqrt{h}H^{abcd}\mathcal{R}_{cd} + \frac{1}{2}h^{ab}\zeta\mathcal{H}\,.\end{aligned} \tag{A.82}$$

The combination $H[N]+V[N^a]$ generates temporal evolution. On the classical solutions, the transformations generated by $H[\zeta]$ can be interpreted geometrically as *deformations* of the surface Σ_t.

Dirac algebra can be written in terms of the smeared quantities $V[\xi]$ and $H[\zeta]$

$$\{V[\xi'^a], V[\xi''^a]\} = V[\xi'^c\partial_c\xi''^a - \xi''^c\partial_c\xi'^a]\,, \tag{A.83}$$

$$\{V[\xi'^a], H[\zeta]\} = H[\xi'^c\partial_c\zeta]\,, \tag{A.84}$$

$$\{H[\zeta'], H[\zeta'']\} = V[h^{ab}\zeta'\partial_b\zeta'' - h^{ab}\zeta''\partial_b\zeta']\,. \tag{A.85}$$

This expressions have the following interpretation

- the Lie algebra of the diffeomorphism generators $\mathcal{H}_a$ can be transported to vector fields,
$$\mathcal{L}^{(\Sigma)}_{\xi'}\,\mathcal{L}^{(\Sigma)}_{\xi''}A - \mathcal{L}^{(\Sigma)}_{\xi''}\,\mathcal{L}^{(\Sigma)}_{\xi'}A = \mathcal{L}^{(\Sigma)}_{[\xi',\xi'']}A \quad ;$$

- the scalar constraint $\mathcal{H}$ transforms as a scalar density;

- deforming the surface Σ with parameter ζ' and then with parameter ζ'' is equivalent to a deformation with parameter ζ'' followed by one with parameter ζ' up to a *metric dependent* diffeomorphism.

A.5 Connection variables from Ashtekar canonical transformation

A.5.1 Extension of the ADM phase space: the triad

The ADM phase space $\Gamma = (h_{ab}, \pi^{ab})$ can be enlarged introducing the triad e^i_a, i.e. a $so(3)$-valued one-form defining a local frame on Σ and using it in place of the metric:

$$h_{ab}(\vec{x}) = \delta_{ij}\, e^i_a(\vec{x}) e^j_b(\vec{x})\,,$$

where δ_{ij} is the Killing metric on $SO(3)$.

The momentum π^a_i conjugate to the triad can be read from the term $\int \pi \dot{h}$ in the action:

$$\int d\vec{x}\, \pi^{ab} \dot{h}_{ab} = \int d\vec{x}\, \pi^{ab} (2\delta_{ij} \dot{e}^i_a e^j_b) = \int d\vec{x}\, (2\delta_{ij} \pi^{ab} e^j_b) \dot{e}^i_a = \int d\vec{x}\, \pi^a_i \dot{e}^i_a\,.$$

Therefore we can rewrite the action in terms of the variables (e^i_a, π^i_a). However, they are certainly reduntant due to the freedom to choose different local frames e^i_a by local $SO(3)$ rotations acting on internal indices $i = 1, 2, 3$. There must be an additional constraint that makes this redundacy manifest: it corresponds to the requirement that the tensor $\pi^{ab} = \frac{1}{2} \delta^{ij} \pi^a_i e^b_j$ calculated from e^i_a and π^a_i is symmetric:

$$\mathcal{G}_a = \epsilon_{abc} \delta^{ij} \pi^b_i e^c_j \approx 0\,.$$

Moreover, it can be useful as a preliminary to next section to introduce a "densitized inverse triad" E^a_i

$$E^a_i = \frac{1}{2} \epsilon^{abc} \epsilon_{ijk} e^j_b e^k_c\,,$$

and use it instead of the triad as a canonical variable. This amounts to a switch between positions and momenta:

$$\begin{aligned} \int d\vec{x}\, \pi^{ab} \dot{h}_{ab} &= \int d\vec{x}\, \pi^a_i \dot{e}^i_a = - \int d\vec{x}\, K^i_a \dot{E}^a_i = \\ &= \int d\vec{x}\, E^a_i \dot{K}^i_a - \frac{d}{dt} \int d\vec{x}\, K^i_a E^a_i\,. \end{aligned}$$

From now on we choose to work with the universal covering group of $SO(3)$, the group $SU(2)$.

A covariant derivative $\mathcal{D}_a$ compatible with the triad can be introduced. It is defined as $\mathcal{D}_a \lambda_i = \partial_a \lambda_i + \epsilon^k{}_{ij} \Gamma^j_a \lambda_k$, in terms of a *spin connection* Γ^i_a. As the triad e^i_a can be written in terms of the densitized inverse triad E^a_i, we have that the covariant derivative is compatible with it, $\mathcal{D}_a E^b_i = 0$. Both the spin connection[7] and the curvature associated with the spin connection, $\mathcal{R}^k_{ab} = \partial_a \Gamma^k_b - \partial_b \Gamma^k_a + \epsilon^k{}_{ij} \Gamma^i_a \Gamma^j_b$, are to be considered as a function of E^a_i.

The constraints in terms of the canonical variables (K^i_a, E^a_i) are given by

$$\mathcal{G}_i = \epsilon^k{}_{ij} K^j_a E^a_k \approx 0 \tag{A.86}$$

$$\mathcal{H}_a = E^b_i (\mathcal{D}_a K^i_b - \mathcal{D}_b K^i_a) \approx 0 \tag{A.87}$$

$$\mathcal{H} = \frac{E^a_i E^b_j}{\sqrt{|\det E^a_i|}} \big((K^j_a K^i_b - K^i_a K^j_b) + \epsilon_k{}^{ij} \mathcal{R}^k_{ab} \big) \approx 0\,. \tag{A.88}$$

Notice that now the position K has the meaning of "extrinsic curvature variable" and is of weight zero while the momentum is the "metric variable" E which is a density of weight one.

A.5.2 Ashtekar new variables

As the theory possesses a local $SU(2)$ invariance, it is desirable to formulate it as a gauge theory for this group. This means that one should identify a $su(2)$ connection A^i_a analogous to the one for Yang-Mills gauge theory and use it as position variable. Actually, the naive candidate, the spin connection Γ^i_a, does not play this role.

In the Yang-Mills case, the gauge transformations are generated by the Gauss constraint (A.27). It is given by the $su(2)$-covariant derivative of the momentum conjugate to the connection - the electric field. In the case of gravity, the constraint (A.86) plays the same role as the Gauss constraint - it generates local $su(2)$ transformations - but it has a different form. Our aim is now to write the constraint $\mathcal{G}_i$ in such a form that it becomes the Gauss constraint for a $SU(2)$ gauge theory. Notice that, as

$$\mathcal{D}_a E^a_i = \partial_a E^a_i + \epsilon^k{}_{ij} \Gamma^j_a E^a_k = 0$$

---

[7] The spin connection Γ^i_a in terms of the triad e^i_a is given by

$$\Gamma^i_a = -\frac{1}{2} \epsilon^{ij}{}_k e^b_j \left(\partial_{[a} e^k_{b]} + \delta^{kl} \delta_{mn} e^c_l e^m_a \partial_b e^n_c \right).$$

It can be written as a function of E^a_i using the relations

$$e^i_a = \frac{1}{2} \frac{\epsilon_{abc} \epsilon^{ijk} E^b_j E^c_k}{\sqrt{|\det(E^a_i)|}} \quad \text{and} \quad e^a_i = \frac{\mathrm{sgn}(\det(E^a_i))\ E^a_i}{\sqrt{|\det(E^a_i)|}}.$$

Notice also that

$$\det h_{ab} = \det(\delta_{ij} e^i_a e^j_b) = |\det(E^a_i)|$$

due to compatibility, we can sum it to the constraint $\mathcal{G}_i$ without modifying it:

$$\begin{aligned}\mathcal{G}_i =& \epsilon^k{}_{ij} K^j_a E^a_k + \gamma^{-1} \mathcal{D}_a E^a_i = \\ =& \gamma^{-1} \big(\partial_a E^a_i + \epsilon^k{}_{ij} (\gamma\, K^j_a + \Gamma^j_a) E^a_k \big) \,.\end{aligned}$$

This equation suggests to introduce the *new connection* A^i_a ,

$$A^i_a = \gamma\, K^i_a + \Gamma^i{}_a \,. \tag{A.89}$$

This is the Ashtekar-Barbero connection. We call D_a the covariant derivative associated with it, $D_a \lambda_i = \partial_a \lambda_i + \epsilon^k{}_{ij} A^j_a \lambda_k$. The constraint (A.86) can now be written in terms of the new connection,

$$\gamma\, \mathcal{G}_i = D_a E^a_i = \partial_a E^a_i + \epsilon^k{}_{ij} A^j_a E^a_k$$

and it is appropriate to call it the *Gauss* constraint.

What turns out to be rather surprising it is that the variables $(A^i_a, \gamma^{-1} E^a_i)$ form a canonically conjugate pair. The canonical Poisson bracket $\{A^i_a(\vec{x}), E^b_j(\vec{x}')\} = \gamma \delta^i_j \delta^b_a \delta(\vec{x}, \vec{x}')$ holds because of the non-trivial relation $\{E^a_i(\vec{x}), \Gamma^b_j(\vec{x}')\} = 0$. It corresponds to the integral

$$\int_\Sigma d\vec{x} E^a_i \delta \Gamma^i{}_a(E) = \frac{1}{2} \int_\Sigma d\vec{x}\, \partial_a (\epsilon^{abc} \delta_{ij} e^i_b \delta e^j_c) = 0 \,, \tag{A.90}$$

and garanties the equality

$$\int dt \int_\Sigma d\vec{x}\, \gamma^{-1} E^a_i \dot{A}^i_a = \int dt \int_\Sigma d\vec{x}\, E^a_i \dot{K}^i_a \,.$$

The other non trivial relation to be checked, $\{A^i_a(\vec{x}), A^b_j(\vec{x}')\} = 0$, can be shown to hold expanding the Poisson bracket

$$\begin{aligned}\{A^i_a(\vec{x}), A^j_b(\vec{x}')\} =& \{\gamma K^i_a(\vec{x}), \Gamma^j_b(\vec{x}')\} + \{\Gamma^i{}_a(\vec{x}), \gamma K^j_b(\vec{x}')\} = \\ =& \gamma \Big(\frac{\delta \Gamma^j_b(\vec{x}')}{\delta E^a_i(\vec{x})} - \frac{\delta \Gamma^i{}_a(\vec{x})}{\delta E^b_j(\vec{x}')} \Big) \,,\end{aligned}$$

and substituting in the relation

$$\Gamma^j_b(\vec{x}') = \frac{\delta}{\delta E^b_j(\vec{x}')} \int d\vec{x}\, E^c_k \Gamma^k_c(E) \,,$$

which in turn can be shown to hold using equation (A.90).

Now we write the other constraints in terms of the variables A_a^i and E_i^a. To that end we expand the curvature of A,

$$F_{ab}^k = \partial_a A_b^k - \partial_b A_a^k + \epsilon^k{}_{ij} A_a^i A_b^j \,,$$

in terms of K and Γ,

$$F_{ab}^k = \gamma(\mathcal{D}_a K_b^k - \mathcal{D}_b K_a^k) + \gamma^2 \epsilon^k{}_{ij} K_a^i K_b^j + \mathcal{R}_{ab}^k \,. \tag{A.91}$$

Contracting it with E_k^b (and remembering that $\mathcal{R}_{ab}^k E_k^b = 0$ due to Bianchi identity) yields the diffeomorphism constraint

$$\mathcal{H}_a = \gamma^{-1} F_{ab}^k E_k^b - \gamma K_a^i \mathcal{G}_i \,.$$

Next we contract equation (A.91) with $\epsilon_k{}^{ij} E_i^a E_j^b$ and find

$$\mathcal{H} = \frac{1}{\sqrt{|\det E_i^a|}} \left(\epsilon_k{}^{ij} E_i^a E_j^b F_{ab}^k - 2(1+\gamma^2) E_i^a E_j^b K_{[a}^i K_{b]}^j \right) + (1+\gamma^2) \mathcal{G}^i \partial_a \big(\sqrt{|\det E|}^{-1} E_i^a \big) \,.$$

Hence, with some redefinitions, we can write Ashtekar action

$$S[A_a^i, E_i^a, N, N^a, \Lambda^i] = \int dt \int_\Sigma d\vec{x}\, E_i^a \dot{A}_a^i - N\mathcal{H} - N^a \mathcal{H}_a - \Lambda^i \mathcal{G}_i \tag{A.92}$$

with the constraints given by

$$\mathcal{G}_i = D_a E_i^a \,, \tag{A.93}$$

$$\mathcal{H}_a = E_k^b F_{ab}^k[A] \,, \tag{A.94}$$

$$\mathcal{H} = \frac{\epsilon_k{}^{ij} E_i^a E_j^b}{\sqrt{|\frac{1}{3!}\epsilon_{abc}\epsilon^{ijk} E_i^a E_j^b E_k^c|}} \left(F_{ab}^k[A] - (1+\gamma^2) \epsilon^k{}_{mn} K_a^m[A,E] K_b^n[A,E] \right) \,. \tag{A.95}$$

In the Euclidean case, the term $(1+\gamma^2)$ is replaced by $(1-\gamma^2)$. In that case the choice $\gamma = 1$ simplyfies greatly the Hamiltonian constraint without modifying the (classical) dynamics.

A.6 The holonomy of the connection and the flux of the electric field

In this chapter we have recast general relativity as a dynamical theory of $SU(2)$-connections and $SU(2)$-electric fields, i.e. a theory defined on the phase space $(A_a^i(\vec{x}), E_i^a(\vec{x}))$. Here we introduce some *elementary* functions on phase space and provide a geometric interpretation for them.

Given an oriented path Υ embedded in Σ, i.e. a 1-dimensional submanifold of Σ given by the set $\Upsilon = \{x^a_\Upsilon(\lambda) \in \Sigma \,|\, \lambda \in [0,1] \subset \mathbb{R}\}$ with a chart provided by the coordinate λ, we define $h_\Upsilon[A,\lambda]$ as the unique solution of the ordinary differential equation

$$\frac{d}{d\lambda} h_\Upsilon[A,\lambda] - i\, A_a(x_\Upsilon(\lambda)) \frac{dx^a_\Upsilon}{d\lambda}(\lambda)\; h_\Upsilon[A,\lambda] = 0\,,$$

with the boundary condition $h_\Upsilon[A,0] = \mathbb{I}$. The holonomy of the connection $A_a(\vec{x}) = A^i_a(\vec{x})\tau_i$ along a path Υ is defined as $h_\Upsilon[A] = h_\Upsilon[A,1]$. By its definition we see that it is independent of the parametrization λ of the path Υ. The solution of the previous differential equation can be formally written in terms of the familiar series expansion

$$\begin{aligned} h_\Upsilon[A] =& \mathbb{I} + i \int_0^1 d\lambda\, \frac{dx^a_\Upsilon}{d\lambda}(\lambda)\, A_a(\vec{x}(\lambda)) + \\ &+ i^2 \int_0^1 d\lambda_1 \int_0^{\lambda_1} d\lambda_2 \frac{dx^{a_1}_\Upsilon}{d\lambda_1}(\lambda_1) \frac{dx^{a_2}_\Upsilon}{d\lambda_2}(\lambda_2)\;\; A_{a_1}(x_\Upsilon(\lambda_1)) A_{a_2}(x_\Upsilon(\lambda_2)) + \\ &+ \ldots, \end{aligned} \tag{A.96}$$

which is usually denoted by a path ordered exponential, $h_\Upsilon[A] = P \exp i \int_\Upsilon A_a dx^a$. Given the path Υ, the holonomy can be seen as a map sending the configuration A to a group element, $h_\Upsilon : \mathcal{C} \to SU(2)$. We list some properties of the holonomy:

(i) The holonomy of a path given by a single point is the identity.

(ii) Consider two oriented paths Υ_1 and Υ_2 such that the end-point of Υ_1 coincides with the starting point of Υ_2 so that we can define the path $\Upsilon = \Upsilon_1 \circ \Upsilon_2$. Then we have that $h_\Upsilon[A] = h_{\Upsilon_1}[A]\, h_{\Upsilon_2}[A]$.

(iii) Denoting Υ^{-1} the path with the same support as Υ but with opposite orientation, we have that $h_{\Upsilon^{-1}}[A] = h_\Upsilon[A]^{-1}$.

Geometrically, the holonomy $h_\Upsilon[A]$ is a functional of the connection that provides a rule for the parallel transport of $SU(2)$ spinors along the path Υ.

Now we shift attention to the electric field $E^a_i(\vec{x})$ and provide a natural smearing for it. As can be easily checked taking the Poisson bracket of $E^a_i(\vec{x})$ with the diffeomorphism constraint, the electric field transforms as a vector density of weight one. Hence it naturally induces a two-form with values in the Lie algebra of $SU(2)$, namely $\epsilon_{abc} E^a_i(\vec{x}) dx^b \wedge dx^c$. This suggests that the smearing should be defined on two-dimensional surfaces. Consider a surface S embedded in Σ with local coordinates σ_1, σ_2 and embedding $x^a(\sigma_1,\sigma_2)$. The flux of the electric field accross the surface S provides exactly such smearing

$$\mathcal{F}_S[\alpha, E] = \frac{1}{2}\int_S \epsilon_{abc}\, \alpha^i\, E^a_i\, dx^b \wedge dx^c = \int d^2\vec{\sigma}\ \alpha^i(\vec{\sigma})\, E^a_i(\vec{x}(\sigma))\, n_a(\vec{\sigma}) \tag{A.97}$$

where $\alpha_i(\vec{\sigma})$ is a smearing function and n_a is the normal one-form on S,

$$n_a(\vec{\sigma}) = \epsilon_{abc}\, \frac{\partial x^b(\vec{\sigma})}{\partial \sigma^1}\frac{\partial x^c(\vec{\sigma})}{\partial \sigma^2}\,. \tag{A.98}$$

The Poisson bracket between the holonomy of the connection and the flux of the electric field can be easily calculated and has a simple, geometrical structure. We give it explicitly here as it plays a key role at the quantum level. Suppose the path Υ intersects in a point σ the surface S and that the orientation of Υ coincides with the orientation of S. Then we have

$$\{\mathcal{F}_S[\alpha, E], h_\Upsilon[A]\} = \alpha^i\ h_{\Upsilon_1}[A]\, \tau_i\, h_{\Upsilon_2}[A]\,, \tag{A.99}$$

where $\Upsilon = \Upsilon_1 \circ \Upsilon_2$ and the target of Υ_1 (which coincides with the source of Υ_2) is the intersection point $\Upsilon \cap S$.

Appendix B

Gravitons in the linearized canonical formulation

The free part of perturbative gravity on Minkowski space is described by the Fierz-Pauli action ([136]). The action is a functional of a symmetric tensor field $\varphi_{\mu\nu}$ propagating in a Minkowski background geometry and defined by the ansatz $g_{\mu\nu}(x) = \eta_{\mu\nu} + \epsilon\varphi_{\mu\nu}(x)$. We restrict attention to the free quadratic part of the action. The Fierz-Pauli action written in Fourier transform is given by

$$S[\varphi_{\mu\nu}] = \frac{1}{2}\int \frac{dk}{(2\pi)^D}\, \varphi_{\mu\nu}(k) D^{\mu\nu\rho\sigma}(k)\varphi_{\rho\sigma}(k)\,, \tag{B.1}$$

with

$$\begin{aligned} D^{\mu\nu\rho\sigma}(k) = -\frac{1}{4}\Big(& k^\mu k^\rho \eta^{\nu\sigma} + k^\mu k^\sigma \eta^{\nu\rho} + k^\nu k^\rho \eta^{\mu\sigma} + k^\nu k^\sigma \eta^{\mu\rho} - 2k^\mu k^\nu \eta^{\rho\sigma} - 2k^\rho k^\sigma \eta^{\mu\nu} \\ & - (\eta^{\mu\rho}\eta^{\nu\sigma} + \eta^{\mu\sigma}\eta^{\nu\rho} - 2\eta^{\mu\nu}\eta^{\rho\sigma})k^2 \Big)\,. \end{aligned}$$

The action is invariant under the gauge transformations $\tilde{\varphi}_{\mu\nu}(x) = \varphi_{\mu\nu}(x) + \partial_\mu\xi_\nu(x) + \partial_\nu\xi_\mu(x)$, i.e. $S[\tilde{\varphi}_{\mu\nu}] = S[\varphi_{\mu\nu}]$. To analyze the dependence of the action on the symmetric tensor field $\varphi_{\mu\nu}$, it is useful to introduce spin projector operators and express the field $\varphi_{\mu\nu}$ in terms of its spin components. In momentum space, we introduce the transverse projector $P^{\mu\nu}$ defined by

$$P^{\mu\nu}(k) = \eta^{\mu\nu} - \frac{k^\mu k^\nu}{k^2}\,.$$

The spin projection operators can be written in terms of the transverse projector:

$$P_{(2)}^{\mu\nu\rho\sigma}(k) = \frac{1}{2}\big(P^{\mu\rho}P^{\nu\sigma} + P^{\mu\sigma}P^{\nu\rho}\big) - \frac{1}{D-1}P^{\mu\nu}P^{\rho\sigma}\,, \tag{B.2}$$

$$P_{(1)}^{\mu\nu\rho\sigma}(k) = \frac{1}{2}\big(\eta^{\mu\rho}\eta^{\nu\sigma} + \eta^{\mu\sigma}\eta^{\nu\rho}\big) - \frac{1}{2}\big(P^{\mu\rho}P^{\nu\sigma} + P^{\mu\sigma}P^{\nu\rho}\big)\,, \tag{B.3}$$

$$P_{(0)}^{\mu\nu\rho\sigma}(k) = \frac{1}{D-1}P^{\mu\nu}P^{\rho\sigma}\,. \tag{B.4}$$

They add up to give the identity matrix,

$$P_{(2)}^{\mu\nu\rho\sigma}(k) + P_{(1)}^{\mu\nu\rho\sigma}(k) + P_{(0)}^{\mu\nu\rho\sigma}(k) = \frac{1}{2}\big(\eta^{\mu\rho}\eta^{\nu\sigma} + \eta^{\mu\sigma}\eta^{\nu\rho}\big)\,.$$

The field $\varphi_{\mu\nu}$ can be decomposed in the three spin components $\varphi_{\mu\nu}^{(s)} = P_{(s)\mu\nu}^{\rho\sigma}\varphi_{\rho\sigma}$, with $s = 0, 1, 2$. Gauge transformations then affect only the spin-1 component,

$$P_{(1)\mu\nu}^{\rho\sigma}(k)\big(k_\rho\xi_\sigma(k) + k_\sigma\xi_\rho(k)\big) = k_\mu\xi_\nu(k) + k_\nu\xi_\mu(k)\,.$$

The kernel $D^{\mu\nu\rho\sigma}(k)$ appearing in the quadratic action (B.1) can be written in terms of the spin projection operators,

$$\begin{aligned} D^{\mu\nu\rho\sigma}(k) &= \frac{1}{4}\big(P^{\mu\rho}P^{\nu\sigma} + P^{\mu\sigma}P^{\nu\rho} - 2P^{\mu\nu}P^{\rho\sigma}\big)k^2 \\ &= \Big(\frac{1}{2}P_{(2)}^{\mu\nu\rho\sigma}(k) - \frac{D-2}{2}P_{(0)}^{\mu\nu\rho\sigma}(k)\Big)k^2\,. \end{aligned} \tag{B.5}$$

Thus the action (B.1) contains both transverse traceless modes (spin 2) and trace modes (spin 0). The longitudinal modes corresponding to gauge transformations are projected out.

The two-point function in gauge $\chi_F(\varphi) = 0$ is defined as

$$G_{\mu\nu\rho\sigma}^F(x,y) = \langle\varphi_{\mu\nu}^F(x)\varphi_{\rho\sigma}^F(y)\rangle = \frac{\displaystyle\int \mathscr{D}\varphi\ \varphi_{\mu\nu}^F(x)\,\varphi_{\rho\sigma}^F(y)\ \delta[\chi_F(\varphi)]\Delta_F[\varphi]\ \exp iS[\varphi]}{\displaystyle\int \mathscr{D}\varphi\ \delta[\chi_F(\varphi)]\Delta_F[\varphi]\ \exp iS[\varphi]}\,,$$

where $\varphi_{\mu\nu}^F(x)$ is such that it satisfies $\chi_F(\varphi^F) = 0$. The tensor field in a different gauge $\chi_{F'}$ is related to $\varphi_{\mu\nu}^F$ by the equation

$$\varphi_{\mu\nu}^{F'}(x) = \varphi_{\mu\nu}^F(x) + \partial_\mu\xi_\nu^{FF'}[\varphi^F(x)] + \partial_\nu\xi_\mu^{FF'}[\varphi^F(x)]\,.$$

The condition $\chi_{F'}(\varphi^{F'}) = 0$ determines $\xi_\mu^{FF'}$ (For a reference on the gauge projection method, see [205]). As a result we have that two-point functions in different gauges are related in the following way:

$$
\begin{aligned}
G^{F'}_{\mu\nu\rho\sigma}(x,y) =& \langle \varphi^{F'}_{\mu\nu}(x)\varphi^{F'}_{\rho\sigma}(y)\rangle \\
=& Z^{-1}\int \mathscr{D}\varphi\; \varphi^{F'}_{\mu\nu}(x)\,\varphi^{F'}_{\rho\sigma}(y)\;\delta[\chi_{F'}(\varphi)]\Delta_{F'}[\varphi]\;\exp iS[\varphi] \\
=& Z^{-1}\int \mathscr{D}\varphi\; \varphi^{F'}_{\mu\nu}(x)\,\varphi^{F'}_{\rho\sigma}(y)\;\delta[\chi_{F}(\varphi)]\Delta_{F}[\varphi]\;\exp iS[\varphi] \\
=& Z^{-1}\int \mathscr{D}\varphi\; \varphi^{F}_{\mu\nu}(x)\,\varphi^{F}_{\rho\sigma}(y)\;\delta[\chi_{F}(\varphi)]\Delta_{F}[\varphi]\;\exp iS[\varphi]+ \\
&+ Z^{-1}\int \mathscr{D}\varphi\; \varphi^{F}_{\mu\nu}(x)\left(\partial_\rho\xi^{FF'}_\sigma[\varphi^F(y)] + \partial_\sigma\xi^{FF'}_\rho[\varphi^F(y)]\right)\;\delta[\chi_{F}(\varphi)]\Delta_{F}[\varphi]\;\exp iS[\varphi]+ \\
&+\ \dots + \dots \\
=& G^{F}_{\mu\nu\rho\sigma}(x,y) + \ \dots
\end{aligned}
$$

Then we find that the propagator is given by the inverse of the kernel $D^{\mu\nu\rho\sigma}(k)$ in the subspace of spin two and spin zero, plus a gauge dependent contribution,

$$
G_{\mu\nu\rho\sigma}(k) = \frac{i}{2}\frac{2P^{\mu\nu\rho\sigma}_{(2)}(k) - \frac{2}{D-2}P^{\mu\nu\rho\sigma}_{(0)}(k)}{k^2 + i\epsilon} + (\text{gauge terms})\,. \tag{B.6}
$$

The gauge terms can be written in the form

$$
(\text{gauge terms}) = A_{\mu\nu}(k)\big(k_\rho\xi_\sigma(k) + k_\sigma\xi_\rho(k)\big) + \big(k_\mu\xi_\nu(k) + k_\nu\xi_\mu(k)\big)A_{\rho\sigma}(k)
$$

and are projected out when the propagator is contracted with gauge invariant sources,

$$
\int dx \int dy\, T^{\mu\nu}(x)G_{\mu\nu\rho\sigma}(x,y)T^{\rho\sigma}(y)\,.
$$

Using the explicit expressions for the projectors we can separate the $(k^2+i\epsilon)^{-1}$ terms from the others in the propagator,

$$
G_{\mu\nu\rho\sigma}(x,y) = \frac{i}{2}\int \frac{dk}{(2\pi)^D}\, e^{ik(x-y)}\frac{(\eta_{\mu\rho}\eta_{\nu\sigma} + \eta_{\mu\sigma}\eta_{\nu\rho} - \frac{2}{D-2}\eta_{\mu\nu}\eta_{\rho\sigma})}{k^2+i\epsilon} + \int \frac{dk}{(2\pi)^D}\, e^{ik(x-y)}\frac{B_{\mu\nu\rho\sigma}(k)}{k^2+i\epsilon}\,.
$$

To $B_{\mu\nu\rho\sigma}(k)$ contribute both projector terms and gauge terms. A gauge can be chosen such that $B = 0$. This is the harmonic gauge $(\eta^{\mu\sigma}k^\rho - \frac{1}{2}k^\mu\eta^{\rho\sigma})\varphi_{\rho\sigma}(k) = 0$, and corresponds to the linear approximation of $g^{\mu\nu}(x)\Gamma^\rho_{\mu\nu}(x) = 0$ when the ansatz $g_{\mu\nu}(x) = \eta_{\mu\nu} + \epsilon\varphi_{\mu\nu}(x)$ is used. It fixes the spin-1 modes of $\varphi_{\mu\nu}$ to be proportional to a certain combination of spin-0 and spin-2 modes. In four dimensions, in harmonic gauge, we have

$$
G_{\mu\nu\rho\sigma}(x,y) = \frac{i}{2}\frac{\eta_{\mu\rho}\eta_{\nu\sigma} + \eta_{\mu\sigma}\eta_{\nu\rho} - \eta_{\mu\nu}\eta_{\rho\sigma}}{\eta_{\mu'\nu'}(x-y)^{\mu'}(x-y)^{\nu'}}\,. \tag{B.7}
$$

B.1 Two-point function from the 3-geometry transition amplitude

The transition amplitude kernel for linearized gravity is given by

$$W_T[\phi'_{ab}, \phi''_{cd}] = \int_{\phi',\phi''} \mathscr{D}\varphi_{\mu\nu}\; \delta[\chi(\varphi)]\Delta[\varphi]\, \exp iS_T[\varphi_{\mu\nu}]\,, \tag{B.8}$$

where χ is a bulk gauge fixing and T the background-time interval. The kernel $W_T[\phi'_{ab}, \phi''_{cd}]$ corresponds to the 3-geometry transition amplitude $W[h'_{ab}, h''_{cd}]$ in the asymptotically flat case with the initial and final geometry approximately flat, $h_{ab}(\vec{x}) = \delta_{ab} + \epsilon\phi_{ab}(\vec{x})$, and T the asymptotic proper time. The two-point correlation function on the vacuum state is given by

$$G_{0\,abcd}(\vec{x},\vec{y},T) = \frac{\langle 0|\hat{\phi}_{cd}(\vec{y})\hat{W}_T\hat{\phi}_{ab}(\vec{x})|0\rangle}{\langle 0|\hat{W}_T|0\rangle}\,.$$

The amplitude kernel (B.8) as been studied in [206] using the temporal gauge. Here we give an Hamiltonian analysis of Fierz-Pauli action and determine the amplitude kernel W_T using phase space path integral techniques.

We start from Fierz-Pauli action (B.1). Notice that $D^{0000} = 0$, so there is no term quadratic in φ_{00} in the action. Similarly, as $D^{0a0b}(k) = (\delta^{ab} - \frac{k^a k^b}{|\vec{k}|^2})|\vec{k}|^2$, there is no term quadratic in time derivatives of φ_{0a}. Also the mixed terms vanish, as $D^{000a} = 0$. As a result the components φ_{00} and φ_{0a} are not dynamical and play the role of Lagrange multipliers in the Hamiltonian formulation. We call them respectively v and v^a. The position variable corresponding to the spatial components of $\varphi_{\mu\nu}$ will be called ϕ_{ab} and represents the fluctuation of the spatial metric off the euclidean metric, $h_{ab}(\vec{x}) = \delta_{ab} + \epsilon\phi_{ab}(\vec{x})$. We introduce the spatial transverse projector,

$$P^{ab}(\vec{k}) = \delta^{ab} - \frac{k^a k^b}{|\vec{k}|^2}$$

and the spatial spin projectors

$$\begin{aligned}
P^{abcd}_{(2)}(\vec{k}) &= \frac{1}{2}\big(P^{ac}P^{bd} + P^{ad}P^{bc}\big) - \frac{1}{d-1}P^{ab}P^{cd}\,,\\
P^{abcd}_{(1)}(\vec{k}) &= \frac{1}{2}\big(\delta^{ac}\delta^{bd} + \delta^{ad}\delta^{bc}\big) - \frac{1}{2}\big(P^{ac}P^{bd} + P^{ad}P^{bc}\big)\,,\\
P^{abcd}_{(0)}(\vec{k}) &= \frac{1}{d-1}P^{ab}P^{cd}\,.
\end{aligned}$$

They are not to be confused with the spatial components of the space-time spin projectors introduced in the previous section: only the spatial impulse $\vec{k}$ appears here. They add up to the identity,

$$P^{abcd}_{(2)}(\vec{k}) + P^{abcd}_{(1)}(\vec{k}) + P^{abcd}_{(0)}(\vec{k}) = \frac{1}{2}\big(\delta^{ac}\delta^{bd} + \delta^{ad}\delta^{bc}\big)\,.$$

The Hamiltonian version of Fierz-Pauli action has the following form[1]

$$S[\phi_{ab}, p^{ab}, v, v^a] = \int dt \left(\int d\vec{x}\, p^{ab}\dot{\phi}_{ab} - H - \int d\vec{x}\, v\mathcal{H} - \int d\vec{x}\, v^a\mathcal{H}_a\right) \tag{B.9}$$

with a true Hamiltonian H representing the energy of the system,

$$\begin{aligned} H = &\int d\vec{x}\, \frac{1}{2}\big(\delta^{ac}\delta^{bd} + \delta^{ad}\delta^{bc} - \frac{2}{d-1}\delta^{ab}\delta^{cd}\big)p^{ab}p^{cd} + \\ &\qquad + \frac{1}{2}\phi_{ab}\Big(\delta^{ac}\partial^b\partial^d - \delta^{ab}\partial^c\partial^d + \frac{1}{2}(\delta^{ab}\delta^{cd} - \delta^{ac}\delta^{bd})\Delta\Big)\phi_{cd} = \\ = &\int \frac{d\vec{k}}{(2\pi)^d}\, \frac{1}{2}\big(\delta^{ac}\delta^{bd} + \delta^{ad}\delta^{bc} - \frac{2}{d-1}\delta^{ab}\delta^{cd}\big)p^{ab}(\vec{k})p^{cd}(-\vec{k}) + \\ &\qquad + \frac{1}{2}\phi_{ab}(\vec{k})\Big(\frac{1}{2}P^{abcd}_{(2)}(\vec{k}) - P^{abcd}_{(0)}(\vec{k})\Big)|\vec{k}|^2\phi_{cd}(-\vec{k}) \end{aligned} \tag{B.10}$$

a scalar constraint and a vector constraint,

$$\int d\vec{x}\, v(\vec{x})\mathcal{H}(\vec{x}) = -\int \frac{d\vec{k}}{(2\pi)^d}\, v(-\vec{k})\; P^{ab}(\vec{k})|\vec{k}|^2\phi_{ab}(\vec{k})\,, \tag{B.11}$$

$$\int d\vec{x}\, v_a(\vec{x})\mathcal{H}^a(\vec{x}) = \int \frac{d\vec{k}}{(2\pi)^d}\, v_a(-\vec{k})\; k_b p^{ab}(\vec{k})\,. \tag{B.12}$$

The scalar constraint kills the spin zero component of the position ϕ_{ab} and generates transformations of the spin zero component of the momentum p^{ab}. The vector constraint kills the spin one component on the momentum and generates transformations of the spin one component of ϕ_{ab} which correspond to linearized diffeomorphism.

[1]A different route could have been followed: the ADM action $S[h_{ab}, \pi^{ab}, N, N^a] = \int dt \int d\vec{x}\pi^{ab}\dot{h}_{ab} - N\mathcal{H} - N^a\mathcal{H}_a$ is highly non-linear in the metric h_{ab}, but it is quadratic in the momentum and linear in the Lagrangian multipliers. Then it would be natural to study perturbation theory in $h_{ab}(\vec{x}) = \delta_{ab} + \epsilon\phi_{ab}(\vec{x})$, without touching the laspe and the shift. As a result we have a totally constrained system. This is at odds with what we have found starting from Fierz-Pauli action: in equation (B.9), H is a true Hamiltonian. We expect this paradox could be solved considering the ADM action in the asymptotically flat case with the appropriate boundary term. The boundary term represents the ADM energy when the constraints are solved. We expect that, in the linearized theory, it can be written as a bulk integral coinciding with the expression (B.10) when the constraints are solved.

The transition amplitude kernel (B.8) can be written as a phase space path integral,

$$
\begin{aligned}
W_T[\phi'_{ab},\phi''_{cd}] = &\int_{\phi'_{ab}}^{\phi''_{cd}} \prod_t \mathcal{D}\phi_{ab} \int \prod_t \mathcal{D}p^{ab} \int \prod_t \mathcal{D}v \int \prod_t \mathcal{D}v^a \; \times \\
&\times \delta[\chi]\,\delta[\chi^a] \left| \det \begin{pmatrix} \{\chi,\mathcal{H}\} & \{\chi^a,\mathcal{H}\} \\ \{\chi,\mathcal{H}_b\} & \{\chi^a,\mathcal{H}_b\} \end{pmatrix} \right| \; \exp iS[\phi_{ab},p^{ab},v,v^a] = \\
= &\int_{\phi'_{ab}}^{\phi''_{cd}} \prod_t \mathcal{D}\phi_{ab} \int \prod_t \mathcal{D}p^{ab}\; \delta[\chi]\,\delta[\chi^a] \left| \det \begin{pmatrix} \{\chi,\mathcal{H}\} & \{\chi^a,\mathcal{H}\} \\ \{\chi,\mathcal{H}_b\} & \{\chi^a,\mathcal{H}_b\} \end{pmatrix} \right| \; \delta[\mathcal{H}]\,\delta[\mathcal{H}_a] \times \\
&\times \exp i \int dt \left(\int d\vec{x}\, p^{ab}\dot{\phi}_{ab} - H[\phi_{ab},p^{ab}] \right) = \\
= &\,\delta[\phi'^{(0)}_{ab}]\,\delta[\phi''^{(0)}_{cd}] \int_{\phi'^{(2)}_{ab}}^{\phi''^{(2)}_{cd}} \prod_t \mathcal{D}\phi^{(2)}_{ab} \int \prod_t \mathcal{D}p^{(2)ab}\; \exp i \int dt \left(\int d\vec{x}\, p^{(2)ab}\dot{\phi}^{(2)}_{ab} - H[\phi^{(2)}_{ab},p^{ab}] \right)
\end{aligned}
$$

A standard calculation involving the Hamilton principal function yields

$$
\begin{aligned}
W_T[\phi'_{ab},\phi''_{cd}] = &\; N^{-1}(T)\;\delta[P^{abcd}_{(0)}\phi'_{cd}]\;\delta[P^{abcd}_{(0)}\phi''_{cd}] \times \\
\times\; \exp i\,\frac{1}{2}\int \frac{d\vec{k}}{(2\pi)^3}\,|\vec{k}| &\left(\frac{P^{abcd}_{(2)}(\vec{k})\Big(\phi''_{ab}(\vec{k})\phi''_{cd}(-\vec{k}) + \phi'_{ab}(\vec{k})\phi'_{cd}(-\vec{k})\Big)}{\tan|\vec{k}|T} - 2\frac{P^{abcd}_{(2)}(\vec{k})\phi'_{ab}(\vec{k})\phi''_{cd}(-\vec{k})}{\sin|\vec{k}|T} \right).
\end{aligned}
$$

The vacuum state can be found as the minimum energy eigenstate of H satisfying the vector constraint[2] and is given by

$$
\Psi_0[\phi_{ab}] = C^{-1} \exp -\frac{1}{2}\int \frac{d\vec{k}}{(2\pi)^3}\,|\vec{k}|\,P^{abcd}_{(2)}(\vec{k})\,\phi_{ab}(\vec{k})\phi_{cd}(-\vec{k})\,.
$$

The two-point function is given by

$$
\begin{aligned}
G^F_{abcd}(\vec{x},\vec{y},T) = Z^{-1} \int \mathcal{D}\phi' \int \mathcal{D}\phi'' \Big(\delta[\chi^F(\phi')]\,\Delta^F[\phi']\Big) \Big(\delta[\chi^F(\phi'')]\Delta^F[\phi'']\Big) \times \\
\times\; \overline{\Psi_0[\phi'']}\;\phi''_{cd}(\vec{y})\;W_T[\phi',\phi'']\;\phi'_{ab}(\vec{x})\;\Psi_0[\phi']\,,
\end{aligned}
$$

where a boundary gauge fixing has been introduced. The gauge fixing terms have the purpose of eliminating the spin one degrees of freedom. The integral on the spin-2

[2] Notice that we do not require the scalar constraint to be satisfied. The physical scalar product is obtained inserting W_T which implements the scalar constraint. Insisting in solving the scalar constraint amounts here to an extra $\delta[\phi^{(0)}_{ab}]$. The limit $T \to \infty$ of the transition amplitude kernel gives the vacuum state with the extra delta function.

component can be easily done using the following relation for moments of a gaussian

$$\frac{\displaystyle\int d^n x \int d^n y \; x^k \, y^l \;\; \exp -\frac{1}{2} x^i M_{ij} y^j}{\displaystyle\int d^n x \int d^n y \;\; \exp -\frac{1}{2} x^i M_{ij} y^j} = M^{-1}_{kl} \, ,$$

and for the inverse of the covariance appearing in the gaussian

$$M = |\vec{k}| \begin{pmatrix} \frac{i}{\tan |\vec{k}| T} - 1 & \frac{i}{\sin |\vec{k}| T} \\ \frac{i}{\sin |\vec{k}| T} & \frac{i}{\tan |\vec{k}| T} - 1 \end{pmatrix} \quad , \quad M^{-1} = \frac{1}{2|\vec{k}|} \begin{pmatrix} -1 & e^{i|\vec{k}|T} \\ e^{i|\vec{k}|T} & -1 \end{pmatrix} .$$

We obtain

$$\begin{aligned} G^F_{abcd}(\vec{x}, \vec{y}, T) &= i \int \frac{d\vec{k}}{(2\pi)^d} \, e^{-i\vec{k}\cdot(\vec{x}-\vec{y})} \, P_{(2)\,abcd}(\vec{k}) \frac{e^{i|\vec{k}|T}}{2|\vec{k}|} + \text{gauge terms} \\ &= i\Big(\frac{1}{2}(\delta_{ac}\delta_{bd} + \delta_{ad}\delta_{bc}) - \frac{1}{d-1}\delta_{ab}\delta_{cd}\Big) \int \frac{d\vec{k}}{(2\pi)^d} \, \frac{e^{-i\vec{k}\cdot(\vec{x}-\vec{y}) + i|\vec{k}|T}}{2|\vec{k}|} + B_{abcd}(\vec{x}-\vec{y}, T) \end{aligned}$$

In spatial harmonic gauge, for $d = 3$, we have

$$G^F_{abcd}(\vec{x}, \vec{y}, T) = \frac{i}{2} \frac{(\delta_{ac}\delta_{bd} + \delta_{ad}\delta_{bc} - \delta_{ab}\delta_{cd})}{|\vec{x}-\vec{y}|^2 - T^2} \, ,$$

which can be compared with equation (B.7) for the graviton propagator.

Bibliography

[1] C. Rovelli, "Quantum gravity,". Cambridge, UK: Univ. Pr. (2004) 455 p.

[2] A. Ashtekar and J. Lewandowski, "Background independent quantum gravity: A status report," *Class. Quant. Grav.* **21** (2004) R53, gr-qc/0404018.

[3] T. Thiemann, "Modern canonical quantum general relativity,". Cambridge University Press 2007.

[4] M. P. Reisenberger and C. Rovelli, "*Sum over surfaces* form of loop quantum gravity," *Phys. Rev.* **D56** (1997) 3490–3508, gr-qc/9612035.

[5] J. Engle, E. Livine, R. Pereira, and C. Rovelli, "LQG vertex with finite Immirzi parameter," *Nucl. Phys.* **B799** (2008) 136–149, 0711.0146.

[6] L. Freidel and K. Krasnov, "A New Spin Foam Model for 4d Gravity," *Class. Quant. Grav.* **25** (2008) 125018, 0708.1595.

[7] H. Ooguri, "Topological lattice models in four-dimensions," *Mod. Phys. Lett.* **A7** (1992) 2799–2810, hep-th/9205090.

[8] R. De Pietri, L. Freidel, K. Krasnov, and C. Rovelli, "Barrett-Crane model from a Boulatov-Ooguri field theory over a homogeneous space," *Nucl. Phys.* **B574** (2000) 785–806, hep-th/9907154.

[9] L. Freidel, "Group field theory: An overview," *Int. J. Theor. Phys.* **44** (2005) 1769–1783, hep-th/0505016.

[10] E. Bianchi, "Loop Quantum Gravity à la Aharonov-Bohm," 0907.4388.

[11] G. 't Hooft, "A locally finite model for gravity," *Found. Phys.* **38** (2008) 733–757, 0804.0328.

[12] C. Rovelli, "A new look at loop quantum gravity," 1004.1780.

[13] C. Rovelli, "Simple model for quantum general relativity from loop quantum gravity," 1010.1939.

[14] M. B. Green, J. H. Schwarz, and E. Witten, "SUPERSTRING THEORY. VOL. 1: INTRODUCTION,". Cambridge, Uk: Univ. Pr. (1987) 469 P. (Cambridge Monographs On Mathematical Physics).

[15] M. B. Green, J. H. Schwarz, and E. Witten, "SUPERSTRING THEORY. VOL. 2: LOOP AMPLITUDES, ANOMALIES AND PHENOMENOLOGY,". Cambridge, Uk: Univ. Pr. (1987) 596 P. (Cambridge Monographs On Mathematical Physics).

[16] J. Polchinski, "String theory. Vol. 1: An introduction to the bosonic string,". Cambridge, UK: Univ. Pr. (1998) 402 p.

[17] J. Polchinski, "String theory. Vol. 2: Superstring theory and beyond,". Cambridge, UK: Univ. Pr. (1998) 531 p.

[18] S. Weinberg, "ULTRAVIOLET DIVERGENCES IN QUANTUM THEORIES OF GRAVITATION,". In *Hawking, S.W., Israel, W.: General Relativity*, 790- 831.

[19] M. Niedermaier and M. Reuter, "The Asymptotic Safety Scenario in Quantum Gravity," *Living Rev. Rel.* **9** (2006) 5.

[20] J. Ambjorn, J. Jurkiewicz, and R. Loll, "Dynamically triangulating Lorentzian quantum gravity," *Nucl. Phys.* **B610** (2001) 347–382, `hep-th/0105267`.

[21] J. Ambjorn, J. Jurkiewicz, and R. Loll, "Emergence of a 4D world from causal quantum gravity," *Phys. Rev. Lett.* **93** (2004) 131301, `hep-th/0404156`.

[22] P. Horava, "Quantum Gravity at a Lifshitz Point," *Phys. Rev.* **D79** (2009) 084008, `0901.3775`.

[23] A. H. Chamseddine and A. Connes, "Noncommutative Geometry as a Framework for Unification of all Fundamental Interactions including Gravity. Part I," *Fortsch. Phys.* **58** (2010) 553–600, `1004.0464`.

[24] S. Weinberg, "The Quantum theory of fields. Vol. 1: Foundations,". Cambridge, UK: Univ. Pr. (1995) 609 p.

[25] S. Weinberg, "The quantum theory of fields. Vol. 2: Modern applications,". Cambridge, UK: Univ. Pr. (1996) 489 p.

[26] J. Polchinski, "Effective field theory and the Fermi surface," `hep-th/9210046`.

[27] J. F. Donoghue, "Introduction to the Effective Field Theory Description of Gravity," `gr-qc/9512024`.

[28] C. P. Burgess, "Quantum gravity in everyday life: General relativity as an effective field theory," *Living Rev. Rel.* **7** (2004) 5, `gr-qc/0311082`.

[29] G. 't Hooft and M. J. G. Veltman, "One loop divergencies in the theory of gravitation," *Annales Poincare Phys. Theor.* **A20** (1974) 69–94.

[30] M. H. Goroff and A. Sagnotti, "QUANTUM GRAVITY AT TWO LOOPS," *Phys. Lett.* **B160** (1985) 81.

[31] C. Rovelli and L. Smolin, "Discreteness of area and volume in quantum gravity," *Nucl. Phys.* **B442** (1995) 593–622, `gr-qc/9411005`.

[32] R. Oeckl, "A 'general boundary' formulation for quantum mechanics and quantum gravity," *Phys. Lett.* **B575** (2003) 318–324, `hep-th/0306025`.

[33] L. Modesto and C. Rovelli, "Particle scattering in loop quantum gravity," *Phys. Rev. Lett.* **95** (2005) 191301, `gr-qc/0502036`.

[34] J. B. Hartle and S. W. Hawking, "Wave Function of the Universe," *Phys. Rev.* **D28** (1983) 2960–2975.

[35] C. J. Isham, "Canonical quantum gravity and the problem of time," `gr-qc/9210011`.

[36] A. Ashtekar, "New Variables for Classical and Quantum Gravity," *Phys. Rev. Lett.* **57** (1986) 2244–2247.

[37] A. Ashtekar, "Lectures on nonperturbative canonical gravity,". Singapore, Singapore: World Scientific (1991) 334 p. (Advanced series in astrophysics and cosmology, 6).

[38] S. Holst, "Barbero's Hamiltonian derived from a generalized Hilbert- Palatini action," *Phys. Rev.* **D53** (1996) 5966–5969, `gr-qc/9511026`.

[39] O. Chandia and J. Zanelli, "Topological invariants, instantons and chiral anomaly on spaces with torsion," *Phys. Rev.* **D55** (1997) 7580–7585, `hep-th/9702025`.

[40] R. Jackiw, "TOPOLOGICAL INVESTIGATIONS OF QUANTIZED GAUGE THEORIES,". Presented at Les Houches Summer School on Theoretical Physics: Relativity Grops and Topology, Les Houches, France, Jun 27 - Aug 4, 1983.

[41] C. Rovelli and L. Smolin, "Loop Space Representation of Quantum General Relativity," *Nucl. Phys.* **B331** (1990) 80.

[42] R. F. Streater and A. S. Wightman, "PCT, spin and statistics, and all that,". Addison-Wesley, 1989.

[43] Barut and Racza, *Theory of group representations and applications.* World Scientific, 1986.

[44] "Roger Penrose, " Angular momentum: An approach to combinatorial space-time" in Quantum Theory and Beyond edited by T. Bastin (Cambridge University Press, Cambridge, 1971); " Combinatorial Quantum Theory and Quantized Directions" in Advances in Twistor Theory, Research Notes in Mathematics 37, edited by L. P. Hughston and R. S. Ward (Pitman, San Fransisco, 1979) pp. 301-307; in Combinatorial Mathematics and its Application edited by D. J. A. Welsh (Academic Press, London, 1971); "Theory of Quantized Directions," unpublished notes. John P. Moussouris, "Quantum Models as Space-time Based on Recoupling Theory" D.Phil. Thesis, Oxford University, Oxford, 1983.,".

[45] L. Landau and E. Lifshits, "Quantum Mechanics Non-Relativistic Theory,". (vol. 3, first ed., Pergamon, UK, 1958).

[46] Ruhl, *The Lorentz group and harmonic analysis.* Benjamin (1970).

[47] G. Ponzano and T. Regge, "Semiclassical limit of Racah coeffecients," *Spectroscopic and Group Theoretical Methods in Physics, edited by F. Block (North Holland, Amsterdam, 1968).*

[48] F. Conrady and L. Freidel, "On the semiclassical limit of 4d spin foam models," *Phys. Rev.* **D78** (2008) 104023, `0809.2280`.

[49] J. W. Barrett, R. J. Dowdall, W. J. Fairbairn, F. Hellmann, and R. Pereira, "Lorentzian spin foam amplitudes: graphical calculus and asymptotics," `0907.2440`.

[50] L. Freidel and S. Speziale, "Twisted geometries: A geometric parametrisation of SU(2) phase space," `1001.2748`.

[51] C. Rovelli and S. Speziale, "On the geometry of loop quantum gravity on a graph," *Phys. Rev.* **D82** (2010) 044018, `1005.2927`.

[52] A. Barbieri, "Quantum tetrahedra and simplicial spin networks," *Nucl. Phys.* **B518** (1998) 714–728, `gr-qc/9707010`.

[53] J. C. Baez and J. W. Barrett, "The quantum tetrahedron in 3 and 4 dimensions," *Adv. Theor. Math. Phys.* **3** (1999) 815–850, `gr-qc/9903060`.

[54] L. Freidel and E. R. Livine, "The Fine Structure of SU(2) Intertwiners from U(N) Representations," *J. Math. Phys.* **51** (2010) 082502, `0911.3553`.

[55] E. Bianchi, P. Dona', and S. Speziale, "Polyhedra in loop quantum gravity," `1009.3402`.

[56] M. Kapovich and J. J. Millson, "The symplectic geometry of polygons in Euclidean space," *J. Differential Geom.* **44**, *3 (1996), 479-513.*

[57] H. Minkowski, "H. Allgemeine Lehrsätze über die konvexe Polyeder," *Nachr. Ges. Wiss., Göttingen, 1897, 198-219.*

[58] E. R. Livine and S. Speziale, "A new spinfoam vertex for quantum gravity," *Phys. Rev.* **D76** (2007) 084028, `0705.0674`.

[59] F. Conrady and L. Freidel, "Quantum geometry from phase space reduction," *J. Math. Phys.* **50** (2009) 123510, `0902.0351`.

[60] A. D. Alexandrov, "Convex Polyhedra," *Springer (2005).*

[61] H. S. M. Coxeter, "Regular Polytopes," *Dover (1973).*

[62] U. Pachner, "PL homeomorphic manifolds are equivalent by elementary shellings," *European Journal of Combinatorics* **12**, *129 (1991).*

[63] G. P. Michon `http://www.numericana.com/data/polyhedra.htm`.

[64] J. B. Lasserre, "An analytical expression and an algorithm for the volume of a Convex Polyhedron in Rn," *J. Optim. Theor. Appl. 39, pp. 363–377.*

[65] P. Gritzmann and V. Klee *On the complexity of some basic problems in computational convexity: II. Volume and mixed volumes, polyhedra: Abstract, Convex and Computational (Boston) (T. Bisztriczky, P. McMullen, R. Schneider, and A. I. Weiss, eds.), Kluwer, 1994, pp. 373-466.*

[66] Büeler, A. Enge, and K. Fukuda, "Exact volume computation for polytopes: A practical study," *Polytopes - Combinatorics and Computation, DMV-Seminars vol. 29., Birkhäuser Verlag, Basel 2000, pp. 131–154.*

[67] Little, "Extended Gaussian images, mixed volumes, shape reconstruction," *SCG '85: Proceedings of the first annual symposium on Computational geometry, pp. 15–23.*

[68] C. Godsil and G. Royle, "Algebraic Graph Theory," *Springer Verlag (2001).*

[69] B. Dittrich and S. Speziale, "Area-angle variables for general relativity," *New J. Phys.* **10** (2008) 083006, `0802.0864`.

[70] C. Rovelli and L. Smolin, "Spin networks and quantum gravity," *Phys. Rev.* **D52** (1995) 5743–5759, `gr-qc/9505006`.

[71] J. C. Baez, "Spin Network States in Gauge Theory," *Adv. Math.* **117** (1996) 253–272, `gr-qc/9411007`.

[72] L. Charles, "On the quantization of polygon spaces," *[arXiv:0806.1585]*.

[73] L. Freidel, K. Krasnov, and E. R. Livine, "Holomorphic Factorization for a Quantum Tetrahedron," *Commun. Math. Phys.* **297** (2010) 45–93, `0905.3627`.

[74] J. Roberts, "Classical 6j-symbols and the tetrahedron," *Geom. Topol.* **3** *(1999), 21-66 [arXiv:math-ph/9812013]*.

[75] M. Kapovich and J. Millson, "Quantization of bending deformations of polygons in E3 , hypergeometric integrals and the Gassner representation," *Canad. Math. Bull., Vol. 44, (2001) p. 36-60*.

[76] V. Guillemin and S. Sternberg, "Geometric quantization and multiplicities of group representations," *Invent. Math., 67(3):515–538, 1982*.

[77] S. A. Major, "Operators for quantized directions," *Class. Quant. Grav.* **16** (1999) 3859–3877, `gr-qc/9905019`.

[78] C. Rovelli and S. Speziale, "A semiclassical tetrahedron," *Class. Quant. Grav.* **23** (2006) 5861–5870, `gr-qc/0606074`.

[79] A. M. Perelomov, "Generalized Coherent States and Their Applications," *Springer-Verlag, 1986*.

[80] B. S. S. John R. Klauder, "Coherent states: applications in physics and mathematical physics," *World Scientific, 1985*.

[81] J. W. Barrett, R. J. Dowdall, W. J. Fairbairn, H. Gomes, and F. Hellmann, "Asymptotic analysis of the EPRL four-simplex amplitude," *J. Math. Phys.* **50** (2009) 112504, `0902.1170`.

[82] L. Freidel and E. R. Livine, "U(N) Coherent States for Loop Quantum Gravity," `1005.2090`.

[83] E. F. Borja, J. Diaz-Polo, I. Garay, and E. R. Livine, "Dynamics for a 2-vertex Quantum Gravity Model," `1006.2451`.

[84] B. Bahr and T. Thiemann, "Gauge-invariant coherent states for Loop Quantum Gravity II: Non-abelian gauge groups," *Class. Quant. Grav.* **26** (2009) 045012, `0709.4636`.

[85] T. Thiemann, "Gauge field theory coherent states (GCS). I: General properties," *Class. Quant. Grav.* **18** (2001) 2025–2064, hep-th/0005233.

[86] T. Thiemann and O. Winkler, "Gauge field theory coherent states (GCS). II: Peakedness properties," *Class. Quant. Grav.* **18** (2001) 2561–2636, hep-th/0005237.

[87] T. Thiemann and O. Winkler, "Gauge field theory coherent states (GCS) III: Ehrenfest theorems," *Class. Quant. Grav.* **18** (2001) 4629–4682, hep-th/0005234.

[88] T. Thiemann and O. Winkler, "Gauge field theory coherent states (GCS). IV: Infinite tensor product and thermodynamical limit," *Class. Quant. Grav.* **18** (2001) 4997–5054, hep-th/0005235.

[89] B. Hall, "Geometric quantization and the generalized SegalBargmann transclass for Lie groups of compact type," *Comm. Math. Phys.* **226** *(2002) 233268.*

[90] E. Bianchi, E. Magliaro, and C. Perini, "LQG propagator from the new spin foams," *Nucl. Phys.* **B822** (2009) 245–269, 0905.4082.

[91] E. Bianchi, C. Rovelli, and F. Vidotto, "Towards Spinfoam Cosmology," *Phys. Rev.* **D82** (2010) 084035, 1003.3483.

[92] E. Bianchi, "The length operator in Loop Quantum Gravity," *Nucl. Phys.* **B807** (2009) 591–624, 0806.4710.

[93] B. Dittrich and J. P. Ryan, "Phase space descriptions for simplicial 4d geometries," 0807.2806.

[94] E. Bianchi, E. Magliaro, and C. Perini, "Coherent spin-networks," *Phys. Rev.* **D82** (2010) 024012, 0912.4054.

[95] L. Freidel and S. Speziale, "Quantum twisted geometries and coherent states," *to appear (2010).*

[96] F. A. Berezin, "Non-wiener continual integrals," *Teor. Mat. Fiz.* **6** *(1971) 194.*

[97] F. A. Berezin, "Feynman Path Integrals In A Phase Space," *Sov. Phys. Usp.* **23** *(1981) 763 [Usp. Fiz. Nauk* **132** *(1980) 497].*

[98] R. J. Glauber, "Coherent and incoherent states of the radiation field," *Phys. Rev.* **131** *(1963) 2766.*

[99] E. C. G. Sudarshan, "Equivalence of semiclassical and quantum mechanical descriptions of statistical light beams," *Phys. Rev. Lett.* **10***, 277 (1963).*

[100] J. Brunnemann and D. Rideout, "Properties of the Volume Operator in Loop Quantum Gravity I: Results," *Class. Quant. Grav.* **25** (2008) 065001, `0706.0469`.

[101] E. Bianchi and H. Haggard, "Volume spectrum from Bohr-Sommerfeld quantization," *to appear (2010)*.

[102] A. Ashtekar and J. Lewandowski, "Quantum theory of geometry. II: Volume operators," *Adv. Theor. Math. Phys.* **1** (1998) 388–429, `gr-qc/9711031`.

[103] R. De Pietri and C. Rovelli, "Geometry Eigenvalues and Scalar Product from Recoupling Theory in Loop Quantum Gravity," *Phys. Rev.* **D54** (1996) 2664–2690, `gr-qc/9602023`.

[104] T. Thiemann, "Closed formula for the matrix elements of the volume operator in canonical quantum gravity," *J. Math. Phys.* **39** (1998) 3347–3371, `gr-qc/9606091`.

[105] K. Giesel and T. Thiemann, "Consistency check on volume and triad operator quantisation in loop quantum gravity. I," *Class. Quant. Grav.* **23** (2006) 5667–5692, `gr-qc/0507036`.

[106] J. Brunnemann and T. Thiemann, "Simplification of the spectral analysis of the volume operator in loop quantum gravity," *Class. Quant. Grav.* **23** (2006) 1289–1346, `gr-qc/0405060`.

[107] T. Thiemann, "Quantum spin dynamics (QSD)," *Class. Quant. Grav.* **15** (1998) 839–873, `gr-qc/9606089`.

[108] C. Flori and T. Thiemann, "Semiclassical analysis of the Loop Quantum Gravity volume operator: I. Flux Coherent States," `0812.1537`.

[109] W. Kaminski, M. Kisielowski, and J. Lewandowski, "Spin-Foams for All Loop Quantum Gravity," *Class. Quant. Grav.* **27** (2010) 095006, `0909.0939`.

[110] J. Engle, R. Pereira, and C. Rovelli, "The loop-quantum-gravity vertex-amplitude," *Phys. Rev. Lett.* **99** (2007) 161301, `0705.2388`.

[111] A. Perez, "Spin foam models for quantum gravity," *Class. Quant. Grav.* **20** (2003) R43, `gr-qc/0301113`.

[112] A. Ashtekar, J. Lewandowski, D. Marolf, J. Mourao, and T. Thiemann, "Coherent state transforms for spaces of connections," *J. Funct. Anal.* **135** (1996) 519–551, `gr-qc/9412014`.

[113] H. Sahlmann, T. Thiemann, and O. Winkler, "Coherent states for canonical quantum general relativity and the infinite tensor product extension," *Nucl. Phys.* **B606** (2001) 401–440, gr-qc/0102038.

[114] T. Thiemann, "Complexifier coherent states for quantum general relativity," *Class. Quant. Grav.* **23** (2006) 2063–2118, gr-qc/0206037.

[115] B. Bahr and T. Thiemann, "Gauge-invariant coherent states for Loop Quantum Gravity I: Abelian gauge groups," *Class. Quant. Grav.* **26** (2009) 045011, 0709.4619.

[116] E. Bianchi, E. Magliaro, and C. Perini, "Spinfoams in the holomorphic representation," 1004.4550.

[117] C. W. Misner, "Feynman quantization of general relativity," *Rev. Mod. Phys.* **29** (1957) 497–509.

[118] S. W. Hawking, "Quantum Gravity and Path Integrals," *Phys. Rev.* **D18** (1978) 1747–1753.

[119] E. Bianchi, D. Regoli, and C. Rovelli, "Face amplitude of spinfoam quantum gravity," *Class. Quant. Grav.* **27** (2010) 185009, 1005.0764.

[120] F. Conrady and L. Freidel, "Path integral representation of spin foam models of 4d gravity," *Class. Quant. Grav.* **25** (2008) 245010, 0806.4640.

[121] R. J. Dowdall, H. Gomes, and F. Hellmann, "Asymptotic analysis of the Ponzano-Regge model for handlebodies," *J.Phys.A* **A43** (2010) 115203, 0909.2027.

[122] F. Bloch, "Nuclear Induction," *Phys. Rev.* **70** *(1946) 460-474.*

[123] B. C. Hall, "The Segal-Bargmann Coherent State Transform for Compact Lie Groups," *J. Funct. Anal. 122 (1994) 103151.*

[124] V. Bonzom, "From lattice BF gauge theory to area-angle Regge calculus," *Class. Quant. Grav.* **26** (2009) 155020, 0903.0267.

[125] D. Oriti and T. Tlas, "Encoding simplicial quantum geometry in group field theories," *Class. Quant. Grav.* **27** (2010) 135018, 0912.1546.

[126] A. Baratin and D. Oriti, "Group field theory with non-commutative metric variables," 1002.4723.

[127] T. Regge, "General Relativity without coordinates," *Nuovo Cim.* **19** (1961) 558–571.

[128] C. Rovelli, "Graviton propagator from background-independent quantum gravity," *Phys. Rev. Lett.* **97** (2006) 151301, gr-qc/0508124.

[129] E. Alesci, E. Bianchi, E. Magliaro, and C. Perini, "Asymptotics of LQG fusion coefficients," *Class. Quant. Grav.* **27** (2010) 095016, 0809.3718.

[130] E. Magliaro, C. Perini, and C. Rovelli, "Numerical indications on the semiclassical limit of the flipped vertex," *Class. Quant. Grav.* **25** (2008) 095009, 0710.5034.

[131] R. Pereira, "Lorentzian LQG vertex amplitude," *Class. Quant. Grav.* **25** (2008) 085013, 0710.5043.

[132] J. Engle and R. Pereira, "Regularization and finiteness of the Lorentzian LQG vertices," *Phys. Rev.* **D79** (2009) 084034, 0805.4696.

[133] R. P. Feynman and A. R. Hibbs, "Quantum Mechanics and Path Integrals,," *McGraw-Hill Companies (1965).*

[134] E. Bianchi and A. Satz, "Semiclassical regime of Regge calculus and spin foams," *Nucl. Phys.* **B808** (2009) 546–568, 0808.1107.

[135] E. Alesci, E. Bianchi, and C. Rovelli, "LQG propagator: III. The new vertex," *Class. Quant. Grav.* **26** (2009) 215001, 0812.5018.

[136] M. J. G. Veltman, "Quantum Theory of Gravitation,". In *Les Houches 1975, Proceedings, Methods In Field Theory*, Amsterdam 1976, 265-327.

[137] J. F. Donoghue, "General relativity as an effective field theory: The leading quantum corrections," *Phys. Rev.* **D50** (1994) 3874–3888, gr-qc/9405057.

[138] E. Bianchi, L. Modesto, C. Rovelli, and S. Speziale, "Graviton propagator in loop quantum gravity," *Class. Quant. Grav.* **23** (2006) 6989–7028, gr-qc/0604044.

[139] E. R. Livine and S. Speziale, "Group Integral Techniques for the Spinfoam Graviton Propagator," *JHEP* **11** (2006) 092, gr-qc/0608131.

[140] E. Bianchi and L. Modesto, "The perturbative Regge-calculus regime of Loop Quantum Gravity," *Nucl. Phys.* **B796** (2008) 581–621, 0709.2051.

[141] J. D. Christensen, E. R. Livine, and S. Speziale, "Numerical evidence of regularized correlations in spin foam gravity," *Phys. Lett.* **B670** (2009) 403–406, 0710.0617.

[142] E. Alesci and C. Rovelli, "The complete LQG propagator: I. Difficulties with the Barrett-Crane vertex," *Phys. Rev.* **D76** (2007) 104012, 0708.0883.

[143] E. Alesci and C. Rovelli, "The complete LQG propagator: II. Asymptotic behavior of the vertex," *Phys. Rev.* **D77** (2008) 044024, `0711.1284`.

[144] S. Speziale, "Background-free propagation in loop quantum gravity," *Adv. Sci. Lett.* **2** (2009) 280–290, `0810.1978`.

[145] R. Oeckl, "General boundary quantum field theory: Foundations and probability interpretation," *Adv. Theor. Math. Phys.* **12** (2008) 319–352, `hep-th/0509122`.

[146] F. Conrady, L. Doplicher, R. Oeckl, C. Rovelli, and M. Testa, "Minkowski vacuum in background independent quantum gravity," *Phys. Rev.* **D69** (2004) 064019, `gr-qc/0307118`.

[147] J. W. Barrett and L. Crane, "Relativistic spin networks and quantum gravity," *J. Math. Phys.* **39** (1998) 3296–3302, `gr-qc/9709028`.

[148] S. Speziale, "Towards the graviton from spinfoams: The 3d toy model," *JHEP* **05** (2006) 039, `gr-qc/0512102`.

[149] E. R. Livine, S. Speziale, and J. L. Willis, "Towards the graviton from spinfoams: higher order corrections in the 3d toy model," *Phys. Rev.* **D75** (2007) 024038, `gr-qc/0605123`.

[150] V. Bonzom, E. R. Livine, M. Smerlak, and S. Speziale, "Towards the graviton from spinfoams: the complete perturbative expansion of the 3d toy model," *Nucl. Phys.* **B804** (2008) 507–526, `0802.3983`.

[151] J. Engle, R. Pereira, and C. Rovelli, "Flipped spinfoam vertex and loop gravity," *Nucl. Phys.* **B798** (2008) 251–290, `0708.1236`.

[152] E. Alesci, E. Bianchi, E. Magliaro, and C. Perini, "Intertwiner dynamics in the flipped vertex," *Class. Quant. Grav.* **26** (2009) 185003, `0808.1971`.

[153] I. Khavkine, "Evaluation of new spin foam vertex amplitudes," *Class. Quant. Grav.* **26** (2009) 125012, `0809.3190`.

[154] I. Khavkine, "Evaluation of new spin foam vertex amplitudes with boundary states," `0810.1653`.

[155] A. Ashtekar and J. Lewandowski, "Quantum theory of geometry. I: Area operators," *Class. Quant. Grav.* **14** (1997) A55–A82, `gr-qc/9602046`.

[156] A. Ashtekar, A. Corichi, and J. A. Zapata, "Quantum theory of geometry. III: Non-commutativity of Riemannian structures," *Class. Quant. Grav.* **15** (1998) 2955–2972, `gr-qc/9806041`.

[157] T. Thiemann, "A length operator for canonical quantum gravity," *J. Math. Phys.* **39** (1998) 3372–3392, `gr-qc/9606092`.

[158] J. W. Barrett, M. Rocek, and R. M. Williams, "A note on area variables in Regge calculus," *Class. Quant. Grav.* **16** (1999) 1373–1376, `gr-qc/9710056`.

[159] L. Hormander, "The analysis of linear partial differential operators. I,". Springer, 1990.

[160] M. Bojowald, "The semiclassical limit of loop quantum cosmology," *Class. Quant. Grav.* **18** (2001) L109–L116, `gr-qc/0105113`.

[161] C. Rovelli and F. Vidotto, "Stepping out of Homogeneity in Loop Quantum Cosmology," *Class. Quant. Grav.* **25** (2008) 225024, `0805.4585`.

[162] M. V. Battisti, A. Marciano, and C. Rovelli, "Triangulated Loop Quantum Cosmology: Bianchi IX and inhomogenous perturbations," *Phys. Rev.* **D81** (2010) 064019, `0911.2653`.

[163] M. Bojowald, "Loop quantum cosmology," *Living Rev. Rel.* **8** (2005) 11, `gr-qc/0601085`.

[164] A. Ashtekar, "Loop Quantum Cosmology: An Overview," *Gen. Rel. Grav.* **41** (2009) 707–741, `0812.0177`.

[165] A. Ashtekar, M. Campiglia, and A. Henderson, "Loop Quantum Cosmology and Spin Foams," *Phys. Lett.* **B681** (2009) 347–352, `0909.4221`.

[166] A. Ashtekar, M. Campiglia, and A. Henderson, "Casting Loop Quantum Cosmology in the Spin Foam Paradigm," *Class. Quant. Grav.* **27** (2010) 135020, `1001.5147`.

[167] C. Rovelli and F. Vidotto, "On the spinfoam expansion in cosmology," *Class. Quant. Grav.* **27** (2010) 145005, `0911.3097`.

[168] K. S. Atsuyuki Okabe, Barry Boots and S. N. Chiu, "patial tessellations: concepts and applications of Voronoi diagrams," *John Wiley & Sons Ltd., Chichester, second edition, 2000.*

[169] A. Ashtekar, M. Bojowald, and J. Lewandowski, "Mathematical structure of loop quantum cosmology," *Adv. Theor. Math. Phys.* **7** (2003) 233–268, `gr-qc/0304074`.

[170] J. B. Hartle, S. W. Hawking, and T. Hertog, "The Classical Universes of the No-Boundary Quantum State," *Phys. Rev.* **D77** (2008) 123537, `0803.1663`.

[171] S. W. Hawking, "THE PATH INTEGRAL APPROACH TO QUANTUM GRAVITY,". In *Hawking, S.W., Israel, W.: General Relativity*, 746- 789.

[172] A. Ashtekar, T. Pawlowski, and P. Singh, "Quantum nature of the big bang," *Phys. Rev. Lett.* **96** (2006) 141301, `gr-qc/0602086`.

[173] A. Ashtekar, T. Pawlowski, and P. Singh, "Quantum nature of the big bang: An analytical and numerical investigation. I," *Phys. Rev.* **D73** (2006) 124038, `gr-qc/0604013`.

[174] A. Ashtekar, T. Pawlowski, and P. Singh, "Quantum nature of the big bang: Improved dynamics," *Phys. Rev.* **D74** (2006) 084003, `gr-qc/0607039`.

[175] A. Ashtekar, T. Pawlowski, P. Singh, and K. Vandersloot, "Loop quantum cosmology of k=1 FRW models," *Phys. Rev.* **D75** (2007) 024035, `gr-qc/0612104`.

[176] P. Singh and K. Vandersloot, "Semi-classical states, effective dynamics and classical emergence in loop quantum cosmology," *Phys.Rev.* **D72** (2005) 084004, `gr-qc/0507029`.

[177] M. Bojowald and A. Tsobanjan, "Effective Constraints and Physical Coherent States in Quantum Cosmology: A Numerical Comparison," `0911.4950`.

[178] M. Bojowald, B. Sandhofer, A. Skirzewski, and A. Tsobanjan, "Effective Constraints for Quantum Systems," *Rev. Math. Phys.* **21** (2009) 111–154.

[179] J. Engle, "Quantum field theory and its symmetry reduction," *Class. Quant. Grav.* **23** (2006) 2861–2894, `gr-qc/0511107`.

[180] J. Engle, "On the physical interpretation of states in loop quantum cosmology," *Class. Quant. Grav.* **24** (2007) 5777–5802, `gr-qc/0701132`.

[181] A. Corichi and P. Singh, "Is loop quantization in cosmology unique?," *Phys. Rev.* **D78** (2008) 024034, `0805.0136`.

[182] V. Baccetti, E. R. Livine, and J. P. Ryan, "The particle interpretation of N = 1 supersymmetric spin foams," *Class. Quant. Grav.* **27** (2010) 225022, `1004.0672`.

[183] A. Perez and C. Rovelli, "Physical effects of the Immirzi parameter," *Phys. Rev.* **D73** (2006) 044013, `gr-qc/0505081`.

[184] L. Freidel, D. Minic, and T. Takeuchi, "Quantum Gravity, Torsion, Parity Violation and all that," *Phys. Rev.* **D72** (2005) 104002, `hep-th/0507253`.

[185] S. A. Major, "Shape in an Atom of Space: Exploring quantum geometry phenomenology," *Class. Quant. Grav.* **27** (2010) 225012, `1005.5460`.

[186] S. B. Giddings and R. A. Porto, "The gravitational S-matrix," *Phys. Rev.* **D81** (2010) 025002, `0908.0004`.

[187] A. Ashtekar, A. Corichi, and P. Singh, "Robustness of key features of loop quantum cosmology," *Phys. Rev.* **D77** (2008) 024046, `0710.3565`.

[188] J. Grain and A. Barrau, "Cosmological footprints of loop quantum gravity," *Phys. Rev. Lett.* **102** (2009) 081301, `0902.0145`.

[189] J. Mielczarek, T. Cailleteau, J. Grain, and A. Barrau, "Inflation in loop quantum cosmology: Dynamics and spectrum of gravitational waves," *Phys. Rev.* **D81** (2010) 104049, `1003.4660`.

[190] **Planck** Collaboration, "Planck: The scientific programme," `astro-ph/0604069`.

[191] H. C. Chiang *et al.*, "Measurement of CMB Polarization Power Spectra from Two Years of BICEP Data," *Astrophys. J.* **711** (2010) 1123–1140, `0906.1181`.

[192] D. Samtleben and f. t. Q. Collaboration, "Measuring the Cosmic Microwave Background Radiation (CMBR) polarization with QUIET," *Nuovo Cim.* **B122** (2007) 1353–1358, `0802.2657`.

[193] A. Ashtekar, J. Baez, A. Corichi, and K. Krasnov, "Quantum geometry and black hole entropy," *Phys. Rev. Lett.* **80** (1998) 904–907, `gr-qc/9710007`.

[194] A. Ashtekar, J. C. Baez, and K. Krasnov, "Quantum geometry of isolated horizons and black hole entropy," *Adv. Theor. Math. Phys.* **4** (2000) 1–94, `gr-qc/0005126`.

[195] J. Engle, A. Perez, and K. Noui, "Black hole entropy and SU(2) Chern-Simons theory," *Phys. Rev. Lett.* **105** (2010) 031302, `0905.3168`.

[196] E. Bianchi, "Black Hole entropy, Loop Gravity, and Polymer Physics," *GR19 - CQG Special Issue (2010).*

[197] R. D. Sorkin, "How wrinkled is the surface of a black hole?," `gr-qc/9701056`.

[198] K. S. Thorne, (Ed.), R. H. Price, (Ed.), and D. A. Macdonald, (Ed.), "BLACK HOLES: THE MEMBRANE PARADIGM,". NEW HAVEN, USA: YALE UNIV. PR. (1986) 367p.

[199] J. W. York, Jr., "Dynamical origin of Black Hole radiance," *Phys. Rev.* **D28** (1983) 2929.

[200] O. Dreyer, "Quasinormal modes, the area spectrum, and black hole entropy," *Phys. Rev. Lett.* **90** (2003) 081301, `gr-qc/0211076`.

[201] W. Fairbairn and C. Rovelli, "Separable Hilbert space in loop quantum gravity," *J. Math. Phys.* **45** (2004) 2802–2814, gr-qc/0403047.

[202] R. M. Wald, "General Relativity,". Chicago, Usa: Univ. Pr. (1984) 491p.

[203] S. W. Hawking and G. F. R. Ellis, "The Large scale structure of space-time,". Cambridge University Press, Cambridge, 1973.

[204] R. L. Arnowitt, S. Deser, and C. W. Misner, "The dynamics of general relativity," gr-qc/0405109.

[205] P. Menotti, G. Modanese, and D. Seminara, "The Radial gauge propagators in quantum gravity," *Ann. Phys.* **224** (1993) 110–138, hep-th/9209028.

[206] F. Mattei, C. Rovelli, S. Speziale, and M. Testa, "From 3-geometry transition amplitudes to graviton states," *Nucl. Phys.* **B739** (2006) 234–253, gr-qc/0508007.